Probiotic Lactobacillus acidophilus NCFM and Bifidobacterium animalis subsp lactis Bl-04 interactions with prebiotic carbohydrates using differential proteomics and protein characterization

Hansen, Morten Ejby; Abou Hachem, Maher ; Svensson, Birte; Jacobsen, Susanne; J. Slotboom, Dirk

Publication date:
2012

Document Version
Publisher's PDF, also known as Version of record

Probiotic *Lactobacillus acidophilus* NCFM and *Bifidobacterium animalis* subsp *lactis* Bl-04 interactions with prebiotic carbohydrates using differential proteomics and protein characterization.

Ph.D. thesis (October 2012)

Morten Ejby Hansen

Enzyme and Protein Chemistry (EPC),

Department of Systems Biology,

Technical University of Denmark (DTU)

Supervisors:

Assoc. Prof. Susanne Jacobsen, EPC, Department of Systems Biology, DTU, DK

Assoc. Prof. Maher Abou Hachem, EPC, Department of Systems Biology, DTU, DK

Prof. Birte Svensson, EPC, Department of Systems Biology, DTU, DK

PREFACE

The present thesis presents the results of my Ph.D. study carried out in the Enzyme and Protein Chemistry group (EPC), Department of Systems Biology, Technical University of Denmark from February 2009 to September 2012 under supervision of Professor Birte Svensson, Associate Professor Susanne Jacobsen and Associate Professor Maher Abou Hachem. The Ph.D. project was performed in collaboration with DuPont Nutrition and Health (former Danisco A/S) and University of Groningen, Membrane Enzymology Group under supervision by Professor Dirk Jan Slotboom. The Ph.D. stipend was funded by EPC and the work was supported by the Danish Strategic Research Council for the project "*Gene discovery and molecular interactions in prebiotics/probiotics systems. Focus on carbohydrate prebiotics*" (project no. 2101-07-0105)

The work of this Ph.D. project has resulted in the following manuscripts:

Majumder, A., Sultan, A., Jersie-Christensen, R.R., **Ejby, M**., Schmidt, B.G., Lahtinen, S.J., Jacobsen, S. and Svensson, B. (2011) Proteome reference map of *Lactobacillus acidophilus* NCFM and quantitative proteomics towards understanding the prebiotic action of lactitol. Proteomics, 11, 3470–3481.

Majumder, A., Cai, L., **Ejby**, **M**., Schmidt, B., Lahtinen, S., Jacobsen, S. and Svensson, B. (2012) 2D-gel based alkaline proteome of the probiotic bacterium *Lactobacillus acidophilus* NCFM. Proteomics, 12**,** 1006–1014.

Ejby, M., Majumder, A., Thorsen, K., Schmidt, B., Lahtinen, S., Jacobsen, S. and Svensson, B. Differential proteome analysis of prebiotic raffinose metabolism by the probiotic bacterium *Lactobacillus acidophilus* NCFM. (*Manuscript to be submitted to BMC Microbiology*).

Ejby, M., Knudsen, A., Majumder, A., Schmidt, B., Lahtinen, S., Svensson, B. and Jacobsen, S. Reference map and proteomic analysis of *Bifidobacterium animalis* subsp. *lactis* Bl-04 grown on galactooligosaccharides, raffinose family oligosaccharides and isomaltooligosaccharides. (*Manuscript to be submitted to PlosOne*).

Ejby, M., Vujicic-Zagar, A., Fredslund, F., Svensson, B., Slotboom, DJ., and Abou Hachem, M. Structural basis for xylooligosaccharide uptake by the probiotic *Bifidobacterium animalis* subsp. *lactis*. Bl-04 (*Manuscript to be submitted to Journal of Biological Chemistry*).

ACKNOWLEDGEMENTS

First and foremost, I should thank my supervisors Associate Professor Maher Abou Hachem, Associate Professor Susanne Jacobsen and Professor Birte Svensson, for the opportunity to do this study and then for their scientific guidance, inspiration and not least their patience. In short thank you for dragging me kicking and screaming through the hellish ordeal of writing this thesis.

A very big thank you to my collaborators and my fellow colleagues on the 'FøSu project': Especially former Post docs Avishek Majumder and Folmer Fredslund for extremely rewarding collaborations, inspirational academic work and good friendship. Ph.D. students Joakim Mark Andersen, Anne Knudsen and Gabriella van Zanten for colorful collaborations, discussions and laughs. Brilliant technical assistance with mass spectrometry from Birgit Andersen and invaluable help with protein purification on ÄKTA systems and a thousand small "details" by Mette Pries. Andreja Vujicic-Zagar and Dirk Slotboom at RUG thank you for introducing me to macromolecular crystallization and structure determination; and not least for trying to keep my spirits up. Thanks to everybody at the Groningen University Membrane Enzymology Group for making my visit an unforgettable experience.

All my dear colleagues present and former, at the Enzyme and Protein Chemistry, Department of Systems Biology, DTU, are thanked for making the days a little less dull.

ABSTRACT

Bacterial communities (microbiota) of great diversity populate the large intestine of animals including humans and influence the physiology, biochemistry and immunology of the host. Microorganisms mainly bacteria that when administered in sufficient amounts promote a beneficial effect to the host are defined as probiotics. The positive clinical effects of probiotics, mainly belonging to the Bifidobacterium and Lactobacillus genera in treatments of irritable bowel syndrome, gut infections and lifestyle diseases are well documented. Compounds that selectively stimulate the beneficial effect of probiotics, primarily non-digestible carbohydrates, are termed prebiotics. The knowledge of prebiotic utilization and in particular the specificities of carbohydrate transport and metabolism are limited, hampering robust understanding for the basis of selective utilization of known prebiotics and the discovery and documentation of novel ones. In this project we set out to investigate the metabolism of carbohydrates that are prebiotic or potential prebiotic compounds utilized by the probiotic organisms *Lactobacillus acidophilus* NCFM (NCFM) and *Bifidobacterium animalis* subsp. *lactis* BL-04 (Bl-04).

The aim of this Ph.D. thesis was the study of probiotic NCFM and Bl-04 interaction with prebiotic carbohydrates using differential proteomics and protein characterization. Proteomics is a potential omics tool to investigate probiotic bacteria and its response to prebiotic carbohydrates at the protein level. The reference proteome of NCFM and Bl-04 was established using 2D based proteomics. The whole cell extract proteome of NCFM grown on glucose until late exponential phase was resolved by two-dimensional gel electrophoresis (2-DE) (pH 3−7 and 6−11). A total of 507 and 150 protein identifications were made from the CBB stained 2D-gel using MALDI-TOF MS and/or MS/MS in the pH 3−7 and 6−11 respectively. While from the whole cell extract 2D proteome of Bl-04 (pH 3−7 and pH 3−10), 870 protein identifications were made using MALDI-TOF MS and/or MS/MS. Differential 2-DE (DIGE) of NCFM and Bl-04 grown on established and potential prebiotics revealed several proteins with differential abundance including the glycoside hydrolases involved in primary breakdown of oligosaccharides and changes in carbohydrate metabolic pathways.

The potential carbohydrates transport systems involved in uptake of potential prebiotic carbohydrates, specifically the ABC-transporter associated solute binding protein *Bl*XBP involved in the transport of XOS from Bl-04 was characterized. Surface plasmon resonance binding assays showed that *Bl*XBP was specific for XOS with a degree of polymerization (DP) 2– 6 with optimal affinity (Kd ~50 nM) for xylotetraose followed by xylotriose. Differences in binding affinity was governed largely by the association rate (k_{on}), while koff had a more modest contribution to binding affinities, except for xylobiose, which displayed the highest k_{off}. The binding affinity and kinetics of arabinose decorated XOS were similar to undecorated counterparts, thus providing evidence that arabinoxylan fragments are efficiently captured by the ABC import system. The binding affinity towards xylotriose and xylotetraose was corroborated using fluorescence emission spectroscopy and isothermal titration. calorimetry that revealed that the binding free energy was dominated by a favourable enthalpy, which was off-set by a large unfavourable entropy change. The crystal structures of *Bl*XBP in complex with xylotriose, xylotetraose and xylohexaose were determined and showed a binding cleft large enough to accommodate the preferred ligand xylotetraose. The helical structure of xylan fragments was recognized by aromatic stacking of xyloxyl rings 1, 3 and 4, in addition to several direct and solvent mediated hydrogen-bonds that contribute to the binding enthalpy. Binding of larger ligands requires conformational changes in a lid loop that contributes to the structural plasticity of *Bl*XBP. This data bring novel insight into the molecular basis for XOS uptake by bifidobacteria, and xylan utilization by the gut microbiome.

DANSK RESUMÉ (SUMMARY IN DANISH)

Tyktarmen hos mennesker og dyr indeholder en mangfoldig og divers population af bakterier, der kan påvirke værtens metabolisme og immunforsvar. Mikroorganismer som indtages i tilstrækkeligt antal udviser en positiv effekt på modtageren, er defineret som probiotika. Det er dokumenteret at probiotika, hovedsageligt fra genera *Bifidobacterium* og *Lactobacillus* kan anvendes i behandlingen af irriteret tyktarm, tarminfektioner og forskellige livsstilssygdomme. Levnedsmiddelskomponenter, der selektivt stimulerer de gavnlige effekter af probitika er defineret som præbiotika. Kendskab til hvordan probiotiske bakterier stimuleres af præbiotiske kulhydrater og i særdeleshed de probiotiske bakteriers kulhydrattransport og metabolisme er begrænset. Dette hindrer forståelsen af den selektive effekt af kendte præbiotika samt opdagelse og dokumentation af nye. Ph.D-projektets målsætning er at undersøge kulhydrat metabolismen hos to probiotiske bakterier *Lactobacillus acidophilus* NCFM (NCFM) og *Bifidobacterium animalis* subsp. *lactis* BL-04 (Bl-04) mens de fermenterer præbiotiske eller potentielt præbiotiske kulhydrater.

Formålet med denne Ph.D-afhandling er at studere de probiotiske bakterier NCFM og Bl-04´s interaktion med præbiotiske kulhydrater ved hjælp af differentiel proteomanalyse og proteinkarakterisering. Proteomics er et ´omics´-værktøj der på proteinniveau kan anvendes til at undersøge probiotiske bakterier og deres interaktion med præbiotiske kulhydrater. Referenceproteomer for NCFM og Bl-04 blev etableret ved hjælp af 2D gel-baseret proteomics.

Proteomet af NCFM dyrket på glukose blev etableret ved 2D- gelelektroforese (pH 3-7 og 6-11). MALDI-TOF massespektromeri resulterede i 507 og 150 protein identifikationer fra coomassie farvede 2D-geler med p*I* intervallerne pH 3-7 og 6-11. For Bl-04 resulterede referenceproteomet (pH 3-7 og pH 3-10), i totalt 870 protein identifikationer. Differential 2-DE (DIGE) af NCFM og Bl-04 dyrket på etablerede og potentielle præbiotika afslørede en række proteiner med differentieret ekspressions mønster herunder glykosidhydrolaser involveret i primær nedbrydning af oligosaccharider og dermed ændringer i kulhydrat stofskiftet.

Et solute binding protein *Bl*XBP tilhørende en ABC-transportør involveret i transport af XOS (Xylooligosaccharider) fra Bl-04 blev karakteriseret. ´Suface plasmon resonance´-

bindingsanalyser viste, at *Bl*XBP var specifik for XOS med en polymerisationsgrad (DP) fra 2 til 6 med optimal affinitet (Kd ~ 50 nM) for xylotetraose efterfulgt af xylotriose. Forskelle i bindingsaffiniteten for forskellige XOS var i vid udstrækning reguleret af associations parameteren k_{on}, mens k_{off} havde et minimalt bidrag til bindingsaffiniteten, bortset fra xylobiose, der viste den højeste k_{off}. Bindings-affinitet og -kinetik for arabinoxylan fragmenter lignede de lineære XOS varianter, hvilket viser, at arabinoxylan fragmenter effektivt opfanges af ABC-transportøren. Bindingsaffiniteten for xylotriose og xylotetraose blev bekræftet ved hjælp af fluorescensemissionsspektroskopi og isotermisk titreringskalorimetri der viste, at den frie bindingsenergi var domineret af enthalpi bidrag, som blev opvejet af en tilsvarende forandring i entropi. Krystalstrukturer af *Bl*XBP i kompleks med xylotriose, xylotetraose og xylohexaose blev løst og viste en bindingskløft der helt kan akkommodere den foretrukne ligand xylotetraose. Binding af større ligander kræver konformationsændringer af et ´loop´ der afgrænser bindings sitet mod solventsiden, denne strukturelle plasticitet af *Bl*XBP er afspejlet i bindingsdata. Observationer giver en hidtil ukendt indsigt i det molekylære grundlag for bifidobacteriers optagelse af XOS samt tarmbakteries udnyttelse af xylan.

CONTENTS

CHAPTER 1

Introduction

ABBREVIATIONS

2-DE	Two-dimensional gel electrophoresis
2D-DIGE	Two-dimensional difference gel electrophoresis
Bl-04	*Bifidobacterium animalis* subsp. *lactis* Bl-04
*Bl*XBP	XOS binding SBP Balac_0514 from Bl-04
CCR	Carbon catabolite repression
DP	Degree of polymerizarion
FAO	Food and agricultural organization
FOS	Fructooligosaccharides
GH	Glycoside hydrolase
GI	Gastro intestinal
GOS	β-Galactooligosaccharides
GPH	Galactose-pentose-hexuronide
HMO	Human milk oligosaccharides
IBS	Irritable bowel syndrome
IMO	Isomaltooligosaccharides
IPG	Immobilized pH gradient
LAB	Lactic acid bacteria
MALDI	Matrix assisted laser desorption/ionization
MFS	Major facilitator superfamily
NBD	Nucleotide binding domain
NCFM	*Lactobacillus acidophilus* NCFM
PTS	Phosphotransferase system
SBP	Solute binding protein
SDS-PAGE	Sodium dodecyl sulfate-polyacrylamide gel electrophoresis
SCFA	Short-chain fatty acids
TMD	Trans-membrane domain
TOF	Time of flight
RFO	Raffinose family oligosaccharides
WHO	World health organization
XOS	Xylooligosaccharides

1 INTRODUCTION

1.1 FUNCTIONAL FOODS

Functional foods refer to food products and beverages, which can produce a positive health effect that surpasses the effect of the nutrients contained by the product and is intended to enhance not replace normal food. Functional food has been defined as “Functional Food is a natural or processed food that contains known biologically-active compounds which when in defined quantitative and qualitative amounts provides a clinically proven and documented health benefit, and thus, an important source in the prevention, management and treatment of chronic diseases of the modern age” [1]. The health benefit in this context means health promotion, disease prevention, relief of symptom or possibly even healing. The concept was originally developed in Japan in the 1980s and in the 1990s the development and availability of functional food products grew especially in the United States, simultaneously the concept of functional foods was specifically defined in Europe [2, 3]. Probiotics and prebiotics are classes of physiologically beneficial components used in functional foods.

1.1.2 PROBIOTICS AND PREBIOTICS

Probiotics meaning “pro life” are defined by the FAO/WHO as: "Live microorganisms which when administered in adequate amounts confer a health benefit on the host". The health claims of live microorganisms in food or fermented foods go long back in history primarily as folklore. The original scientific proposal of the positive role played by certain bacteria was first introduced by Élie Metchnikoff in 1907 [4], who suggested that it would be possible to modify the gut flora and to replace harmful microbes with useful microbes. This was at the beginning of the modern microbiology and probiotics were thought to beneficially affect the host by improving its intestinal microbial balance, by inhibiting pathogens and toxin producing bacteria [4]. The term probiotics was first used by Lilly and Stillwell [5] as the opposite of antibiotics “substances secreted by one microorganism which stimulates the growth of another”, later the term came to include the microorganisms in question. In recent

years specific health effects of probiotic microorganisms in combination with selectively metabolized compounds (prebiotics), mainly carbohydrates [6] have been investigated and documented, including alleviation of chronic intestinal inflammatory diseases [7], prevention and treatment of pathogen-induced diarrhea [8], urogenital infections, and atopic diseases [9]. Furthermore probiotics have been suggested to play a role in some cases of obesity [10] (see Table 1). Most attention has been given to the probiotic potential of bifidobacteria and LAB (Lactic acid bacteria) especially various lactobacillus species of the latter group. But other gut inhabiting microorganisms have also been shown to have probiotic effects. Probiotic organisms have been suggested in species of *Bacteriodes, Bifidobacterium, Enterococcus, Escherichia, Lactobacillus, Lactococcus, Leuconostoc, Pediococcus, Ruminococcus, Saccharomyces* and *Streptococcus* [11-13], in this context it is worth noting that *Bacteriodes, Escherichia, Enterococcus,* and *Streptococcus* double as both beneficial and detrimental genera. The determinants of beneficial or detrimental effect may be species specific and could also be dependent on the diversity and composition of the gut microbiota

Table 1. Studies investigating human health benefits of consuming probiotics

Effect on ailment	**References**
Common infections	[14-18]
Diarrheal illness	[18-22]
Inflammatory bowel disease	[23-27]
Age dependent effects	[28-30]
Allegies	[31-33]
Colonic cancer	[34, 35]

The term prebiotic has been defined twice by Gibson and Robberfroid [11, 14] and has ended up in the form: “A prebiotic is a selectively fermented ingredient that allows specific changes, both in the composition and/or activity in the gastrointestinal microflora that confers benefits upon host well-being and health”. The prebiotic definition does not emphasize a specific bacterial group. Generally, however, it is assumed that a prebiotic should increase the number

and/or activity of probiotic bifidobacteria or lactic acid bacteria. So far most attention has been given to bifidobacteria and lactic acid bacteria in the role of probiotic bacteria and as a consequence most evidence has been on the beneficial effects of these groups, especially in terms of improving digestion and the effectiveness and intrinsic strength of the immune system. Synbiotics is the less frequently used term for the combined use of probiotic organisms and prebiotic compounds to increase their effect.

1.1.2.1 PREBIOTIC CARBOHYDRATES

Intake of prebiotic non digestible dietary carbohydrates is another approach to obtain the health benefits of intestinal probiotic microbes already present in the gastrointestinal tract (GI). A healthy and balanced gut microbiota has been proposed to be one that is primarily saccharolytic with significant numbers of lactobacilli and bifidobacteria [15]. Accoding to the definition given earlier and [16] a food ingredient has to fulfill the following criteria in order to be classified as a prebiotic:

1) Resist gastric acidity, hydrolysis by mammalian enzymes and gastrointestinal absorption
2) Be fermented by the intestinal microbes
3) Selectively stimulate the growth and/or activity of intestinal bacteria associated with the health benefit and well being

So far only fructooligosaccharides (FOS), galactooligosaccharides (GOS) and lactulose have been classified as prebiotic carbohydrates [16]. Other carbohydrates that are being evaluated as promising emerging prebiotics are lactitol, isomaltooligosaccharides (IMO), xylooligosaccharides (XOS) and raffinose family oligosaccharides (RFO). One of the major aspects of the prebiotic concept is the selective stimulation of prebiotic bacteria such as lactobacilli and bifidobacteria at the expense of other bacteria especially potential pathogenic bacterial groups [17]. Such selectivity may be conferred by carbohydrate characteristics such as the type of glycosidic linkage, degree and type of branching or added modifications and degree of polymerization (DP). The DP may influence where in the colon the carbohydrates

are fermented as longer polymers are supposed to travel longer into the colon before they are broken down [18].

Recent studies have focused on investigate the potential of nondigestible carbohydrates (Table 2) to act as a prebiotic. Lactitol (4-O-*β*-D-galactopyranosyl-D-glucitol) is a synthetic sugar alcohol obtained from lactose and is accessible to the microbiota in the colon [7]. It has been shown to stimulate growth and metabolism of intestinal *Bifidobacterium* and *Lactobacillus* species, thus creating unfavourable conditions for pathogens such as *Clostridia* and *Enterobacteriaceae* [8]. Daily consumption of the synbiotic combination of NCFM and lactitol by elderly volunteers increased stool frequency, fecal levels of NCFM and genus *Bifidobacterium*, and modulated fecal immune biomarkers, reflecting stimulation of intestinal mucosal functions [9]. RFO are an emerging class of prebiotic carbohydrates derived from soybean and lupins. Raffinose was been shown to modulate the human intestinal microbiota for beneficial effects [15] and the administration of raffinose has shown to increase the levels of bifidobacteria sp. in the gut from 12.5% to 37% [19]. GOS and FOS supplementation has shown a bifidogenic effect in infants and adults and results in increased amounts of bifidobacteria in the gut [20, 21]. IMO are known to be selectively fermented by bifidobacteria and increase their numbers in the presence of the human gut microflora [22].

Table 2. A list of various nondigestible carbohydrates with their chemical structure and potential sources

Common names	Chemical Structure	Source	Ref.
Fructo-oligosaccharides (FOS)	[β-D-Fru*f*-(1-2)]$_a$ -(β2,α1)-D-Glc*p*	Hydrolysis of chicory inulin or enzymatic synthesis	[23]
Inulin	As FOS with a > 20	Onion, banana, garlic,leek, chicory root	[24]
β-galacto-oligosaccharides (GOS)	[β-D-Gal*p*-(1–4)]$_b$-D-Glc*p*	Milk or enzymatic synthesis from lactose	[25]
Lactitol	β-D-Gal*p*-(1–4)-D-Glc-ol	enzymatic sunthesis from milk sugar	[26]
Lactulose	β-D-Gal*p*-(1–4)-D-Fru*f*	Enzymatic isomerization of lactose	[25]
Raffinose family oligosaccharides (RFO)	[α-D-Gal*p*-(1–6)]$_c$- D-Glc*p*-(α1,β2)-D-Fru*f*	Soybean, beans, cabbage, brussels sprouts, broccoli and asparagus	[27]
Melibiose	α-D-Gal*p*-(1–6)- D-Glc*p*	Produced from RFOs	
Isomaltooligosaccharides (IMO)	[α-D-Glc*p*-(1–6)]$_d$-D-Glc*p*	Enzymatic degradation from starch.	[28]
Panose	α-D-Glc*p*(1–6)-α-D-Glc*p*-(1–4)-D-Glc*p*	Enzymatic degradationfrom starch.	[29]
Gentio-oligosaccharides	[β-D-Glc*p*-(1–6)]$_e$-D-Glc*p*	Enzymatic synthesis by trans-glycosylation	[30]
β-xylo-oligosaccharides (XOS)	[β- D-xyl*p*-(1–4)]$_f$-D-xyl*p*	Bamboo shoots, plant cell walls, produced comercially by enzymatic treatment of xylan rich material e.g. corncob	[31]
Arabinose-decorated XOS (AXOS)	α-D-Ara*f*-(1–2) and/or α-D-Ara*f*-(1–3) linked to XOS	Bamboo shoots, plant cell walls, produced comercially by enzymatic treatment of xylan rich material e.g. corncob	[31]
Xylitol	β- D-xyl*p*-(1–4)-D-xyl*p*-ol	Enzymatic synthesis	
Polydextrose mostly mixed α-glucans, DP=2–30		Chemical synthesis by random polymerization of glucose	[31]
Rhamnogalacturonan I (RG-I) fraction of pectin	[α-L-Rha*p*-(1,2)-α-D-GalA*f*-(1,4)]$_g$	Plant cell walls, commercially produced from citrus and apple solids	[32]
Manno-oligosaccharides	[α- D-Man*p*-(1–4)]-D-Man*p*	yeast cell wall, Konjac (plant)	[33]

a = [1–5]; b = [1–5]; c = [1=raffinose, 2=stachyose, 3=verbascose]; d = [1–5]; e = [1–5]; f = [1–7]; g = [1–4]

1.2 THE GUT MICROBIOME

The continuum of microorganisms inhabiting the GI tract has a few collective names, including gut microflora, microbiota and gut microbiome. The big majority of the gut microbiome consists of bacteria, between 300–500 species per individual [34], but also yeasts and archaea inhabit the gut microbiome. The varied conditions along the GIT have led to development of niche specific microbial communities (Fig. 1). The small intestine has the lowest density of microbes, while the large intestine has the highest density of microbes (Fig. 1) [35]. The density of bacteria in human feces is quite high 10^{11} - 10^{12} cells per gram which is equivalent to 50–60 % of fecal solids [36]. This makes the gut microbiome one of the most densely populated natural ecosystems. The combined genome of the gut microbiome is estimated to be over 100 times larger than the human genome and is often in popular terms referred to as our second genome or the genome within [37, 38]. The metabolic capabilities of the combined microbiome are beyond what is found in the human genome which corresponds to the role of the microbiome. It contains a wide array of activities for utilization of carbohydrates that would otherwise escape processing. Furthermore minerals are made more accessible to the host by the microbiomes activities [39] and helps to get rid of potential toxic components [40].

Given this relatively large and complex microbial community living in our digestive system it seems almost natural that both its composition and the products of its combined metabolism may have an impact on human health. The relationship is mutual, as our diet to a very large degree determines the composition of the gut microbiome. Digestion of food and absorption of nutrients is a complex process performed by the GI system. The small intestine is the part of the gastrointestinal tract, where most of the human digestion and absorption of nutrients take place. Carbohydrates that resist degradation in the small intestine reach the cecum and colon, where they are available for bacterial fermentation [41]. The major end-products of bacterial metabolism in the gut include short-chain fatty acids (SCFA), pyruvate, lactic acid, ethanol, and succinic acid [42].

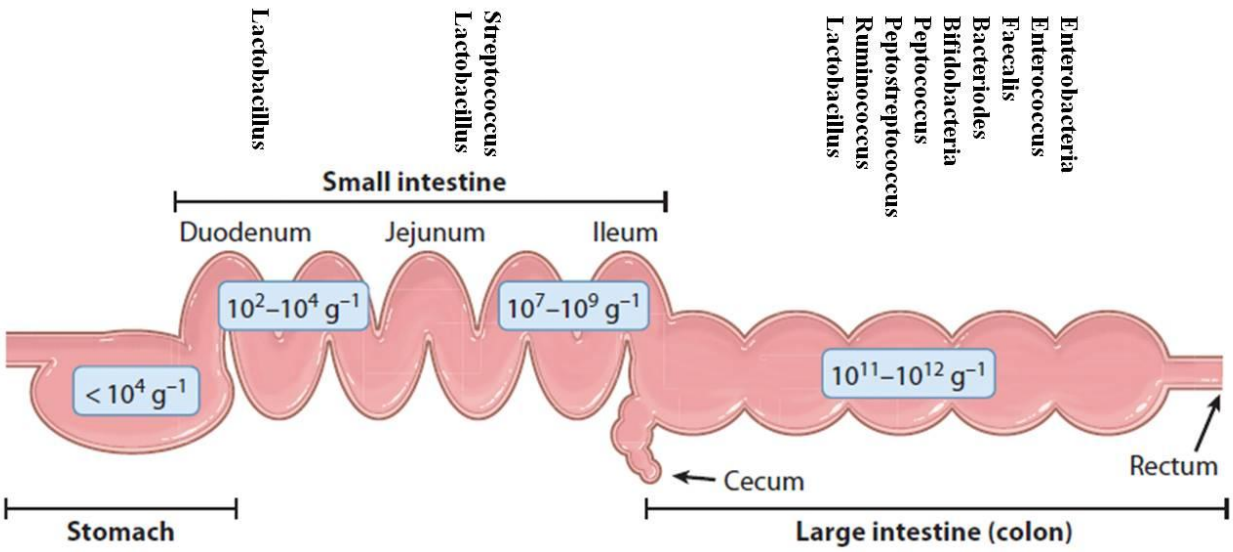

Fig. 1. The distribution of microbial flora in the human intestine. The schematic representation of the intestine indicates the different regions and the overall sizes of the residing bacterial populations (*blue boxes*) (modified from [43]).

The highest density and diversity of bacteria is found in the large intestine (10^{11}–10^{12} CFU/g). The human GIT microbiota is a complex ecosystem that has co-evolved with its human host [44]. As mentioned above it contains three domains of life, bacteria, archaea and eukaryote, where the bacteria are the most abundant and diversely represented [34, 45]. The intestinal microflora is established at birth or shortly after and develops with the host through life. Breast-fed infants are colonized by high numbers of bifidobacteria opposed to formula-fed infants whose fecal samples contain high numbers of bacteriodes and clostridia [46-48]. The intestinal microbiota stabilizes after weaning and resembles the adult composition when the child is approximately 3 years old. Our GIT microbiome varies through our life, between geographical regions and with different diet. The diet seems to be major factor determining the composition of gut microflora and clear separations are observed between populations with the major food intake being of plant origin as opposed to western (US or European) diet [49-52]. There is much diversity in the gut microbiome even between individuals from the same geographical area that are supposed to have a more similar diet, but interestingly the combined metabolic capabilities of the gut microbiome is found to be a lot more stable [53]. The

combined metabolic function of the whole gut microbiome rather than the type of bacteria seems to plays a detrimental role of a healthy gut. (Fig. 2)

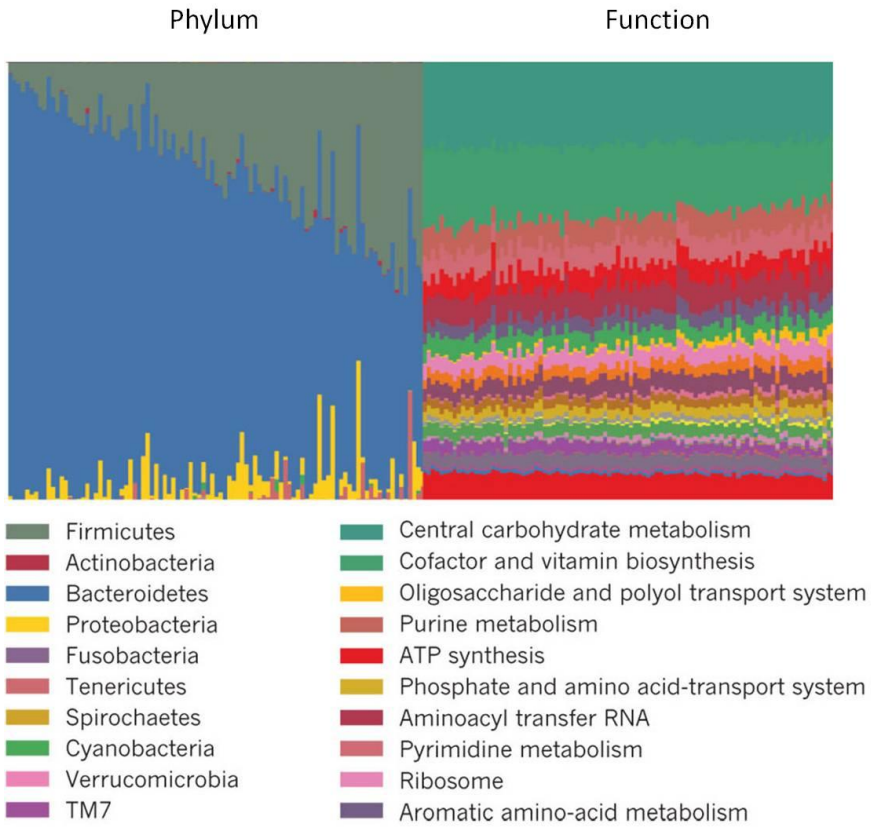

Fig. 2. Biodiversity of the gut microbiome and their genome content divided into functional groups from 242 healthy individuals (modified from [53]).

The organisms of the gut microflora are thought to have 3 types of interactions with the host; commensalism where one organisms benefits without affecting the other, mutualism where both organisms benefits and parasitism where one benefits and the other is harmed. Probiotic bacteria belong to the mutualists and can in some cases inhibit colonization by pathogens [54, 55]. A huge determinant of a well functioning gut microbiota in balance is the diversity and the exact composition. Imbalances have been observed with several gut diseases e.g. inflammatory bowel disease and irritable bowel disease [55, 56]. A huge effort has recently been established to characterize the GIT microbiome diversity and its gene contents through phylogenetic studies and sequencing of gut bacterial genomes [53]. This study involving stool

samples from 242 individuals, showed large differences in content of microbial taxa between individual but the little variance in the metabolic pathways present. This effort has added greatly to our understanding of the system, but is still in the early days of emergence. Some of the complicating factors are the differences between different species of the same genera and even at the strain level, crucial differences between choice of life style (commensal, mutualist or pathogen). In order to understand what a healthy balanced gut microbiome is, we need to investigate the differences between normal healthy gut microbiome and the composition found in different bowel diseases. It has been reported that individuals with inflammatory bowel disease and irritable bowel syndrome (IBS) have an over representation of bacteriodes in feces and in the intestinal mucosa combined with an under representation of bifidobaceria (Fig. 3) [56-58].

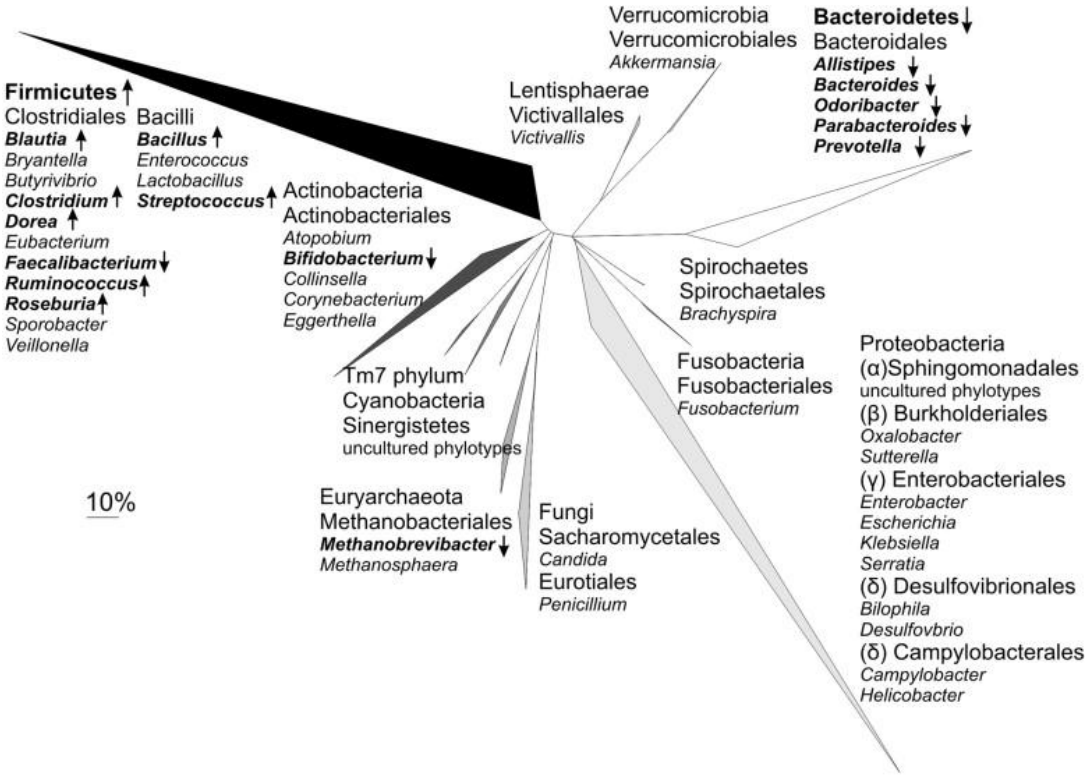

Fig. 3. Phylogenetic tree representing the diversity of the human gut microbiome. Taxa are presented in *bold* when found to be significantly different between IBS patients and healthy subjects. The direction of the changes are indicated by the *arrows* (*down arrow*, higher in healthy; *up arrow*, higher in IBS). The reference bar indicates 10% sequence divergence [59].

The main carbon source arriving in the colon are the so called recalcitrant insoluble carbohydrates deriving from insoluble plant fibers from plant cell wall structures and resistant or partly degraded storage polysaccharides like inulin and resistant starches. But also animal derived carbohydrates from *e.g.* cartilage will reach the colon. Of all the different species of bacteria in the gut only a few have the cellolytic activity associated with breakdown and growth on recalcitrant carbohydrates. In humans bacterial species capable of degrading recalcitrant carbohydrates have been identified within the genera bacteriodes, roseburia, ruminococcus, enterococcus and bifidobacteria [60]. Plant cell walls are composed of cellulose (polymer of glucose linked via α-1→4 glycosidic linkages) fibrils, held together by a matrix of hemicellulose (heteropolymers such as arabinoxylans) and pectin (polysaccharide rich in galacturonic acids). The degradation of cellulose is the first step in the breakdown of plant cell-wall derived structures, and this ability is primarily found in Gram-positive firmicutes of the genera ruminococcus and enterococcus and Gram-negative bacteriodes and they are often termed primary degraders [61]. The cellulytic glycoside hydrolases are located on the cell surface of the primary degraders either in large functional units called cellulosomes that co-localizes different glycoside hydrolase activities on a common protein scaffold (in Gram-positives) or as lipid anchored proteins on the surface of Gram-negatives like bacteriodes [60]. Cellulytic gut bacteria have acquired the ability to degrade matrix polysaccharides like xylans and pectins in order to make the cellulose fibrils available, but they do not necessarily use the solubilized matrix polysaccharides which therefore can be available for other gut bacteria, a phenomenon known as cross-feeding [61]. The secondary degraders, cross feeders or scavengers are basically the rest of the non pathogenic species found in the colon. The substrates that the secondary degraders cross-feed on are end or by-products from other species metabolic activity. First there is the cross-feeding on solubilized oligosaccharides (DP=2–10) and polysaccharides (DP > 10) of both branched and unbranched structure, then there is the cross feeding of anaerobic fermentation end-products; hydrogen, carbon dioxide, short chain fatty acids and lactate. Apart from being used as carbon source by colonic bacteria, the short chain fatty acids butyrate and acetate are also taken up by the host and used as energy source by the colonic epithelium (butyrate) and the heart and brain (acetate) [62].

The probiotic bacteria of the genera bifidobacteria and lactobacilli are saccharolytic and use oligosaccharides and monosaccharides as carbon source. They are also among the first colonizers of the infant gut and are found in especially high amounts in breast fed infants [63]. In the infant gut bifidobacteria and lactobacilli catabolize different carbohydrates, lactobacilli seem to prefer lactose and monosaccharide components while bifidobacteria are able to directly metabolize human milk oligosaccharides (HMO), suggesting that they cooperate synergistically to digest the human milk sugars [64-66]. In the mature gut the lactobacilli and bifidobacteria derive oligosaccharides from the activity of the primary degraders or from the partial breakdown of plant polysaccharides from other secondary degraders for instance xylooligosaccharides from the activity of roseburia and bacteroides on solubilized hemicelluloses [58]. The probiotic bifidobacteria and lactobacilli bacteria often have their own (often limited) set of secreted glycoside hydrolases in order to degrade polysaccharides into oligo or monosaccharides that can be transported to the inside of the cell for further utilization. Once inside the cell oligosaccharides are hydrolysed by glycoside hydrolases (GH) into monosaccharides that are ultimately metabolized via the glycolysis (Embden-Meyerhof pathway) for lactobacilli [67] or through the bifid shunt (Pentose phosphate pathway) for bifidobacteria, that also have a specialized pathway for HMO and mucin-derived carbohydrates [68].

1.3 LACTOBACILLUS AND BIFIDOBACTERIA

Lactobacilli are low G+C gram positive firmicutes, and microaerophilic. They have been isolated from various habitats including milk plant and animal sources. The lactobacilli residing in the gut are characterized by their ability to adapt to bile stress [69] and utilize a diverse range of carbohydrates [70, 71]. The lactobacilli are either homofermentative in which lactic acid is the primary product or heterofermentative in which lactic acid, CO_2, acetic acid, and/or ethanol are produced [67]. The lactobacilli isolated from gut include *L. acidophilus*, *L. gasseri*, *L. crispatus*, *L. johnsonii*, *L. salivarius*, *L. casei*, *L. rhamnosus*, *L. reuteri* [72].

Bifidobacteria are high G+C gram positive of the phylum actinobacteria. They are endosymbiotic inhabitants of the gastrointestinal tract. Bifidobacteria are known to colonize the GIT of infants during the first days to weeks of life, and *B. bifidum*, *B. infantis*, *B. breve*,

and *B. parvulorum* were isolated from infant feces [43]. The adult GIT hosts *B. animalis*, *B. adolescentis*, *B. bifidum* and *B. longum*. Bifidobacteria are heterofermentative resulting in production of acetate, lactate and formate when fermenting carbohydrates [54].

1.3.1 CARBOHYDRATE METABOLISM IN LACTOBACILLUS AND BIFIDOBACTERIA

The carbohydrates are metabolized via the glycolysis (Embden-Meyerhof pathway) for lactobacilli [67] and through the bifid shunt (pentose phosphate pathway) for bifidobacteria [73]. In homofermentative lactobacilli, fructose 1,6-bisphosphate is converted to two triose phosphate moieties which are funneled into the end product metabolite lactate (Fig. 4). Bifidobacteria are heterofermentative, fructose 6-phosphate is converted to acetyl phosphate and erythrose-4-phosphate by phosphoketolase (Fig. 4). The end product metabolites of carbohydrate metabolism in bifidobacteria are acetate lactate and formate at changing molar ratios depending on the carbohydrate metabolized [74, 75].

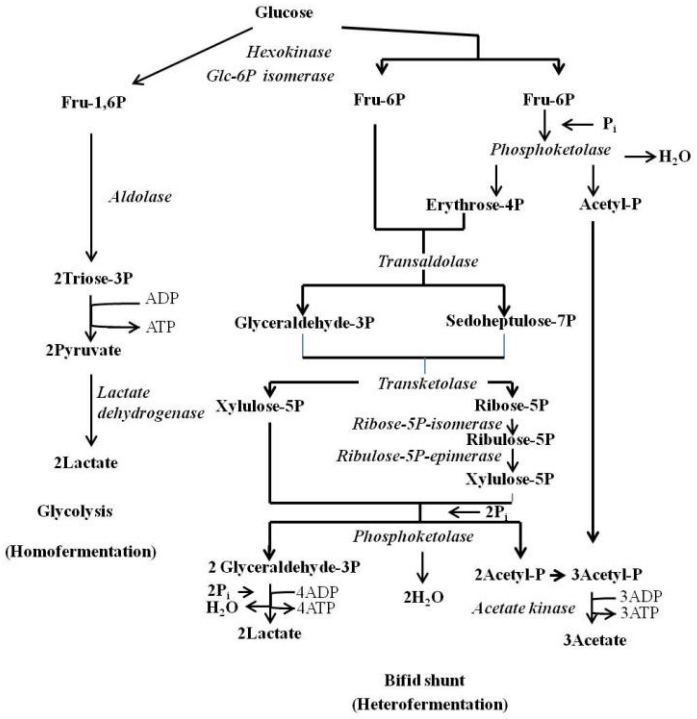

Fig. 4. Hexose metabolism in lactobacilli via the glycolysis (Embden-Meyerhof pathway) and through the bifid shunt (Pentose phosphate pathway) for bifidobacteria.

The carbon flux in the metabolism of low G+C Gram-positive lactic acid bacteria is tightly regulated by carbon catabolite repression (CCR) (Fig. 5) [76], thus in the presence of glucose, genes not needed for growth with glucose are repressed. The regulation of the repression is brought upon by transcriptional control and regulation at the protein level by phosphorylation [76]. CCR is a global gene regulation system that ensures only one set of sugar utilization genes are expressed at a given time. This achieved through three known mechanisms; inducer exclusion, inducer expulsion, and control of the activity of transcriptional regulators through phosphorylation [77, 78]. CCR has been extensively studied for low G+C Gram-positive bacteria utilizing sugars transported by a phosphoenolpyruvate dependent carbohydrate phosphotransferase system (PTS) [79]. The regulation of carbohydrate utilization for high G+C bifidobacteria is by an uncharacterized CCR under the control of LacI-type repressors [75]. CCR plays an important role in the survival of lactobacilli and bifidobacteria in the GIT, where they compete with gut microbiota for scant carbohydrate sources.

In lactobacilli and other low G+C Gram-positive bacteria, CCR involves negative regulation of genes encoding catabolic enzymes by the protein CcpA [80]. CcpA binds to DNA target sites called catabolite response elements (*cre*) and thereby inhibits transcription of the genes downstream from the *cre* site. The most important effector of CcpA is the phosphorylated form of HPr, the phosphocarrier protein of the PTS transporters. The phosphorylation state of HPr reflects the glycolytic activity of the cell. Hpr is phosphorylated at Ser-46 by the HPr-kinase that in turn is allosterically regulated by the levels of fructose-1,6-bisphosphate and P_i. The phosphorylated form of HPr can mediate inducer exclusion by interaction with non-PTS transporters which blocks their transport activity [81, 82]. Phosphorylated HPr also interacts with CcpA and thereby stimulates binding to *cre* sites (Fig. 5) [83].

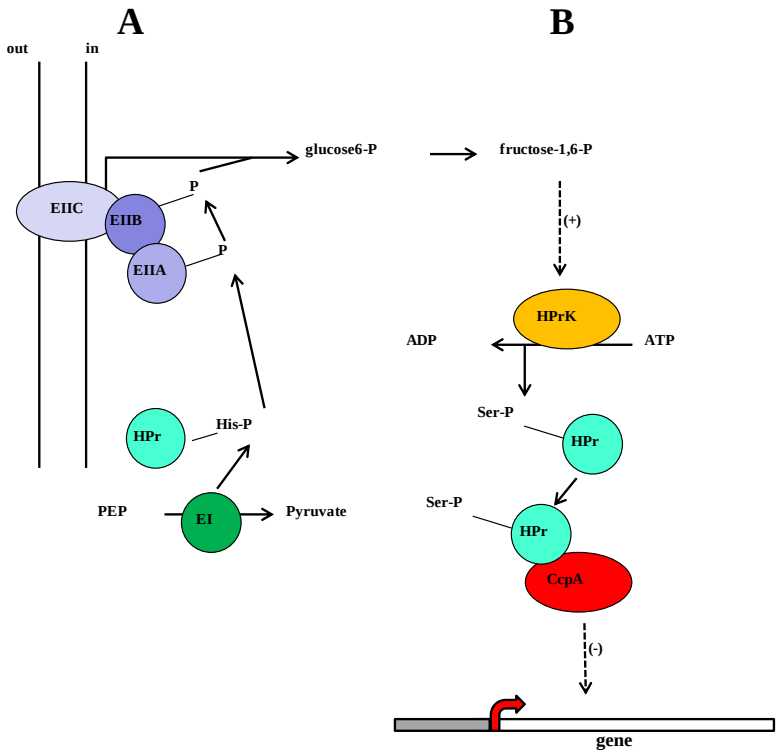

FIG. 5. Schematic representation of CcpA-dependent carbon catabolite repression in low G+C Gram-positive bacteria. **A**. Glucose is phosphorylated to glucose-6-phosphate during PTS mediated transport. Histidine-containing phosphocarrier protein (HPr) is phosphorylated by enzyme I (EI) at the histidine residue. The histidine phosphorylated phospho-carrier protein HPr transfers the phosphate group to glucose moiety via the EIIABC. **B.** Fructose-1,6-bisphosphate produced from glucose-6-phosphate activates HPr kinase (HPrK) that phosphorylates HPr at the regulatory-site serine. Binding of HPr-Ser-P to catabolite control protein A (CcpA) results in a complex that inhibits the transcription of target genes (negative regulation) (modified from [84]).

Preference for specific carbohydrates has been demonstrated in bifidobacteria. Little is known about the exact mechanisms of CCR in bifidobacteria, but the system is surely different from that found in lactobacilli. In *B. longum* NCC2705 glucose transporter *glcP* was shown to be under lactose repression [85]. Bifidobacteria do not have an obvious CcpA homologue and no *cre* sites have been predicted in the generea as well [85]. Secondly carbohydrate transport in bifidobacteria does not seem to be primarily facilitated by PTS-type transport systems but rather by ABC-transporters or MFS or GPH permeases where no substrate phosporylation

occurs during the translocation event, which rules out a PTS-HPr circuit for most carbohydrates. In one case it has been indicated that *B. lactis* exhibited glucose repression of a sucrose and raffinose active sucrose phosphorylase gene *scrP*. When expressed in *E. coli*. induction of the *scrP* gene was mediated through a GalR-LacI type transcriptional regulator in the presence of sucrose or raffinose [86] . The exact mechanism of the glucose repression in this system is not known and elucidation is hampered by the lack of genetic tools like cloning vector and transformation techniques for bifidobacteria [86].

1.3.2 CARBOHYDRATE TRANSPORT IN LACTOBACILLUS AND BIFIDOBACTERIA

In general transport mechanisms in prokaryotes are classified as simple transport, group translocation and ABC systems. In simple transport, the substrate is carried across the cell membrane without being chemically altered. The transport is driven by energy from the proton-motive force. There are three different types of simple transport events, performed by uniporters, antiporters and symporters. In group translocation the transported molecule is altered during the transport sequence *e.g*. by adding a charge to the transported compound. A classic example is the prokaryotic sugar phospho-enol-pyruvate phosphostransferase system (PTS-transporters), where a high-energy phosphate group from phosphoenolpyruvate is transferred to the sugar. Energy for the transport process comes from the stepwise transfer of the phosporyl group from phosphoenolpyruvate to the sugar. ATP-binding cassette (ABC) transporters use the energy derived from ATP hydrolysis to drive the translocation event but do not chemically alter the transported substrate.

There are four main classes of carbohydrate transporters identified within bacteria [87] major facilitator superfamily (MFS) permeases; and glycoside-pentoside-hexuronide permeases (GPH) that form a sub-group of MFS permeases, PTS-transporters and ABC-transporters. Classification and annotation of transporters have mainly been accomplished by sequence homology based classification [88-90]. The probiotic *Lactobacillus acidophilus* NCFM (NCFM) and *Bifidobacterium animalis* subsp *lactis* Bl-04 (Bl-04), which have been used for the present study, are known to possess transporters for utilizing several different carbohydrates [91, 92]. NCFM genome has of 17 PTS, two MFS/GPH permeases and three

ABC transporters predicted to be carbohydrate transporters (family 1 solute binding proteins, SBP_bac_1 (Pfam PF01547)). In Bl-04 carbohydrate transport is carried out by MFS/GPH permeases, and ABC-transporters [93] and the genome of Bl-04 has five MFS/GPH permeases and five ABC-transporters predicted to be involved in carbohydrate uptake [93]. A section of the thesis focuses on the solute binding domain of the ABC-transporters and has been described below.

1.3.2.1 ABC TRANSPORTERS

ABC-transporters are part of one of the largest protein-families epresentatives in all phyla from prokaryotes to mammals [94]. They facilitate uptake of vitamins, carbohydrates, oligo-peptides, amino acids, ions and a wide variety of other compounds [95]. The broad range of transported compounds is reflected by diversity in the oligomerization of the domains that constitute the transportes [96]. The classic architecture consists of two nucleotide binding (NBDs) and two transmembrane domains (TMDs) (Fig. 6). This configuration facilitates ATP-driven transport of a large variety of substrates in all known phyla. Among these; import and export systems are differentiated. Import systems are so far only found in prokaryotes and archaea and require an additional solute binding protein (SBP), which binds the substrate in the periplasmic space or extracellularly on the cell surface and delivers it to the transmembrane permease part of the transporter. SBPs have been classified using different approaches, sequence alignment [88], structural connectivity of the secondary elements [97] and most recently by structural alignment of 107 3D models from the PDB database (http://www.pdb.org/pdb/home/home.do) [98]. The reason for the different classification studies is that SBPs have relatively low sequence similarity, but share an overall similar tertiary structure [99] . Another interesting observation from these studies is that contrary to what might be expected, the different groupings did not correlate with ligand specificity of the SBPs. Crystal structures of SBP have shown two possible conformations; open without substrate and closed with substrate bound. In theory though four different states may exist; open-unliganded, closed-unliganded, open-liganded and closed-liganded. SBPs consist of two globular lobes of different size, creating a cleft between them where the

substrate binding-site is located. In the closed-liganded complex the two domains have rotated towards each other along a hinge region and closed around the substrate. This mechanism is named the Venus Fly-trap model and describes the SBP conformation change upon ligand binding and the burying of the substrate in the closed confirmation [100]. Bacterial carbohydrate ABC-importers are typically arranged as pentamers composed of an extracellular cell wall/cell membrane lipid anchored solute SBP in Gram-positive bacteria whereas Gram-negative bacteria secrete the SBP into the periplasmic space. Two membrane-spanning domains forms the heterodimeric permease that recruits the closed-liganded SBP. The channel is formed between the two transmembrane domains as their transmembrane helices align on each side along a hypothetical axis perpendicular to the membrane. Two nucleotide (ATP) binding proteins dock with each its transmembrane domain on the cytoplasmic side of the membrane [96]. The mechanism of carbohydrate uptake by ABC transporters has been studied based on structural work [101, 102]. The transport sequence of events starts with the SBP, which upon substrate binding undergoes a conformational change capturing the substrate which allows docking onto the membrane embeded permease for release of the substrate into a transmembrane funnellike channel. ATP loading in the NBDs is thought to cause a perturbation of the SBP conformation destroying the highaffinity binding site and releasing the substrate into the funnel of the outward open conformation of the permease. Translocation is facilitated by an altering access mechanism where conformational change in the permease subunits driven by hydrolysis of ATP by the nucleotide binding proteins, changes the funnel shaped channel from outward open to inward open allowing the substrate to diffuse into the cytoplasm (Fig. 6).

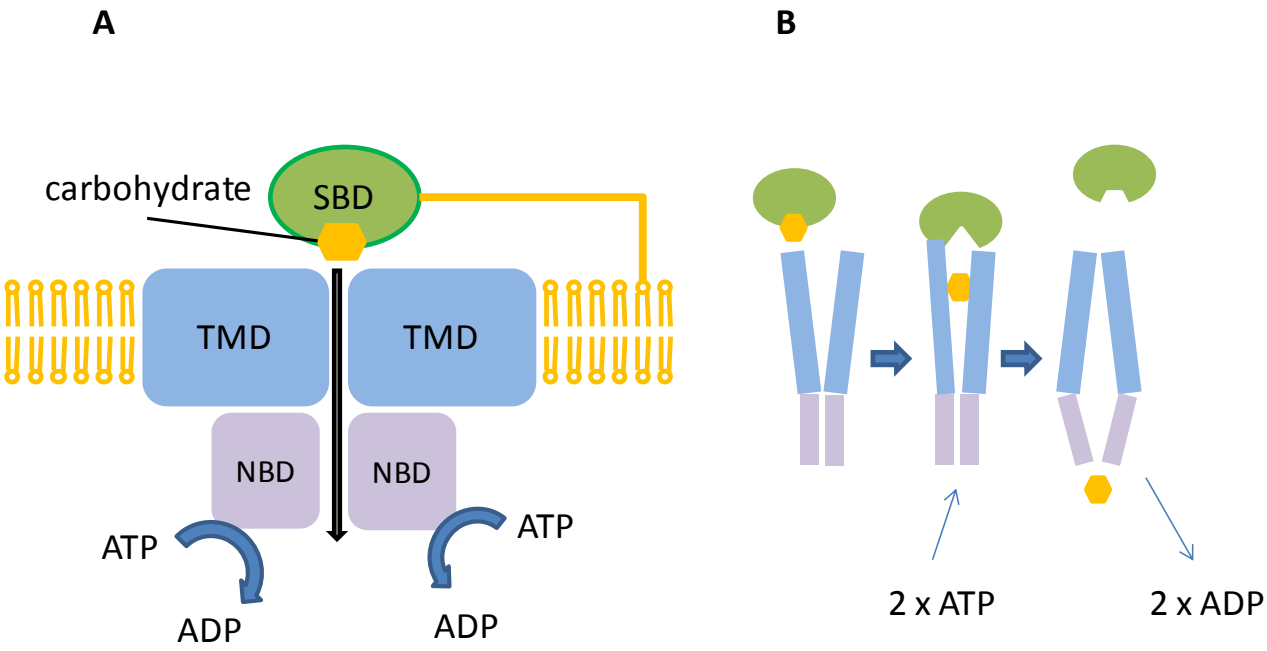

FIG. 6. Schematic representation of carbohydrate ABC-importers in Gram-positive bacteria. **A**. The architecture of ABC-type importers in Gram-positive bacteria. **B.** The proposed alternating access mechanism of transport for ABC-importers.

1.3.3. THE PROBIOTIC LACTOBACILLUS ACIDOPHILUS NCFM

Lactobacillus acidophilus NCFM was isolated and from a human source [103] and is a probiotic with benefits to human health [104]. The probiotic characteristics of NCFM include, i) its ability to survive the GIT, ii) modulate host immune response, ii) maintain GIT microflora balance and iv) alleviation of lactose intolerance [104]. A lot of effort has been put into understanding the basis of NCFM probiotic effects on human health. The 2.0 Mb genome of NCFM encodes for 1864 proteins, including 39 glycoside hydrolases for carbohydrate utilization [105]. The carbohydrate utilization [70, 91, 106] , acid stress [107], and bile stress [108, 109] of NCFM have been studied by transcriptomics.

Prebiotic carbohydrates in combination with NCFM have shown to beneficially effect human health. Daily consumption of the combination of NCFM and lactitol by elderly volunteers has shown to increase stool frequency, fecal levels of NCFM and genus *Bifidobacterium*, and modulated fecal immune biomarkers, reflecting stimulation of intestinal mucosal functions

[110, 111]. Complementary beneficial effects with this synbiotic were also observed in a semi-continuous colon fermentation model [112].

Previous studies on NCFM have been focused on gene inactivation studies and transcriptomics. Proteomics is an *omics* tool to investigate NCFM and its response to prebiotic carbohydrates at the protein level. During the past years a number of proteome 2-DE profiles were described for lactic acid bacteria mostly related to changes associated with growth [113-115], growth medium [116], and adaptations to the gut [117, 118]. However, only very few proteome reference maps were reported [113, 119, 120]. For example using narrow range pH windows of 4–7 and 4.5–5.5 a reference map of *Lactococcus lactis* IL14103 contained 230 proteins, corresponding to 25% coverage of the predicted acidic proteome [120]. Proteome analysis of cytosolic proteins of *L. plantarum* WCFS1 at pH range 3−10 covered 3.3% of all genes [113]. Studies however are lacking with regards to NCFM proteome and the proteome adaptation to different carbohydrates abundant in the gut.

1.3.4 The Probiotic Bifidobacterium animalis subsp. lactis Bl-04

Bifidobacterium animalis subsp. *lactis* Bl-04 (also known as DGCC2908 and RB 4825) was originally isolated from a fecal sample from a healthy adult and is a widely used commercial probiotic bacteria. Bl-04 has a 1.9 Mb genome with a ~60% GC content, encoding 1655 predicted ORFs of which 1072 has been annotated with a function [93]. The Bl-04genome contains 38 glycoside hydrolases (GH) divided into 16 GH families (http://www.cazy.org/b982.html). However this is somewhat fewer than what has been observed in strains of *B. longum* and *B. adolescentis*, (~50-70 GHs in 20–25 families) which also have larger genomes (2.0-2.5 Mb) [121]. The relatively small size of the *B. animalis* subsp. *lactis* Bl-04 genome compared to those of other bifidobacteria could indicate a genome simplification process that reduces biosynthetic capabilities and favors the retention and acquisition of genes involved in the utilization of nutrient sources in a specific nutritionally rich ecological niche [122, 123]. This could also explain the smaller number of GHs in Bl-04 than in *B. longum* and *B. adolescentis*. Notably, the genes involved in the catabolism of human

milk oligosaccharides in *B. longum* subsp. *infantis* and in the degradation and utilization of mucin (endo-α-N-acetylgalactosaminidase) are not present in Bl-04 [93].

Probiotic treatment with *Bifidobacteria animalis* subsp. *lactis* has been reported to reduce symptoms associated with irritable bowel syndrome [124, 125], activate immune system by increase the proportions of total, helper ($CD4^+$) and activated ($CD25^+$) T lymphocytes and natural killer cells [126, 127] and inhibit infection rates of the pathogen *E.coli* O157:H7 [128]. Recent studies with colon simulator models have shown that potential prebiotic carbohydrates (xylobiose, melibiose, raffinose and maltotriose) increased the numbers of Bl-04 in the colon simulator. As a result the concentrations of acetate and butyric acid increased and the ratio of bacteriodes/firmicutes decreased, suggesting direct link between the activity of bifidobacteria to the composition of the gut microbiota [129].

1.4 EXPERIMENTAL WORK INCLUDED IN THE PRESENT THESIS

In this thesis, I have used two fundamentally different approaches to study the uptake and utilization of potential prebiotic carbohydrates by the probiotic bacteria *Lactobacillus acidophilus* NCFM and *Bifidobacterium animalis* subsp. *lactis* Bl-04. First, 2-DE based proteomics approach was used to establish the reference proteomes of *Lactobacillus acidophilus* NCFM and *Bifidobacterium animalis* subsp. *lactis* Bl-04. Next 2DE-DIGE was used to study the changes in proteome profiles during growth on different prebiotic carbohydrate carbon sources. Secondly, the biochemical protein characterization was carried out for an ABC-transporter associated solute binding protein (SBP) from *Bifidobacterium animalis* subsp. *lactis* Bl-04, to evaluate the binding and recognition of different xyloligosaccharides. The work carried out has been described in the following chapters.

1.4.1 CHAPTER 2

— describes the reference proteome (pH 4−7) of *Lactobacillus acidophilus* NCFM established using 2-DE. A total of 275 unique proteins assigned to various physiological processes were

identified from 650 spots. Differential 2-DE (DIGE) (pH 4−7) with the prebiotic lactitol, revealed proteome changes of NCFM with lactitol.

1.4.2 CHAPTER 3

— describes the reference proteome (pH 6−11) of *Lactobacillus acidophilus* NCFM established using 2-DE. A total of 102 unique proteins assigned to various physiological processes were identified from 202 spots.

1.4.3 CHAPTER 4

— describes the differential proteome (pH 4−7) of *Lactobacillus acidophilus* NCFM with the potential prebiotic raffinose using 2D-DIGE. Various proteins involved in the metabolism of raffinose including α-galactosidase, sucrose phophorylase, maltose phosphorylase and β-galactosidase were identified.

1.4.4 CHAPTER 5

— describes the reference proteome (pH 3−7 and 3−10) of *Bifidobacterium animalis* subsp. *lactis* Bl-04 established using 2-DE. A total of 328 unique proteins assigned to various physiological processes were identified from 960 spots. Differential 2-DE (DIGE) (pH 4−7) with various prebiotics including, galactooligosaccharides, melibiose, raffinose family oligosaccharides and isomaltooligosaccharides, revealed various proteins involved in prebiotic metabolism.

1.4.5 CHAPTER 6

— describes the characterization of the SBP of the ABC transport system from the XOS operon of *Bifidobacterium animalis* subsp. *lactis* Bl-04 (*Bl*XBP). *Bl*XBP was produced and purified, its ligand preference and affinity determined and optimal affinity (K_d ~100 nM) for xylotetraose was found. The crystal structure of *Bl*XBP in complex with xylotriose, xylotetraose and xylohexaose was determined, thus providing a structural rationale to the binding data and highlighting structural elements responsible for XOS recognition and capture.

REFERENCES

1. Martirosyan DM: *Functional Foods and Chronic Diseases. Science and Practice*: Food Science Publisher, Dallas, USA; 2011.
2. Roberfroid MB: **A European consensus of scientific concepts of functional foods**. *Nutrition* 2000, **16**:689-691.
3. Hasler CM, Brown AC: **Position of the American dietetic association: Functional Foods**. *J Am Diet Assoc* 2009, **109**:735-746.
4. Metchnikoff E: *The prolongation of life - Optimistic Studies*: William Heinemann, London, UK; 1907.
5. Lilly DM, Stillwell RH: **Probiotics: Growth-promoting factors produced by microorganisms**. *Science* 1965, **147**:747-748.
6. Roberfroid M, Gibson GR, Hoyles L, McCartney AL, Rastall R, Rowland I, Wolvers D, Watzl B, Szajewska H, Stahl B *et al*: **Prebiotic effects: metabolic and health benefits**. *Br J Nutr* 2010, **104**:S1-63.
7. Foligne B, Nutten S, Grangette C, Dennin V, Goudercourt D, Poiret S, Dewulf J, Brassart D, Mercenier A, Pot B: **Correlation between *in vitro* and *in vivo* immunomodulatory properties of lactic acid bacteria**. *World J Gastroenterol* 2007, **13**:236-243.
8. Salminen S, Gueimonde M: **Human studies on probiotics: What is scientifically proven**. *J Food Sci* 2004, **69**:M137-M140.
9. Moller C, De Vrese M: **Probiotic effects of selected acid bacteria**. *Milchwiss* 2004, **59**:597-601.
10. Flint HJ: **Obesity and the gut microbiota**. *J Clin Gastroenterol* 2011, **45**:S128-S132 110.1097/MCG.1090b1013e31821f31844c31824.
11. Gibson GR, Roberfroid MB: **Dietary Modulation of the human colonic microbiota - introducing the concept of prebiotics**. *J Nutr* 1995, **125**:1401-1412.
12. McFarland LV, Bernasconi P: *Saccharomyces boulardii*- A review of an innovative biotherapeutic agent. *Microb Ecol Health Dis* 1993, **6**:157-171.
13. Wang JQ, Yin FG, Zhu C, Yu H, Niven SJ, de Lange CFM, Gong J: **Evaluation of probiotic bacteria for their effects on the growth performance and intestinal**

microbiota of newly-weaned pigs fed fermented high-moisture maize. *Livest Sci*, **145**:79-86.

14. Roberfroid M: **Prebiotics: The concept revisited**. *J Nutr* 2007, **137**:830S-837S.
15. Cummings JH, Antoine J-M, Azpiroz F, Bourdet-Sicard R, Brandtzaeg P, Calder PC, Gibson GR, Guarner F, Isolauri E, Pannemans D *et al*: **PASSCLAIM-gut health and immunity**. *Eur J Nutr* 2004, **43**: Suppl 2:II118–II173.
16. Gibson GR, Probert HM, Van Loo J, Rastall RA, Roberfroid MB: **Dietary modulation of the human colonic microbiota: updating the concept of prebiotics**. *Nutr Res Rev* 2004, **17**:259-275.
17. Macfarlane S, Macfarlane GT, Cummings JH: **Prebiotics in the gastrointestinal tract**. *Aliment Pharmacol Ther* 2006, **24**:701-714.
18. Kelly G: **Inulin-type prebiotics - A review: Part 1**. *Altern Med Rev* 2008, **13**:315-329.
19. Dinoto A, Suksomcheep A, Ishizuka S, Kimura H, Hanada S, Kamagata Y, Asano K, Tomita F, Yokota A: **Modulation of rat cecal microbiota by administration of raffinose and encapsulated *Bifidobacterium breve***. *Appl Environ Microbiol* 2006, **72**:784-792.
20. Bakker-Zierikzee AM, Alles MS, Knol J, Kok FJ, Tolboom JJ, Bindels JG: **Effects of infant formula containing a mixture of galacto- and fructo-oligosaccharides or viable *Bifidobacterium animalis* on the intestinal microflora during the first 4 months of life**. *Br J Nutr* 2005, **94**:783-790.
21. Shadid R, Haarman M, Knol J, Theis W, Beermann C, Rjosk-Dendorfer D, Schendel DJ, Koletzko BV, Krauss-Etschmann S: **Effects of galactooligosaccharide and long-chain fructooligosaccharide supplementation during pregnancy on maternal and neonatal microbiota and immunity-a randomized, double-blind, placebo-controlled study**. *Am J Clin Nutr* 2007, **86**:1426-1437.
22. Rycroft CE, Jones MR, Gibson GR, Rastall RA: **A comparative in vitro evaluation of the fermentation properties of prebiotic oligosaccharides**. *J Appl Microbiol* 2001, **91**:878-887.
23. Roberfroid MB, Delzenne NM: **Dietary fructans**. *Ann Rev Nutr* 1998, **18**:117-143.

24. Vanloo J, Coussement P, Deleenheer L, Hoebregs H, Smits G: **On the presence of inulin and oligofructose as natural ingredients in the western diet**. *Crit Rev Food Sci Nutr* 1995, **35**:525-552.
25. Gänzle MG: **Enzymatic synthesis of galacto-oligosaccharides and other lactose derivatives (hetero-oligosaccharides) from lactose**. *Int Dairy J* 2011, **22**:116-122.
26. Vanvelthuijsen JA: **Food-additives derived from lactose-lactitol and lactitol plamitate**. *J Agric Food Chem* 1979, **27**:680-686.
27. Martinez-Villaluenga C, Frias J, Vidal-Valverde CN: **Raffinose family oligosaccharides and sucrose contents in 13 Spanish lupin cultivars**. *Food Chem* 2005, **91**:645-649.
28. Lee H-S, Auh J-H, Yoon H-G, Kim M-J, Park J-H, Hong S-S, Kang M-H, Kim T-J, Moon T-W, Kim J-W *et al*: **Cooperative action of alpha-glucanotransferase and maltogenic amylase for an improved Process of isomaltooligosaccharide (IMO) Production**. *J Agric Food Chem* 2002, **50**:2812-2817.
29. Killey M, Dimler RJ, Cluskey JE: **Preparation of panose by the action of NRRL B-512 dextransucrase on a sucrose-maltose Mixture[2]**. *J Am Chem Soc* 1955, **77**:3315-3318.
30. Kim T-Y, Lee D-S, Shin H-J: **Gentiobiose synthesis from glucose using recombinant β-glucosidase from *Thermus caldophilus* GK24**. *Biotechnol Bioproc Eng* 2003, **8**:210-212.
31. Crittenden RG, Playne MJ: **Production, properties and applications of food-grade oligosaccharides**. *Trends Food Sci Technol* 1996, **7**:353-361.
32. Mohnen D: **Pectin structure and biosynthesis**. *Curr Opin Plant Biol* 2008, **11**:266-277.
33. Jahn M, Stoll D, Warren RAJ, Szabo L, Singh P, Gilbert HJ, Ducros VMA, Davies GJ, Withers SG: **Expansion of the glycosynthase repertoire to produce defined manno-oligosaccharides**. *Chem Commun* 2003, **12**:1327-1329.
34. Eckburg PB, Bik EM, Bernstein CN, Purdom E, Dethlefsen L, Sargent M, Gill SR, Nelson KE, Relman DA: **Diversity of the human intestinal microbial flora**. *Science* 2005, **308**:1635-1638.
35. Walter J, Ley R: **The human gut microbiome: Ecology and recent evolutionary changes**. *Ann Rev Microbiol,* 2011, **65**: 411-429.

36. Stephen AM, Cummings JH: **The microbial contribution to human faecal mass**. *J Med Microbiol* 1980, **13**:45-56.
37. Gill SR, Pop M, DeBoy RT, Eckburg PB, Turnbaugh PJ, Samuel BS, Gordon JI, Relman DA, Fraser-Liggett CM, Nelson KE: **Metagenomic analysis of the human distal gut microbiome**. *Science* 2006, **312**:1355-1359.
38. Grice EA, Segre JA: **The human microbiome: Our second genome**. *Annu Rev Genomics Hum Genet* 2012, **13**:151-170.
39. Scholz-Ahrens KE, Ade P, Marten B, Weber P, Timm W, Acil Y, Gluer CC, Schrezenmeir J: **Prebiotics, probiotics, and synbiotics affect mineral absorption, bone mineral content, and bone structure**. *J Nutr* 2007, **137**:838S-846S.
40. Wallace TC, Guarner F, Madsen K, Cabana MD, Gibson G, Hentges E, Sanders ME: **Human gut microbiota and its relationship to health and disease**. *Nutr Rev* 2011, **69**:392-403.
41. Patterson JK, Yasuda K, Welch RM, Miller DD, Lei XG: **Supplemental dietary inulin of variable chain lengths alters intestinal bacterial populations in young pigs**. *J Nutr* 2010, **140**:2158-2161.
42. Gibson GR: **Dietary modulation of the human gut microflora using the prebiotics oligofructose and inulin**. *J Nutr* 1999, **129**:1438S-1441S.
43. Kleerebezem M, Vaughan EE: **Probiotic and gut lactobacilli and bifidobacteria: Molecular approaches to study diversity and activity**. *Ann Rev Microbiol* 2009, **63**: 269-290.
44. Xu J, Mahowald MA, Ley RE, Lozupone CA, Hamady M, Martens EC, Henrissat B, Coutinho PM, Minx P, Latreille P *et al*: **Evolution of symbiotic bacteria in the distal human intestine**. *PLoS Biol* 2007, **5**:1574-1586.
45. Samonis G, Gikas A, Toloudis P, Maraki S, Vrentzos G, Tselentis Y, Tsaparas N, Bodey G: **Prospective study of the impact of broad-spectrum antibiotics on the yeast flora of the human gut**. *Eur J Clin Microbiol Infect Dis* 1994, **13**:665-667.
46. Fallani M, Young D, Scott J, Norin E, Amarri S, Adam R, Aguilera M, Khanna S, Gil A, Edwards CA *et al*: **Intestinal microbiota of 6-week-old infants across Europe:**

Geographic influence beyond delivery mode, breast-feeding, and antibiotics. *J Pediatr Gastroenterol Nutr* 2010, **51**:77-84.

47. Fanaro S, Chierici R, Guerrini P, Vigi V: **Intestinal microflora in early infancy: composition and development**. *Acta Paediatrica* 2003, **92**:48-55.
48. Penders J, Stobberingh EE, Thijs C, Adams H, Vink C, van Ree R, van den Brandt PA: **Molecular fingerprinting of the intestinal microbiota of infants in whom atopic eczema was or was not developing**. *Clin Exp Allergy* 2006, **36**:1602-1608.
49. De Filippo C, Cavalieri D, Di Paola M, Ramazzotti M, Poullet JB, Massart S, Collini S, Pieraccini G, Lionetti P: **Impact of diet in shaping gut microbiota revealed by a comparative study in children from Europe and rural Africa**. *Proc Natl Acad Sci USA* 2010, **107**:14691-14696.
50. Ley RE, Peterson DA, Gordon JI: **Ecological and evolutionary forces shaping microbial diversity in the human intestine**. *Cell* 2006, **124**:837-848.
51. Yatsunenko T, Rey FE, Manary MJ, Trehan I, Dominguez-Bello MG, Contreras M, Magris M, Hidalgo G, Baldassano RN, Anokhin AP *et al*: **Human gut microbiome viewed across age and geography**. *Nature* 2012, **486**:222-227.
52. Wu GD, Chen J, Hoffmann C, Bittinger K, Chen YY, Keilbaugh SA, Bewtra M, Knights D, Walters WA, Knight R *et al*: **Linking long-term dietary patterns with gut microbial enterotypes**. *Science* 2011, **333**:105-108.
53. Huttenhower C: **Structure, function and diversity of the healthy human microbiome**. *Nature* 2012, **486**:207-214.
54. Fukuda S, Toh H, Hase K, Oshima K, Nakanishi Y, Yoshimura K, Tobe T, Clarke JM, Topping DL, Suzuki T *et al*: **Bifidobacteria can protect from enteropathogenic infection through production of acetate**. *Nature* 2011, **469**:543-547.
55. Parkes GC, Sanderson JD, Whelan K: **Treating irritable bowel syndrome with probiotics: the evidence**. *Proc Nutr Soc* 2010, **69**:187-194.
56. Parkes GC, Rayment NB, Hudspith BN, Petrovska L, Lomer MC, Brostoff J, Whelan K, Sanderson JD: **Distinct microbial populations exist in the mucosa-associated microbiota of sub-groups of irritable bowel syndrome**. *Neurogastroenterol Motil* 2012, **24**:31-39.

57. Hedin C, Whelani K, Lindsay JO: **Evidence for the use of probiotics and prebiotics in inflammatory bowel disease: A review of clinical trials**. *Proc Nutr Soc* 2007, **66**:307-315.
58. Chassard C, Goumy V, Leclerc M, Del'homme C, Bernalier-Donadille A: **Characterization of the xylan-degrading microbial community from human faeces**. *FEMS Microbiol Ecol* 2007, **61**:121-131.
59. Rajilic-Stojanovic M, Biagi E, Heilig H, Kajander K, Kekkonen RA, Tims S, de Vos WM: **Global and deep molecular analysis of microbiota signatures in fecal samples from patients with irritable bowel syndrome**. *Gastroenterology* 2011, **141**:1792-1801.
60. Flint HJ, Bayer EA, Rincon MT, Lamed R, White BA: **Polysaccharide utilization by gut bacteria: potential for new insights from genomic analysis**. *Nat Rev Microbiol* 2008, **6**:121-131.
61. Flint HJ, Duncan SH, Scott KP, Louis P: **Interactions and competition within the microbial community of the human colon: links between diet and health**. *Environ Microbiol* 2007, **9**:1101-1111.
62. Roberfroid MB: **Introducing inulin-type fructans**. *Br J Nutr* 2005, **93**:S13-S25.
63. Palmer C, Bik EM, DiGiulio DB, Relman DA, Brown PO: **Development of the human infant intestinal microbiota**. *PLoS Biol* 2007, **5**:1556-1573.
64. Martinez RCR, Aynaou AE, Albrecht S, Schols HA, De Martinis ECP, Zoetendal EG, Venema K, Saad SMI, Smidt H: **In vitro evaluation of gastrointestinal survival of *Lactobacillus amylovorus* DSM 16698 alone and combined with galactooligosaccharides, milk and/or *Bifidobacterium animalis* subsp. *lactis* Bb-12**. *Int J Food Microbiol* 2011, **149**:152-158.
65. Rodriguez-Diaz J, Monedero V, Yebra MJ: **Utilization of natural fucosylated oligosaccharides by three novel alpha-L-fucosidases from a probiotic *Lactobacillus casei* strain**. *Appl Environ Microbiol* 2011, **77**:703-705.
66. Schwab C, Ganzle M: **Lactic acid bacteria fermentation of human milk oligosaccharide components, human milk oligosaccharides and galactooligosaccharides**. *FEMS Microbiol Lett* 2011, **315**:141-148.

67. Kandler O: Carbohydrate metabolism in lactic acid bacteria. *Antonie Van Leeuwenhoek* 1983, **49**:209-224.
68. Fushinobu S: **Unique sugar metabolic pathways of bifidobacteria**. *Biosci Biotechnol Biochem* 2011, **75**:188-188.
69. Koskenniemi K, Laakso K, Koponen J, Kankainen M, Greco D, Auvinen P, Savijoki K, Nyman TA, Surakka A, Salusjarvi T *et al*: **Proteomics and transcriptomics characterization of bile stress response in probiotic *Lactobacillus rhamnosus* GG**. Mol Cell Proteomics 2011, **10**: M110.002741.
70. Barrangou R, Azcarate-Peril MA, Duong T, Conners SB, Kelly RM, Klaenhammer TR: **Global analysis of carbohydrate utilization by *Lactobacillus acidophilus* using cDNA microarrays**. *Proc Natl Acad Sci USA* 2006, **103**:3816-3821.
71. Francl AL, Thongaram T, Miller MJ: **The PTS transporters of *Lactobacillus gasseri* ATCC 33323**. *BMC Microbiol* 2010, **10**:77.
72. Holzapfel WH, Haberer P, Snel J, Schillinger U, Huis in't Veld JHJ: **Overview of gut flora and probiotics**. *Int J Food Microbiol* 1998, **41**:85-101.
73. Schell MA, Karmirantzou M, Snel B, Vilanova D, Berger B, Pessi G, Zwahlen MC, Desiere F, Bork P, Delley M *et al*: **The genome sequence of *Bifidobacterium longum* reflects its adaptation to the human gastrointestinal tract**. *Proc Natl Acad Sci USA* 2002, **99**:14422-14427.
74. Palframan RJ, Gibson GR, Rastall RA: **Carbohydrate preferences of bifidobacterium species isolated from the human gut**. *Curr Issues Intest Microbiol* 2003, **4**:71-75.
75. Pokusaeva K, Fitzgerald GF, van Sinderen D: **Carbohydrate metabolism in bifidobacteria**. *Genes and Nutr* 2011, **6**:285-306.
76. Tsai YK, Lin TH: **Sequence, organization, transcription and regulation of lactose and galactose operons in *Lactobacillus rhamnosus* TCELL-1**. *J Appl Microbiol* 2006, **100**:446-459.
77. Saier MH: **Regulatory interactions controlling carbon metabolism: An overview**. *Res Microbiol* 1996, **147**:439-447.
78. Bachem S, Stulke Jr: **Regulation of the *Bacillus subtilis* GlcT antiterminator protein by components of the phosphotransferase system**. *J Bacteriol* 1998, **180**:5319-5326.

79. Deutscher J, Francke C, Postma PW: **How phosphotransferase system-related protein phosphorylation regulates carbohydrate metabolism in bacteria**. *Microbiol Mol Biol Rev* 2006, **70**:939-1031.
80. Mahr K, Hillen W, Titgemeyer F: **Carbon catabolite repression in *Lactobacillus pentosus*: Analysis of the ccpA region**. *Appl and Environ Microbiol* 2000, **66**:277-283.
81. Saier MH, Crasnier M: **Inducer exclusion and the regulation of sugar transport**. *Res Microbiol* 1996, **147**:482-489.
82. Ye JJ, Saier MH: **Regulation of sugar uptake via the phosphoenolpyruvate-dependent phosphotransferase systems in *Bacillus subtilis* and *Lactococcus lactis* is mediated by ATP-dependent phosphorylation of seryl residue 46 in HPr**. *J Bacteriol* 1996, **178**:3557-3563.
83. Fujita Y, Miwa Y, Galinier A, Deutscher J: **Specific recognition of the *Bacillus subtilis* gnt cis-acting catabolite responsive element by a protein complex formed between CcpA and seryl-phosphorylated Hpr**. *Mol Microbiol* 1995, **17**:953-960.
84. Warner JB, Lolkema JS: **CcpA-dependent carbon catabolite repression in bacteria**. *Microbiol Mol Biol Rev* 2003, **67**:475-490.
85. Parche S, Beleut M, Rezzonico E, Jacobs D, Arigoni F, Titgemeyer F, Jankovic I: **Lactose-over-glucose preference in *Bifidobacterium longum* NCC2705: glcP, encoding a glucose transporter, is subject to lactose repression**. *J Bacteriol* 2006, **188**:1260-1265.
86. Trindade MI, Abratt VR, Reid SJ: **Induction of sucrose utilization genes from *Bifidobacterium lactis* by sucrose and raffinose**. *Appl Environ Microbiol* 2003, **69**:24-32.
87. Lorca GL, Barabote RD, Zlotopolski V, Tran C, Winnen B, Hvorup RN, Stonestrom AJ, Nguyen E, Huang LW, Kim DS *et al*: **Transport capabilities of eleven Gram-positive bacteria: Comparative genomic analyses**. *Biochim Biophys Acta-Biomembranes* 2007, **1768**:1342-1366.
88. Tam R, Saier MH, Jr.: **Structural, functional, and evolutionary relationships among extracellular solute-binding receptors of bacteria**. *Microbiol Rev* 1993, **57**:320-346.

89. Saier MH, Ren QH: **The bioinformatic study of transmembrane molecular transport**. *J Mol Microbiol Biotechnol* 2006, **11**:289-290.
90. Saier MH, Yen MR, Noto K, Tamang DG, Elkan C: **The transporter classification database: recent advances**. *Nucleic Acids Res* 2009, **37**:D274-D278.
91. Andersen JM, Barrangou R, Abou Hachem M, Lahtinen SJ, Goh YJ, Svensson B, Klaenhammer TR: **Transcriptional analysis of prebiotic uptake and catabolism by Lactobacillus acidophilus NCFM**. *PLoS One* 2012, **7**:e44409.
92. Parche S, Amon J, Jankovic I, Rezzonico E, Beleut M, Barutcu H, Schendel I, Eddy MP, Burkovski A, Arigoni F *et al*: **Sugar transport systems of *Bifidobacterium longum* NCC2705**. *J Mol Microbiol Biotechnol* 2007, **12**:9-19.
93. Barrangou R, Briczinski EP, Traeger LL, Loquasto JR, Richards M, Horvath P, Coute-Monvoisin A-C, Leyer G, Rendulic S, Steele JL *et al*: **Comparison of the complete genome sequences of *Bifidobacterium animalis* subsp. *lactis* DSM 10140 and Bl-04**. *J Bacteriol* 2009, **191**:4144-4151.
94. Jones PM, George AM: **The ABC transporter structure and mechanism: perspectives on recent research**. *Cell Mol Life Sci* 2004, **61**:682-699.
95. Davidson AL, Dassa E, Orelle C, Chen J: **Structure, function, and evolution of bacterial ATP-binding cassette systems**. *Microbiol Mol Biol Rev* 2008, **72**:317-364.
96. Eitinger T, Rodionov DA, Grote M, Schneider E: **Canonical and ECF-type ATP-binding cassette importers in prokaryotes: diversity in modular organization and cellular functions**. *FEMS Microbiol Rev* 2011, **35**:3-67.
97. Fukami-Kobayashi K, Tateno Y, Nishikawa K: **Domain dislocation: a change of core structure in periplasmic binding proteins in their evolutionary history**. *J Mol Biol* 1999, **286**:279-290.
98. Berntsson RPA, Smits SHJ, Schmitt L, Slotboom DJ, Poolman B: **A structural classification of substrate-binding proteins**. *FEBS Lett* 2010, **584**:2606-2617.
99. Quiocho FA, Ledvina PS: **Atomic structure and specificity of bacterial periplasmic receptors for active transport and chemotaxis: Variation of common themes**. *Mol Microbiol* 1996, **20**:17-25.

100. Mao B, Pear MR, McCammon JA, Quiocho FA: **Hinge bending in L-arabinose binding protein. The "Venus's fly trap model"**. *J Biol Chem* 1982, **257**:1131-1133.
101. Oldham ML, Davidson AL, Chen J: **Structural insights into ABC transporter mechanism**. *Curr Opin Struct Biol* 2008, **18**:726-733.
102. Oldham ML, Khare D, Quiocho FA, Davidson AL, Chen J: **Crystal structure of a catalytic intermediate of the maltose transporter**. *Nature* 2007, **450**:515-521.
103. Gilliland SE, Speck ML, Morgan CG: **Detection of *Lactobacillus acidophilus* in feces of humans, pigs and chickens**. *Appl Microbiol* 1975, **30**: 541-545.
104. Sanders ME, Klaenhammer TR: **The scientific basis of *Lactobacillus acidophilus* NCFM functionality as a probiotic**. *J Dairy Sci* 2001, **84**:319-331.
105. Altermann E, Russell WM, Azcarate-Peril MA, Barrangou R, Buck BL, McAuliffe O, Souther N, Dobson A, Duong T, Callanan M *et al*: **Complete genome sequence of the probiotic lactic acid bacterium *Lactobacillus acidophilus* NCFM**. *Proc Natl Acad Sci USA* 2005, **102**(11):3906-3912.
106. Barrangou R, Altermann E, Hutkins R, Cano R, Klaenhammer TR: **Functional and comparative genomic analyses of an operon involved in fructooligosaccharide utilization by *Lactobacillus acidophilus***. *Proc Natl Acad Sci USA* 2003, **100**:8957-8962.
107. Azcarate-Peril MA, McAuliffe O, Altermann E, Lick S, Russell WM, Klaenhammer TR: **Microarray analysis of a two-component regulatory system involved in acid resistance and proteolytic activity in *Lactobacillus acidophilus***. *Appl Environ Microbiol* 2005, **71**:5794-5804.
108. Pfeiler EA, Azcarate-Peril MA, Klaenhammer TR: **Characterization of a novel bile-inducible operon encoding a two-component regulatory system in *Lactobacillus acidophilus***. *J Bacteriol* 2007, **189**:4624-4634.
109. Pfeiler EA, Klaenhammer TR: **Role of transporter proteins in bile tolerance of *Lactobacillus acidophilus***. *Appl Environ Microbiol* 2009, **75**:6013-6016.
110. Björklund M, Ouwehand A, Forssten S, Nikkilä J, Tiihonen K, Rautonen N, Lahtinen S: **Gut microbiota of healthy elderly NSAID users is selectively modified with the**

administration of *Lactobacillus acidophilus* NCFM and lactitol. *AGE* 2012, **34**:987-999.

111. Ouwehand AC, Tiihonen K, Saarinen M, Putaala H, Rautonen N: **Influence of a combination of *Lactobacillus acidophilus* NCFM and lactitol on healthy elderly: intestinal and immune parameters**. *Br J Nutr* 2009, **101**:367-375.
112. Makivuokko H, Forssten S, Saarinen M, Ouwehand A, Rautonen N: **Synbiotic effects of lactitol and *Lactobacillus acidophilus* NCFM™ in a semi-continuous colon fermentation model**. *Benef Microbes* 2010, 1:131-137.
113. Cohen DPA, Renes J, Bouwman FG, Zoetendal EG, Mariman E, de Vos WM, Vaughan EE: **Proteomic analysis of log to stationary growth phase *Lactobacillus plantarum* cells and a 2-DE database**. *Proteomics* 2006, **6**:6485-6493.
114. Koistinen KM, Plumed-Ferrer C, Lehesranta SJ, Karenlampi SO, von Wright A: **Comparison of growth-phase-dependent cytosolic proteomes of two *Lactobacillus plantarum* strains used in food and feed fermentations**. *FEMS Microbiol Lett* 2007, **273**:12-21.
115. Palmfeldt J, Levander F, Hahn-Hagerdal B, James P: **Acidic proteome of growing and resting *Lactococcus lactis* metabolizing maltose**. *Proteomics* 2004, **4**:3881-3898.
116. Koskenniemi K, Koponen J, Kankainen M, Savijoki K, Tynkkynen S, de Vos WM, Kalkkinen N, Varmanen P: **Proteome analysis of *Lactobacillus rhamnosus* GG using 2-D DIGE and mass spectrometry shows differential protein production in laboratory and industrial-type growth media**. *J Proteome Res* 2009, **8**:4993-5007.
117. Roy K, Meyrand M, Corthier G, Monnet V, Mistou MY: **Proteomic investigation of the adaptation of *Lactococcus lactis* to the mouse digestive tract**. *Proteomics* 2008, **8**:1661-1676.
118. Izquierdo E, Horvatovich P, Marchioni E, Aoude-Werner D, Sanz Y, Ennahar S: **2-DE and MS analysis of key proteins in the adhesion of *Lactobacillus plantarum*, a first step toward early selection of probiotics based on bacterial biomarkers**. *Electrophoresis* 2009, **30**:949 - 956.

119. Gitton C, Meyrand M, Wang JH, Caron C, Trubuil A, Guillot A, Mistou MY: **Proteomic signature of *Lactococcus lactis* NCDO763 cultivated in milk**. *Appl Environ Microbiol* 2005, **71**:7152-7163.
120. Guillot A, Gitton C, Anglade P, Mistou MY: **Proteomic analysis of *Lactococcus lactis*, a lactic acid bacterium**. *Proteomics* 2003, **3**:337-354.
121. Bottacini F, Medini D, Pavesi A, Turroni F, Foroni E, Riley D, Giubellini V, Tettelin H, van Sinderen D, Ventura M: **Comparative genomics of the genus bifidobacterium**. *Microbiology* 2012, **156**:3243-3254.
122. Makarova K, Slesarev A, Wolf Y, Sorokin A, Mirkin B, Koonin E, Pavlov A, Pavlova N, Karamychev V, Polouchine N *et al*: **Comparative genomics of the lactic acid bacteria**. *Proc Natl Acad Sci USA* 2006, **103**:15611-15616.
123. Makarova KS, Koonin EV: **Evolutionary genomics of lactic acid bacteria**. *J Bacteriol* 2007, **189**:1199-1208.
124. Ringel-Kulka T, Palsson OS, Maier D, Carroll I, Galanko JA, Leyer G, Ringel Y: **Probiotic bacteria *Lactobacillus acidophilus* NCFM and *Bifidobacterium lactis* Bi-07 versus placebo for the symptoms of bloating in patients with functional bowel disorders: A double-blind Study**. *J Clin Gastroenterol* 2011, **45**:518-525.
125. Larsen N, Vogensen FK, Gøbel R, Michaelsen KF, Al-Soud WA, Sørensen SJ, Hansen LH, Jakobsen M: **Predominant genera of fecal microbiota in children with atopic dermatitis are not altered by intake of probiotic bacteria *Lactobacillus acidophilus* NCFM and *Bifidobacterium animalis* subsp. *lactis* Bi-07**. *FEMS Microbiol Ecol* 2010, **75**:482-496.
126. Gill HS, Rutherfurd KJ, Cross ML, Gopal PK: **Enhancement of immunity in the elderly by dietary supplementation with the probiotic *Bifidobacterium lactis* HN019**. *Am J Clin Nutr* 2001, **74**:833-839.
127. Chiang BL, Sheih YH, Wang LH, Liao CK, Gill HS: **Enhancing immunity by dietary consumption of a probiotic lactic acid bacterium (*Bifidobacterium lactis* HN019): optimization and definition of cellular immune responses**. *Eur J Clin Nutr* 2000, **54**:849-855.

128. Shu Q, Gill HS: **A dietary probiotic (*Bifidobacterium lactis* HN019) reduces the severity of *Escherichia coli* O157:H7 infection in mice**. *Med Microbiol Immunol* 2001, **189**:147-152.
129. van Zanten GC, Knudsen A, Röytiö H, Forssten S, Lawther M, Blennow A, Lahtinen SJ, Jakobsen M, Svensson B, Jespersen L: **The effect of selected synbiotics on microbial composition and short-chain fatty acid production in a model system of the human Colon**. *PLoS One* 2012, **7**:e47212.
130. Unlu M, Morgan ME, Minden JS: **Difference gel electrophoresis: a single gel method for detecting changes in protein extracts**. *Electrophoresis* 1997, **18**:2071-2077.

CHAPTER 2

Proteome reference map of *Lactobacillus acidophilus* NCFM and quantitative proteomics towards understanding the prebiotic action of lactitol

Proteome reference map of *Lactobacillus acidophilus* NCFM and quantitative proteomics towards understanding the prebiotic action of lactitol

Avishek Majumder[1], Abida Sultan[1,†], Rosa R. Jersie-Christensen[1,†], Morten Ejby[1], Bjarne Gregers Schmidt[1], Sampo J. Lahtinen[2], Susanne Jacobsen[1*] and Birte Svensson[1*]

1. Enzyme and Protein Chemistry, Department of Systems Biology, Technical University of Denmark, Søltofts Plads, Building 224, DK-2800 Kgs. Lyngby, Denmark.

2. Danisco Bioactives, Health & Nutrition, Sokeritehtaantie 20, 02460 Kantvik, Finland.

***Corresponding authors:** Birte Svensson & Susanne Jacobsen, Enzyme and Protein Chemistry, Department of Systems Biology, Technical University of Denmark, Søltofts Plads, Building 224, DK-2800 Kgs. Lyngby, Denmark

Phone: +45 45252740; +45 45252741; Fax:+45 45886307

Email: bis@bio.dtu.dk; sja@bio.dtu.dk

Footnote: [†]These authors contributed equally

Abbreviations:

CAAI, codon-anticodon adaptation index; CcpA, catabolite control protein A; CCR, carbon catabolite repression; GIT, gastrointestinal tract; GH, glycoside hydrolase; HPr, histidine-containing phosphocarrier protein; HPrK/P, HPr kinase/phosphorylase; KEGG, Kyoto Encyclopedia of Genes and Genomes; LAB, lactic acid bacteria; LABSEM, lactic acid bacteria semisynthetic medium; L-LDH, L-lactate dehydrogenase; NCFM, North Carolina Food Microbiology; note that NCFM is used as short for *Lactobacillus acidophilus* NCFM; PEP-PTS, phosphoenolpyruvate-phosphotransferase system; PTM, post-translational modification

Key words: *Lactobacillus acidophilus* NCFM, lactitol, prebiotics, 2D-DIGE, RT-PCR

Abstract

Lactobacillus acidophilus NCFM is a probiotic bacterium adapted to survive in the gastrointestinal tract and with potential health benefits to the host. Lactitol is a synthetic sugar alcohol used as a sugar replacement in low calorie foods and selectively stimulating growth of *L. acidophilus* NCFM. In the present study the whole cell extract proteome of *L. acidophilus* NCFM grown on glucose until late exponential phase was resolved by two-dimensional gel electrophoresis (2-DE) (pH 3−7). A total of 275 unique proteins assigned to various physiological processes were identified from 650 spots. Differential 2-DE (DIGE) (pH 4−7) of *L. acidophilus* NCFM grown on glucose and lactitol, revealed 68 spots with modified relative intensity. Thirty-two unique proteins were identified in 41 of these spots changing 1.6−12.7 fold in relative abundance by adaptation of *L. acidophilus* NCFM to growth on lactitol. These proteins included *β*-galactosidase small subunit, galactokinase, galactose-1-phosphate uridylyltransferase and UDP-glucose 4-epimerase, which all are potentially involved in lactitol metabolism. This first comprehensive proteome analysis of *L. acidophilus* NCFM provides insights into protein abundance changes elicited by the prebiotic lactitol.

Introduction

Lactobacillus acidophilus NCFM (NCFM) is a well-documented probiotic [1] with a 2.0 Mb genome of low G+C content (34.7%) and encoding 1862 predicted ORFs (http://www.ncbi.nlm.nih.gov; NCBI:CP000033) [2], including several transport systems and 37 glycoside hydrolases (GH) (http://www.cazy.org/) involved in uptake and utilization of carbohydrates [1, 3, 4]. NCFM has the capacity to adapt its metabolic machinery in response to the gut nutrient composition by negative transcriptional regulation. This metabolic flexibility ensures survival of NCFM in a low nutrient and highly competitive environment [5]. In addition, NCFM contains a suite of mucus binding proteins as an adaptation to survive in the GIT [6].

Lactitol (4-O-*β*-D-galactopyranosyl-D-glucitol) is a synthetic sugar alcohol obtained from lactose and used as a prebiotic. It is not metabolized by humans due to lack of a suitable *β*-galactosidase and is also not absorbed in the small intestine. Lactitol therefore becomes readily accessible to the microbiota in the colon [7] and has been shown to stimulate growth and metabolism of intestinal *Bifidobacterium* and *Lactobacillus* species, thus creating unfavourable conditions for pathogens such as *Clostridia* and *Enterobacteriaceae* [8]. Daily consumption of the synbiotic combination of NCFM and lactitol by elderly volunteers increased stool frequency, fecal levels of NCFM and genus *Bifidobacterium*, and modulated fecal immune biomarkers, reflecting stimulation of intestinal mucosal functions [9]. Complementary beneficial effects with this synbiotic were also observed in a semi-continuous colon fermentation model [10].

In the present work, a comprehensive whole cell extract reference proteome of NCFM grown with glucose as carbon source was established using 2D-gel electrophoresis (pH 3−7). This signature proteome with most proteins distributed in the pI 4−7 range was used for understanding the protein abundance dynamics associated with stimulation by the prebiotic lactitol. Comparative proteomics using 2D-DIGE (pH 4−7) coupled with mass spectrometric protein identification, revealed proteins involved in the lactitol metabolism.

Materials and Methods

Growth Conditions and Protein Extraction

Lactobacillus acidophilus NCFM (Danisco USA Inc., Madison, US-WI) was grown under aerobic conditions without agitation at 37 °C in 40 ml batch cultures in semisynthetic medium for lactic acid bacteria (LABSEM) [3] supplemented with 1% of either glucose or lactitol (Danisco) for soluble whole cell proteome (pI 3−7) and DIGE analyses. Cultures were sub-cultured in the LABSEM for three cycles prior to analysis to avoid chemical carry-over effects. Late-log phase cells with an A_{600nm} of 2.0 for glucose and 0.4 for lactitol (Supplementary Fig. 1) were harvested from four independent cultures by centrifugation (3,200 *g*, 10 min, 4 °C). Cell pellets were washed twice with 0.9% NaCl, vacuum-dried without heating for approx. 2 h until dry (SpeedVac, Savant, SC110A with Vacuum unit UVS400A; GMI Inc., Ramsey, US-MN) and kept at −80 °C until use. Cells were disrupted by manual mechanical grinding with a small number of acid washed glass beads (<100 μm diameter) using a rounded glass Pasteur pipette.

Sample Preparation for 2-DE and DIGE

Disrupted cells from 40 ml cultures were added 60 μl sample buffer (28 mM Tris-HCl, 22 mM Tris-base pH 8.5, 0.3% SDS, 100 mM DTT), heated (100 ºC, 2 min), and incubated at room temperature (5 min) followed by addition of 240 μl pharmalyte buffer (8 M urea, 2 M thiourea, 100 mM DTT, 2% pharmalyte pH 4−7 (GE Healthcare, Uppsala, Sweden), 0.52% Triton X-100). The mixture was vortexed, centrifuged (10,000 *g*, 10 min), and the supernatant was collected. Protein concentration of the supernatant was quantified (2D Quant kit; GE Healthcare) and the samples were stored at −80 °C. Whole cell extract proteome (400 μg protein) was added with rehydration buffer (8 M urea, 2 M thiourea, 2% CHAPS, 0.5% pharmalyte 4−7, 0.3% DTT) up to 450 μl and applied on IPG strips (linear pH 3−7; 24 cm). For DIGE analysis, dye-swapping approach was used to avoid bias due to the interference from gel fluorescence properties at different wavelengths [11]. Protein aliquots (50 μg) of each of four biological replicates grown on glucose or lactitol were labeled interchangeably with 400 pmol of either Cy3 or Cy5, vortexed, and left in the dark (30 min, 4 °C). In a similar

manner, aliquots (25 μg protein) of each sample were combined for internal standard and labeled with 400 pmol Cy2. Labeling reactions were quenched by 1 μl 10 mM lysine in the dark (10 min). The internal standard and the samples were mixed and the volume was made to 450 μl with rehydration buffer for IPG strips (linear pH 4−7, 24 cm).

2-DE for Whole Cell Extract Proteome and Differential Proteomics

Separation in the first dimension was performed using IPG strips (pH 3−7; 24 cm; GE Healthcare) on Ettan^{TM} IPGphor (GE Healthcare). The reference map showed few proteins of pI < 4, hence for DIGE pH 4−7 IPG strips were used. After rehydration at 20 °C for 12 h at 50 μA/strip, IEF was performed at a total of 78 kVh (1 h at 150 V, 1 h at 300 V, 1 h at 1,000 V, gradient to 8,000 V, hold at 8,000 V until a total of at least 78 kVh was reached). Subsequently, strips were equilibrated (2 × 15 min) in 5 ml equilibration buffer (6 M urea, 30% glycerol, 50 mM Tris-HCl, pH 8.8, 2% SDS, 0.01% bromophenol blue) supplemented with 1% DTT and 2.5% iodoacetamide in the first and second equilibration step, respectively. The strips and molecular weight (*Mr*) markers (Mark 12^{TM}, Invitrogen) were placed on 12.5% SDS-PAGE gels and overlaid with 0.5% molten agarose in 1 × SDS running buffer (0.25 M Tris-base, 1.92 M glycine, 1% SDS). The second dimension (SDS-PAGE) was performed on Ettan^{TM} DALT *twelve* Electrophoresis Unit (GE Healthcare) overnight at 1 W/gel until the dye front reached the gel bottom. The proteome reference map gels (pH 3−7) were stained by colloidal CBB as described previously [12].

Image Analysis

Images of colloidal CBB stained gels were generated (Microtek scanner; Scan maker 9800XL; Microtek, Carson, USA) using Photoshop CS4 software and image analysis was done using the algorithm for blob images [13]. Imaging of DIGE gels (four biological replicates and four internal standard gels) was done immediately after the second dimension run at excitation/emission wavelengths of Cy2 (488/520 nm), Cy3 (532/580 nm) and Cy5 (633/670 nm), respectively (100 μm resolution; Typhoon 9410 Variable Mode Imager; GE Healthcare, Uppsala, Sweden). Gel images were aligned by automated calculation of ten manually

assigned alignment landmark vectors (Progenesis SameSpots version 3.3, nonlinear Dynamics Ltd, Newcastle upon Tyne, UK). Scanned gels were analyzed by intra-gel (difference in-gel) and inter-gel (biological variance) analysis. A 1.5-fold threshold (spot volume ratio change and ANOVA $p \leq 0.05$ and a false discovery rate of $q \leq 0.05$) was chosen as criterion in the identification of differentially expressed protein candidates. The 1.5 fold threshold value used was based on the Power analysis, which has a recommended value of 80%. Power analysis can be used to calculate the minimum sample size required to accept the outcome of a statistical test with a particular level of confidence [14]. The experimental set up had enough statistical power with the four replicate gels. False discovery rate estimates the number of false positives within statistically significant changes in the experiment [15]. The q value was set to ≤ 0.05 giving a false discovery rate of 5%. Gels were post-stained with colloidal CBB prior to spot protein identification.

In-gel Digestion and Protein Identification by MS

Spots on 2-DE reference map and DIGE gels were excised manually and subjected to in-gel tryptic digestion with modifications as described below [16]. Gel pieces were washed with 100 µl 40% ethanol (10 min) followed by 50 µl 100% ACN, and incubated 45 min on ice with 2 µl 12.5 ng μl^{-1} trypsin (Promega) in 25 mM ammonium bicarbonate followed by addition of 10 µl 25 mM ammonium bicarbonate for rehydration, and incubated at 37 °C overnight. A supernatant aliquot (1 µl) was applied to the Anchor Chip target (Bruker-Daltonics, Bremen, Germany), covered by 1 µl matrix solution (0.5 µg μl^{-1} α-cyano-4-hydroxycinnamic acid in 90% ACN, 0.1% TFA) and washed in 0.02% TFA. MS and MS/MS spectra were obtained by Ultraflex II MALDI-TOF MS mass spectrometer (Bruker-Daltonics) in auto-mode using Flex Control v3.0 (Bruker-Daltonics) and processed by Flex Analysis v3.0 (Bruker-Daltonics). Peptide mass maps were acquired in reflectron mode with 500 laser shots per spectrum. Spectra were externally calibrated using a tryptic digest of β-lactoglobulin (5 pmol μl^{-1}); MS/MS data were acquired with stop conditions so that 1000–1600 laser shots were accumulated for each spectrum. The MS together with MS/MS spectra were searched against the NCBInr database for bacteria (NCBInr 20090826; 9523564 sequences; 3256669569

residues) using the MASCOT 2.0 software (http://www.matrixscience.com) integrated together with BioTools v3.1 (Bruker-Daltonics). Search parameters were: monoisotopic peptide mass accuracy of 80 ppm, fragment mass accuracy to $\pm$ 0.7 Da; maximum of one missed cleavage; carbamidomethylation of cysteine and partial oxidation of methionine. Filtering of peaks was done for known keratin and autocatalytic trypsin peaks; the signal to noise threshold ratio was set to 1:6. Protein identifications by PMF were confirmed with a Mascot score of 80, $p \leq 0.05$ and should have a minimum of 6 matched peptides. Single peptide based protein identifications by MS/MS analysis were confirmed with a Mascot score of 40, $p \leq 0.05$.

Semiquantitative RT-PCR

Total RNA from glucose and lactitol grown cultures was extracted using the Trizol (Invitrogen) method according to manufacturer's instructions. RNA was purified by Pure link RNA mini kit with on-column DNase treatment to remove contaminating DNA. The primer pairs were designed using Primer3 software (http://frodo.wi.mit.edu/primer3/), 1 µg of total RNA was used as the template for reverse transcription of 9 selected genes with Omniscript reverse transcriptase by OneStep RT-PCR (Qiagen) according to manufacturer's instructions. PCR was carried out with the primer pairs (Supplementary Table 1) in a Thermal cycler (PTC-200 Peltier Thermal Cycler, GMI Inc., Ramsey, US-MN) (50 °C for 30 min, 95 °C for 15 min, followed by 22 three-step cycles of 94 °C for 1 min, 55 °C for 1 min and 72 °C for 1 min). NCFM 16S ribosomal DNA (rDNA) (LBA2001 and LBA2071) transcript whose expression is always constant, was used as internal control [17]. The absence of DNA contamination in the RNA preparation was confirmed according to the manufacturer's instructions (Qiagen), by heat inactivation of Omniscript reverse transcriptase. The PCR products were detected by 2% agarose gel electrophoresis with ethidium bromide staining.

***In silico* Analysis**

The codon-anticodon adaptation index (CAAI) of all ORFs of NCFM was obtained using DAMBE (http://dambe.bio.uottawa.ca/dambe.asp) [18] in two steps. Firstly CAAI values were created using the codon table based on tRNA anticodons frequency, without a reference set of

highly expressed genes. The CAAI values were then adjusted to a range of 0−1 [18]. GRAVY values were calculated using the ProtParam tool (http://www.expasy.ch/tools/protparam.html).

Results

Growth of NCFM on Glucose and Lactitol

Detailed growth curves and pH profiles of NCFM grown with glucose or lactitol as carbohydrate source (Supplementary Fig. 1) showed higher cell density and larger decrease in pH of cultures with glucose as compared to lactitol. Proteome changes with the prebiotic was determined at late exponential phase cultures under controlled conditions, because this is the stage with maximum synthesis of macromolecules [19] and where accumulation of stress proteins is minimal. The growth phase significantly affects the proteome pattern and in the stationary phase, stress-sensing and stress-related proteins are produced due to depletion of nutrients [19-21].

The Reference Map of the NCFM Proteome (pH 3−7)

A reference map using whole cell extract of NCFM grown on LABSEM medium was established to identify constitutively expressed proteins and describe the dynamics of this proteome in response to carbohydrate prebiotics. Initially the wide range of pH 3−10 (linear; 18 cm; data not shown) was used for separation in the first dimension to get an overview of the NCFM proteome distribution on the 2-DE. However, since the vast majority of spots clustered at pH 4−7, IEF in pH 3−7 was applied to optimize spot resolution in the densely populated area of the 2D-gel. Six hundred and fifty well-resolved spots were selected for identification from the CBB stained 2D-gel (Fig. 1), which led to 507 protein identifications using MALDI-TOF MS and/or MS/MS (Supplementary Tables 2 and 3). Several proteins appeared in more than one spot and in total 275 unique proteins were identified (Supplementary Tables 2 and 3). Only 16 of the 275 unique proteins have theoretical pI > 7.0; most of these were identified from spots shaped as horizontal streaks in the pH range 3−7 (Fig. 1). Proteins present in more than one spot showing pI and *Mr* heterogeneity were probably

post-translationally modified (PTM) or found as highly similar isoforms. Isoelectric heterogeneity in 2-DE is very common in proteomics [19, 22-24] and has been attributed to PTM or to artifacts, *e.g.* carbamylation by urea or deamidation [22]. Carbamylation generally leads to spot charge trains, not observed on the NCFM 2-DE (Fig. 1 and 4A) and the multiple protein forms probably stem from PTM.

In silico Analysis and the Experimental Proteome

The NCFM *in silico* proteome generated using the bioinformatics tool JVirGel version 2 (http://www.jvirgel.de/) contains 705 intracellular proteins of pI 3−7 and *Mr* 5−200 kDa. The 259 identified proteins (pI 3−7 range) thus constitute 36% of the theoretical proteome. Grouping the identified proteins according to functionality using Gene Role Category annotation (http://cmr.jcvi.org/tigr-scripts/CMR/CmrHomePage.cgi) (Fig. 2; Supplementary Tables 2 and 3) showed the majority are important in protein synthesis and energy metabolism. The cellular localization was predicted using PSORT version 3.0 (http://www.psort.org/) (Supplementary Tables 2 and 3), which indicated that 218 of the 275 identified proteins were cytoplasmic, 10 belonged to the cytoplasmic membrane, 2 were extracellular, 2 were associated with cell wall formation, and 43 had unknown cellular localization.

One of the limitations of 2D-gel based proteomics is poor detection of low abundance proteins. The theoretical abundance of proteins on 2D-gels can be calculated using the codon-anticodon adaptive index (CAAI), which is based on the codon usage bias and the relative frequencies of tRNA anticodons [18]. CAAI is an indicator of translation efficiency used to predict gene expression levels in bacteria. Several recent reference proteomes used CAAI analyses to assess the genome with respect to translation efficiency [21, 21, 25, 26]. The relative protein abundance in *L. acidophilus* NCFM on 2D-gels (pH 3–7) correlated with CAAI (Fig. 1 and 3A), proteins with low copy numbers being hard to identify. CAAI for proteins from the most intensely stained spots, *e.g.* elongation factor Tu (EF-Tu) (spot 140, 147, 215), L-LDH (spot 261, 299, 290), glyceraldehyde-3-p dehydrogenase (spot 230, 232, 210), pyruvate kinase (spot 46, 50, 60) and phosphopyruvate hydratase (spot 169, 166, 140) have value in the 0.581−0.69 range. Noticeably, among 23 proteins in the theoretical proteome with CAAI < 0.2, indicating

low abundance, 10 were identified from the 2D-gel. The GRAVY index for hydrophobicity of all NCFM coding sequences were calculated (Fig. 3B) and proteins identified from the 2D-gel have values from 0.179 to -1.244 (Fig. 3B). Only 18 identified proteins have a GRAVY value > 0, and hydrophobic proteins with values $\geq$ 0.2 were not identified due to loss during sample preparation and / or electrophoresis. The present percentage of hydrophobic proteins identified on the 2D-gel is similar to the previous reference proteomes of bacteria [21, 26].

Identification of Differentially Abundant Proteins with NCFM Grown on Lactitol

Proteome changes of NCFM elicited by growth on lactitol compared to glucose (Supplementary Fig. 1) were identified using 2D-DIGE. The predicted cytosolic proteome has a total of 17 proteins of pI $\leq$ 4.0, but only one, DNA-directed RNA polymerase subunit delta (LBA0232) (spot 463), was identified on the reference 2D-gel (Supplementary Table 2). DIGE was therefore performed at pI 4–7 to obtain better spot resolution. A total of 68 spots changed $\geq$ 1.5-fold in relative abundance. Forty-one identified spots representing, 32 unique proteins were differentially abundant in response to lactitol (Table 1), with 25 up-regulated (1.6–12.7 fold) and 16 down-regulated (1.6–4.8 fold) proteins/protein forms (Fig. 4A; Table 1). Certain proteins such as galactokinase (spot 628, 629), mannose-6-phosphate isomerase (spot 630), fructokinase (spot 637) and deoxyadenosine kinase (spot 634), were identified from the DIGE experiment (Fig. 4A), but absent in the reference 2D-map. As further discussed below, proteins of the Leloir pathway; β-galactosidase small subunit; galactokinase; galactose-1-phosphate uridylyltransferase; and UDP-glucose 4-epimerase were abundant by a significant fold (4.5–12.7 fold) (Fig. 4A).

Validation of Differentially Abundant Proteins by Semiquantitative RT-PCR

To confirm the differential abundance of proteins found by DIGE, semiquantitative RT-PCR was carried out for 7 gene transcripts of the Leloir pathway; β-galactosidase large subunit; β-galactosidase small subunit; galactokinase; galactose-1-phosphate uridylyltransferase; lactose

permease, phosphoglucomutase and fructokinase. The results showed different expression patterns with glucose and lactitol consistent with the 2D-DIGE analysis (Fig. 4B).

Discussion

The Reference Map of the Soluble NCFM Proteome

During the past years a number of proteome 2-DE profiles were described for lactic acid bacteria (LAB) [27] mostly related to changes associated with growth [19, 20, 24], growth medium [28], and adaptations to the gut [29, 30]. However, very few proteome reference maps were reported [19, 25, 31]. For example using narrow range pH windows of 4–7 and 4.5–5.5 a reference map of *Lactococcus lactis* IL14103 contained 230 proteins, corresponding to 25% coverage of the predicted acidic proteome [25]. Proteome analysis of cytosolic proteins of *L. plantarum* WCFS1 at pH range 3−10 covered 3.3% of all genes [19]. The present 275 unique proteins identified in the NCFM proteome, comprising 259 proteins of pI 3–7 and 16 proteins with pI > 7, constitute approximately 15% coverage of the theoretical proteome and 36% of the predicted intracellular acidic proteome. Proteome coverage was 3.3–21.4% in proteome studies of other Gram-positive bacteria [19, 21, 25, 26].

The present proteome analysis used late exponential phase NCFM cultures to focus on enzymes associated with carbon metabolism and to avoid accumulation of stress proteins. Proteins associated with protein synthesis were dominated by components of the translational machinery, while proteins related to energy metabolism were dominated by enzymes of the glycolysis/gluconeogenesis. The current proteomics data complements an earlier transcriptome analysis of global gene expression patterns of NCFM grown on 8 different carbohydrate sources with glycolysis genes being consistently highly expressed [5].

Differential Proteomics of NCFM in the Presence of Glucose and Lactitol

Genome annotation showed that NCFM possesses transporter and fermentative capability to survive in the GIT and has the capacity of versatile utilization of an array of carbohydrate sources. The carbon flux in the metabolism of low G+C Gram-positive bacteria is tightly

regulated by carbon catabolite repression (CCR) [32], thus in the presence of glucose, genes not needed for growth with glucose are repressed. The regulation of the repression is brought upon by transcriptional control or regulation at the protein level by phosphorylation [32]. The present DIGE data show that abundant enzymes apparently responsible for utilization of lactitol are essentially identical to the metabolic machinery for utilization of lactose, *i.e.* the Leloir pathway. As will be further discussed below, it offers a view of how the physiology of NCFM adapts to lactitol and its hydrolysis products galactose and glucitol/sorbitol.

Galactose Metabolism in NCFM

Lactose has to be hydrolyzed either by a phospho-*β*-galactosidase (LacG), generating glucose and galactose-6-P, or by a *β*-galactosidase (LacZ or LacLM) to glucose and galactose [33]. In this context, *β*-galactosidase small subunit (LacM, LBA1468) was highly abundant (12.7 fold) on lactitol. The heterodimeric *β*-galactosidase (LacLM) belongs to GH2 (CAZy; http://www.cazy.org/); only the small, not the large subunit, was identified on the gel. Similarly, most enzymes for galactose metabolism were identified on 2D-gels of *L. lactis* grown on lactose, but not the *β*-galactosidase [25]. The other highly abundant proteins (4.5–5.0 fold) include galactokinase, galactose-1-phosphate uridylyltransferase and UDP-glucose 4-epimerase from the Leloir pathway (Fig. 4B, 5). Galactose-1-P generated by ATP dependent galactokinase is transferred to UDP-glucose by galactose-1-phosphate uridylyltransferase in exchange with glucose-1-P. UDP-glucose 4-epimerase converts the generated UDP-galactose to UDP-glucose, which enters the glycolysis after phosphorylation to glucose-6-P by phosphoglucomutase, which was also abundant by 1.6 fold (Fig. 5, Table 1).

The genes for lactose and galactose metabolism are distributed in two adjacent loci LBA1457−1459 and LBA1462−1469 in NCFM. In LAB the organization of *lac* and *gal* clusters can vary significantly, possessing or lacking operon-like structures and genes interspersed with insertion sequences [34]. The presence of lactose permease belonging to the glycoside-pentoside-hexuronide:cation symporter family, and the enzymes of the Leloir pathway suggests lactitol is transported into NCFM by lactose permease, rather than by a PEP-PTS system [35]. The RT-PCR analysis confirms the clear up-regulation of *lacS* in lactitol

compared to glucose (Fig. 4B). These results complement previous extensive transcriptomic studies of NCFM grown on different carbohydrates [3, 5]. In the transcriptomic study with lactose and galactose, 10 different genes within the *lac* and *gal* loci were shown to be significantly up-regulated, *galKTME* being increased 2.7–17.6 fold, and *lacSZL* 2.8–29.5 fold [5]. The *lac-gal* locus region has two *β*-galactosidase genes *lacZ* (LBA1462) and *lacLM* (LBA1467-68) of GH42 and GH2 families, respectively. The *lacZ* gene was significantly overexpressed in an earlier transcriptome study [5]. The two *β*-galactosidases, were not identified in the present 2-DE, except for the small subunit of *β*-galactosidase (LacM). It was not possible to conclude from the proteome analysis which of the two *β*-galactosidases acts on lactitol, but the large subunit of *β*-galactosidase (*lacL*) was found to be highly expressed by semiquantitative RT-PCR (Fig. 4B).

Sorbitol Metabolism in NCFM

The DIGE analysis showed various enzymes involved in glucitol/sorbitol metabolism to be differentially abundant (1.7 to 4.3 fold; Table 1, Fig. 5). Sorbitol in NCFM is metabolized to fructose-6-P, ultimately leading to either glycolysis or fructose and mannose metabolism, according to the KEGG pathway (Kyoto Encyclopedia of Genes and Genomes; www.genome.ad.jp/kegg) [36]. Sorbitol has been described as a carbon source for certain Gram-positive bacteria, including LAB and enzymes for sorbitol metabolism are encoded by an operon-like structure and subject to catabolite repression by glucose in Gram-positive bacteria [37, 38]. This kind of organization for sorbitol utilization was not identified in the NCFM genome. The phosphotransferase system enzyme II (PTS EII, LBA0655) based on its conserved domains belongs to the class of PEP-PTS specific for glucitol (http://pfam.sanger.ac.uk/) [39]. The PTS components are involved in the phosphorylation of carbohydrate by the histidine-containing phosphocarrier protein (HPr). HPr is in turn phosphorylated by the PEP system or by ATP-dependent auto-phosphorylation [32]. PTS EII (LBA0655), phosphorylating glucitol to glucitol-6-phosphate, was abundant by 1.7 fold (Fig. 5), and the two oxidoreductases (LBA1023 and LBA1027) were abundant by 2.9 and 3.9 fold, respectively. Oxidoreductase (LBA1023 and LBA1027) may be involved in the interconversion of D-glucitol-6-P to L-sorbose-1-P, and maintain the concentrations of

glucitol-6-P (KEGG). Glucitol-6-P has to be converted to *β*-D-fructose-6-P by 6-phosphogluconate dehydrogenase, which was not identified by DIGE (Fig. 5). *β*-D-Fructose-6-P is the central metabolite that can either enter glycolysis, amino sugar metabolism, or be converted to other carbohydrate metabolites. The other significantly differentially abundant enzymes were mannose-6-phosphate isomerase and fructokinase, which increased by 4.3 and 2.4 fold, respectively. The *β*-D-fructose-6-P generated by sorbitol catabolism may thus enter either fructose or mannose metabolism or it enters glycolysis after being converted to *β*-D-fructose-1, 6-bis-P by phosphofructokinase. Fructose-bisphosphate aldolase decreased (2.2 fold) and there was an increase of glyceraldehyde-3-p dehydrogenase (2.2 fold) and dihydroxyacetone kinase (2.8 fold) (Table 1), which might channel all *β*-D-fructose-1, 6-bis-P into glycolysis.

Carbon Catabolite Repression (CCR) and the Enzymes of Glycolysis

In low G+C Gram-positive bacteria, PTS protein and HPr are the master regulators of carbon flow and metabolism. The phosphorylation and dephosphorylation of these proteins control the carbon metabolism via CCR [32, 40]. The CCR regulatory network in NCFM was also observed by microarray data with the presence of a flexible transcriptome controlled by CCR [5]. The key gene products involved in the regulation, *i.e.* catabolite control protein A (CcpA), HPr, HPrK/P, and PTS, were consistently highly abundant in the NCFM transcriptome, which suggested the regulation to occur at the protein rather than the transcriptional level [5]. PTS phosphotransferase activity and the phosphoenolpyruvate-to-pyruvate ratio regulates the concentrations of metabolites like fructose-1, 6-bis-P, ATP, PP_i and P_i, which in turn control the HPr kinase activity [32, 41, 42]. Various enzymes indicating the regulation in the presence of lactitol were identified by DIGE analysis. In *Streptococcus* sp. transport of lactose via lactose permease containing the IIA domain was found to be regulated at the protein level by different HPr forms [43]. A similar mechanism is possible in NCFM owing to the absence of other transporters for lactose and the presence of a highly homologous lactose permease with IIA domain. The cellular concentration of pyruvate kinase, which has control over the phosphoenolpyruvate-to-pyruvate ratio, was 1.9 fold abundant, which indicates CCR. Lactate

dehydrogenase converts the generated pyruvate to lactate and noticeably, of two different NCFM lactate dehydrogenase forms, one increased in 3.1 fold abundance and the other decreased by 4.8 fold (Table 1).

In Gram-positive bacteria when readily metabolized carbohydrate is available as energy source, the intracellular concentration of fructose-1, 6-bis-P increases and the concentrations of ATP and P_i decrease, while the opposite is true for unfavorable carbohydrate sources [32]. The presence of abundant enzymes for the intermediary metabolite β-D-fructose-6-P to fructose and mannose metabolism, abundant enzymes glyceraldehyde-3-p dehydrogenase (2.3 fold), dihydroxyacetone kinase (2.8 fold) and a lower fructose-bisphosphate aldolase (2.2 fold) indicates β-D-fructose-6-P being converted to fructose, mannose or glyceraldehyde-3-p. This might lead to lowered concentrations of fructose-1, 6-bis-P, and therefore a complete switch in the metabolic machinery (35).

More recently, glycolytic enzymes from low G+C bacteria have been ascribed multiple roles like mucus adhesion [30], mRNA processing [44] and interactions with key regulatory proteins. These proteins are often overlooked as housekeeping genes in proteome studies, but changes in their abundance may have significant effects on the metabolic pathways. Glucose-6-phosphate 1-dehydrogenase, which is very important in maintaining the redox potential of the cell by generating NADPH, was found to be 1.6 fold lower in abundance, and phosphoglucomutase, which maintains a balance between the glucose-6-P and glucose-1-P, was found to be more abundant by 1.6 fold. Glucose-6-P is the metabolite that enters the glycolysis, and lower abundance of glucose-6-phosphate 1-dehydrogenase and higher abundance of phosphoglucomutase may lead to accumulation of glucose-1-P.

Variation of Abundance in other Proteins Elicited by Lactitol

The other differentially abundant proteins include elongation factor Tu (EF-Tu), putative stress-related phosphate starvation inducible protein both involved in protein synthesis (http://cmr.jcvi.org/tigr-scripts/CMR/CmrHomePage.cgi) Along with its function in protein translation, EF-Tu has been reported to have a role in other cellular processes, including acting as chaperone and protein folding in *E. coli* [45]. In several LAB, EF-Tu was localized to the

cell wall and described as a 'moonlighting protein', *i.e.* a protein which has multiple, apparently unrelated functions in different cell locations [46]. EF-Tu was moreover suggested to participate in intestinal cell adhesion [30, 46-48] and its 2.6 fold increase may be connected to the higher number of NCFM in the GIT during lactitol administration [9]. The proposed involvement of EF-Tu in intestinal adhesion of bacteria agrees with its increased abundance by lactitol. This effect presents a novel putative mechanism for synbiotic interactions between probiotics and specific prebiotics.

At harvest pH of glucose and lactitol cultures was 5.2 and 6.3, respectively and the difference is due to higher growth rates in glucose and increased production of lactic acid. F_0F_1 ATP synthase subunit gamma was 1.8 fold higher in glucose compared to the lactitol grown cultures (Table 1). The increased abundance of F_0F_1 ATP synthase subunit gamma is due to its role in maintaining the proton motive force at lower pH [49]. Also the 1.9 fold increase of chaperonin GroEL in NCFM grown on glucose may be attributed to the low pH (Table 1). Chaperonin GroEL was reported to be induced as acid stress response in *L. acidophilus* [49], *Lactococcus lactis* and *Enterococcus faecalis*, which are all Gram-positive LAB [27].

Several NCFM proteins lowered in abundance in the presence of lactitol, including ribonucleoside triphosphate reductase, deoxyadenosine kinase, inosine-5′-monophosphate dehydrogenase, adenylosuccinate synthase, trigger factor, and citrate lyase α-chain, most of which are involved in nucleotide metabolism. *L. lactis* grown on lactose showed a similar down-regulation of pyrimidine-regulated enzymes [25]. The catabolism of galactose-1-P to glucose-1-P, a process involving UDP-glucose and UDP-galactose and the enzymes UDP-glucose-4-epimerase and galactose-1-phosphate uridylyltransferase, has been suggested to participate in the lower abundance of pyrimidine enzymes [25], and a similar physiological response may occur with lactitol.

Concluding Remarks

The present reference soluble whole cell extract proteome (pH 3−7) for *L. acidophilus* NCFM is the most comprehensive analysis for a probiotic bacterium to date. A dynamic view of the proteome at the late exponential phase of NCFM grown on lactitol as sole carbon source

provides insights into probiotic-prebiotic interactions, which are essential for understanding how a prebiotic source can benefit a probiotic strain and lead to selective stimulation of its growth. *L. acidophilus* NCFM has the capacity to metabolize the carbohydrate moieties generated from lactitol. Galactose thus likely enters the Leloir pathway, while glucitol is metabolized by a PTS-II component. Other proteins showing differential abundance in lactitol were indirectly involved in the CCR. Finally, lactitol increases EF-Tu that can participate in adhesion processes, which presumably constitute an important consequence of intake of the synbiotic combination of NCFM and lactitol.

Acknowledgements

Birgit Andersen is acknowledged for technical assistance with mass spectrometric analysis. Dr. Rodolphe Barrangou is thanked for helpful comments to the manuscript. This work was supported by the Danish Strategic Research Council's Programme Committee on Health, Food and Welfare (FøSu), the Danish Research Council for Natural Science and the Danish Center for Advanced Food Studies (LMC). AM is grateful to the Technical University of Denmark for a Hans Christian Ørsted postdoctoral fellowship. AS thanks Danisco for a student scholarship.

References

[1] Sanders, M. E., Klaenhammer, T. R., The scientific basis of *Lactobacillus acidophilus* NCFM functionality as a probiotic. *J. Dairy Sci.* 2001, *84*, 319-331.

[2] Altermann, E., Russell, W. M., Azcarate-Peril, M. A., Barrangou, R. *et al.*, Complete genome sequence of the probiotic lactic acid bacterium *Lactobacillus acidophilus* NCFM. *Proc. Natl. Acad. Sci. U. S. A.* 2005, *102*, 3906-3912.

[3] Barrangou, R., Altermann, E., Hutkins, R., Cano, R., Klaenhammer, T. R., Functional and comparative genomic analyses of an operon involved in fructooligosaccharide utilization by *Lactobacillus acidophilus*. *Proc. Natl. Acad. Sci. U. S. A.* 2003, *100*, 8957-8962.

[4] Buck, B. L., Altermann, E., Svingerud, T., Klaenhammer, T. R., Functional analysis of putative adhesion factors in *Lactobacillus acidophilus* NCFM. *Appl. Environ. Microbiol.* 2005, *71*, 8344-8351.

[5] Barrangou, R., Azcarate-Peril, M. A., Duong, T., Conners, S. B. *et al.*, Global analysis of carbohydrate utilization by *Lactobacillus acidophilus* using cDNA microarrays. *Proc. Natl. Acad. Sci. U. S. A.* 2006, *103*, 3816-3821.

[6] Ventura, M., O'Flaherty, S., Claesson, M. J., Turroni, F. *et al.*, Genome-scale analyses of health-promoting bacteria: Probiogenomics. *Nat. Rev. Microbiol.* 2009, *7*, 61-71.

[7] Grimble, G. K., Patil, D. H., Silk, D. B. A., Assimilation of lactitol, an unabsorbed disaccharide in the normal human-colon. *Gut* 1988, *29*, 1666-1671.

[8] Finney, M., Smullen, J., Foster, H. A., Brokx, S., Storey, D. M., Effects of low doses of lactitol on faecal microflora, pH, short chain fatty acids and gastrointestinal symptomology. *Eur. J. Nutr.* 2007, *46*, 307-314.

[9] Ouwehand, A. C., Tiihonen, K., Saarinen, M., Putaala, H., Rautonen, N., Influence of a combination of *Lactobacillus acidophilus* NCFM and lactitol on healthy elderly: intestinal and immune parameters. *Br. J. Nutr.* 2009, *101*, 367-375.

[10] Makivuokko, H., Forssten, S., Saarinen, M., Ouwehand, A., Rautonen, N., Synbiotic effects of lactitol and *Lactobacillus acidophilus* NCFM^{TM} in a semi-continuous colon fermentation model. *Benef. Microbes* 2010, *1*, 131-137.

[11] Tannu, N. S., Hemby, S. E., Two-dimensional fluorescence difference gel electrophoresis for comparative proteomics profiling. *Nat. Protoc.* 2006, *1*, 1732-1742.

[12] Candiano, G., Bruschi, M., Musante, L., Santucci, L. *et al.*, Blue silver: A very sensitive colloidal Coomassie G-250 staining for proteome analysis. *Electrophoresis* 2004, *25*, 1327-1333.

[13] dos Anjos, A., Møller, A. L. B., Ersbøll, B. K., Finnie, C., Shahbazkia, H. R., New approach for segmentation and quantification of two-dimensional gel electrophoresis images. *Bioinformatics* 2010, 27, 368-375.

[14] Karp, N. A., Lilley, K. S., Maximising sensitivity for detecting changes in protein expression: Experimental design using minimal CyDyes. *Proteomics* 2005, *5*, 3105-3115.

[15] Karp, N. A., McCormick, P. S., Russell, M. R., Lilley, K. S., Experimental and statistical considerations to avoid false conclusions in proteomics studies using differential in-gel electrophoresis. *Mol. Cell Proteomics* 2007, *6*, 1354-1364.

[16] Hellman, U., Wernstedt, C., Gonez, J., Heldin, C. H., Improvement of an in-gel digestion procedure for the micropreparation of internal protein-fragments for amino-acid sequencing. *Anal. Biochem.* 1995, *224*, 451-455.

[17] Goh, Y. J., Zhang, C., Benson, A. K., Schlegel, V. *et al.*, Identification of a putative operon involved in fructooligosaccharide utilization by *Lactobacillus paracasei*. *Appl. Environ. Microbiol.* 2006, *72*, 7518-7530.

[18] Xia, X. H., An improved implementation of codon adaptation index. *Evolut. Bioinform. Online* 2007, *3*, 53-58.

[19] Cohen, D. P. A., Renes, J., Bouwman, F. G., Zoetendal, E. G. *et al.*, Proteomic analysis of log to stationary growth phase *Lactobacillus plantarum* cells and a 2-DE database. *Proteomics* 2006, *6*, 6485-6493.

[20] Koistinen, K. M., Plumed-Ferrer, C., Lehesranta, S. J., Karenlampi, S. O., von Wright, A., Comparison of growth-phase-dependent cytosolic proteomes of two *Lactobacillus plantarum* strains used in food and feed fermentations. *FEMS Microbiol. Lett.* 2007, *273*, 12-21.

[21] Wu, R., Wang, W. W., Yu, D. L., Zhang, W. Y. *et al.*, Proteomics analysis of *Lactobacillus casei* zhang, a new probiotic bacterium isolated from traditional home-made koumiss in Inner Mongolia of China. *Mol. Cell Proteomics* 2009, *8*, 2321-2338.

[22] Len, A. C. L., Harty, D. W. S., Jacques, N. A., Stress-responsive proteins are upregulated in *Streptococcus mutans* during acid tolerance. *Microbiology-Sgm* 2004, *150*, 1339-1351.

[23] Pessione, E., Mazzoli, R., Giuffrida, M. G., Lamberti, C. *et al.*, A proteomic approach to studying biogenic amine producing lactic acid bacteria. *Proteomics* 2005, *5*, 687-698.

[24] Palmfeldt, J., Levander, F., Hahn-Hagerdal, B., James, P., Acidic proteome of growing and resting *Lactococcus lactis* metabolizing maltose. *Proteomics* 2004, *4*, 3881-3898.

[25] Guillot, A., Gitton, C., Anglade, P., Mistou, M. Y., Proteomic analysis of *Lactococcus lactis*, a lactic acid bacterium. *Proteomics* 2003, *3*, 337-354.

[26] Yuan, J., Zhu, L., Liu, X. K., Zhang, Y. *et al.*, A proteome reference map and proteomic analysis of *Bifidobacterium longum* NCC2705. *Mol. Cell Proteomics* 2006, *5*, 1105-1118.

[27] Champomier-Verges, M. C., Maguin, E., Mistou, M. Y., Anglade, P., Chich, J. F., Lactic acid bacteria and proteomics: Current knowledge and perspectives. *J. Chromatogr. B Analyt. Technol. Biomed. Life Sci.* 2002, *771*, 329-342.

[28] Koskenniemi, K., Koponen, J., Kankainen, M., Savijoki, K. *et al.*, Proteome analysis of *Lactobacillus rhamnosus* GG using 2-D DIGE and mass spectrometry shows differential protein production in laboratory and industrial-type growth media. *J. Proteome Res.* 2009, *8*, 4993-5007.

[29] Roy, K., Meyrand, M., Corthier, G., Monnet, V., Mistou, M. Y., Proteomic investigation of the adaptation of *Lactococcus lactis* to the mouse digestive tract. *Proteomics* 2008, *8*, 1661-1676.

[30] Izquierdo, E., Horvatovich, P., Marchioni, E., Aoude-Werner, D. *et al.*, 2-DE and MS analysis of key proteins in the adhesion of *Lactobacillus plantarum*, a first step toward early selection of probiotics based on bacterial biomarkers. *Electrophoresis* 2009, *30*, 949-956.

[31] Gitton, C., Meyrand, M., Wang, J. H., Caron, C. *et al.*, Proteomic signature of *Lactococcus lactis* NCDO763 cultivated in milk. *Appl. Environ. Microbiol.* 2005, *71*, 7152-7163.

[32] Deutscher, J., Francke, C., Postma, P. W., How phosphotransferase system-related protein phosphorylation regulates carbohydrate metabolism in bacteria. *Microbiol. Mol. Biol. Rev.* 2006, *70*, 939-1031.

[33] Tsai, Y. K., Lin, T. H., Sequence, organization, transcription and regulation of lactose and galactose operons in *Lactobacillus rhamnosus* TCELL-1. *J. Appl. Microbiol.* 2006, *100*, 446-459.

[34] Fortina, M. G., Ricci, G., Mora, D., Guglielmetti, S., Manachini, P. L., Unusual organization for lactose and galactose gene clusters in *Lactobacillus helveticus*. *Appl. Environ. Microbiol.* 2003, *69*, 3238-3243.

[35] Devos, W. M., Vaughan, E. E., Genetics of lactose utilization in lactic-acid bacteria. *FEMS Microbiol. Rev.* 1994, *15*, 217-237.

[36] Kanehisa, M., Araki, M., Goto, S., Hattori, M. *et al.*, KEGG for linking genomes to life and the environment. *Nucleic Acids Res.* 2008, *36*, D480-D484.

[37] Yebra, M. J., Perez-Martinez, G., Cross-talk between the L-sorbose and D-sorbitol (D-glucitol) metabolic pathways in *Lactobacillus casei*. *Microbiology-Sgm* 2002, *148*, 2351-2359.

[38] Alcantara, C., Sarmiento-Rubiano, L. A., Monedero, V., Deutscher, J. *et al.*, Regulation of *Lactobacillus casei* sorbitol utilization genes requires DNA-binding transcriptional activator GutR and the conserved protein GutM. *Appl. Environ. Microbiol.* 2008, *74*, 5731-5740.

[39] Finn, R. D., Tate, J., Mistry, J., Coggill, P. C. *et al.*, The Pfam protein families database. *Nucleic Acids Res.* 2008, *36*, D281-D288.

[40] Monedero, V., Maze, A., Boel, G., Zuniga, M. *et al.*, The phosphotransferase system of *Lactobacillus casei*: Regulation of carbon metabolism and connection to cold shock response. *J. Mol. Microbiol. Biotechnol.* 2007, *12*, 20-32.

[41] Kotrba, P., Inui, M., Yukawa, H., Bacterial phosphotransferase system (PTS) in carbohydrate uptake and control of carbon metabolism. *J. Biosci. Bioeng.* 2001, *92*, 502-517.

[42] Dossonnet, V., Monedero, V., Zagorec, M., Galinier, A. *et al.*, Phosphorylation of HPr by the bifunctional HPr kinase/P-ser-HPr phosphatase from *Lactobacillus casei* controls catabolite repression and inducer exclusion but not inducer expulsion. *J. Bacteriol.* 2000, *182*, 2582-2590.

[43] Hols, P., Hancy, F., Fontaine, L., Grossiord, B. *et al.*, New insights in the molecular biology and physiology of *Streptococcus thermophilus* revealed by comparative genomics. *FEMS Microbiol. Rev.* 2005, *29*, 435-463.

[44] Commichau, F. M., Rothe, F. M., Herzberg, C., Wagner, E. *et al.*, Novel activities of glycolytic enzymes in *Bacillus subtilis*. *Mol. Cell Proteomics* 2009, *8*, 1350-1360.

[45] Caldas, T. D., El Yaagoubi, A., Richarme, G., Chaperone properties of bacterial elongation factor EF-Tu. *J. Biol. Chem.* 1998, *273*, 11478-11482.

[46] Siciliano, R. A., Cacace, G., Mazzeo, M. F., Morelli, L. *et al.*, Proteomic investigation of the aggregation phenomenon in *Lactobacillus crispatus*. *BBA-Proteins Proteom*. 2008, *1784*, 335-342.

[47] Granato, D., Bergonzelli, G. E., Pridmore, R. D., Marvin, L. *et al.*, Cell surface-associated elongation factor tu mediates the attachment of *Lactobacillus johnsonii* NCC533 (La1) to human intestinal cells and mucins. *Infect. Immun.* 2004, *72*, 2160-2169.

[48] Kelly, P., Maguire, P. B., Bennett, M., Fitzgerald, D. J. *et al.*, Correlation of probiotic *Lactobacillus salivarius* growth phase with its cell wall-associated proteome. *FEMS Microbiol. Lett.* 2005, *252*, 153-159.

[49] Lorca, G. L., de Valdez, G. F., Ljungh, A., Characterization of the protein-synthesis dependent adaptive acid tolerance response in *Lactobacillus acidophilus*. *J. Mol. Microbiol. Biotechnol.* 2002, *4*, 525-532.

Figure Legends

Fig. 1. A detailed 2-DE of the 400 µg whole cell extract soluble proteins (pH 3−7) of *Lactobacillus acidophilus* NCFM grown on LABSEM with 1% glucose. Numbered spots are chosen for analysis by in-gel digestion and mass spectrometry.

Fig. 2. Functional grouping of the 275 identified unique proteins on the 2-DE (pH 3–7) of *Lactobacillus acidophilus* NCFM.

Fig. 3 A. CAAI distribution of 1862 ORFs of *Lactobacillus acidophilus* NCFM (black bars) and of the 275 genes encoding proteins identified on 2-DE (pH 3–7) (open bars). **B.** GRAVY distribution of 1862 ORFs of *Lactobacillus acidophilus* NCFM (black bars) and of the 275 genes encoding proteins identified on 2-DE (pH 3–7) (open bars).

Fig. 4 A. Representative 2D-DIGE images of whole cell extract soluble proteins of *Lactobacillus acidophilus* NCFM grown on glucose (Cy3 green) and lactitol (Cy5 red) and the corresponding gray scale image of the CBB stained gel. The numbers on the gel indicate spots picked for identification by mass spectrometry. **B.** The semiquantitative RT-PCR amplified fragments of selected genes of *Lactobacillus acidophilus* NCFM grown on SEM medium with 1% glucose and 1% lactitol. The expression of 16S rDNA was used as an internal control. LacM, *β*-galactosidase small

subunit; GalK, galactose kinase; GalT, galactose-1-phosphate uridylyltransferase; PGM, phosphoglucomutase; FK, fructokinase; LacL, β-galactosidase large subunit; LacS, lactose permease.

Fig. 5. Schematic representation of the proposed proteins involved in lactitol metabolism. The proteins shaded in grey were identified by 2D-DIGE and MS, while the proteins in white were hypothesized to be involved in the metabolism of lactitol. Blue arrows by their orientation show differentially abundant proteins. Dashed red arrow shows proteins and metabolites involved in CCR. LacS, lactose permease; LacL, β-galactosidase large subunit; LacM, β-galactosidase small subunit; GalK, galactose kinase; GalT, galactose-1-phosphate uridylyltransferase; GalE, UDP-glucose-4-epimerase; PGM, phosphoglucomutase; FK, fructokinase; MPI, mannose-6-p-isomerase; PTSII, phosphotransferase component specific for glucitol; PGD, 6-phosphogluconate dehydrogenase; PFK, phosphofructokinase; FBA; fructose-bisphosphate aldolase; GAPDH; glyceraldehyde-3-p dehydrogenase; DHAK; dihydroxyacetone kinase; PK; pyruvate kinase; EI; enzyme I; HPr; histidine-containing phosphocarrier protein; HPrK/P; HPr kinase/phosphorylase. Black dashed arrow indicates the entry of glyceraldehyde-3-P into glycolysis

Table 1: Protein identifications of differentially abundant spots (≥ 1.5-fold spot volume ratio change and ANOVA $P \leq 0.05$) of *Lactobacillus acidophilus* NCFM grown on SEM medium with 1% glucose and 1% lactitol. Protein identifications were confirmed with a Mascot score of 80 for peptide mass fingerprint and ANOVA $p \leq 0.05$, and a minimum of 6 matched peptides

Spot	Accesion number	Protein description	Score	Sequence coverage %	Peptides matched / searched	MW/pI	Fold change
254	gi|58337734	beta-galactosidase small subunit	124	38	10/45	35966/ 5.53	+12.7
628	gi|58337726	galactokinase	100	37	12/56	43521/4.74	+5.0
29	gi|58337725	galactose-1-phosphate uridylyltransferase	146	43	20/68	55735/5.48	+4.8
311	gi|58336405	D-lactate dehydrogenase	135	38	13/34	39177/4.96	-4.8
255	gi|58337735	UDP-glucose 4-epimerase	163	37	14/36	36458/5.95	+4.7
457	gi|58336994	phosphate starvation inducible protein stressrelated	113	48	12/71	21503/5.46	+4.4
630	gi|58337059	mannose-6-phosphate isomerase	98	37	11/48	36677/6.03	+4.3
458	gi|58336994	phosphate starvation inducible protein stressrelated	130	63	15/77	21503/5.46	+4.2
631	Mixture						+3.9
	gi|58337735	UDP-glucose 4-epimerase	235	76	25/92	36458/5.95	
	gi|58336950	UTP-glucose-1-phosphate uridylyltransferase	118	57	15/92	33875/5.90	
632	gi|58337322	oxidoreductase	124	42	13/63	31816/5.19	+3.9
211	gi|58336405	D-lactate dehydrogenase	141	50	18/67	39177/4.96	+3.3
633	gi|58337735	UDP-glucose 4-epimerase	303	83	30/85	36458/5.95	+3.1
623	gi|58337488	hypothetical protein LBA1206	170	42	12/42	31352/5.15	+3.1
16	gi|58336392	ribonucleoside triphosphate reductase	289	46	33/73	83982/5.62	+2.9
634	gi|58338190	deoxyadenosine kinase	79	30	7/44	24765/5.70	-2.9
635	gi|58336733	putative oxalyl-CoA decarboxylase	228	42	25/71	60969/5.03	-2.9
213	gi|58337704	dihydroxyacetone kinase	110	36	12/44	36307/5.16	-2.9
636	gi|58336994	phosphate starvation inducible protein stressrelated	79	33	7/24	21503/5.46	+2.8
436	gi|58337318	oxidoreductase	104	49	9/23	23070/5.78	+2.6
140	gi|58337152	elongation factor Tu	176	50	19/68	43609/4.97	+2.6
637	gi|58336369	fructokinase	161	50	17/45	32016/5.08	+2.4
232	gi|58337019	glyceraldehyde-3-p dehydrogenase	138	37	12/35	36643/5.92	+2.3
321	gi|58337860	fructose-bisphosphate aldolase	206	65	21/85	33560/4.94	-2.2
114	gi|58336560	UDP-N-acetylglucosamine pyrophosphorylase	100	30	13/46	50162/5.57	-2.2
195	gi|58336608	ala racemase	81	29	10/39	41801/6.02	+2.1
295	gi|58337322	oxidoreductase	116	44	12/50	31816/5.19	+2.1

50	gi|58337255	pyruvate kinase	233	38	29/79	63136/5.23	+1.9
15	gi|58336392	ribonucleoside triphosphate reductase	91	13	10/26	83982/5.62	-1.9
638	gi|58336743	chaperonin GroEL	167	45	15/97	57785/4.98	-1.9
280	gi|58337019	glyceraldehyde-3-p dehydrogenase	239	76	24/97	36643/5.92	+1.8
256	gi|58337089	F_0F_1 ATP synthase subunit gamma	136	42	18/73	35512/5.93	-1.8
130	gi|58336600	serine hydroxymethyl transferase	112	26	12/44	45276/5.56	-1.8
91	gi|58337153	trigger factor	93	34	17/90	49275/4.72	-1.7
546	gi|58336978	phosphotransferase system enzyme II	105	55	9/38	13904/4.84	+1.7
84	gi|58337008	phosphoglucomutase	186	47	26/100	64122/5.18	+1.6
204	gi|58336540	inosine-5' monophosphate dehydrogenase	247	63	24/96	39816/5.75	-1.6
115	gi|58336750	glucose-6-P 1-dehydrogenase	157	39	17/43	55824/5.57	-1.6
75	gi|58337220	citrate lyase alpha chain	116	29	13/36	55315/5.53	-1.6
108	gi|58338136	adenylosuccinate synthetase	157	51	21/82	47851/5.38	-1.6
131	gi|58338136	adenylosuccinate synthetase	185	55	23/95	47851/5.38	-1.6

Fig. 1.

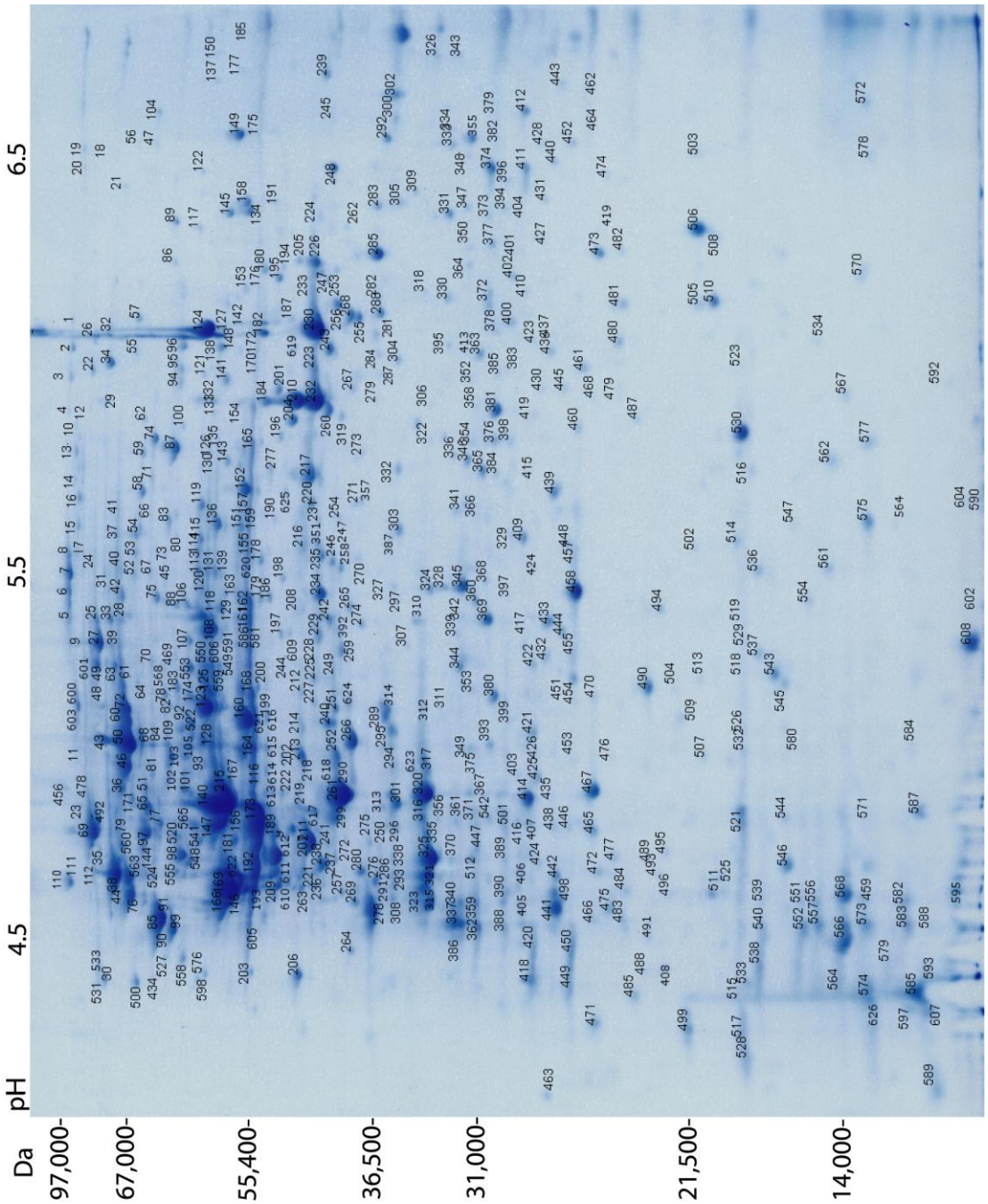

Fig. 2.

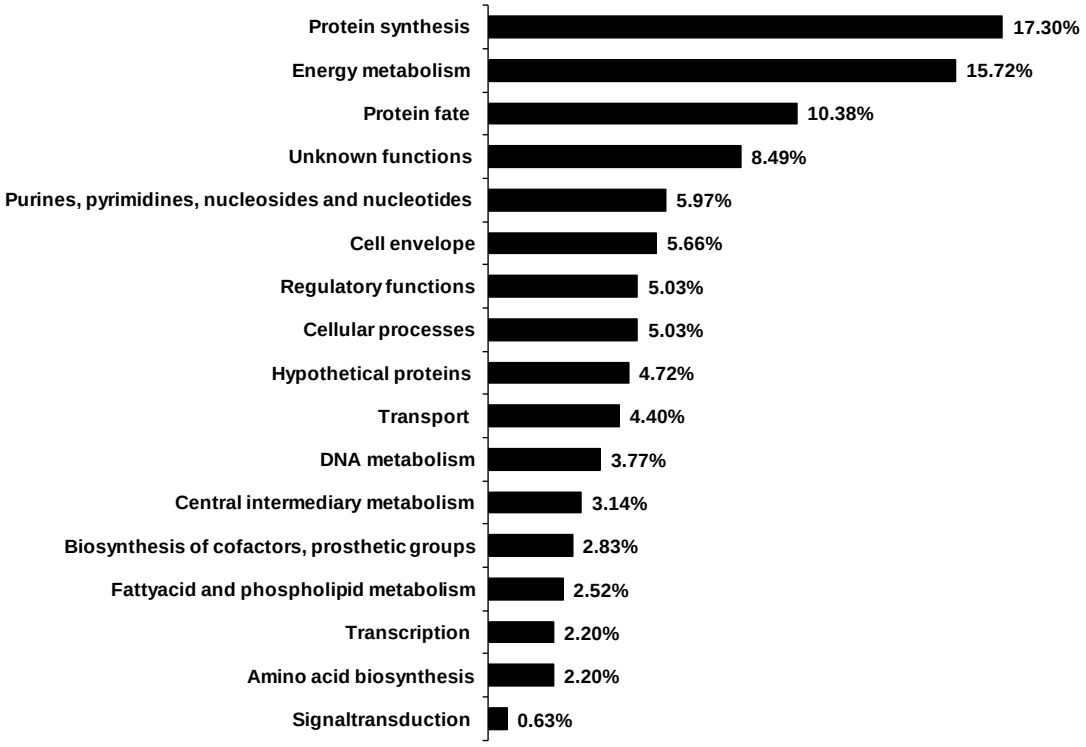
Protein synthesis
17.30%
Energy metabolism
15.72%
Protein fate
10.38%
Unknown functions
8.49%
Purines, pyrimidines, nucleosides and nucleotides
5.97%
Cell envelope
5.66%
Regulatory functions
5.03%
Cellular processes
5.03%
Hypothetical proteins
4.72%
Transport
4.40%
DNA metabolism
3.77%
Central intermediary metabolism
3.14%
Biosynthesis of cofactors, prosthetic groups
2.83%
Fattyacid and phospholipid metabolism
2.52%
Transcription
2.20%
Amino acid biosynthesis
2.20%
Signaltransduction
0.63%

Fig. 3A.

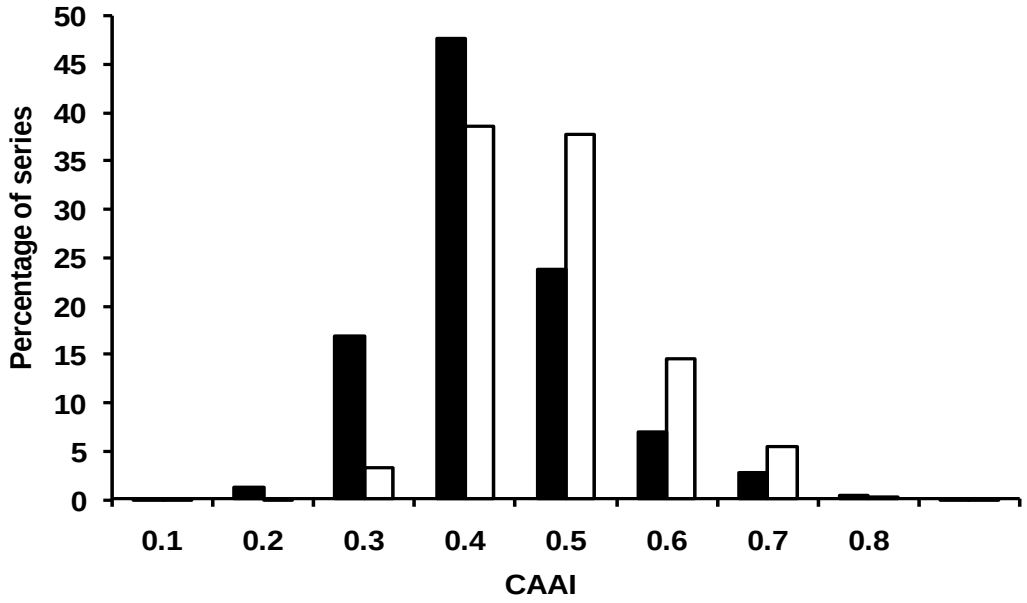
Percentage of series
50
45
40
35
30
25
20
15
10
5
0
0.1
0.2
0.3
0.4
0.5
0.6
0.7
0.8
CAAI

Fig. 3B.

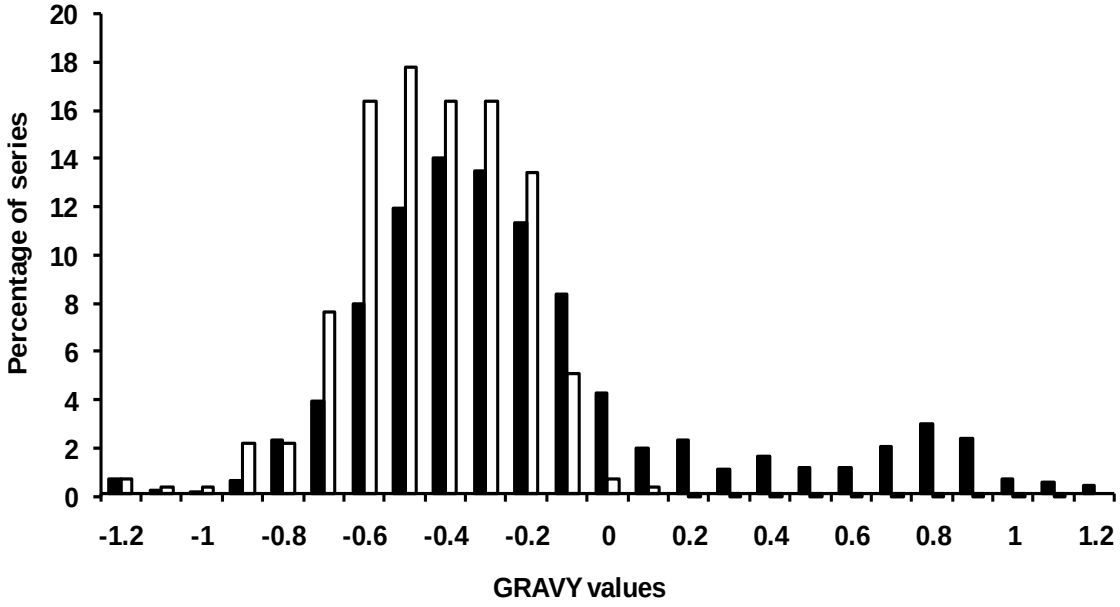
Percentage of series
20
18
16
14
12
10
8
6
4
2
0
-1.2
-1
-0.8
-0.6
-0.4
-0.2
0
0.2
0.4
0.6
0.8
1
1.2
GRAVY values

Fig. 4A.

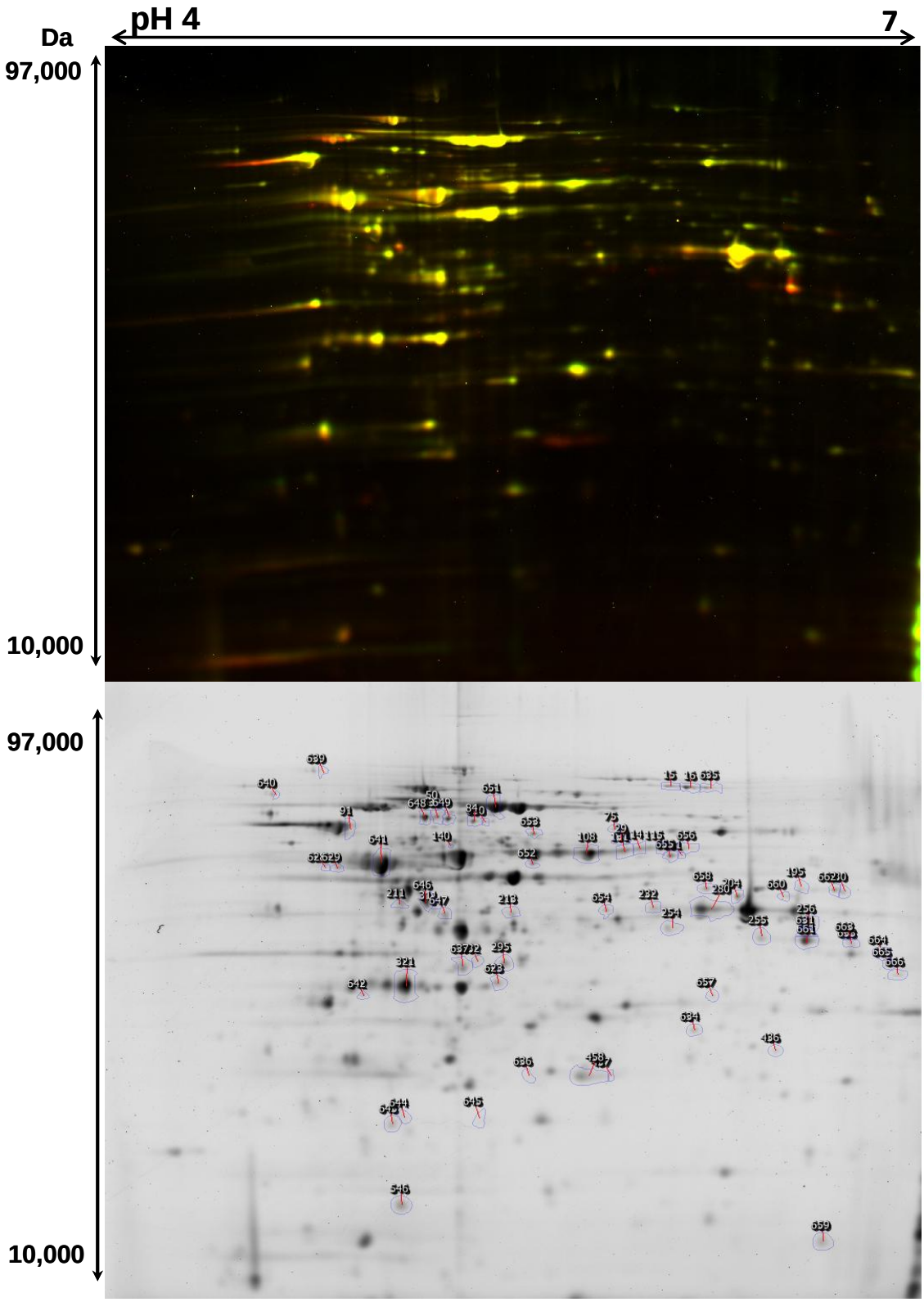

Fig. 4B.

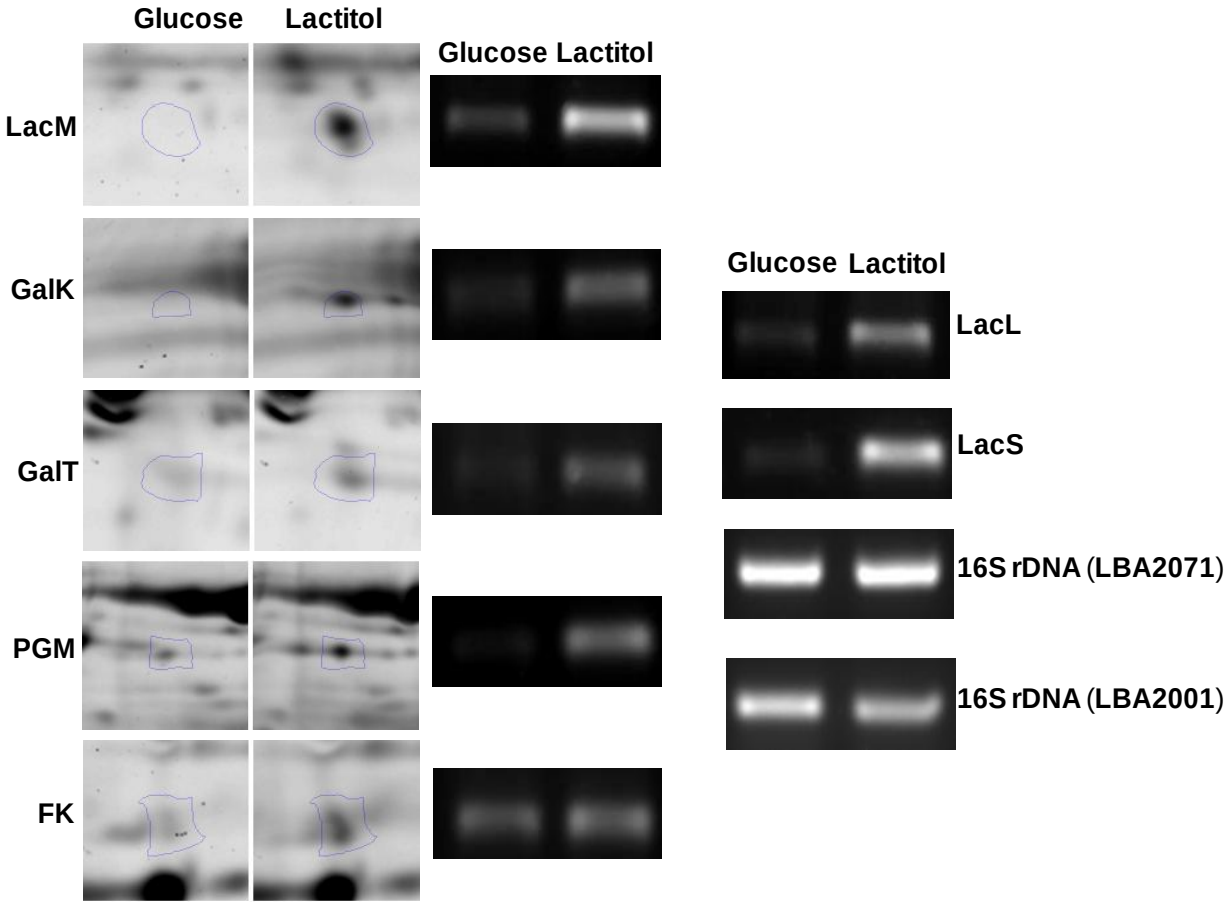
Glucose
Lactitol
LacM
GalK
GalT
PGM
FK
Glucose Lactitol
Glucose Lactitol
LacL
LacS
16S rDNA (LBA2071)
16S rDNA (LBA2001)

Fig. 5.

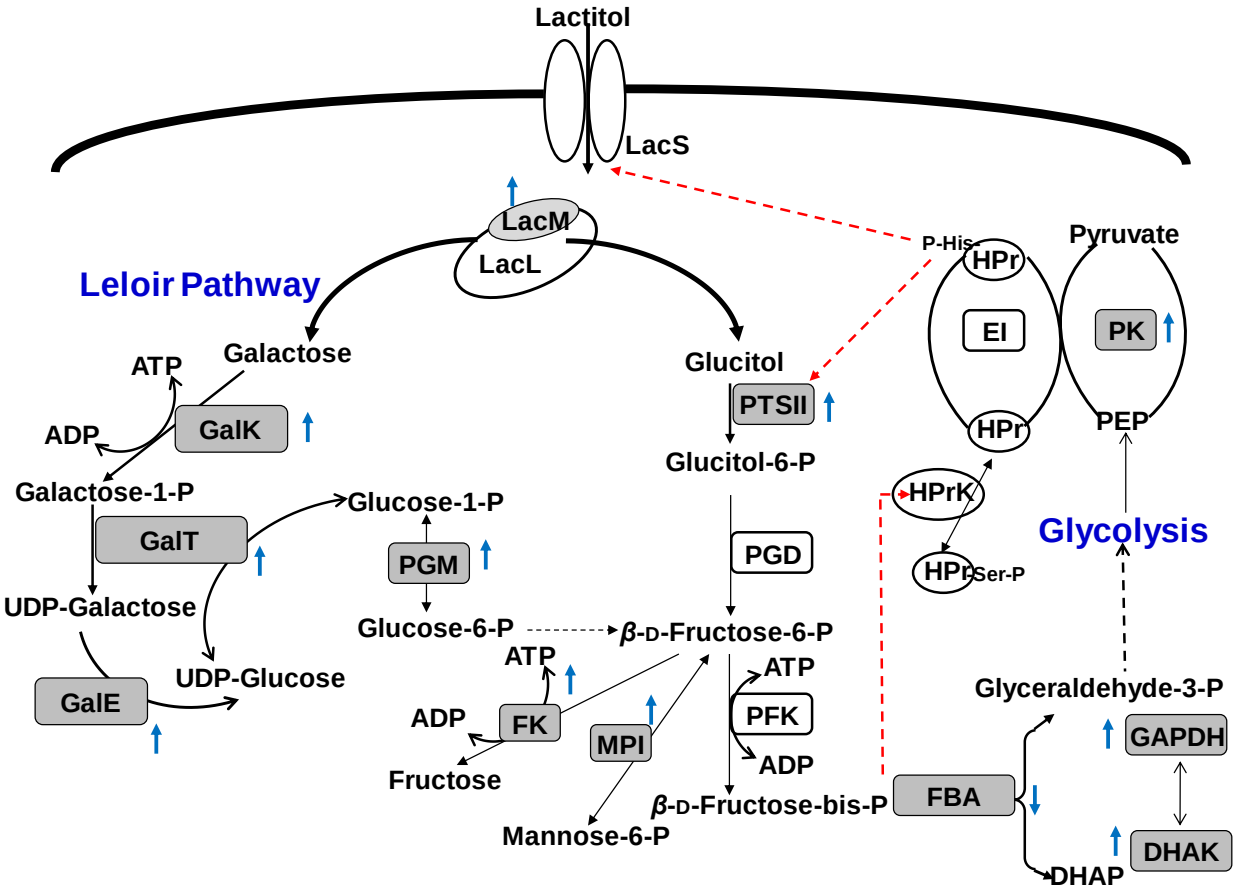
Lactitol
LacS
LacM
LacL
Leloir Pathway
Galactose
ATP
ADP
GalK
Galactose-1-P
GalT
Glucose-1-P
PGM
UDP-Galactose
GalE
UDP-Glucose
Glucose-6-P
β-D-Fructose-6-P
ATP
ADP
FK
Fructose
MPI
Mannose-6-P
ATP
PFK
ADP
β-D-Fructose-bis-P
Glucitol
PTSII
Glucitol-6-P
PGD
P-His
HPr
EI
HPr
HPrK
HPr-Ser-P
Pyruvate
PK
PEP
Glycolysis
Glyceraldehyde-3-P
GAPDH
FBA
DHAK
DHAP

CHAPTER 3

2D-gel based alkaline proteome of the probiotic bacterium *Lactobacillus acidophilus* NCFM

2D-gel based alkaline proteome of the probiotic bacterium *Lactobacillus acidophilus* NCFM

Avishek Majumder[1], Liyang Cai[1], Morten Ejby[1], Bjarne Gregers Schmidt[1], Sampo J. Lahtinen[2], Susanne Jacobsen[1*] and Birte Svensson[1*]

1. Enzyme and Protein Chemistry, Department of Systems Biology, Technical University of Denmark, Søltofts Plads, Building 224, DK-2800 Kgs. Lyngby, Denmark.
2. Danisco Bioactives, Health & Nutrition, Sokeritehtaantie 20, 02460 Kantvik, Finland.

***Corresponding authors:**

Birte Svensson & Susanne Jacobsen
Enzyme and Protein Chemistry
Department of Systems Biology
Technical University of Denmark
Søltofts Plads, Building 224
DK-2800 Kgs. Lyngby
Denmark
Phone: +45 45252740; +45 45252741; Fax:+45 45886307
Email: bis@bio.dtu.dk; sja@bio.dtu.dk

Abbreviations:

CAAI, codon-anticodon adaptation index; LAB, lactic acid bacteria; NCFM, *Lactobacillus acidophilus* NCFM; SEM, semi-defined medium; SLAP domain, surface layer protein domain; SLH, S-layer homology.

Key words: *Lactobacillus acidophilus* NCFM, alkaline proteome, probiotic, cup-loading, 2-DE

Abstract

Lactobacillus acidophilus NCFM (NCFM) is a well documented probiotic bacterium isolated from human gut. Detailed 2D-gel based NCFM proteomics addressed the so-called alkaline range, *i.e.* pH 6−11. Proteins were identified in 150 of the 202 spots picked from the Coomassie brilliant blue stained 2D-gel using MALDI-TOF-MS. The 102 unique gene products among the 150 protein identifications were assigned to different functional categories, and evaluated by considering a calculated distribution of abundance as well as GRAVY values. None of the very few available lactic acid bacteria proteome reference maps available included the range of p*I* > 7.0. The present report of such data on the proteome of NCFM fundamentally complements current knowledge on protein profiles limited to the acid and neutral pH range.

Lactobacillus acidophilus NCFM (NCFM) is a well documented probiotic Gram-positive, homo-fermentative bacterium isolated from a human source [1]. While, the carbohydrate utilization and bile stress tolerance of NCFM have been studied previously by transcriptomics [2, 3], gel-based proteomics was applied to gain insights into physiological processes (see [4] for a review). Thus various proteome analyses of lactic acid bacteria (LAB) address physiological changes associated with *e.g.* growth [5], culture medium composition [6] and adaptation to the intestinal environment [7]. A shortcoming of gel-based proteomics *per se* that also applies to LAB, stems from that only a sub-set of the soluble proteome is described at p*I* 3−7. Technical challenges associated with IEF at pH > 7 include migration of DTT causing streaky 2-DE patterns and the electro endosmosis that perturbs the steady-state position of the proteins [8]. Sample application strategies like cup loading and paper bridge loading have been reported to improve analysis of alkaline proteomes [9]. Thus, bacterial alkaline proteomes have been established for *e.g.* *Bacillus subtilis* by using cup-loading [10], by enrichment using acid incubation of the *Escherichia coli* alkaline proteome [11], by cup-loading in case of *Lactococcus lactis* [12], and by paper-bridge sample loading for *Trypanosoma cruzi* [13].

The NCFM genome encompasses a total of 1862 open reading frames (ORFs) (http://www.ncbi.nlm.nih.gov; NCBI: CP000033) and gives a characteristic bimodal distribution of the p*I* values which for 1104 proteins are predicted to p*I* > 7.0. The goal of the present study is to establish an NCFM proteome reference map for the alkaline region. The whole cell protein extract from the late-log phase of NCFM grown in semi-defined media (SEM) was cup-loaded onto IPG strips of pH 6−11. In-gel protein digestion and MALDI-TOF MS for 202 CBB stained spots resulted in 150 identifications that provide the first overview of an alkaline proteome from *Lactobacillus* sp.

NCFM (Danisco USA Inc., Madison, WI, USA) was grown (in triplicate) under aerobic conditions without agitation at 37 °C in 40 mL batch culture in SEM for LAB [14] supplemented with 1% glucose as carbon source. The cells were harvested at late-log phase (A_{600} of 2.0) by centrifugation (3,200 *g*, 10 min, 4 °C), and washed twice with 0.9% NaCl. The cell pellet was added an approximately equal volume of acid washed glass beads (<100 µm diameter; Sigma, Brøndby, Denmark) followed by 300 µL phenol (Tris saturated pH 8.0) and

300 µL 10 mM Tris, 10 mM DTT (pH 8.0). Disruption was carried out (Bio 101 Savant FastPrep FP 120 bead beater, Savant, Farmingdale, USA) at a speed of 6.5 m/s for four cycles of 45 s each with intermittent cooling on ice. The cell lysate was centrifuged (10,000 *g*, 10 min, 4 ºC) resulting in three distinct phases. The phenol phase was transferred to a microtube, added ice-cold ethanol (four volumes), kept at −20 ºC overnight and centrifuged (15,000 *g*, 10 min, 4 ºC). The resulting precipitate was dissolved in 300 µl rehydration buffer (7 M urea, 2 M thiourea, 48 mM CHAPS, 200 mM bis(2-hydroxyethyl) disulfide (HED), 5% glycerol, 10% 2-propanol, and 2% pharmalyte pH 6−11 (GE Life Sciences, Uppsala, Sweden)). The protein concentration was determined (2D Quant kit; GE Healthcare) and the samples kept at −80 °C until use.

IPG strips (pH 6−11, 18 cm; GE Life Sciences), were passively rehydrated (340 µL rehydration buffer) overnight (Immobiline DryStrip Reswelling Tray) at room temperature. Proteins (350 µg) from whole cell extract in 100 µL rehydration buffer were applied using cup-loading (Cup Loading Manifold; GE Life Sciences) according to the manufacturer's instructions and IEF was performed at 30 V for 10 min, 150 V for 2 h, 1000 V for 30 min, gradient to 8000 V for 4 h, and kept at 8000 V to a total of 31 kVh.

Subsequently, strips were equilibrated in two steps of 15 min with 5 mL equilibration buffer (6 M urea, 30% glycerol, 50 mM Tris-HCl, pH 8.8, 2% SDS, 0.01% bromophenol blue) supplemented with 1% DTT and 2.5% iodoacetamide, respectively. The second dimension (SDS-PAGE; Ettan^{TM} DALT *six* Electrophoresis Unit; GE Life Sciences) was run at 1 W/gel for 1 h followed by 12 W/gel until the dye front reached the gel bottom and stained by colloidal CBB [15]. Images of the gels were generated (Microtek scanner; Scan maker 9800XL; Microtek, Carson, USA) using Photoshop CS4 software and image analysis was done using the algorithm for blob images [16]. The 202 gel spots consistently present (three biological and two technical replicates) were manually excised from a master gel (Fig. 1) and subjected to in-gel digestion by trypsin as described [17]. Aliquots (1 µL) of the trypsin spot-digests were applied to the Anchor Chip target plate (Bruker-Daltonics, Bremen, Germany), covered by 1 µL matrix solution (0.5 µg μL^{-1} CHCA in 90% ACN, 0.1% TFA) and washed in 0.02% TFA. MS and MS/MS spectra were obtained in auto-mode (Ultraflex II MALDI-TOF MS mass spectrometer; Bruker-Daltonics) operating in a result-dependent acquisition mode.

Peptide mass maps were acquired in reflectron mode with 500 laser shots per spectrum. Spectra were calibrated externally and internally using a tryptic digest of β-lactoglobulin (5 pmol μl^{-1}) and porcine trypsin autolysis products, respectively, to mass accuracy within 80 ppm and $\pm$ 0.7 Da. MS/MS data were acquired with stop conditions so that 1000–1600 laser shots were accumulated for each spectrum. MS together with MS/MS spectra were searched against NCBInr database for bacteria (NCBInr 20090826 (9523564 sequences; 3256669569 residues) by using the MASCOT software (http://www.matrixscience.com), applying the search parameters; monoisotopic peptide mass accuracy of 80 ppm; maximum of one missed cleavage; carbamidomethylation of cysteine; and partial oxidation of methionine. There were no restrictions with respect to protein *Mr* and p*I*. Spectra were filtered for known autocatalytic trypsin peaks. Signal to noise threshold ratio was set to 1:6. Protein identifications were confirmed by a Mascot score of 80 for PMF, $p \leq 0.05$ and a minimum of 6 matched peptides and for MS/MS by a Mascot score of 50 and $p \leq 0.05$.

A total of 150 proteins representing 102 unique gene products were identified from 202 2-DE spots. The majority of these proteins (61%) showed p*I* 8.0–10.0 agreeing with the theoretical proteome of p$I \geq 7.0$. The proteins were grouped into different functional categories (Fig. 2; Table 1) using Gene Role Category annotation (http://cmr.jcvi.org/tigr-scripts/CMR/CmrHomePage.cgi). The CAAI (codon-anticodon adaptability index) values of the proteins obtained using DAMBE (http://dambe.bio.uottawa.ca/dambe.asp) were applied to calculate the theoretical relative abundance [18]. The present theoretical CAAI values are in the range 0.21–0.76. Noticeably CAAI values of 0.50–0.76 for the 15 ribosomal proteins indicated constant high abundance in the cell and a similar abundance pattern was observed for these proteins on the 2D-gel. The most intensely stained spots contain 30S ribosomal proteins S8 (spot 196) and S7 (spots 179 and 180) and 50S ribosomal proteins L1 (spot 108, 118, 119 and 122), L5 (spots 157 and 158), L21 (spot 177) and L13 (spots 183 and 184) having CAAI 0.48–0.66. The cell wall associated S-layer protein (CAAI = 0.43) appeared to be the most abundant protein (spots 39a–d) on the 2D-gel. Five proteins, hypothetical protein LBA1408, 16s pseudouridylate synthase, PhoH family phosphate starvation-induced protein, GTP-binding protein and pantothenate metabolism flavoprotein-like protein (Table 1) with low theoretical abundance (CAAI < 0.3) were identified on the 2D-gel (Table 1,

Supplementary Fig. 1A). The GRAVY index of hydrophobicity was calculated using ProtParam tool (http://www.expasy.ch/tools/protparam.html) for all NCFM coding sequences (Supplementary Fig. 1B). Proteins identified from the 2D-gel have GRAVY index of –0.907 - –0.063 (Supplementary Fig. 1B), whereas no hydrophobic proteins (GRAVY index $\geq$ 0.0) were identified probably due to loss during sample preparation and / or electrophoresis. The cellular localization predicted by PSORT version 3.0 (http://www.psort.org/) (Table 1) for the 102 unique gene products indicated 68 proteins to belong to the cytoplasm, 8 to be associated with cytoplasmic membranes and three and two being cell wall and extracellular, respectively. The extracellular and cell wall associated proteins including the S-layer protein may have particularly important roles in the host-microbial interactions of a probiotic bacterium. Twenty one proteins were not assigned a cellular localization.

The many identified proteins involved in protein synthesis (23%) were dominated by proteins of the ribosomal subunits, thus 15 of the 55 proteins forming the ribosome were identified on the 2D-gel. Proteins of unknown function constitute another large fraction (10%). Furthermore, the identifications confirmed the existence for 13 hypothetical proteins (Supplementary Table 1). A BLAST search of these against the Conserved Domain Database (http://www.ncbi.nlm.nih.gov/Structure/cdd/cdd.shtml) and similarity to homologs allowed prediction of a possible function for 10 hypothetical proteins based on the conserved domains (Supplementary Table 1). A motif search using SMART (http://smart.embl-heidelberg.de/) for three hypothetical proteins, whose nearest homologs were identified as conserved hypothetical proteins, showed hypothetical protein LBA0695 to comprise a signal peptide sequence and Big_3 domain (PFAM accession number: PF07523). This entry represents bacterial domains with an Ig-like fold and is found in a variety of bacterial surface proteins. No domains, however were identified for the hypothetical proteins LBA0157, LBA0229 and LBA0864, but LBA0864, has a signal peptide and might be secreted to the extracellular milieu. Eighty-three of the 102 unique proteins were identified from a single spot, while 19 were found in spots with different p*I* indicating the presence of PTMs. Thus spots migrating with similar apparent molecular mass and varying p*I* from bacterial proteomes have been suggested to arise by phosphorylation [19] or deamidation [20]. Of the proteins showing such charge heterogeneity nine are ribosomal proteins. Furthermore, the 50S ribosomal protein L6 (spot

168) was present in 18 different spots showing both mass and charge heterogeneity. Some of the L6 forms were found at the site of cup-loading probably due to protein precipitation (Table 1, Fig. 1), other forms of lower *Mr* indicated possible cleavage of the protein during sample preparation.

The S-layer protein (LBA0169) was seen to be the most abundant on the 2D-gel (spots 39a-d) having an *Mr* of 46.5 kDa and p*I* of 9.59. S-layer proteins have been identified in major bacterial phyla and were documented to function in maintaining and determining the cell shape, protection against mechanical forces, and in interactions with the environment [21]. Noticeably interaction with the host is important for the probiotic function [22]. S-layer proteins from different bacterial genera have p*I* of 4−6, but S-layer proteins in *Lactobacillus* sp. are alkaline p*I* (9−10) and lack the SLH (S-layer homology) motif common (PF00395) to S-layer proteins (http://pfam.janelia.org/) [23]. The S-layer proteins from *Lactobacillus* contain SLAP (surface layer protein) domain (PFO3217) and recognize neutral polysaccharide as a binding site. In NCFM the S-layer protein has an important role in adhesion to intestinal cells and was shown to interact with dendritic cells *via* the dendritic cell specific ICAM-3-grabbing nonintegrin receptor [22].

Very few bacterial proteome maps include information on proteins of p*I* > 7 [10, 12, 13, 24] and the present study adds knowledge on proteins of p*I* 6–11. The reference map with 102 identified unique proteins is the first report of *Lactobacillus* sp. in the alkaline region. It represents a useful dataset for Gram-positive bacteria, and would aid studies into various physiological processes at the proteome level.

Acknowledgements

Birgit Andersen is acknowledged for technical assistance with mass spectrometric analysis. This work was supported by the Danish Strategic Research Council's Programme Committee on Health, Food and Welfare (FøSu), the Danish Research Council for Natural Science and the Danish Center for Advanced Food Studies (LMC). AM is grateful to the Technical University of Denmark for a Hans Christian Ørsted postdoctoral fellowship.

References

[1] Sanders, M. E., Klaenhammer, T. R., The scientific basis of *Lactobacillus acidophilus* NCFM functionality as a probiotic. *J. Dairy Sci.* 2001, *84*, 319-331.

[2] Barrangou, R., Azcarate-Peril, M. A., Duong, T., Conners, S. B. *et al.*, Global analysis of carbohydrate utilization by *Lactobacillus acidophilus* using cDNA microarrays. *Proc. Natl. Acad. Sci. U. S. A.* 2006, *103*, 3816-3821.

[3] Pfeiler, E. A., Azcarate-Peril, M. A., Klaenhammer, T. R., Characterization of a novel bile-inducible operon encoding a two-component regulatory system in *Lactobacillus acidophilus*. *J. Bacteriol.* 2007, *189*, 4624-4634.

[4] Hecker, M., Antelmann, H., Buettner, K., Bernhardt, J., Gel-based proteomics of Gram-positive bacteria: A powerful tool to address physiological questions. *Proteomics* 2008, *8*, 4958-4975.

[5] Cohen, D. P. A., Renes, J., Bouwman, F. G., Zoetendal, E. G. *et al.*, Proteomic analysis of log to stationary growth phase *Lactobacillus plantarum* cells and a 2-DE database. *Proteomics* 2006, *6*, 6485-6493.

[6] Koskenniemi, K., Koponen, J., Kankainen, M., Savijoki, K. *et al.*, Proteome analysis of *Lactobacillus rhamnosus* GG using 2-D DIGE and mass spectrometry shows differential protein production in laboratory and industrial-type growth media. *J. Proteome Res.* 2009, *8*, 4993-5007.

[7] Roy, K., Meyrand, M., Corthier, G., Monnet, V., Mistou, M. Y., Proteomic investigation of the adaptation of *Lactococcus lactis* to the mouse digestive tract. *Proteomics* 2008, *8*, 1661-1676.

[8] Olsson, I., Larsson, K., Palmgren, R., Bjellqvist, B., Organic disulfides as a means to generate streak-free two-dimensional maps with narrow range basic immobilized pH gradient strips as first product dimension. *Proteomics* 2002, *2*, 1630-1632.

[9] Bak-Jensen, K. S., Laugesen, S., Roepstorff, P., Svensson, B., Two-dimensional gel electrophoresis pattern (pH 6-11) and identification of water-soluble barley seed and malt proteins by mass spectrometry. *Proteomics* 2004, *4*, 728-742.

[10] Ohlmeier, S., Scharf, C., Hecker, M., Alkaline proteins of *Bacillus subtilis*: First steps towards a two-dimensional alkaline master gel. *Electrophoresis* 2000, *21*, 3701-3709.

[11] Wang, S. Y., Zhu, R., Peng, B., Liu, M. M. *et al.*, Identification of alkaline proteins that are differentially expressed in an overgrowth-mediated growth arrest and cell death of *Escherichia coli* by proteomic methodologies. *Proteomics* 2006, *6*, 5212-5220.

[12] Drews, O., Reil, G., Parlar, H., Görg, A., Setting up standards and a reference map for the alkaline proteome of the gram-positive bacterium *Lactococcus lactis*. *Proteomics* 2004, *4*, 1293-1304.

[13] Magalhaes, A. D., Charneau, S., Paba, J., Guercio, R. A. P. *et al.*, *Trypanosoma cruzi* alkaline 2-DE: Optimization and application to comparative proteome analysis of flagellate life stages. *Proteome Sci.* 2008, *6*, 24.

[14] Barrangou, R., Altermann, E., Hutkins, R., Cano, R., Klaenhammer, T. R., Functional and comparative genomic analyses of an operon involved in fructooligosaccharide utilization by *Lactobacillus acidophilus*. *Proc. Natl. Acad. Sci. U. S. A.* 2003, *100*, 8957-8962.

[15] Candiano, G., Bruschi, M., Musante, L., Santucci, L. *et al.*, Blue silver: A very sensitive colloidal coomassie G-250 staining for proteome analysis. *Electrophoresis* 2004, *25*, 1327-1333.

[16] dos Anjos, A., Møller, A. L. B., Ersbøll, B. K., Finnie, C., Shahbazkia, H. R., New approach for segmentation and quantification of two-dimensional gel electrophoresis images. *Bioinformatics* 2011, *27*, 368-375.

[17] Majumder, A., Sultan, A., Jersie-Christensen, R. R., Ejby, M. *et al.*, Proteome reference map of *Lactobacillus acidophilus* NCFM and quantitative proteomics towards understanding the prebiotic action of lactitol. *Proteomics* 2011, *11*, 3470-3481.

[18] Xia, X. H., An improved implementation of codon adaptation index. *Evol. Bioinform.Online* 2007, *3*, 53-58.

[19] Rosen, R., Becher, D., Buttner, K., Biran, D. *et al.*, Highly phosphorylated bacterial proteins. *Proteomics* 2004, *4*, 3068-3077.

[20] Robinson, N. E., Protein deamidation. *Proc. Natl. Acad. Sci. U. S. A.* 2002, *99*, 5283-5288.

[21] Li, P., Yin, Y., Yu, Q., Yang, Q., *Lactobacillus acidophilus* S-layer protein-mediated inhibition of *Salmonella*-induced apoptosis in caco-2 cells. *Biochem. Biophys. Res. Commun.* 2011, *409*, 142-147.

[22] Konstantinov, S. R., Smidt, H., de Vos, W. M., Bruijns, S. C. M. *et al.*, S layer protein A of *Lactobacillus acidophilus* NCFM regulates immature dendritic cell and T cell functions. *Proc. Natl. Acad. Sci. U. S. A.* 2008, *105*, 19474-19479.

[23] Finn, R. D., Mistry, J., Tate, J., Coggill, P. *et al.*, The pfam protein families database. *Nucleic Acids Res.* 2010, *38*, D211-D222.

[24] Wang, S. Y., Zhu, R., Peng, B., Liu, M. M. *et al.*, Identification of alkaline proteins that are differentially expressed in an overgrowth-mediated growth arrest and cell death of *Escherichia coli* by proteomic methodologies. *Proteomics* 2006, *6*, 5212-5220.

Figure Legends

Fig. 1. A detailed 2-DE of 350 μg whole cell extract soluble proteins (pH 6−11) of *Lactobacillus acidophilus* NCFM grown on LABSEM with 1% glucose. Numbered spots are chosen for analysis by in-gel digestion and mass spectrometry.

Fig. 2. Functional grouping of the 102 identified unique proteins on the 2-DE (pH 6−11) of *Lactobacillus acidophilus* NCFM.

Table 1. Protein identifications from 2D-gel (pH 6−11) of whole cell extract of *L. acidophilus* NCFM grown on SEM medium with 1% glucose. Protein identifications were confirmed with a Mascot score of 80 for peptide mass fingerprint, ANOVA $\leq$ 0.05 and a minimum of 6 matched peptides. Single peptide based protein identifications were confirmed with a Mascot score of 50, ANOVA $\leq$ 0.05[a]

Proteins identified by peptide mass fingerprint									
Spot	**Accession number**	**Protein description**	**Score**	**ANOVA**	**Sequence coverage%**	**Peptides matched/ searched**	***Mr*/p*I***	**Localization[b]**	**Functional role[c]**
3	gi|58336758	mismatch repair protein	162	3.3e-010	19%	18/33	88092/7.75	C	DM
4	gi|58337413	DNA topoisomerase IV subunit A	201	4.1e-014	26%	23/36	92270/8.1	C	DM
6	gi|58336622	ATPase	314	2.1e-025	44%	34/61	91966/7.71	C	PF
9	gi|58338020	Oligopeptidase	104	0.00021	15%	9/16	68213/4.84	C	PF
11	gi|58338214	tRNA uridine 5-carboxymethylaminomethyl modification enzyme GidA	106	0.00013	17%	12/16	70719/6.99	C	UF
14	gi|58337150	hypothetical protein LBA0843	87	0.01	14%	8/14	65599/8.78	C	UF
19	gi|58337016	hypothetical protein LBA0695	293	2.6e-023	38%	31/61	61777/9.24	U	HP
24	gi|58336504	hypothetical protein LBA0157	133	2.6e-007	35%	14/32	53966/8.76	C	UF
25	gi|58336866	RNA methyltransferase	241	4.1e-018	52%	31/78	50867/8.99	C	PS
26	gi|58337604	exodeoxyribonuclease VII (large subunit) EX7L	207	1.00E-14	50%	33/80	52626/9.1	C	DM
28	gi|58336533	fibronectin domain-containing protein	190	5.2e-013	44%	22/45	52088/9.59	U	T
30	gi|58337996	GTP-binding protein	229	6.5e-017	54%	24/38	47084/8.35	C	UF
31	gi|58337169	hypothetical protein LBA0864	93	0.0038	30%	14/79	54757/9.66	U	HP
34	gi|58337078	UDP-N-acetylmuramyl tripeptide synthetase	86	0.017	25%	11/51	50447/8.77	C	CE
35	gi|58337245	GTPase ObgE	143	2.6e-008	36%	19/38	47592/6.31	C	UF
36	gi|58337078	UDP-N-acetylmuramyl tripeptide synthetase	152	3.3e-009	34%	19/46	50447/8.77	C	CE
37	gi|58337101	thiazole biosynthesis protein	120	5.2e-006	18%	14/21	45812/6.24	C	BCPC; PS
39a	gi|58336516	S-layer	119	6.5e-006	32%	15/56	46542/9.59	CW	CE
39b	gi|58336516	S-layer	202	3.3e-014	46%	22/69	46542/9.59	CW	CE
39c	gi|58336516	S-layer	268	8.2e-021	48%	23/63	46542/9.59	CW	CE
39d	gi|58336516	S-layer	245	1.6e-018	40%	23/46	46542/9.59	CW	CE

40	gi|58337078	UDP-N-acetylmuramyl tripeptide synthetase	86	0.017	25%	11/51	50447/8.77	C	CE
42	gi|58336608	ala racemase	116	1.3e-005	36%	12/29	41801/6.02	C	CE
45	gi|58337118	N-acetylglucosaminyl transferase	110	5.2e-005	29%	13/49	40718/8.56	U	CE
46	gi|58337238	pantothenate metabolism flavoprotein-like protein	99	0.0007	31%	12/43	43914/8.67	C	BCPC
47	gi|58336952	hydroxymethylglutaryl-CoA reductase	222	3.3e-016	43%	21/48	44143/8.91	U	FP
48	gi|58337440	hypothetical protein LBA1155	204	2.1e-014	43%	22/52	42521/9.18	C	CIM
51	gi|58337436	pseudouridine synthase	129	6.5e-007	44%	14/63	34227/9.11	C	PS
52	gi|58336409	penicillin-binding protein	125	1.6e-006	20%	9/22	42206/9.37	E	CP
53	gi|58337247	metallo-beta-lactamase superfamily	116	1.3e-005	52%	15/94	34806/8.84	C	UF
54	gi|58337019	glyceraldehyde-3-p dehydrogenase	182	3.3e-012	67%	22/90	36643/5.92	C	EM
55	gi|58337019	glyceraldehyde-3-p dehydrogenase	242	3.3e-018	67%	25/81	36643/5.92	C	EM
56	gi|58337019	glyceraldehyde-3-p dehydrogenase	284	2.1e-022	76%	30/74	36643/5.92	C	EM
57	gi|58336550	tryptophanyl-tRNA synthetase II	283	2.6e-022	52%	25/57	38302/6.49	C	PS
58	gi|58337019	glyceraldehyde-3-p dehydrogenase	290	5.2e-023	70%	26/50	36643/5.92	C	EM
59	gi|58336998	HPr kinase/phosphorylase	146	1.3e-008	44%	14/44	36305/6.73	C	RF; T
60	gi|58337430	site-specific tyrosine recombinase XerS	137	1.0e-07	35%	13/28	39747/9.54	U	DM
63	gi|58337483	GTP-binding protein Era	163	2.6e-010	52%	16/43	34097/7.03	CM	CP; RF
65	gi|58337012	hypothetical protein LBA0691	109	6.5e-005	36%	15/43	33454/7.72	C	UF
66	gi|58337089	F0F1 ATP synthase subunit gamma	141	4.1e-008	38%	15/28	35512/5.93	C	EM
67	gi|58337580	oligopeptide ABC transporter ATP-binding protein	141	4.1e-008	40%	14/38	37703/6.29	CM	T
68	gi|58336442	putative regulatory protein	263	2.6e-020	49%	21/33	35831/8.81	U	RF
69	gi|58337485	PhoH family phosphate starvation-induced protein	83	0.027	30%	7/25	35008/8.69	C	UF
70	gi|58337977	UTP-glucose-1-phosphate uridylyltransferase	152	3.3e-009	38%	11/20	33055/7.04	C	CE
71	gi|58336950	UTP-glucose-1-phosphate uridylyltransferase	184	2.1e-012	47%	19/52	33875/5.9	C	CE
72	gi|58337485	PhoH family phosphate starvation-induced protein	224	2.1e-016	67%	21/43	35008/8.69	C	PS
74	gi|58338074	chromosome partitioning protein	157	1.0e-09	60%	19/52	33130/9.15	C	CP
75	gi|58338074	chromosome partitioning protein	196	1.3e-013	60%	20/37	33130/9.15	C	CP
77	gi|58337302	penicillin-binding protein	112	3.3e-005	31%	15/65	40946/9.63	E	CP

78	gi|58336456	hypothetical protein LBA0109	94	0.0026	29%	10/39	36207/8.62	C	DM
79	gi|58337735	UDP-glucose 4-epimerase	196	1.3e-013	39%	13/22	36458/5.95	U	EM
81	gi|58337028	UDP-N-acetylenolpyruvoylglucosamine reductase	81	0.05	23%	7/39	32470/6.19	C	CE
82	gi|58336565	ribose-p-pyrophosphokinase	195	1.6e-013	43%	18/40	35684/6.01	C	PPNN
83	gi|58337241	glyoxylate reductase	191	4.1e-013	49%	15/28	35749/6.01	C	CIM
84	gi|58337595	methionyl-tRNA formyltransferase FMT	150	5.2e-009	53%	18/47	34223/6.37	C	PS
85	gi|58338076	chromosome partitioning protein	205	1.6e-014	67%	25/73	31473/7.71	C	CP
86	gi|58338137	guanosine 5'-monophosphate oxidoreductase	162	3.3e-010	45%	16/39	36748/8.24	C	PPNN
89	gi|58337517	cysteine synthase	129	6.5e-007	44%	16/32	32655/6.99	C	AA
90	gi|58337517	cysteine synthase	100	0.00058	40%	11/34	32655/6.99	C	AA
92	gi|58337517	cysteine synthase	189	6.5e-013	61%	21/21	32655/6.99	C	AA
93	gi|58337532	tRNA pseudouridine synthase B	119	6.5e-006	31%	11/21	33657/8.78	C	PS
94	gi|58336431	putative heat shock related serine protease	102	0.00033	26%	7/27	43695/9.42	U	PF
96	gi|58336485	hypothetical protein LBA0138	163	2.6e-010	62%	17/44	28157/8.48	C	HP
97	gi|58337102	16s pseudouridylate synthase	108	8.2e-005	36%	10/26	26359/9.24	C	PS
99	gi|58337781	L-LDH	161	4.1e-010	30%	12/24	33804/7.03	C	EM
100	gi|58337781	L-LDH	219	6.5e-016	52%	18/55	33804/7.03	C	EM
101	gi|58336499	alkylphosphonate ABC transporter	144	2.1e-008	43%	12/26	28462/9.38	CM	T
102	gi|58336609	hypothetical protein LBA0270	83	0.026	34%	7/26	26569/6.31	C	UF
105	gi|58337187	transcriptional regulator	174	2.1e-011	39%	13/31	28083/7.82	C	RF
106	gi|58336702	phosphate ABC transporter ATP-binding protein	83	0.041	27%	7/26	29680/8.94	CM	T
108	gi|58336698	50S ribosomal protein L1			36%	7/51	24717/8.89	C	PS
109	gi|58336650	adenylate kinase	135	1.6e-007	49%	11/43	24743/6.36	C	PPNN
110	gi|58337948	hypothetical protein LBA1690	89	0.0067	34%	8/26	30975/9.66	U	CE
111	gi|58336650	adenylate kinase	142	3.3e-008	51%	12/35	24743/6.36	C	PPNN
112	gi|58336650	adenylate kinase	200	5.2e-014	61%	19/76	24743/6.36	C	PPNN
114	gi|58336630	50S ribosomal protein L3	228	8.2e-017	66%	20/49	23129/9.94	U	PS
115	gi|58336630	50S ribosomal protein L3	185	1.6e-012	54%	15/38	23129/9.94	U	PS
117	gi|58337938	ABC transporter ATP-binding protein	116	1.3e-005	45%	12/25	27358/6.93	CM	T
118	gi|58336698	50S ribosomal protein L1	83	0.028	28%	6/19	24717/8.89	C	PS

119		mixture							
119	gi|58336698	50S ribosomal protein L1	123	2.6e-006	58%	15/55	24717/8.89	C	PS
119	gi|58337445	endonuclease III	105	0.00016	57%	12/55	23783/8.47	C	DM
121	gi|58337938	ABC transporter ATP-binding protein	98	0.00076	39%	10/23	27358/6.93	CM	T
122	gi|58336698	50S ribosomal protein L1	142	3.3e-008	61%	15/55	24717/8.89	C	PS
123	gi|58338086	ABC transporter ATP-binding protein	146	1.3e-008	60%	17/42	24611/9.24	CM	T
125	gi|58337845	methlytransferase	94	0.0021	27%	6/10	25401/6.84	U	PS
126	gi|58336844	transcriptional regulator	182	3.3e-012	57%	14/35	26627/8.8	C	RF
127	gi|58336636	30S ribosomal protein S3	147	1.0e-08	44%	12/27	25055/10.13	C	PS
128	gi|58336636	30S ribosomal protein S3	175	1.6e-011	50%	15/40	25055/10.13	C	PS
130	gi|58336636	30S ribosomal protein S3	156	1.3e-009	47%	14/45	25055/10.13	C	PS
131	gi|58336936	nitroreductase	97	0.0011	29%	10/28	24616/8.67	U	EM
132	gi|58337558	DNA polymerase	152	3.3e-009	57%	13/39	24927/9.11	C	DM
133	gi|58336905	glutamine ABC transporter ATP-binding protein	137	1.0e-07	40%	14/43	27895/6.4	CM	CP; T
134	gi|58337795	putative nicotinate-nucleotide adenyltransferase	119	6.5e-006	28%	13/31	24802/9.32	C	BCPC
136	gi|58337545	uridine mono phosphate kinase	93	0.0028	21%	7/22	25872/7.81	C	PPNN
137	gi|58337545	uridine mono phosphate kinase	108	8.2e-005	37%	13/56	25872/7.81	C	PPNN
138	gi|58337545	uridine mono phosphate kinase	91	0.0043	29%	12/51	25872/7.81	C	PPNN
139	gi|58337679	hypothetical protein LBA1408	152	3.3e-009	49%	15/36	24360/8.65	C	HP
142	gi|58338161	lysin	99	0.00065	35%	9/37	34603/10.28	CW	AA
143	gi|58337098	30S ribosomal protein S4	201	4.1e-014	60%	18/47	23453/9.89	C	PS
144	gi|58337811	dephospho-CoA kinase	134	2.1e-007	48%	11/24	22693/8.79	U	BCPC
145	gi|58337426	lysin	92	0.0049	15%	7/24	41475/9.64	CW	AA
148	gi|58337654	bifunctional pyrimidine regulatory protein PyrR uracil phosphoribosyltransferase	84	0.033	37%	7/27	20099/6.21	C	PPNN
150	gi|58338089	putative phosphoglycerate mutase	153	2.6e-009	52%	15/37	22750/6.31	C	EM
152	gi|58336528	pyrrolidone carboxyl peptidase	159	6.5e-010	55%	12/22	21848/8.85	C	PF
153	gi|58336611	peptidyl-tRNA hydrolase	95	0.0015	52%	9/25	21042/6.97	U	PS
154	gi|58337416	peptidyl-prolyl cis-trans isomerase	97	0.0011	29%	7/20	22351/6.84	C	PF
155	gi|58336389	putative cobalamin adenosyltransferase	114	2.1e-005	40%	9/28	21499/9.1	C	BCPC
156	gi|58337521	adenine phosphoribosyltransferase	189	6.5e-013	60%	11/23	19335/6.1	C	PPNN

157	gi|58336642	50S ribosomal protein L5	222	3.3e-016	88%	19/32	20252/8.72	C	PS
158	gi|58336642	50S ribosomal protein L5	209	6.5e-015	88%	21/41	20252/8.72	C	PS
166	gi|58336644	50S ribosomal protein L6	145	1.6e-008	48%	10/25	19161/9.15	U	PS
167	gi|58336644	50S ribosomal protein L6	157	1e-009	56%	11/29	19161/9.15	U	PS
168	gi|58336644	50S ribosomal protein L6	146	1.3e-008	56%	11/41	19161/9.15	U	PS
169	gi|58336365	50S ribosomal protein L9	155	1.6e-009	79%	19/78	16941/9.54	C	PS
172	gi|58336644	50S ribosomal protein L6	107	0.0001	41%	8/22	19161/9.15	U	PS
173	gi|58336644	50S ribosomal protein L6	82	0.036	32%	6/21	19161/9.15	U	PS
175	gi|58336644	50S ribosomal protein L6	99	0.00065	32%	6/11	19161/9.15	U	PS
176	gi|58337095	hypothetical protein LBA0783	183	2.6e-012	78%	12/25	17028/5.93	C	CP
178	gi|58336644	50S ribosomal protein L6	83	0.024	32%	6/18	19161/9.15	U	PS
179	gi|58336627	30S ribosomal protein S7	198	8.2e-014	83%	17/43	17920/9.81	C	PS
180	gi|58336627	30S ribosomal protein S7	211	4.1e-015	80%	23/69	17920/9.81	C	PS
181	gi|58337810	transcriptional regulator NrdR	84	0.022	53%	9/67	18189/8.68	C	HP
182	gi|58336644	50S ribosomal protein L6	85	0.023	32%	6/32	19161/9.15	U	PS
183	gi|58336661	50S ribosomal protein L13	161	4.1e-010	82%	15/56	16479/9.54	U	PS
184	gi|58336661	50S ribosomal protein L13	128	8.2e-007	77%	12/42	16479/9.54	U	PS
185	gi|58336644	50S ribosomal protein L6	99	0.00065	32%	6/11	19161/9.15	U	PS
186	gi|58336644	50S ribosomal protein L6	82	0.05	32%	6/25	19161/9.15	U	PS
187	gi|58336644	50S ribosomal protein L6	93	0.0028	32%	6/22	19161/9.15	U	PS
188	gi|58336644	50S ribosomal protein L6	122	3.3e-006	39%	7/16	19161/9.15	U	PS
191	gi|58336635	50S ribosomal protein L22	135	1.6e-007	71%	9/36	12806/9.91	C	PS
193	gi|58336635	50S ribosomal protein L22	124	2.1e-006	35%	6/42	12806/9.91	C	PS
195	gi|58336643	30S ribosomal protein S8	104	0.00021	53%	9/59	14523/9.33	C	PS
197	gi|58336643	30S ribosomal protein S8	83	0.029	53%	9/53	14523/9.33	C	PS
199	gi|58336644	50S ribosomal protein L6	82	0.036	36%	7/39	19161/9.15	U	PS
200	gi|58336644	50S ribosomal protein L6	99	0.00065	32%	6/14	19161/9.15	U	PS
202	gi|58336644	50S ribosomal protein L6	90	0.0052	32%	6/15	19161/9.15	U	PS
203	gi|58336644	50S ribosomal protein L6	99	0.00065	32%	6/13	19161/9.15	U	PS
204	gi|58336644	50S ribosomal protein L6	99	0.00067	32%	6/13	19161/9.15	U	PS

206	gi|58336644	50S ribosomal protein L6	93	0.0028	32%	6/13	19161/9.15	U	PS
212	gi|58336629	30S ribosomal protein S10	140	5.2e-008	71%	13/57	11455/9.63	U	PS
225	gi|58337267	DNA-binding protein II HB	92	0.003	60%	6/32	9726/9.52	U	DM; T
228	gi|58336604	50S ribosomal protein L31 type B	140	5.2e-008	88%	11/57	9174/8.86	C	PS

Proteins identified by MS/MS

Spot	Accession number	Protein description	Sequence coverage%	Mr/p*I*	Peptides	Peptide sequence	Score	ANOVA	Localization [b]	Functional role [c]
95	gi|58337812	formamidopyrimidine-DNA glycosylase	4%	31651/8.95	1	DKHDHVEFVFTDK	53	0.03	C	DM
98	gi|58337993	exopolysaccharide biosynthesis protein	6%	28517/9.0	1	SPIAEQFR	52	0.048	C	CE
141	gi|58337498	acetyltransferase	13%	22876/7.6	2	DYNLLADTDKEER	67	0.001	C	UF
						DVPDNSLVVGVPG	89	7e-006		
151	gi|58336556	putative primase like	15%	21682/9.17	2	NFDAVIVVEGKDDTIR	70	0.00052	C	UF
						QIIVFTDPDFNGER				
177	gi|58337611	50S ribosomal protein L21	20%	11334/9.18	2	VAEGDSVFVEK	90	6.3e-006	U	PS
						VGTPLVDGAK	61	0.0043		
189	gi|58337486	hypothetical protein LBA1204	19%	16556/8.63	1	LGHDLTPDEELTVLNR	113	2.3e-008	C	PS
194	gi|58336643	30S ribosomal protein S8	21%	14523/9.33	2	DIILRPVITEK	51	0.021	C	PS
						NAVEEIFDVK	63	0.0034		
196	gi|58336643	30S ribosomal protein S8	9%	14523/9.33	1	VMTDPIADYLTR	72	0.00032	C	PS

a) Individual ion scores >50 indicate identity or extensive homology.

b) Localization: C – cytoplasmic; CM – cytoplasmic membrane; CW – cell wall; E – extracellular; U – unknown functions.

c) Functional role: AA - Amino acid biosynthesis; BCPC - Biosynthesis of cofactors; prosthetic groups, and carriers; CE - Cell envelope; CIM - Central intermediary metabolism; CP - Cellular processes; DM - DNA metabolism; EM - Energy metabolism; FP - Fatty acid and phospholipid metabolism; HP - Hypothetical proteins; PF - Protein fate; PPNN - Purines, pyrimidines, nucleosides and nucleotides; PS - Protein synthesis; RF - Regulatory functions; T - Transport; UF - Unknown functions.

Fig. 1.

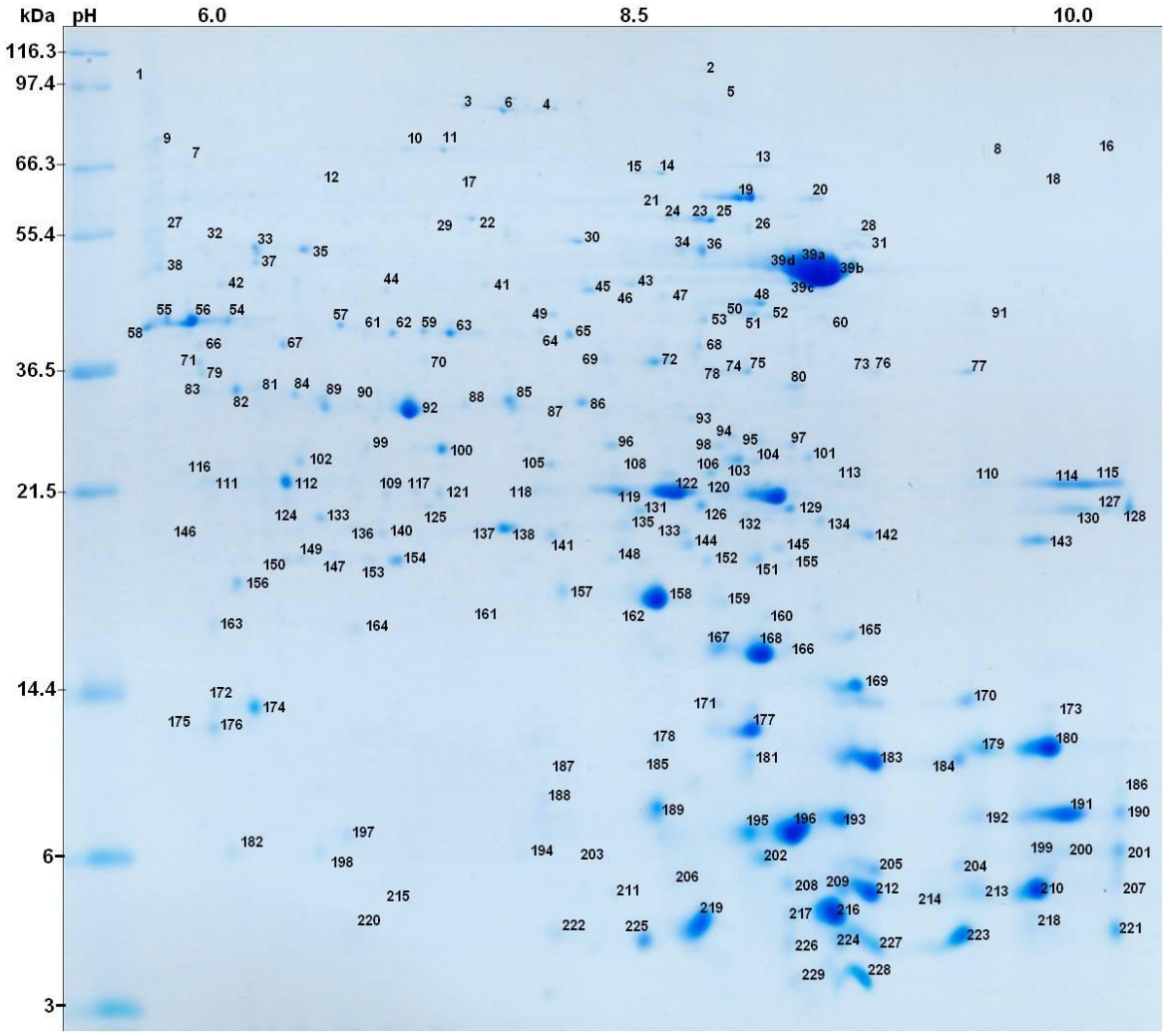

Fig. 2.

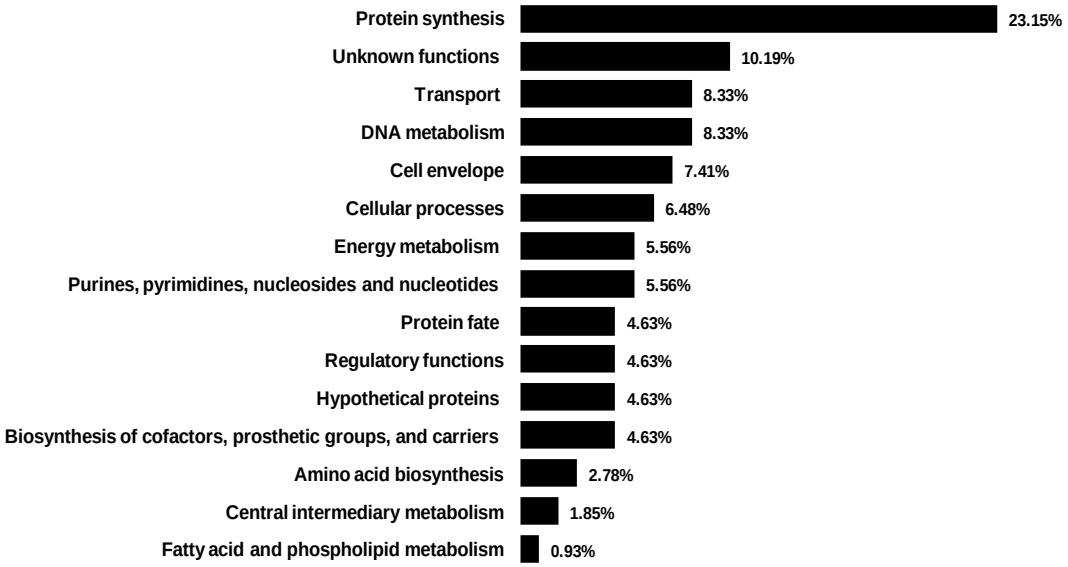
Protein synthesis
23.15%
Unknown functions
10.19%
Transport
8.33%
DNA metabolism
8.33%
Cell envelope
7.41%
Cellular processes
6.48%
Energy metabolism
5.56%
Purines, pyrimidines, nucleosides and nucleotides
5.56%
Protein fate
4.63%
Regulatory functions
4.63%
Hypothetical proteins
4.63%
Biosynthesis of cofactors, prosthetic groups, and carriers
4.63%
Amino acid biosynthesis
2.78%
Central intermediary metabolism
1.85%
Fatty acid and phospholipid metabolism
0.93%

CHAPTER 4

Differential proteome analysis of potential prebiotic raffinose metabolism by the probiotic bacterium *Lactobacillus acidophilus* NCFM

Differential proteome analysis of potential prebiotic raffinose metabolism by the probiotic bacterium *Lactobacillus acidophilus* NCFM

Morten Ejby[1], Avishek Majumder[1], Kristian Thorsen[1], Sampo Lahtinen[2], Susanne Jacobsen[1*] and Birte Svensson[1*]

1. Enzyme and Protein Chemistry, Department of Systems Biology, Technical University of Denmark, Søltofts Plads, Building 224, DK-2800 Kgs. Lyngby, Denmark.
2. DuPont, Health & Nutrition, Sokeritehtaantie 20, 02460 Kantvik, Finland.

***Corresponding authors:**

Birte Svensson & Susanne Jacobsen
Enzyme and Protein Chemistry
Department of Systems Biology
Technical University of Denmark
Søltofts Plads, Building 224
DK-2800 Kgs. Lyngby
Denmark
Phone: +45 45252740; +45 45252741; Fax:+45 45886307
Email: bis@bio.dtu.dk; sja@bio.dtu.dk

Abbreviations:

ACN; Acetonitrile

ANOVA; Analysis of variance

CBB; Coomassie brilliant blue

CHAPS; 3-[(3-Cholamidopropyl)dimethylammonio]-1-propanesulfonate

CFU; Colony forming units

DIGE; Difference gel electrophoresis

DTT; Dithiothreitol

IEF; Isoelectric focusing

LABSEM; Lactic acid bacteria semi-defined media

MALDI-TOF MS; Matrix-assisted laser desorption/ionization – time of flight mass spectrometry

MS/MS-MS; Tandem mass spectrometry

SDS-PAGE; sodium dodecyl sulfate polyacrylamide gel electrophoresis

Key words: *Lactobacillus acidophilus* NCFM, 2D-DIGE, probiotics, prebiotics, raffinose

Abstract

A comparative differential proteome study of *Lactobacillus acidophilus* NCFM grown in semi-defined media (LABSEM) supplemented by glucose (control) or raffinose was performed to explore the carbohydrate metabolism pathways. The proteome analysis by 2D-DIGE showed that the intracellular family GH36 α-galactosidase (MelA) is highly abundant in growth on raffinose together with sucrose-6-phosphate hydrolase (LBA0400), maltose phosphorylase (LBA1870) and β-galactosidase (LBA1467 and LBA1468). Sugar kinases specific for galactose, glucose and fructose also were found in the proteome of NCFM grown on raffinose. Furthermore the Lelior pathway for galactose utilization was found to be differentially expressed together with various enzymes from the glycolysis. D-lactate dehydrogenase (LBA0055) and L-lactate dehydrogenase (LBA0910) were found to be differentially abundant with upregulation of L-lactate dehydrogenase and downregulation of D-lactate dehydrogenase, indicating a shift from the end product enatiomer ratio of lactic acid.

Introduction

Functional foods *i.e.* food products with significant health benefits are being widely accepted by the consumers [1]. To be a probiotic microorganism there are certain basic characteristics to be fulfilled such as, being safe, identification to the strain level by using biochemical and genetic techniques, and have proven beneficial effect on human health [2]. *Lactobacillus acidophilus* NCFM (NCFM) according to the requirements is a probiotic bacterium and has been extensively studied [3]. The 2 Mb genome of NCFM has been sequenced [4] and transcriptomics analyses of the carbohydrate utilization of NCFM have been carried out [5, 6].

Prebiotics are food ingredients that promote the growth of selected bacterial species in the gut microbiota for the benefit of host health [7]. Raffinose (*O*-α-D-galactopyranosyl-(1→6)-α-D-glucopyranosyl-(1→2)-β-D-fructofuranoside) is a trisaccharide with galactose α-(1→6) linked to the glucose moiety of sucrose and a major constituent of different legume seeds [8]. The absence of α-galactosidase in the intestinal mucosa leads to accumulation of raffinose and the raffinose family oligosaccharides (RFO) from the diet in the gut [9]. Raffinose has been shown to modulate the human intestinal microbiota and promote intestinal health [10]. The presence of α-galactosidase activity of various *L. acidophilus* strains has been documented [11]. The supplementation of milk with raffinose increased the viability of *L. acidophilus* in fermented milk during refrigerated storage [12]. The utilization of raffinose by NCFM and the high abundance of raffinose in various legumes in the diet [8] makes it imminent to study how the probiotic NCFM takes up and metabolizes raffinose.

Gel-based proteomics has been used to describe the probiotic potential of *Lactobacillus* sp. related to bile tolerance [13, 14], acid tolerance [15] and interactions with the gut epithelium [16]. Studies are lacking, with regard to interaction and adaptation of probiotic *Lactobacillus* sp to different carbohydrates abundant in the gut. The present work focuses on proteome changes by the utilization of raffinose by NCFM using two-dimensional fluorescence-based difference gel electrophoresis (2D-DIGE) coupled with mass spectrometry.

Materials and Methods

Growth Conditions

Freeze dried commercial *Lactobacillus acidophilus* NCFM (NCFM 150B, FloraFIT® Probiotics; Danisco USA Inc., Madison, US) with 150 X 10^9 CFU/g was used in the present study. The culture was revived in semisynthetic medium for lactic acid bacteria (LABSEM) [17] supplemented with 1% glucose and grown under aerobic conditions without agitation at 37 °C. For DIGE analyses the cultures were sub-cultured in LABSEM supplemented with either 1% glucose or 1% raffinose for three cycles prior to analysis. Cells from late-log phase cultures of A_{600} of 1.1 for glucose and 0.9 for raffinose (pH 5.3 for both) were harvested from four independent 40 ml cultures (centrifugation at 3,200 *g*, 10 min, 4 °C). Cell pellets were washed twice with 0.9% NaCl, vacuum-dried without heating to dryness (SpeedVac, Savant, SC110A with Vacuum unit UVS400A; GMI Inc., Ramsey, US) and kept at −80 °C until use.

Protein Extraction

To prepare the whole cell extract proteins, cells were disrupted by mechanical grinding with a small number of acid washed glass beads (<100 µm diameter; Sigma, Brøndby, Denmark). The cell pellet was added an equal volume of glass beads, 300 µl phenol (Tris saturated pH 8.0) and 300 µl 10 mM Tris, 10 mM DTT (pH 8.0). Disruption was carried out using a Bio 101 Savant FastPrep FP 120 bead beater (Savant, Farmingdale, USA) at a speed of 6.5 m/s for four cycles of 45 s each with intermittent cooling on ice. The cell lysate was centrifuged (10,000 *g*, 10 min, 4 ºC) resulting in three distinct phases. The phenol phase were transferred to a fresh microtube, added ice-cold ethanol (four volumes) and kept at −20 ºC overnight. After centrifugation (15,000 *g*, 10 min, 4 ºC), the precipitate was dissolved in 300 µl rehydration buffer (8 M urea, 2 M thiourea, 2% CHAPS, and 1% pharmalyte pH range 4−7 (GE Life Sciences, Uppsala, Sweden)). The protein concentration was determined (2D Quant kit; GE Life Sciences) prior to storage at −80 °C until use.

CyDye labeling

CyDye minimal-labeling for DIGE analysis was performed using a dye-swapping approach to avoid bias due to the interference from fluorescence properties of gels at different wavelengths. Protein aliquots (50 µg) of each of four biological replicates grown on glucose or raffinose were labeled interchangeably with 250 pmol of either Cy3 or Cy5 dye, vortexed, and left in the dark (30 min, 4 ºC). In a similar manner, aliquots (25 µg protein) of each sample were combined for internal standard and labeled with 250 pmol Cy2. Labeling reactions were quenched by 1 µl 10 mM lysine in the dark (10 min). The internal standard and the samples were mixed and the volume made to 450 µl with rehydration buffer (8 M urea, 2 M thiourea, 2% CHAPS, 0.3% DTT and 1% pharmalyte pH range 4−7 (GE Life Sciences)).

2-D Differential gel electrophoresis

Separation in the first dimension (isoelectric focusing, IEF) was performed using IPG strips (pH 4−7; 24 cm; GE Life Sciences) on Ettan^{TM} IPGphor (GE Life Sciences). Rehydration was carried out at 20 ºC for 12 h at 30 V. IEF was performed at a total of 78 kVh (1 h at 150 V, 1 h at 300 V, 1 h at 1,000 V, gradient to 8,000 V, hold at 8,000 V until a total of at least 78 kVh was reached). Subsequently, the strips were equilibrated for 2 x 15 min in 5 ml equilibration buffer (6 M urea, 30% glycerol, 50 mM Tris-HCl, pH 8.8, 2% SDS and 0.01% bromophenol blue) supplemented with 1% DTT and 2.5% iodoacetamide in the first and second equilibration step, respectively. The second dimension (SDS-PAGE) was performed on ETTAN^{TM} DALT *twelve* Electrophoresis unit (GE Lifesciences) overnight at 1 W/gel until the dye front reached the gel bottom.

Image Analysis

Imaging of the DIGE gels was done immediately after the second dimension run at excitation/emission wavelengths of Cy2 (488/520 nm), Cy3 (532/580 nm) and Cy5 (633/670 nm), respectively (100 µm resolution; Typhoon 9410 Variable Mode Imager; GE Lifesciences). Gel images were analyzed by Progenesis SameSpots version 3.2 (nonlinear Dynamics Ltd, Newcastle upon Tyne, UK). The gel images were aligned by automated

calculation of manually assigned landmark vectors. Aligned gels were subjected to intra-gel (difference in-gel) and inter-gel (biological variance) analyses. Spot volume ratio change of $\geq$ 1.5 fold, ANOVA $p \leq 0.05$ and false discovery rate $q \leq 0.05$ were chosen as criterion in the identification of differentially abundant protein spots. Gels were post-stained with CBB [18] for spot picking.

In-gel Digestion and Protein Identification by MS/MS-MS

Spots of interest were excised manually and subjected to in-gel digestion with some modifications as described below [19]. Gel pieces were washed with 100 µl 40% ethanol (10 min) followed by 50 µl 100% acetonitrile (ACN), and incubated 45 min on ice with 2 µl 12.5 ng μl^{-1} trypsin (Promega, Nacka, Sweden) in 25 mM ammonium bicarbonate followed by addition of 10 µl 25 mM ammonium bicarbonate for rehydration, and incubated at 37 ºC overnight. A supernatant aliquot (1 µl) was applied to the Anchor Chip target plate (Bruker-Daltonics, Bremen, Germany), covered by 1 µl matrix solution (0.5 µg μl^{-1} α-cyano-4-hydroxycinnamic acid in 90% ACN, 0.1% TFA) and washed in 0.02% TFA. MS and MS/MS spectra were obtained by Ultraflex II MALDI-TOF MS mass spectrometer (Bruker-Daltonics) in auto-mode using Flex Control v3.0 (Bruker-Daltonics) and processed by Flex Analysis v3.0 (Bruker-Daltonics). Peptide mass maps were acquired in reflectron mode with 500 laser shots per spectrum. Spectra were externally calibrated using a tryptic digest of β-lactoglobulin (5 pmol μl^{-1}); MS/MS data were acquired with stop conditions so that 1000–1600 laser shots were accumulated for each spectrum. The MS together with MS/MS spectra were searched against NCBInr database for bacteria (NCBInr 20100323 (10606545 sequences; 3615943919 residues) using MASCOT 2.0 software (http://www.matrixscience.com) integrated together with Biotools v3.1 (Bruker-Daltonics). Search parameters were as follows: monoisotopic peptide mass accuracy of 80 ppm, fragment mass accuracy to $\pm$ 0.7 Da; maximum of one missed cleavage; carbamidomethylation of cysteine and partial oxidation of methionine. There were no restrictions with respect to protein *Mr* and p*I*. Filtering of peaks was done for known autocatalytic trypsin peaks and keratin peaks; the signal to noise threshold ratio was set to 1:6. A Mascot score of $\geq$ 80 ($p \leq 0.05$) was used to confirm proteins identified by peptide

mass fingerprint and should have a minimum of six matched peptides. For single peptide based MS/MS identification of proteins, a Mascot score of ≥ 40 ($p \leq 0.05$) was used.

Results and Discussion

Raffinose family of oligosaccharides (RFO) represented by raffinose, stachyose, verbascose and related oligosaccharides have been shown to be well documented prebiotics [10]. They confer positive bifidogenic effects during the manufacture of probiotic milk products [8] and have also been shown to have beneficial effects on the survival of probiotic cultures e.g. *L. acidophilus* and *B. lactis* [12]. The administration of raffinose and *B. breve* increased the number of bifidobacteria and lactobacilli in rat cecal microbiota [20]. Transcriptomic analysis of raffinose metabolism by NCFM showed induction of raffinose operon [5]. However, knowledge of raffinose metabolism in probiotic bacteria at the protein level is lacking and the present study addresses changes in protein profiles of NCFM grown on raffinose to gain insight into uptake and metabolism of raffinose by the probiotic NCFM.

Differential abundance of proteins of NCFM grown on raffinose

In total 108 spots were found by 2D-DIGE and image analysis to differ in relative abundancy for NCFM grown on raffinose compared to glucose (Fig. 1). Ninety spots were excised as detected by CBB staining for further identification by mass spectrometry after trypsin digestion. Among these 90 spots, proteins in 63 spots were identified by MS/MS-MS (Table 1), and 48 showed higher (1.5–13.9 fold), while 15 showed lower (1.5–2.3 fold) relative abundance. The 63 identifications corresponding to 43 unique proteins are distributed among 12 functional categories based on the Comprehensive Microbial Research (CMR) database (http://cmr.jcvi.org) (Fig. 2) as follows; 3 with biosynthesis of cofactors, prosthetic groups and carriers; 23 from energy metabolism; 3 from the functional role cell envelope, protein synthesis and purines, pyrimidines, nucleosides and nucleotides; 1 protein each from the functional role cellular processes, hypothetical proteins, regulatory functions, transcription and transport; and 2 of unknown function.

Proteins involved in raffinose metabolism

Several glycoside hydrolases with +2.5–13.9 fold change in the range were identified using 2D-DIGE to be differentially abundant with growth of NCFM on raffinose compared to glucose (Table 1). These include α-galactosidase (MelA) in the raffinose operon, β-galactosidase large and small subunit (LacLM) from the lactose gene locus, and sucrose-6-p hydrolase (ScrB) of the sucrose gene locus (Fig 3). The glycoside hydrolases α-galactosidase (spot 1, fold change +13.9; spot 10, fold change +7.3), β-galactosidase large (spot 19, fold change +6.9; spot 36, fold change +3.3; spot 53, fold change +2.5) and small subunit (spot 6, fold change +5.7; spot 7, fold change +5.7) were identified on the 2D-gel in multiple forms of different p*I* (Fig 4). Raffinose in NCFM induces the raffinose operon, consisting of genes encoding the ABC transporter msmEFGK (*msmEFGK*), α-galactosidase (*melA*) and sucrose phosphorylase (*gftA*), and the MsmEFGK transporter from the raffinose operon, has been shown to be involved in the uptake of raffinose in NCFM (Fig. 3) [5]. The NCFM α-galactosidase (E.C. 3.2.1.22) belongs to glycoside hydrolase family 36 and catalyzes hydrolysis of the galactose residue from raffinose [21]. In the present study α-galactosidase is the primary enzyme for raffinose metabolism to galactose and sucrose and was found to be significantly abundant (spot 1, fold change +13.9; spot 10, fold change +7.3) (Fig. 3). A similar induction of the raffinose operon in the presence of raffinose was observed in low G+C bacterium *Streptococcus mutans* [22].

Sucrose phosphorylase (GftA) of the raffinose operon may be involved in the conversion of sucrose to glucose-1-phosphate and fructose. This enzyme was significantly upregulated at the transcriptome level [17], but it has not been identified among the differentially abundant proteins by 2D-DIGE. Sucrose and galactose, catalyzed products of raffinose by α-galactosidase, could potentially induce the expression of sucrose, galactose and lactose gene loci. Indeed sucrose-6-p hydrolase (E.C. 3.2.1.26) (spot 20) was found to be upregulated by +5.4 fold in the presence of raffinose. The transcriptomic analysis of NCFM and low G+C *S. mutans* growth with sucrose shows induction of the sucrose locus [5]. Utilization of sucrose in most low G+C Gram-positive bacteria is under the regulation of the LacI/GalR transcriptional regulator [23] that controls the induction of the sucrose locus, encoding sucrose-6-p hydrolase, and the sucrose PTS transporter EIIBCA^{Suc} [5, 23, 24]. The sucrose 6-p hydrolase of glycoside hydrolase family 32, has been shown to hydrolyze sucrose-6-phosphate and sucrose to glucose-6-phosphate and fructose

(http://www.uniprot.org/uniprot/P27217) [25]. Sucrose-6-p hydrolase has been shown to be active on sucrose and sucrose-6-phosphate with a similar catalytic efficiency [25, 26]. Noticeably, while the enzymes of the Lelior pathway for galactose utilization and fructokinase were found to be differentially expressed in NCFM during growth on raffinose and also the for entry of fructose into the glycolysis was identified, no glucose or sucrose active kinases were found. Multiple forms of phosphoglucomutase (spot 21, 34 and 54) and maltosephosphorylase (spot 15 and 28) were found to be differentially abundant during growth on raffinose, with a fold change of +5.3–2.4 and +6.2–4.5 respectively (Table 1). Both of these enzymes have been shown to be involved in glycolysis and glyconeogenesis [27]. Transcriptomics of galactose utilization has shown that galactose induce 10 different genes from two different loci in NCFM [5]. A similar induction of the galactose and lactose loci was found in the present study, with a differential abundance of +1.7–9.9 fold (Table 1). The proteins of the Leloir pathway, galactokinase (GalK) (spot 38, fold change +3.1; spot 43, fold change +2.9), galactose-1-epimerase (GalM) (spot 79, fold change +1.7), galactose-1-phosphate uridylyltransferase (GalT) (spot 4, fold change +8) and UDP-glucose 4-epimerase (GalE) (spot 11, fold change +9.6 and spot 24, fold change +5.4) are involved in the conversion of galactose to glucose-1-P. Glucose-1-P is converted to glucose-6-P by phosphoglucomutase (pgm) (spot 21, fold change +5.3; spot 34, fold change +3.3 and spot 54, fold change +2.4). The β-galactosidase large and small subunits from a different locus were also found to be differentially abundant (Table 1). The lactose transcriptional regulator (LacR) regulates the expression of LacLM and is induced by galactose [5]. Similar observation of lactose locus induction by galactose was observed in the low G+C bacteria *S. gordonii* [28]. Low G+C gram positive bacteria adapt to changing carbohydrate conditions by catabolite repression [29]. Catabolite control protein A (CcpA) involved in regulation of sugar utilization by maintaining sugar uptake and catabolic/metabolic balance [30] was found be +1.9 fold abundant (spot 71).

Other abundant proteins

Proteins with a functional role in energy predominate proteins upregulated by raffinose. These include enzymes of glycolysis, glyceraldehyde-3-p dehydrogenase; phosphofructokinase, L-lactate dehydrogenase; D-lactate dehydrogenase; pyruvate kinase;

pyruvate oxidase; maltose phosphorylase; and NAD-dependent aldehyde dehydrogenase (Table 1). The end product of anaerobic fermentation for lactic acid bacteria is lactate, which is formed as the end-product of glycolysis when pyruvate is reduced to lactate with NADH as a cofactor [31]. L-lactate dehydrogenase was found to be abundant (spot 18, fold change +5.4; spot 90, fold change +1.6); while pyruvate kinase was lower in abundance (spot 60, fold change -2.3; spot 80, fold change -1.7) with raffinose. Noticeably D-lactate dehydrogenase was found be lower in abundance (spot 83, fold change -1.7). NCFM ferments glucose to produce 33.8 % D-lactic acid and 66.2% L-lactic acid [3], The change in abundance of L-lactate dehydrogenase and D-lactate dehydrogenase indicates a change in the ratio of enantiomers of lactic acid during raffinose fermentation. Carbohydrate sources have been shown to influence the ratio of produced lactic acid enantiomers in *L. acidophilus* [32]. F_0F_1 ATP synthase maintains the proton motive force by ATP synthesis/hydrolysis and was found to be differentially abundant in conditions of acid and bile stress [13, 15]. Subunits of the multimeric F_0F_1 ATP synthase, subunit beta (spot 87), and subunit delta (spot 108) was reduced in abundance by -1.6 and -1.5 fold respectively.

Conclusions

The present investigation of the interaction of prebiotic raffinose with the probiotic NCFM at a proteome level revealed the abundance of various proteins involved in the raffinose utilization. α-Galactosidase cleaves raffinose to galactose and sucrose, which possibly induce the sucrose, galactose and lactose loci. NCFM was found to utilize galactose by the Leloir pathway and sucrose by sucrose 6-p hydrolase. Furthermore, various proteins of the glycolysis are shown to be differentially abundant, indicating regulation of the glycolytic flux. Interestingly, various proteins involved in raffinose metabolism were found in multiple isoforms and further characterization of these proteins may contribute to understanding the role of posttranslational modifications in prebiotic carbohydrate utilization.

This study has so far only relied on data obtained by 2DE electrophoresis. Before submission to BMC microbiology the 2DE-DIGE data are to be verified by semi-quantitative RT-PCR, DNA-microarrays or equivalent methods. Furthermore it is planned to make small organic acid profiles for the media in fermentations, to verify that the

changes observed in lactate dehydrogenase L and D forms in the 2D-DIGE experiments have a biological effect and changes the ratio between the produced lactic acid enantiomers.

Acknowledgements

Birgit Andersen is acknowledged for technical assistance with mass spectrometric analysis. ME is grateful to the Technical University for Denmark for the Ph.D. scholarship. AM is grateful to the Technical University for Denmark for a Hans Christian Ørsted postdoctoral fellowship. This work was supported by the Danish Strategic Research Council's Program Committee on Health, Food and Welfare (FøSu), the Danish Research Council for Natural Science and the Danish Center for Advanced Food Studies (LMC).

References

1. Lynn F, Joachim S, Nigel L: **Consumer acceptance of functional foods: issues for the future**. *Br Food J* 2003, **105**:714-731.
2. Douglas LC, Sanders ME: **Probiotics and prebiotics in dietetics practice**. *J Am Diet Assoc* 2008, **108**:510-521.
3. Sanders ME, Klaenhammer TR: **The scientific basis of *Lactobacillus acidophilus* NCFM functionality as a probiotic**. *J Dairy Sci* 2001, **84**:319-331.
4. Altermann E, Russell WM, Azcarate-Peril MA, Barrangou R, Buck BL, McAuliffe O, Souther N, Dobson A, Duong T, Callanan M *et al*: **Complete genome sequence of the probiotic lactic acid bacterium *Lactobacillus acidophilus* NCFM**. *Proc Natl Acad Sci USA 2005,* **102**:3906-3912.
5. Barrangou R, Azcarate-Peril MA, Duong T, Conners SB, Kelly RM, Klaenhammer TR: **Global analysis of carbohydrate utilization by *Lactobacillus acidophilus* using cDNA microarrays**. *Proc Natl Acad Sci USA 2006,* **103**:3816-3821.
6. Andersen JM, Barrangou R, Abou Hachem M, Lahtinen S, Goh YJ, Svensson B, Klaenhammer TR: **Transcriptional and functional analysis of galactooligosaccharide uptake by lacS in *Lactobacillus acidophilus***. *Proc Natl Acad Sci USA,* **108**:17785-17790.
7. Gibson GR, Roberfroid MB: **Dietary modulation of the human colonic microbiota - introducing the concept of prebiotics**. *J Nutr* 1995, **125**:1401-1412.

8. Martinez-Villaluenga C, Frias J, Vidal-Valverde CN: **Raffinose family oligosaccharides and sucrose contents in 13 Spanish lupin cultivars**. *Food Chem* 2005, **91**:645-649.
9. LeBlanc JG, Garro MS, de Giori GS: **Effect of pH on *Lactobacillus fermentum* growth, raffinose removal, alpha-galactosidase activity and fermentation products**. *Appl Microbiol Biotechnol* 2004, **65**:119-123
10. Fernando W, Hill J, Zello G, Tyler R, Dahl W, Van Kessel A: **Diets supplemented with chickpea or its main oligosaccharide component raffinose modify faecal microbial composition in healthy adults**. *Benef Microbes* 2010, **1**:197-207.
11. Yeo S-K, Liong M-T: **Effect of prebiotics on viability and growth characteristics of probiotics in soymilk**. *J Sci Food Agric* 2009, **90**:267-275.
12. Martinez-Villaluenga C, Frias J, Gomez R, Vidal-Valverde C: **Influence of addition of raffinose family oligosaccharides on probiotic survival in fermented milk during refrigerated storage**. *Int Dairy J* 2006, **16**:768-774.
13. Hamon E, Horvatovich P, Izquierdo E, Bringel F, Marchioni E, Aoude-Werner D, Ennahar S: **Comparative proteomic analysis of *Lactobacillus plantarum* for the identification of key proteins in bile tolerance**. *BMC Microbiol* 2011, **11**:63
14. Koskenniemi K, Koponen J, Kankainen M, Savijoki K, Tynkkynen S, de Vos WM, Kalkkinen N, Varmanen P: **Proteome analysis of *Lactobacillus rhamnosus* GG using 2-D DIGE and mass spectrometry shows differential protein production in laboratory and industrial-type growth media**. *J Proteome Res* 2009, **8**:4993-5007.
15. Koponen J, Laakso K, Koskenniemi K, Kankainen M, Savijoki K, Nyman TA, de Vos WM, Tynkkynen S, Kalkkinen N, Varmanen P: **Effect of acid stress on protein expression and phosphorylation in *Lactobacillus rhamnosus* GG**. *Proteomics* 2012, **75**:1357-1374.
16. Siciliano RA, Cacace G, Mazzeo MF, Morelli L, Elli M, Rossi M, Malorni A: **Proteomic investigation of the aggregation phenomenon in *Lactobacillus crispatus***. *BBA Proteins and Proteomics* 2008, **1784**:335-342.
17. Barrangou R, Altermann E, Hutkins R, Cano R, Klaenhammer TR: **Functional and comparative genomic analyses of an operon involved in fructooligosaccharide utilization by *Lactobacillus acidophilus***. *Proc Natl Acad Sci USA 2003,* **100**:8957-8962.

18. Candiano G, Bruschi M, Musante L, Santucci L, Ghiggeri GM, Carnemolla B, Orecchia P, Zardi L, Righetti PG: **Blue silver: A very sensitive colloidal Coomassie G-250 staining for proteome analysis**. *Electrophoresis* 2004, **25**:1327-1333.
19. Hellman U, Wernstedt C, Gonez J, Heldin CH: **Improvement of an in-gel digestion procedure for the micropreparation of internal protein-fragments for amino-acid sequencing**. *Anal Biochem* 1995, **224**:451-455.
20. Dinoto A, Suksomcheep A, Ishizuka S, Kimura H, Hanada S, Kamagata Y, Asano K, Tomita F, Yokota A: **Modulation of rat cecal microbiota by administration of raffinose and encapsulated *Bifidobacterium breve***. *Appl Environ Microbiol* 2006, **72**:784-792.
21. Fredslund F, Abou Hachem M, Larsen RJ, Sorensen PG, Coutinho PM, Lo Leggio L, Svensson B: **Crystal structure of alpha-galactosidase from *Lactobacillus acidophilus* NCFM: Insight into tetramer formation and substrate binding**. *J Mol Biol*, 412:466-480.
22. Ajdic D, Pham VTT: **Global transcriptional analysis of *Streptococcus mutans* sugar transporters using microarrays**. *J Bacteriol* 2007, **189**:5049-5059.
23. Wang B, Kuramitsu HK: **Control of enzyme IIscr and sucrose-6-phosphate hydrolase activities in *Streptococcus mutans* by transcriptional repressor ScrR binding to the cis-active determinants of the scr regulon**. *J Bacteriol* 2003, **185**:5791-5799.
24. Iyer R, Camilli A: **Sucrose metabolism contributes to *in vivo* fitness of *Streptococcus pneumoniae***. *Mol Microbiol* 2007, **66**:1-13.
25. Thompson J, Robrish SA, Immel S, Lichtenthaler FW, Hall BG, Pikis A: **Metabolism of sucrose and its five linkage-isomeric alpha-D-glucosyl-D-fructoses by *Klebsiella pneumoniae*. Participation and properties of sucrose-6-phosphate hydrolase and phospho-alpha-glucosidase**. *J Biol Chem* 2001, **276**:37415-37425.
26. Chassy BM, Victoria Porter E: **Initial characterization of sucrose-6-phosphate hydrolase from *Streptococcus mutans* and its apparent identity with intracellular invertase**. *Biochem Biophys Res Commun* 1979, **89**:307-314.
27. Laakso K, Koskenniemi K, Koponen J, Kankainen M, Surakka A, Salusjarvi T, Auvinen P, Savijoki K, Nyman TA, Kalkkinen N *et al*: **Growth phase-associated**

changes in the proteome and transcriptome of *Lactobacillus rhamnosus* GG in industrial-type whey medium. *Microb Biotechnol* 2011, **4**:746-766.

28. Zeng L, Martino NC, Burne RA: **Two gene clusters coordinate galactose and lactose metabolism in *Streptococcus gordonii***. *Appl Environ Microbiol* 2012, **78**: 5597-5605.
29. Deutscher J, Francke C, Postma PW: **How phosphotransferase system-related protein phosphorylation regulates carbohydrate metabolism in bacteria**. *Microbiol Mol Biol Rev* 2006, **70**:939-1031.
30. Bruckner R, Titgemeyer F: **Carbon catabolite repression in bacteria: choice of the carbon source and autoregulatory limitation of sugar utilization**. *FEMS Microbiol Lett* 2002, **209**:141-148.
31. Ramos A, Neves AR, Ventura R, Maycock C, LÃ³pez P, Santos H: **Effect of pyruvate kinase overproduction on glucose metabolism of *Lactococcus lactis***. *Microbiology* 2004, **150**:1103-1111.
32. Goderska K. NJ, Czarnecki Z.: **Comparision of growth of *Lactobacillus acidophilus* and *Bifidobacterium bifidum* species in media suplemented with selected saccharides including prebiotics**. *Acta Sci Pol Technol Aliment* 2008, **7**:5-20.

Figure Legends

Fig. 1 **A.** Pseudocolor map of whole cell extract proteome of NCFM by 2D-DIGE. Proteins from glucose and raffinose grown cells were labeled with Cy5 (green) and Cy3 (red) respectively. A pooled internal standard of glucose and raffinose cells extract was labeled with Cy2 (blue) (not shown). The image overlays of Cy5- and Cy3-labeled proteins appear yellow. **B.** Progenesis SameSpots image of analyzed 2D-DIGE gel with spot numbers. The spots identified by mass spectrometry have been listed in Table 1, with their fold changes.

Fig. 2 **A.** Functional role category chart reporting the percentage of unique proteins identified by differential proteome analysis of NCFM grown on raffinose compared to glucose.

Fig. 3. Schematic representation of the differentially abundant proteins involved in utilization of raffinose. The genetic organization of the raffinose induced, raffinose operon, sucrose, lactose and galactose gene loci are shown. The proteins identified by 2D-DIGE and MS analysis of cytosolic proteome (pH 4−7) are shown as arrows in black, while the arrows in white were found to be differentially expressed in the transcriptome analysis of NCFM grown on raffinose (Barrangou et al. 2006). The following abbreviations are used, msmEFGK, multiple sugar metabolism transporter; melA, α-galactosidase; gftA, sucrose phosphorylase; scrR, transcriptional regulator; scrB, sucrose-6 phosphate hydrolase; scrA, sucrose PTS transporter EIIBCA^{suc}; lacR, lacR transcription repressor; lacL, *β*-galactosidase large subunit; lacM, *β*-galactosidase small subunit; galK, galactose kinase; galT, galactose-1-phosphate uridylyltransferase; galM, galactose epimerase.

Fig. 4 A. Inset image with fold changes of some spots from the 2D-DIGE analysis of NCFM growth on raffinose compared to glucose. **B.** Image with the position of glycoside hydrolases on the 2D-DIGE, marked with red circles. The proteins were found in isoforms differing in their p*I*.

Fig. 1.

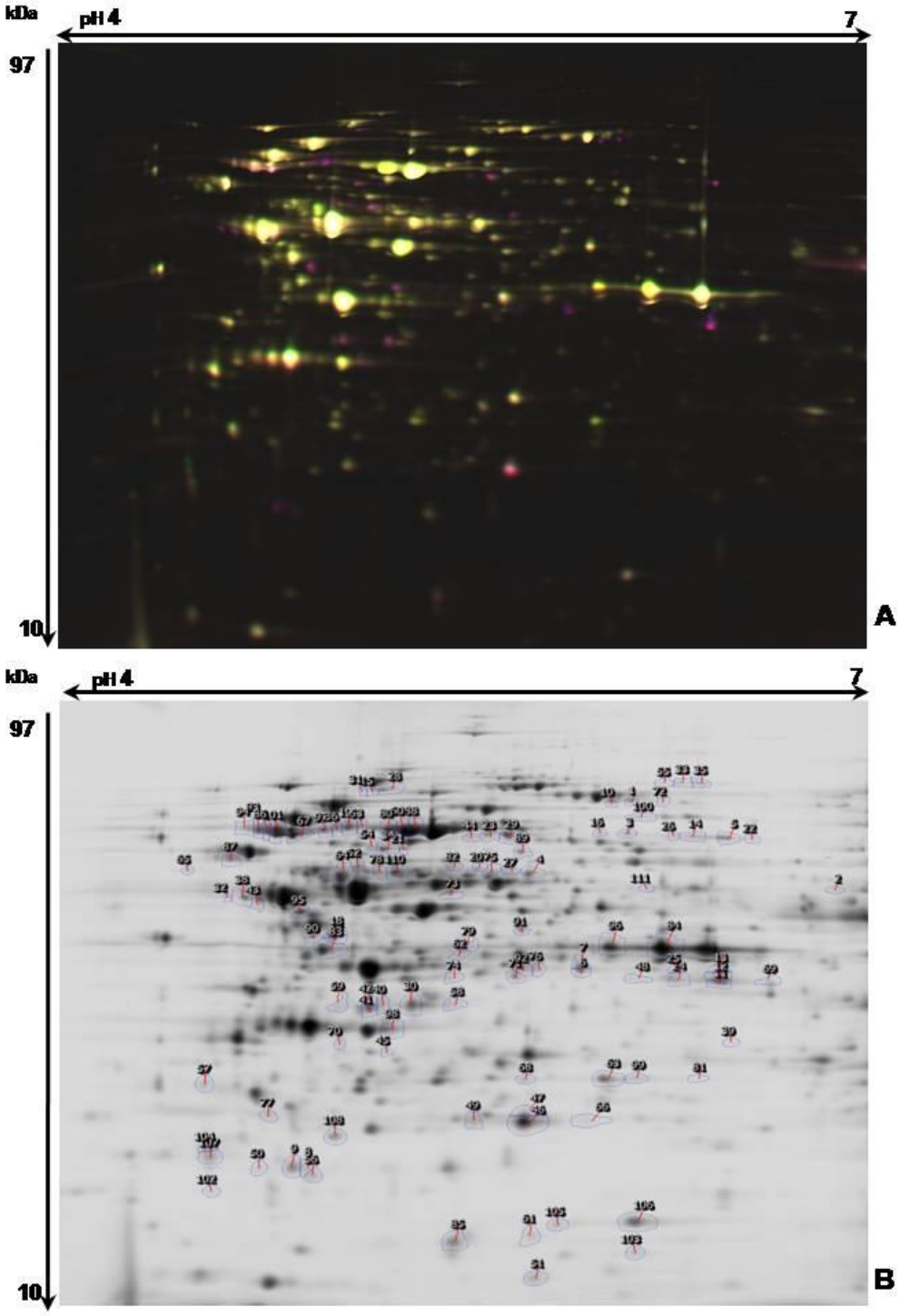

Fig. 2.

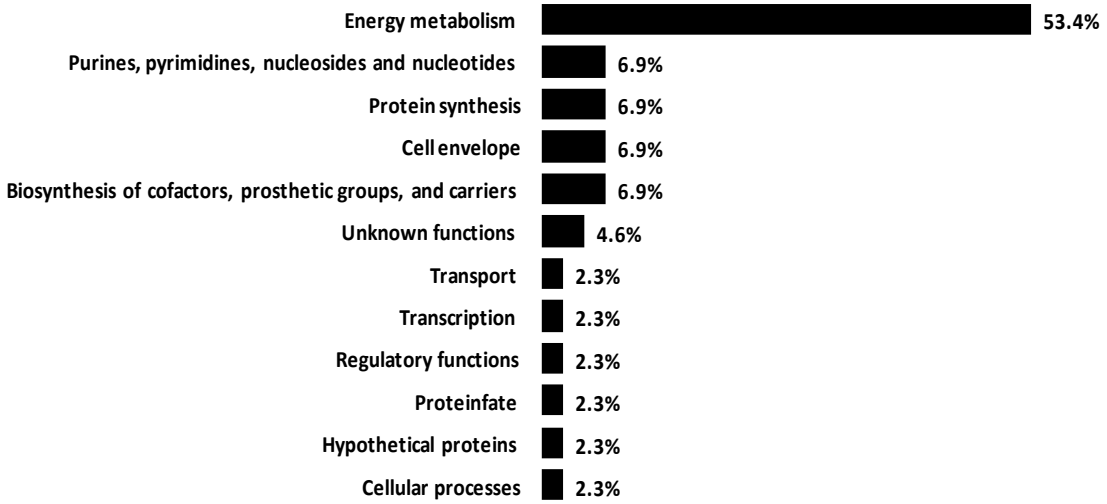
Energy metabolism
53.4%
Purines, pyrimidines, nucleosides and nucleotides
6.9%
Protein synthesis
6.9%
Cell envelope
6.9%
Biosynthesis of cofactors, prosthetic groups, and carriers
6.9%
Unknown functions
4.6%
Transport
2.3%
Transcription
2.3%
Regulatory functions
2.3%
Proteinfate
2.3%
Hypothetical proteins
2.3%
Cellular processes
2.3%

Fig. 3.

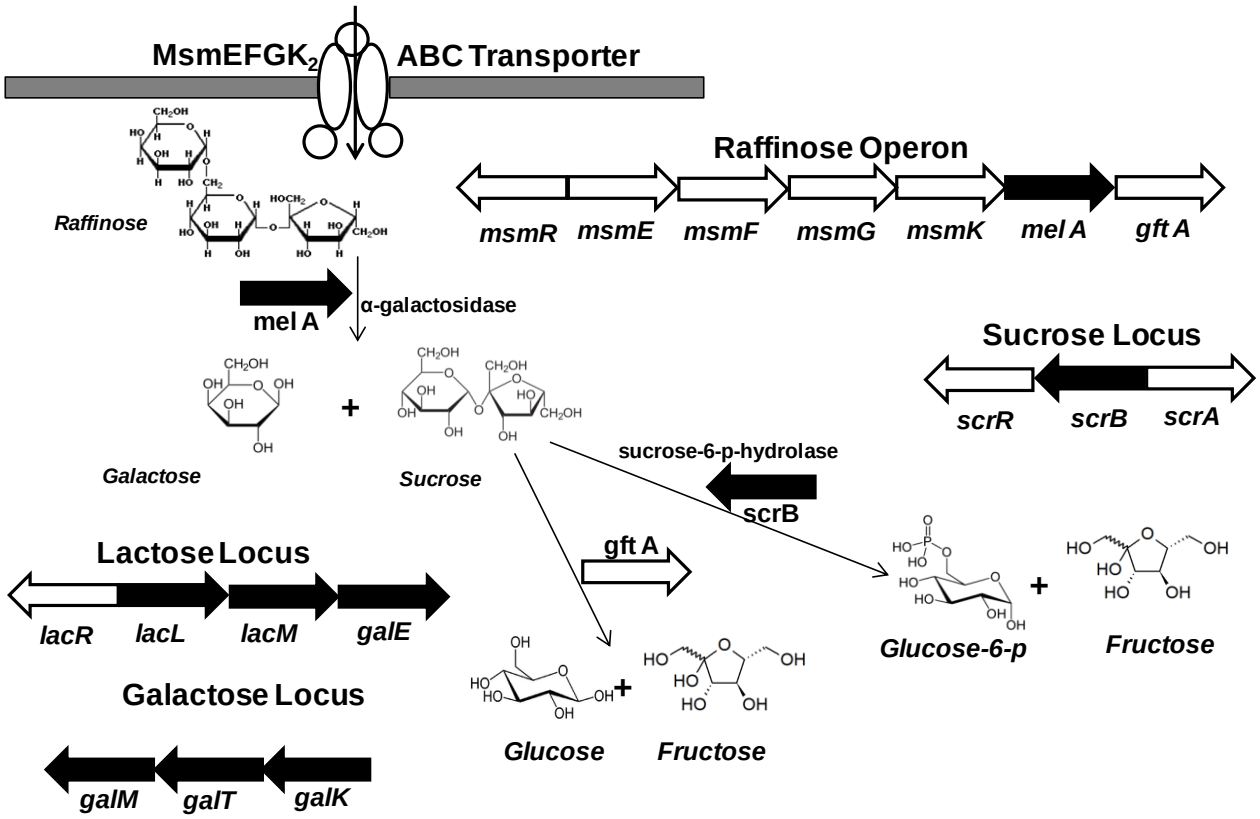
MsmEFGK2 ABC Transporter
Raffinose
Raffinose Operon
msmR msmE msmF msmG msmK mel A gft A
mel A
α-galactosidase
Sucrose Locus
scrR scrB scrA
Galactose
Sucrose
sucrose-6-p-hydrolase
scrB
Lactose Locus
gft A
lacR lacL lacM galE
Glucose-6-p
Fructose
Galactose Locus
Glucose
Fructose
galM galT galK

Fig. 4.

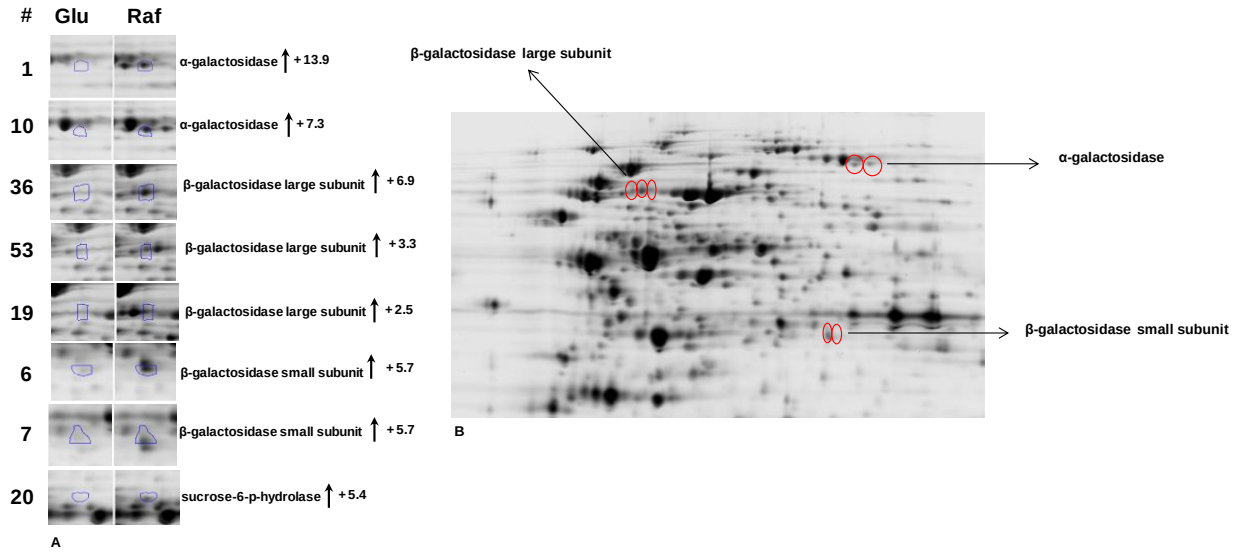
#
Glu
Raf
1
α-galactosidase +13.9
10
α-galactosidase +7.3
36
β-galactosidase large subunit +6.9
53
β-galactosidase large subunit +3.3
19
β-galactosidase large subunit +2.5
6
β-galactosidase small subunit +5.7
7
β-galactosidase small subunit +5.7
20
sucrose-6-p-hydrolase +5.4
A
β-galactosidase large subunit
α-galactosidase
β-galactosidase small subunit
B

Table 1: Protein identifications of differentially abundant spots (≥ 1.5-fold spot volume ratio change and ANOVA $p \leq 0.05$) of *Lactobacillus acidophilus* NCFM grown on SEM medium with 1% glucose and 1% raffinose. Protein identifications were confirmed with a Mascot score of 80 for peptide mass fingerprint and ANOVA $p \leq 0.05$, and a minimum of 6 matched peptides. A Mascot ion score of 40 and ANOVA $p \leq 0.05$ were used for single peptide based identifications.

Spot	Fold Change	Accession number	Protein Name	PMF Score	Mr/pI	Sequence Coverage	Peptides Identified /Searched	Identified Peptides	Ion Score
1	+13.9	gi|58337709	alpha-galactosidase	83	84653/5.63	30%	20/95	-	
2	+10.9	gi|58337861	arginyl-tRNA synthetase	83	63274/5.60	13%	7/13	-	
4	+8.0	gi|58337725	galactose-1-phosphate uridylyltransferase	147	55735/5.48	42%	20/51	FADQVVNSGAYEPLDR	144
								FWNQYSDPAR	54
5	+7.6	gi|58336882	myosin-crossreactive antigen	89	67700/5.91	16%	8/24	GVPEVFASAFDVR	84
6	+5.7	gi|58337734	beta-galactosidase small subunit	122	35966/5.53	53%	13/46	NFHYLFSYER	56
								EGKFHVDGLPVTK	71
7	+5.7	gi|58337734	beta-galactosidase small subunit	87	35966/5.53	20%	6/16	-	
10	+7.3	gi|58337709	alpha-galactosidase	233	84653/5.63	45%	33/84	EVTQFGTLYR	66
11	+9.6	gi|58337735	udp-glucose 4-epimerase	263	36458/5.95	67%	20/39	-	
13	+7.3	gi|58336950	UTP-glucose-1-phosphate uridylyltransferase	153	33875/5.90	60%	13/37	QPHPAGLGDAIYR	111
								HPEIKDQLR	58
15	+6.2	gi|58338116	maltose phosphorylase	94	87353/5.05	12%	8/17	-	
18	+5.4	gi|58337213	L-lactate dehydrogenase	150	33442/4.95	49%	14/31	ISGFPKDR	54
19	+6.9	gi|58337733	beta-galactosidase large subunit (lactase)	220	73492/4.98	43%	29/78	DHDIHIVFEGAER	103
20	+5.4	gi|58336737	sucrose-6-p hydrolase	83	55364/5.30	13%	6/9	-	
21	+5.3	gi|58337008	phosphoglucomutase	136	64122/5.18	19%	11/14	-	
23	+5.2	gi|58336799	hypothetical protein LBA0466	138	63103/5.39	21%	11/17	-	
24	+5.4	gi|58337735	udp-glucose 4-epimerase	128	36458/5.95	30%	8/10	-	
28	+4.5	gi|58338116	maltose phosphorylase	93	87353/5.05	17%	8/20	-	
29	+4.4	gi|58336799	hypothetical protein LBA0466	281	63103/5.39	55%	25/45	-	
30	+4.1	gi|58337322	oxidoreductase	151	31816/5.19	40%	11/28	HIDTASAYGNEDSVGR	154

								SGINRHELFITTK	67
								AIGVSNFR	53
34	+3.3	gi|58337008	phosphoglucomutase	212	64122/5.18	40%	22/45	INLFTVGR	59
								GVVIAFDSR	64
								YGVAYEITR	71
36	+3.3	gi|58337733	beta-galactosidase large subunit (lactase)	202	73492/4.98	38%	25/75	-	
38	+3.1	gi|58337726	galactokinase	173	43521/4.74	41%	15/38	-	
40	+3.9	gi|58337322	oxidoreductase	99	31816/5.19	37%	8/21	-	
41	+2.8	gi|58336369	fructokinase	121	32016/5.08	41%	9/25	FIVAVQDVETGKEVAR	134
43	+2.9	gi|58337726	galactokinase	187	43521/4.74	44%	17/37	HAVSENQR	71
46	+2.8	gi|58336994	putative phosphate starvation inducible protein stressrelated	117	21503/5.46	52%	10/26	YNVRGENIEVTDALR	86
								GENIEVTDALR	104
								SIDFVSEKLER	91
								GLQDFFVEQPEEEKKPSEFDIVR	190
47	+2.7	gi|58336994	putative phosphate starvation inducible protein stressrelated	92	21503/5.46	45%	9/43	YNVRGENIEVTDALR	97
								SIDFVSEKLER	90
								NDGRYGLIETNE	63
								GLQDFFVEQPEEEKKPSEFDIVR	152
49	+2.6	gi|58336994	putative phosphate starvation inducible protein stressrelated	118	21503/5.46	43%	8/15	GENIEVTDALR	90
								SIDFVSEKLER	82
52	+2.5	gi|58337043	phospho-beta-galactosidase II	123	56703/5.04	24%	13/35	-	
53	+2.5	gi|58337733	beta-galactosidase large subunit (lactase)	154	73492/4.98	32%	16/38	-	
54	+2.4	gi|58337008	phosphoglucomutase	114	64122/5.18	14%	9/11	-	
56	+2.4	gi|58337890	putative deoxyribosyltransferase		18978/4.88	32%	4/12	IYLGTPFYNDDQR	98
60	-2.3	gi|58337255	pyruvate kinase	267	63136/5.23	48%	25/42	IVSTLGPASNDIETITALANAGA NVFR	188
								TTEQEGGKFTINTGDTIR	95
								FNFSHGDHEEHR	87
								EGINFIFASFAR	76
63	-2.1	gi|58338190	deoxyadenosine kinase	142	24765/5.70	42%	10/25	LAQINQAIQEK	70

								SFEQISTDPSLKDYYAR	135
								SIYEDALFFK	61
64	-2.1	gi|58337152	elongation factor Tu	225	43609/4.97	60%	22/43	DLLTEYDYPGDDIPVVR	151
								LMDIVDEYIPTPER + Oxidation (M)	83
								QTDKPFLMPVEDVFTITGR + Oxidation (M)	70
65	-2.1	gi|58337537	transcription elongation factor NusA	85	43534/4.55	20%	7/21		
67	-1.9	gi|58338213	pyruvate oxidase	187	66629/4.85	45%	21/50	TPELIPVLTDEAIR	115
								GVVEDKFPAYIGTIGR	102
								ALIEEGEERSESPLYK	80
								ADDNAIFAIDVGNVNVDSCR	180
70	+1.9	gi|58338125	phosphomethylpyrimidine kinase	82	29557/5.06	25%	5/8	-	
71	+1.9	gi|58336768	catabolite control protein A	163	37154/5.43	41%	13/23	YNIIITSIENR	56
73	+1.9	gi|58337214	aminopeptidase	99	50308/5.31	37%	13/38	-	
74	+1.8	gi|58337254	phosphofructokinase	100	34511/5.15	29%	7/15	-	
75	+1.8	gi|58336848	nicotinate phosphoribosyltransferase	211	56238/5.35	40%	22/47	NAVFETFYR	68
								AAYIGGFDSTSNVR	98
78	+1.7	gi|58337891	NAD-dependent aldehyde dehydrogenase	99	50588/5.14	21%	9/25	IQGVALTGSER	67
79	+1.7	gi|58337724	galactose-1-epimerase	152	36971/5.29	39%	12/26	-	
80	-1.7	gi|58337255	pyruvate kinase	261	63136/5.23	39%	25/42	TTEQEGGKFTINTGDTIR	118
								FEAYKGSNVTEAIGESVVR	154
								TIIAATNSGYTAR	101
83	-1.7	gi|58336405	D-lactate dehydrogenase	203	39177/4.96	63%	20/56	-	
84	-1.6	gi|58337019	glyceraldehyde-3-p dehydrogenase	240	36643/5.92	78%	23/58	KYESPSFEYEPNNVVSSDILGR	196
								YESPSFEYEPNNVVSSDILGR	171
								TVAWYDNEYSFTCQMVR	74
85	+1.6	gi|58336496	putative nucleotide-binding protein		18166/5.28	19%		VKESILVPVDGSESAER	148
								DGAHVDVLNVIDTR	119
86	+1.6	gi|58336965	p-enolpyruvate-protein p-transferase PTSI	155	63886/4.79	44%	23/63	GFITDVGGR	78
								GNDNVSYLYQPYNPSVLR	106
87	-1.6	gi|58337090	F0F1 ATP synthase subunit beta	319	52183/4.69	63%	31/51	VIDLLEPYVR	74

								FTQAGSEVSALLGR	118
								LILDGHLDDLPEDAFR	116
88	-1.6	gi|58337255	pyruvate kinase	282	63136/5.23	54%	32/68	IVSTLGPASNDIETITALANAGA NVFR	192
								TTEQEGGKFTINTGDTIR	152
								FNFSHGDHEEHR	89
								EGINFIFASFAR	101
89	-1.6	gi|58337220	citrate lyase alpha chain	113	55315/5.53	26%	10/21	-	
90	+1.6	gi|58337213	L-lactate dehydrogenase	97	33442/4.95	20%	6/8	-	
93	+1.5	gi|58336965	p-enolpyruvate-protein p-transferase PTSI	138	63886/4.79	44%	19/49	GFITDVGGR	54
								LSLMNEEIFR + Oxidation (M)	70
								GNDNVSYLYQPYNPSVLR	109
95	-1.5	gi|58336484	d-alanine-d-alanine ligase	160	40278/4.86	52%	17/52	LQIPADLPQDIVDTVR	96
								LFEEAGIPYTELITR	136
								KVYEITECSGMAR + Oxidation (M)	53
96	-1.5	gi|58337019	glyceraldehyde-3-p dehydrogenase	166	36643/5.92	54%	14/47	KYESPSFEYEPNNVVSSDILGR	190
								YESPSFEYEPNNVVSSDILGR	149
98 (Mixture)	+1.7								
		gi|58337488	hypothetical protein LBA1206	139	31352/5.15	47%	13/36	GFLEADVVLLGVSR	114
		gi|58336527	phosphoglyceromutase	100	26509/5.00	43%	9/36	-	
101	+1.5	gi|58338213	pyruvate oxidase	105	66629/4.85	35%	15/66	TPELIPVLTDEAIR	100
								GVVEDKFPAYIGTIGR	100
								ALIEEGEERSESPLYK	75
								ADDNAIFAIDVGNVNVDSCR	145
106	+1.5	gi|58338023	hypothetical protein LBA1769	162	13558/5.65	68%	9/17	VLDDGHLIYLEK	100
								AAVVVADVPTHTNVR	139
107	-1.5	gi|58336492	2-deoxyribosyltransferase	90	18297/4.62	27%	5/12	ISELKDFDFNKPR	93
								DFDFNKPR	56
108	-1.5	gi|58337087	F0F1 ATP synthase subunit delta	140	20326/4.93	43%	9/17	KYDLNAVR	55
110	+1.9	gi|58337891	NAD-dependent aldehyde dehydrogenase	200	50588/5.14	48%	19/57	IQGVALTGSER	91

CHAPTER 5

Reference map and proteomic analysis of *Bifidobacterium animalis* subsp. *lactis* Bl-04 grown on galactooligosaccharides, raffinose family oligosaccharides and isomaltooligosaccharides

Reference map and proteomic analysis of *Bifidobacterium animalis* subsp. *lactis* Bl-04 grown on galactooligosaccharides, raffinose family oligosaccharides and isomaltooligosaccharides

Morten Ejby[1], Anne Knudsen[1], Avishek Majumder[1], Bjarne Schmidt[1], Sampo Lahtinen[2], Birte Svensson[1*] and Susanne Jacobsen[1*]

1. Enzyme and Protein Chemistry, Department of Systems Biology, Technical University of Denmark, Søltofts Plads, Building 224, DK-2800 Kgs. Lyngby, Denmark.

2. DuPont, Nutrition & Health, Sokeritehtaantie 20, 02460 Kantvik, Finland.

***Corresponding authors:** Susanne Jacobsen & Birte Svensson, Enzyme and Protein Chemistry, Department of Systems Biology, Technical University of Denmark, Søltofts Plads, Building 224, DK-2800 Kgs. Lyngby, Denmark.

Phone: +45 45252740; +45 45252741; Fax:+45 45886307

Email: sja@bio.dtu.dk; bis@bio.dtu.dk

Abstract

Bifidobacterium animalis subsp. *lactis* Bl-04 is a well known probiotic bacteria used in many fermented milk products. In the present study a reference proteome map of *Bifidobacterium animalis* subsp. *lactis* Bl-04 was established using two-dimensional gel electrophoresis (2-DE) and the differential abundance of proteins with different prebiotic carbohydrates was studied using differential 2-DE (2D-DIGE). Whole-cell protein extracts were separated by 2DE in the pH ranges 3−10 and 3−7. A total of 328 unique proteins were identified by MS/MS-MS analysis from the 960 spots picked from the 2D gel. The identified spots were distributed among the 22 functional classes and the major fraction of the identifications possesses to the functional role translation and ribosomal structure. The 2D-DIGE analysis with galactooligosaccharides, raffinose family oligosaccharides and isomaltooligosaccharides revealed various proteins involved in the metabolism of these prebiotic carbohydrates. The glycoside hydrolase β-galactosidace (Balac_0484) was found to be 2.0 fold more abundant with galactooligosaccharides than on glucose. The glycoside hydrolases α-galactosidase (Balac_1601), oligo-1,6-glucosidase (Balac_1593) and sucrose phosphorylase (Balac_0138) were found to be upregulated with 1.5−11.2 fold for melibiose, raffinose family oligosaccharides raffinose, and stachyose and isomaltooligosaccharides panose and isomaltose. Various proteins of the bifid shunt including L-ribulose-5-phosphate 4-epimerase, phosphoketolase, phosphoglucomutase, transketolase, 2,3-bisphosphoglycerate-dependent phosphoglycerate mutase, glyceraldehyde-3-phosphate dehydrogenase, pyruvate kinase and L-lactate dehydrogenase were found to be differentially abundant with these prebiotic oligosaccharides candidates as carbon source.

Introduction

Bifidobacteria are high G+C Gram-positive non-motile anaerobic rod-shaped bacteria from the actinobacterial branch of bacteria [1]. They are found in the large intestines of most mammals, including humans and different species from the genus bifidobacteria have been linked to health promoting probiotic traits. Bifidobacteria represents a significant genus of the gastro intestinal tract (GIT) microbiota (up to 3% of the total fecal microflora of adults) [2]. Bifidobacteria have been shown to survive in the GIT, to adhere to human epithelial cells *in vitro*, modify fecal flora, modulate the host immune response and to prevent microbial gastroenteritis as well as colitis [3,4,5,6,7,8]. Currently bifidobacteria are used with increasing frequency in the food industry as health-promoting microorganisms. Efforts have been made to increase the diversity and number of bifidobacterial species in the intestinal tract by supplying certain bifidobacteria strains or prebiotic food ingredients that can stimulate the growth of bifidobacteria or a combination of both. The therapeutic effects of these practices have been described by treatment and prevention of gastrointestinal disorders [9]. Bifidobacteria are thought to act as scavengers of carbohydrate oligosaccharides in the large intestine [1,10,11]. They possess a range of carbohydrate transporters and glycoside hydrolases that confer a growth advantage where readily fermentable carbohydrates are in low supply [1,12].

Bifidobacterium animalis subsp. *lactis* Bl-04 (Bl-04) has been isolated from different sources *e.g*. human and animal feces, sewage and fermented milk [13]. The 1.94 Mb genome of Bl-04 encodes for 1567 proteins (http://www.ncbi.nlm.nih.gov/genome/844?project_id=59359), comprising of 38 glycoside hydrolases (http://www.cazy.org/b982.html) capable of hydrolyzing carbohydrates of varying linkage type and monosaccharide composition. Three different groups of prebiotic carbohydrates including, β-galactosyl linked galactooligosaccharides (GOS), α-galactosyl linked melibiose, and raffinose family oligosaccharides (RFO) as well as isomaltooligosaccharides (IMO) i.e α-(1→6) linked glucose oligomers were used in the present study using 2D-DIGE, to monitor the specific effects of potential prebiotic carbohydrates. GOS are well described prebiotics able to promote growth and beneficial activities of bifidobacteria [14]. Furthermore GOS have been proposed to act as a molecular decoy that mimic the epithelial carbohydrate binding sites recognized by pathogens and thereby suppress infection of pathogenic species [15]. RFO constitute an

emerging class of prebiotic carbohydrates derived from soybean and lupins. Raffinose was been shown to modulate the human intestinal microbiota with beneficial effects [16]. Finally IMO are known to be selectively fermented by bifidobacteria and increase their number in the presence of the human gut microflora [14].

Proteome studies of bifidobacteria primarily focused on establishing reference proteome of *B. longum* [17,18], utilization of different carbohydrate sources [19,20], and adaptation to stress conditions [21,22]. There are no previous reports on the reference proteome of *B. animalis* and this is the first report of *B. animalis* reference proteome and the adaptations to various prebiotics. The whole cell extract reference proteome of Bl-04 grown MRS-glucose was established by using 2D-gel electrophoresis (pH 3−7 and pH 3−10) to provide a basis for subsequent differential proteome studies of the prebiotic metabolism. CyDye minimal labeling using a dye swapping approach was used for the differential proteome analysis using 2-DE DIGE.

Material and Methods

Growth Conditions and Protein Extraction

Bifidobacterium animalis subsp. *lactis* Bl-04 (Bl-04); (DuPont Nutrition & Health, Kantvik, Finland) was grown under anaerobic conditions without agitation at 37 °C in 50 mL batch cultures in MRS media [23] for analyzing the soluble whole cell reference proteome (pH 3−7 and pH 3−10). Bl-04 was grown under anaerobic conditions without agitation at 37 °C in 50 mL batch cultures in semi-synthetic medium (LABSEM) [24], supplemented with 1% of carbohydrate carbon source for the DIGE analysis (pH 3−7). Cultures were sub-cultured in the LABSEM media for three cycles prior to analysis, to avoid chemical carry-over effects. The cells were harvested at late-log phase by centrifugation (3200 *g*, 10 min, 4 °C), and washed twice with 0.9% NaCl. The cell pellet was added an approximately equal volume of acid washed glass beads (<100 μm diameter; Sigma, Brøndby, Denmark) followed by 300 μL phenol (Tris saturated, pH 8.0) and 300 μL 10 mM DTT, 10 mM Tris (pH 8.0). Disruption was carried out (Bio 101 Savant FastPrep FP 120 bead beater, Savant, Farmingdale, USA) at a speed of 6.5 m/s for four cycles of 45 s each with intermittent cooling on ice. The cell lysate was centrifuged (10,000 *g*, 10 min, 4 ºC) resulting in three distinct phases. The phenol phase was transferred to a microtube, added ice-cold ethanol (four volumes), kept at −20 ºC overnight and centrifuged (15000 *g*, 10 min, 4 ºC). The

resulting precipitate was dissolved in 300 µL rehydration buffer (7 M urea, 2 M thiourea, 2 % CHAPS, 200 mM bis(2-hydroxyethyl) disulfide (HED), and 2% pharmalyte pH 3−10 (GE Life Sciences, Uppsala, Sweden). The protein concentration was determined (2D Quant kit; GE Life Sciences) and the samples kept at −80 °C until use.

Sample Preparation for 2-DE and DIGE

For the MRS grown whole cell soluble proteome an extract containing 300 µg protein was diluted with rehydration buffer (8 M urea, 2 M thiourea, 2 % CHAPS, 0.5% pharmalyte pH 4−7 , 0.3% DTT) up to 450 µL and applied on immobilized pH gradient (IPG) strips (linear pH 3−7 and pH 3−10; 24 cm). For the DIGE analysis, a dye-swapping approach was used to avoid bias due to the interference from fluorescence properties of gels at different wavelengths [25]. A protein aliquot (50 µg) of each of four biological replicates grown with the same carbon source was labeled interchangeably with 400 pmol of either Cy3 or Cy5 dye. For the internal standard, aliquots (25 µg protein) of each sample in the experiment were pooled and labeled with 400 pmol Cy2. The Cy dye labeled samples were vortexed, and left in the dark (30 min, 4 °C). Labeling reactions were quenched by 2 µL 200 mM lysine in the dark (20 min). The internal standard and the samples were mixed and the volume was made to 450 µL with rehydration buffer for IPG strips (linear pH 3−7, 24 cm).

2-D gel electrophoresis

Separation in the first dimension (isoelectric focusing, IEF) was performed using IPG strips (pH 3−7 and 3−10; 24 cm; GE Lifesciences) on Ettan™ IPGphor (GE Lifesciences). Rehydration was carried out at 20 °C for 12 h. IEF was performed at a total of 70 kVh (1 h at 150 V, 1 h at 300 V, 1 h at 1,000 V, gradient to 8,000 V, hold at 8,000 V until a total of at least 70 kVh was reached). Subsequently, strips were equilibrated for 2 × 15 min in 5 mL equilibration buffer (6 M urea, 30% glycerol, 50 mM Tris-HCl, pH 8.8, 2% SDS, and 0.01% bromophenol blue) supplemented with 1% DTT and 2.5% iodoacetamide in the first and second equilibration step, respectively. The strips were placed on 12.5% SDS-PAGE gels and overlaid with 0.5% molten agarose in 1 × SDS running buffer (0.25 M Tris-base, 1.92 M glycine, and 1% SDS). The second dimension (SDS-PAGE) was performed on Ettan™

DALT *twelve* Electrophoresis Unit (GE Lifesciences) overnight at 1 W/gel until the dye front reached the gel bottom. The reference map gels for whole cell extract proteome (pH 3−7 and pH 3−10) were stained by colloidal Coomassie Brilliant Blue (CBB) as described previously [26].

Image Analysis

Images of CBB stained gels were generated (Microtek scanner; Scan maker 9800XL; Microtek, Carson, USA) using Photoshop CS4 software. Imaging of DIGE gels (four biological replicates and four internal standard gels) was done immediately after the second dimension run at excitation/emission wavelengths of Cy2 (488/520 nm), Cy3 (532/580 nm) and Cy5 (633/670 nm), respectively (100 μm resolution; Typhoon 9410 Variable Mode Imager; GE Lifesciences). Gel images were analyzed by Progenesis SameSpots version 3.3 (nonlinear Dynamics Ltd, Newcastle upon Tyne, UK). Scanned gels were analyzed by intra-gel (difference in-gel analysis) and inter-gel (biological variance analysis) analysis. A 1.5-fold threshold (spot volume ratio change and ANOVA $p \leq 0.05$) and false discovery rate $q \leq 0.05$ was chosen as criterion in the identification of differentially abundant protein spots. Gels were post-stained with CBB prior to spot protein identification.

In-gel Digestion and Protein Identification by MS

Spots on the 2-DE reference map and DIGE gels were excised manually and subjected to in-gel tryptic digestion with some modifications as described below [27]. Gel pieces were washed with 100 μL 40% ethanol (10 min) followed by 50 μl 100% acetonitrile (ACN), and incubated 45 min on ice with 2 μL 12.5 ng μL^{-1} trypsin (Promega, Nacka, Sweden) in 25 mM ammonium bicarbonate followed by addition of 10 μL 25 mM ammonium bicarbonate for rehydration, and incubated at 37 °C overnight. A supernatant aliquot (1 μL) was applied to the Anchor Chip target plate (Bruker Daltonics, Bremen, Germany), covered by 1 μL matrix solution (0.5 μg μL^{-1} α-cyano-4-hydroxycinnamic acid in 90% ACN, 0.1% TFA) and washed in 0.02% TFA. MS and MS/MS spectra measurements were performed on a Bruker Ultraflex II TOF/TOF-MS (Bruker Daltronics) equipped with a nitrogen laser, working in reflecton mode. Spectra were externally calibrated using a

tryptic digest of β-lactoglobulin (5 pmol μL^{-1}). The MS together with MS/MS spectra were searched against the NCBInr database for bacteria (NCBInr 20091112; 10032801 sequences; 3422028181 residues) using the MASCOT 2.4 software (http://www.matrixscience.com) integrated together with BioTools v3.1 (Bruker-Daltonics). Database search parameters used were, peptide charge of +1, peptide mass accuracy of 80 ppm, maximum one partial cleavage, fragment mass accuracy was set to $\pm$ 0.5 Da, carbamidomethylation was set as fixed modification of cysteine and partial oxidation of methionine. Filtering of peaks was done for known autocatalytic trypsin peaks and keratin peaks; the signal to noise threshold ratio was set to 1:6. Protein identifications were confirmed with a Mascot score cutoff of 84 for peptide mass fingerprint (PMF) and 42 for single peptide based MS/MS analysis which refer to significant *P*-values ($p \leq 0.05$). Mascot uses probability based scoring and is described by $-10 \times \text{Log}_{10}(P)$, where P is the probability that the observed match is a random event. Protein scores greater than 84 are significant ($p \leq 0.05$). PMF identifications with low scores were confirmed by additional MS/MS identification.

Results and Discussion

Reference Proteome of *Bifidobacterium animalis* subsp. *lactis* Bl-04

The Bl-04 genome with 1631 annotated genes encodes a proteome comprosing 1567 proteins. The cytosolic proteome excluding predicted secreted and membrane proteins is predicted to encompass ~800 proteins. The cytosolic proteins are predicted to be distributed in the p*I* 3.5−12 and *Mr* 5−200 kDa and are the primary focus in the present proteome study. Bacterial proteomes show a bimodal distribution based on p*I*, with proteins moving away from the cytoplasmic pH [28]. The bimodal pattern of proteome distribution of Bl-04 is similar to reported proteomes of gut microbiota [19,29,30] with a high concentration of proteins in the p*I* 3−7. The *in silico* virtual gel of the cytosolic proteins show a high density of proteins in the p*I* 3−7 and constitute to ~75 % of the total cytosolic proteins (http://web.expasy.org/protparam/). A similar distribution corresponding to the virtual gel was observed for the reference gel in the pH 3−10 (Fig. 1). 585 spots were picked for identification by MALDI MS/MS-MS and resulted in 517 protein identifications (Supplementary Table 1A). To better resolve proteins in the dense pH 3−7 range, the whole

cell extract proteome was resolved on a 2D-gel within the pH 3−7 (Fig. 2). A total of 375 spots were picked from the 2D-gel in the pH 3−7 and resulted in 353 protein identifications (Supplementary Table 1B). From the 2D-gels of pH 3−7 and pH 3−10 a total of 960 spots were picked and 870 spots were identified (Supplementary Table 1A and B). The observation that only 328 unique protein identifications were made from the 870 protein identifications, possibly reflects PTMs. A similar pattern was observed for the *B. longum* 2-DE based reference map, where 369 unique identifications were made from 708 spots identified [18]. In the present study the proteome coverage was ~21% and previous proteome studies of Bifidobacteria have reported coverage of 6−22% [17,31]. Other proteome studies of Gram-positive bacteria have reported identification rates of 3.3−22% [18,32,33,34].

A relatively large part of the proteins identified in the composite reference proteome (~18%) are involved in protein synthesis including ribosomal proteins, translational factors and tRNA-synthases (Fig. 3; Supplementary Table 1A and B). This suggests that cells were propagating at a relatively high growth rate at the time of harvest since ribosomal proteins are growth rate regulated in most bacteria [35,36]. Another dominant class found in the Bl-04 reference map was proteins involved in carbohydrate metabolism and energy conversion, 11% and 6% respectively. The proteins of the metabolic pathway "bifid shunt", including the taxonomic marker enzyme phosphoketolase (Fig. 2, spot 50−54 and 357) were found in the 2-DE maps, within the pH 3−7. The key enzymes of the bifid shunt where found in multiple spots indicating PTMs. Putative xylulose-5-phosphate/fructose-6-phosphate (X5P/F6P) phosphoketolase (Balac_0971) (Fig. 2, spot 50−54), transketolase (Balac_0842) (Fig. 2, spot 23−26), and transaldolase (Balac_0843) (Fig. 2, spot 175 and 176), were identified in multiple spots of differing p*I* values and *Mr*. Post translational modifications are in regulating the activity of glycolytic enzymes [37] and this multiple spot pattern has often been observed in 2-DE proteomic studies [18,19]. Noticeably proteins involved in the metabolism of carbohydrates other than glucose were also identified in the reference proteome. For example proteins involved in galactose metabolism, galactokinase (Fig. 1, spot 207; Supplementary Table 1A) and UDP-glucose 4-epimerase (Fig. 1, spot 231 and 232; Fig. 2, spot 169,192 and 193; Supplementary Table 1A and 1B); in sucrose metabolism, sucrose phosphorylase (Fig. 2, spot 100; Supplementary Table 1B); and in degradation of β-linked glucans, β-D-

glucosideglucohydrolase (Fig. 2, spot 8 and 9) and β-glucosidase (Fig. 2 spot 104; Supplementary Table 1B) ; in degradation of maltodextrins, 4-α-glucanotransferase (Fig. 1, spot 334−337; Supplementary Table 1A). A third prominent group of proteins identified in the Bl-04 2-DE reference map were involved in amino acid and nucleotide transport and metabolism corresponding to ~10 % and ~8 % respectively (Fig. 3). Especially enzymes catalyzing steps in the metabolism of threonine, glutamine, arginine, histidine and serine were observed.

2DE-DIGE

Molecular mechanisms of adaptation of probiotic bacteria to prebiotic carbohydrates have been previously studied in lactobacillus and bifidobacteria using transcriptomic and proteomic approaches [38,39,40,41]. Bifidobacteria are able to ferment several oligosaccharides, including GOS, RFO and IMO. Here we apply differential proteomics using (2DE-DIGE) to gain insights into Bl-04 utilization of various oligosaccharides at proteome level. Carbohydrate utilization in bifidobacteria is characterized by the channeling of the carbohydrate via the bifid shunt (pentose phosphate pathway). The ratio of the end products of carbohydrate metabolism *i.e*. lactate to acetate changes with the type of sugar fermented in bifidobacteria [19,42]. The differential abundance of proteins in the whole cell proteome of Bl-04 grown on glucose was compared to growth on GOS, RFO and IMO.

Differential abundance of proteins in Bl-04 with GOS

2D-DIGE analysis of the differential proteome revealed a total of 35 spots to have ≥ 1.5-fold difference in relative abundance (Fig. 4). Thirty protein identifications were possible from the 35 spots and represent, 27 unique proteins (Table 1). Identified proteins of the carbohydrate metabolism include, β-galactosidase (Balac_0484) (spot 286); UDP-glucose-4-epimerase (spot 620); L-ribulose-5-phosphate 4-epimerase (spot 849); X5P/F6P-phosphoketolase (spot 238); phosphoglucomutase (spot 353); transketolase (spot 274); 2,3-bisphosphoglycerate-dependent phosphoglycerate mutase (spot 478); glyceraldehyde-3-phosphate dehydrogenase (spot 633); and pyruvate kinase (spot 361). Bifidobacteria are known to poses multiple copies of β-galactosidase (http://www.cazy.org/), while the Bl-04

genome encodes three β-galactosidases. β-Galactosidase (spot 286) was found to be +2.0 fold upregulated in the presence of GOS and is the primary glycoside hydrolase hydrolysing β-linked galactose oligomers. UDP-glucose-4-epimerase and phosphoglucomutase involved in the conversion of galactose moieties to α-D-glucose-6-P were found to be 2.4 and 1.6 fold upregulated. α-D-Glucose-6-P enters the bifid shunt [43] and L-ribulose-5-phosphate 4-epimerase, transketolase, and putative phosphoketolase of the bifid shunt were found to be differentially abundant (+1.6−(+3.7) fold) (Table 1). The glycerate-3-P generated by glyceraldehyde-3-phosphate dehydrogenase is converted to glycerate-2-P and finally to pyruvate by 2,3-bisphosphoglycerate-dependent phosphoglycerate mutase and pyruvate kinase, which were found to be lower in abundance by 1.5 and 1.7 fold respectively. The end products of bifidobacteria carbohydrate fermentation include acetate, L-lactate, ethyl alcohol, and formate [42]. The bifunctional acetaldehyde-CoA/alcohol dehydrogenase (spot 110) involved in the inter conversion of acetaldehyde to ethyl alcohol was found to be 2.6 fold upregulated when grown on GOS. The differential abundance of proteins of the end product carbohydrate metabolism in the GOS proteome suggests a change in the lactate to acetate ratio. Proteome investigation of *B. longum* grown on galactose resulted in similar differential abundance UDP-glucose-4-epimerase and phosphoglucomutase and lowered acetate to lactate ratio [19]. Additional noticeable observations from the proteome of GOS grown Bl-04 cells is the down regulation (−1.6−2.2 fold) of proteins belonging to the COG group involved in transcription and translation.

Differential abundance of proteins in Bl-04 grown on RFO

Raffinose family oligosaccharides (RFO) are α-galactosyl derivatives of sucrose. In the present study, the trisaccharide raffinose (α-D-Gal*p*-(1→6)-D-Glc*p*-(α1,β2)-D-Fru*f*) and tetrasaccharide stachyose (α-D-Gal*p*-(1→6)-D-Gal*p*-(1→6)-D-Glcp-(α1,β2)-D-Fru*f*) were used along with the disaccharide melibiose (α-D-Gal*p*-(1→6)-D-Glc*p*). The administration of raffinose has shown to increase the levels of bifidobacteria sp. in the gut [44]. In the present study a total of 61, 39 and 63 spots were found to be differentially abundant with ≥ 1.5-fold relative abundance and 52, 33 and 63 protein identifications were possible, with growth on α-galactose linked carbohydrates, stachyose, raffinose and melibiose

respectively (Fig. 5; Table 2A, B and C). The glycoside hydrolases α-galactosidase (GH36; Balac_1601) and the oligo-1-6-glucosidase (GH31; Balac_1593) were found to be abundant in the proteome of Bl-04 with growth on the three oligosaccharides. α-Galactosidase was found in the three corresponding proteomes as two multiple forms differing in p*I*, with a fold change abundance of 2.7−5.0 fold (Fig. 4; Table 3). The α-galactosidase, releases the galactose moiety liberating glucose, sucrose and raffinose from melibiose, raffinose and staychose respectively [45]. The liberated galactose enters the central metabolism via the Leloir pathway, and UDP-glucose-4-epimerase of this pathway was 2.2−3.7 fold upregulated. Sucrose is generated from the hydrolysis of raffinose and stachyose and sucrose phosphorylase (GH 13_18; Balac_0138) acts on sucrose to liberate fructose and glucose-1-P [46]. Sucrose phosphorylase could be identified on 2D-DIGE gels of cultures grown on melibiose (spot 416, fold +1.6) and stachyose (spot 416, fold +1.6) but not raffinose. Induction of sucrose phosphorylase was found to be under the transcriptional regulation of GalR-LacI-type regulator and was induced in the presence of sucrose and raffinose in *B. lactis* and *B. longum* [47,48]. Melibiose also seems to induce the synthesis of Bl-04 sucrose phosphorylase. Sucrose phosphorylase mutants of the Gram-positive bacteria *Streptococcus mutans* failed to utilize melibiose, and require a functional sucrose phosphorylase for metabolizing melibiose [49]. A similar interaction with sucrose phosphorylase for utilization of melibiose in Bl-04 is a plausible explanation for the induction of sucrose phosphorylase with melibiose.

In addition to changes in abundance of various proteins of the bifid shunt (Table 2A, B and C), notably, is the change in abundance of glycoside hydrolase oligo-1,6-glucosidase (+1.5−(+2.2) fold) with growth in all the three carbohydrates (Table 2A, B and C). The gene cluster involved in the metabolism of α-galactose linked sugars includes two α-galactosidases (Balac_1596 and Balac_1601), components of the ABC transporter for sugars, oligo-1,6-glucosidase and two transcriptional regulators (Fig. 7). The gene cluster is similar to the multiple sugar metabolism gene cluster in Gram-positive bacteria capable of utilizing melibiose, raffinose and isomalooligosaccharides [50,51,52]. Only one of the α-galactosidases (Balac_1601) was found to be differentially abundant in cultures grown on α-galactose linked sugars (Table 2A, B and C). The presence and induction of oligo-1-6-glucosidase indicates transcriptional regulation and induction by α-galactose linked sugars and the capability of the gene cluster in Bl-04 to utilize multiple sugars.

Differential abundance of proteins in Bl-04 grown on IMO

IMO are glucose oligomers with α-D-(1→6)-linkages, and in the present study the disaccharide isomaltose (α-D-Glc*p*(1→6)-α-D-Glc*p*) and trisaccharide panose (α-D-Glc*p*(1→6)-α-D-Glc*p*-(1→4)-D-Glc*p*) were used. A total of 105 and 96 spots were found to be differentially expressed with ≥ 1.5- relative fold change and 92 and 84 protein identifications were possible after growth on IMO isomaltose and panose respectively (Fig. 6; Table 4A and B). Oligo-1-6-glucosidase (GH 13) shows preferential activity towards panose and isomaltose in bifidobacteria [43] and was found to be 1.6−3.1 fold upregulated, by growth on isomaltose and panose (Fig. 6; Table 4A and B). Oligo-1,6-glucosidase (Balac_1593) liberates two molecules of glucose from isomaltose and glucose together with the α-1→4 linked glucose disaccharide maltose from panose. The gene encoding oligo-1,6-glucosidase is located in the gene cluster involved in the metabolism of α-galactose linked sugars, and α-galactosidase was upregulated 3.1−11.2 fold (Fig. 6; Table 4A and B). The coexpression of the proteins for melibiose, isomaltose and raffinose utilization in similar gene clusters has been reported for Gram-positive bacteria [53]. Remarkably sucrose phosphoryalase was also found to be differentially abundant with +1.5−(+1.7) fold change during growth on isomaltose and panose. Similarly, in *B. lactis*, sucrose phosphorylase was found to be induced by oligofructose in addition to sucrose and raffinose and was repressed by glucose [48]. The increase in abundancy of sucrose phosphorylase (Balac_0138), during growth on the carbohydrates melibiose, isomaltose and panose for Bl-04, suggests differences in regulation of GalR-LacI-type transcriptional regulator from other Gram-positive bacteria. The exact mechanism of regulation in bifidobacteria is not known, but the divergent evolution of GalR-LacI type repressor from other Gram-positive bacteria has been suggested to the differences in regulation from other known regulatory mechanisms [48].

Similar to the differential abundance of proteins of the bifid shunt during growth on GOS and RFO's, growth on IMO, alters the abundance of proteins from this pathway (Fig. 6; Table 4A and B). Carbohydrate sources have been shown to influence the end products of their metabolism, primarily influencing the lactate to acetate ratio [19,54]. The isoforms of L-lactate dehydrogenase 2 (spots 640 and 643; Fig. 6; Table 4A and B) involved in the inter conversion of pyruvate to L-lactate was found to be lower in abundance by 2.0−2.9 fold (Table 4A and B). The lowered abundance of L-lactate dehydrogenase indicates a

change in the ratio of lactate to acetate. Degradation of inulin-type fructans has been shown to increase acetic acid production in *B. animalis* [55]. It has been suggested in bifidobacteria that the presence of high intracellular sugar concentrations leads to lactic acid production, while low intracellular sugar concentrations with less fermentable sugars leads to short chain fatty acids like formic and acetic acid production to maintain the redox balance in the cell [55,56].

Concluding Remarks

The bifidobacteria in the gut are shown to promote human health. Proteome analyses of bifidobacteria have been previously carried out for *B. longum* sp. involving reference proteomes, adaptation to bile stress and carbohydrate sources have been studied. In the present work 2D-gel based proteomics to establish the cytosolic proteome of *Bifidobacterium animalis* subsp *lactis* Bl-04 and the molecular mechanisms of prebiotic carbohydrate metabolism of Bl-04 with different carbohydrate sources was analyzed using 2D-DIGE. On the reference cytosolic proteome of Bl-04, 870 protein spots were identified representing 328 unique proteins. The differential proteome analysis of Bl-04 with prebiotic carbohydrates GOS, ROS and IMO identified proteins involved in the metabolism of carbohydrates with different glycosidic linkages and composition. The prebiotic carbohydrate sources have been shown to influence abundance of the proteins of the bifid shunt and play a role in the production of end product metabolites. A single gene cluster was found to be involved in the metabolism of multiple sugars like α-galactosides melibiose, raffinose, stachyose and the α-glucosides isomaltose and panose.

This study has so far only relied on data obtained by 2DE electrophoresis. Before submission to *PLOS ONE* the 2DE-DIGE data are to be verified by semi-quantitative RT-PCR, DNA-microarrays or equivalent methods. Furthermore it is planned to make small organic acid profiles for the media in the different fermentations in the study, to verify that the changes observed in pyruvate metabolism in the 2D-DIGE experiments have a biological effect.

Acknowledgements

Birgit Andersen is acknowledged for technical assistance with mass spectrometric analysis. This work was supported by the Danish Strategic Research Council's Programme Committee on Health, Food and Welfare (FøSu), the Danish Research Council for Natural Science and the Danish Center for Advanced Food Studies (LMC). M.E. is grateful to the Technical University of Denmark for a Ph.D. scholarship. A.M. is grateful to the Technical University of Denmark for a Hans Christian Ørsted postdoctoral fellowship.

References

1. Schell MA, Karmirantzou M, Snel B, Vilanova D, Berger B, et al. (2002) The genome sequence of *Bifidobacterium longum* reflects its adaptation to the human gastrointestinal tract. Proc Natl Acad Sci USA 99: 14422-14427.
2. Bezkorovainy A (2001) Probiotics: determinants of survival and growth in the gut. Am J Clin Nutr 73: 399S-405S.
3. Briczinski EP, Phillips AT, Roberts RF (2008) Transport of glucose by *Bifidobacterium animalis subsp. lactis* occurs via facilitated diffusion. Appl Environ Microbiol 74: 6941-6948.
4. Paineau D, Carcano D, Leyer G, Darquy S, Alyanakian M-A, et al. (2008) Effects of seven potential probiotic strains on specific immune responses in healthy adults: a double-blind, randomized, controlled trial. FEMS Immunol Med Microbiol 53: 107-113.
5. Gopal PK, Prasad J, Smart J, Gill HS (2001) In vitro adherence properties of *Lactobacillus rhamnosus* DR20 and *Bifidobacterium lactis* DR10 strains and their antagonistic activity against an enterotoxigenic *Escherichia coli*. Int J Food Microbiol 67: 207-216.
6. Bartosch S, Woodmansey EJ, Paterson JCM, McMurdo MET, Macfarlane GT (2005) Microbiological effects of consuming a synbiotic containing *Bifidobacterium bifidum, Bifidobacterium lactis,* and oligofructose in elderly persons, determined by real-time polymerase chain reaction and counting of viable bacteria. Clin Infect Dis 40: 28-37.
7. Ventura M, O'Flaherty S, Claesson MJ, Turroni F, Klaenhammer TR, et al. (2009) Genome-scale analyses of health-promoting bacteria: probiogenomics. Nat Rev Microbiol 7: 61-71.

8. Wallace TC, Guarner F, Madsen K, Cabana MD, Gibson G, et al. (2011) Human gut microbiota and its relationship to health and disease. Nutr Rev 69: 392-403.
9. Gagnon M, Kheadr EE, Le Blay G, Fliss I (2004) In vitro inhibition of *Escherichia coli* O157:H7 by bifidobacterial strains of human origin. Int J Food Microbiol 92: 69-78.
10. Turroni F, Strati F, Foroni E, Serafini F, Duranti S, et al. (2012) Analysis of predicted carbohydrate transport systems encoded by *Bifidobacterium bifidum* PRL2010. Appl Environ Microbiol 78: 5002-5012.
11. Turroni F, van Sinderen D, Ventura M (2011) Genomics and ecological overview of the genus bifidobacterium. Int J Food Microbiol 149: 37-44.
12. Yin XH, Chambers JR, Barlow K, Park AS, Wheatcroft R (2005) The gene encoding xylulose-5-phosphate/fructose-6-phosphate phosphoketolase (xfp) is conserved among Bifidobacterium species within a more variable region of the genome and both are useful for strain identification. FEMS Microbiol Letters 246: 251-257.
13. Masco L, Ventura M, Zink R, Huys G, Swings J (2004) Polyphasic taxonomic analysis of *Bifidobacterium animalis* and *Bifidobacterium lactis* reveals relatedness at the subspecies level: reclassification of *Bifidobacterium animalis* as *Bifidobacterium animalis subsp. animalis subsp. nov.* and *Bifidobacterium lactis* as *Bifidobacterium animalis subsp. lactis subsp. nov*. Int J Syst Evol Microbiol 54: 1137-1143.
14. Rycroft CE, Jones MR, Gibson GR, Rastall RA (2001) A comparative in vitro evaluation of the fermentation properties of prebiotic oligosaccharides. J Appl Microbiol 91: 878-887.
15. Quintero M, Maldonado M, Perez-Munoz M, Jimenez R, Fangman T, et al. (2011) Adherence inhibition of *Cronobacter sakazakii* to intestinal epithelial cells by prebiotic oligosaccharides. Curr Microbiol 62: 1448-1454.
16. Fernando W, Hill J, Zello G, Tyler R, Dahl W, et al. (2010) Diets supplemented with chickpea or its main oligosaccharide component raffinose modify faecal microbial composition in healthy adults. Benef Microbes 1: 197-207.
17. Yuan J, Zhu L, Liu X, Li T, Zhang Y, et al. (2006) A proteome reference map and proteomic analysis of *Bifidobacterium longum* NCC2705. Mol Cell Proteomics 5: 1105-1118.
18. Guillaume E, Berger B, Affolter M, Kussmann M (2009) Label-free quantitative proteomics of two *Bifidobacterium longum* strains. J Proteomics 72: 771-784.

19. Liu DW, Wang SA, Xu B, Guo YH, Zhao JL, et al. (2011) Proteomics analysis of *Bifidobacterium longum* NCC2705 growing on glucose, fructose, mannose, xylose, ribose, and galactose. Proteomics 11: 2628-2638.
20. He T, Priebe MG, Zhong Y, Huang C, Harmsen HJM, et al. (2008) Effects of yogurt and bifidobacteria supplementation on the colonic microbiota in lactose-intolerant subjects. J Appl Microbiol 104: 595-604.
21. Sanchez B, Champomier-Verges MC, Collado MD, Anglade P, Baraige F, et al. (2007) Low-pH adaptation and the acid tolerance response of *Bifidobactetium longum* biotype *longum*. Appl Environ Microbiol 73: 6450 - 6459.
22. Yuan J, Wang B, Sun Z, Bo X, Yuan X, et al. (2008) Analysis of host-inducing proteome changes in *Bifidobacterium longum* NCC2705 grown *in vivo*. J Proteome Res 7: 375-385.
23. De Man JC, Rogosa M, Sharpe ME (1960) A medium for the cultivation of lactobacilli. J Appl Bact 23: 130-135.
24. Barrangou R, Altermann E, Hutkins R, Cano R, Klaenhammer TR (2003) Functional and comparative genomic analyses of an operon involved in fructooligosaccharide utilization by *Lactobacillus acidophilus*. Proc Natl Acad Sci USA 100: 8957-8962.
25. Tannu NS, Hemby SE (2006) Two-dimensional fluorescence difference gel electrophoresis for comparative proteomics profiling. Nat Protocols 1: 1732-1742.
26. Candiano G, Bruschi M, Musante L, Santucci L, Ghiggeri GM, et al. (2004) Blue silver: A very sensitive colloidal Coomassie G-250 staining for proteome analysis. Electrophoresis 25: 1327-1333.
27. Hellman U, Wernstedt C, Gonez J, Heldin CH (1995) Improvement of an in-gel digestion procedure for the micropreparation of internal protein-fragments for amino-acid sequencing. Anal Biochem 224: 451-455.
28. Knight CG, Kassen R, Hebestreit H, Rainey PB (2004) Global analysis of predicted proteomes: Functional adaptation of physical properties. Proc Natl Acad Sci USA 101: 8390-8395.
29. Ashida N, Yanagihara S, Shinoda T, Yamamoto N (2011) Characterization of adhesive molecule with affinity to Caco-2 cells in *Lactobacillus acidophilus* by proteome analysis. J Biosci Bioeng 112: 333-337.

30. Koskenniemi K, Koponen J, Kankainen M, Savijoki K, Tynkkynen S, et al. (2009) Proteome analysis of *Lactobacillus rhamnosus* GG using 2-D DIGE and mass spectrometry shows differential protein production in laboratory and industrial-type growth media. J Proteome Res 8: 4993-5007.
31. Vitali B, Wasinger V, Brigidi P, Guilhaus M (2005) A proteomic view of *Bifidobacterium infantis* generated by multi-dimensional chromatography coupled with tandem mass spectrometry. Proteomics 5: 1859-1867.
32. Cohen DPA, Renes J, Bouwman FG, Zoetendal EG, Mariman E, et al. (2006) Proteomic analysis of log to stationary growth phase *Lactobacillus plantarum* cells and a 2-DE database. Proteomics 6: 6485-6493.
33. Wu R, Wang WW, Yu DL, Zhang WY, Li Y, et al. (2009) Proteomics analysis of *Lactobacillus casei* Zhang, a new probiotic bacterium isolated from traditional home-made koumiss in Inner Mongolia of China. Mol Cell Proteomics 8: 2321-2338.
34. Guillot A, Gitton C, Anglade P, Mistou MY (2003) Proteomic analysis of *Lactococcus lactis*, a lactic acid bacterium. Proteomics 3: 337-354.
35. Lindahl L, Zengel JM (1982) Expression of ribosomal genes in bacteria. Adv Genet 21: 53-121.
36. Gourse RL, Gaal T, Bartlett MS, Appleman JA, Ross W (1996) rRNA transcription and growth rate-dependent regulation of ribosome synthesis in *Escherichia coli*. Annu Rev Microbiol 50: 645-677.
37. Deribe YL, Pawson T, Dikic I (2010) Post-translational modifications in signal integration. Nat Struct Mol Biol 17: 666-672.
38. Yuan J, Zhu L, Liu XK, Zhang Y, Ying TY, et al. (2006) A proteome reference map and proteomic analysis of Bifidobacterium longum NCC2705. Mol Cell Proteomics 5: 1105-1118.
38. Gilad O, Jacobsen S, Stuer-Lauridsen B, Pedersen MB, Garrigues C, et al. (2010) Combined transcriptome and proteome analysis of *Bifidobacterium animalis* subsp. *lactis* BB-12 Grown on xylo-oligosaccharides and a model of their utilization. Appl Environ Microbiol 76: 7285-7291.
39. Gilad O, Svensson B, Viborg AH, Stuer-Lauridsen B, Jacobsen S (2011) The extracellular proteome of *Bifidobacterium animalis* subsp. *lactis* BB-12 reveals proteins with putative roles in probiotic effects. Proteomics 11: 2503-2514.

40. Andersen JM, Barrangou R, Abou Hachem M, Lahtinen S, Goh YJ, et al. (2011) Transcriptional and functional analysis of galactooligosaccharide uptake by lacS in *Lactobacillus acidophilus*. Proc Natl Acad Sci 108: 17785-17790.
41. Andersen JM, Barrangou R, Abou Hachem M, Lahtinen SJ, Goh YJ, et al. (2012) Transcriptional analysis of prebiotic uptake and catabolism by *Lactobacillus acidophilus* NCFM. PLoS One 7: e44409.
42. deVries W, Stoutham AH (1968) Fermentation of glucose, lactose, galactose, mannitol and xylose by bifidobacteria. J Bacteriol 96: 472-478.
43. Pokusaeva K, Fitzgerald GF, van Sinderen D (2011) Carbohydrate metabolism in bifidobacteria. Genes Nutr 6: 285-306.
44. Dinoto A, Suksomcheep A, Ishizuka S, Kimura H, Hanada S, et al. (2006) Modulation of rat cecal microbiota by administration of raffinose and encapsulated *Bifidobacterium breve*. Appl Environ Microbiol 72: 784-792.
45. Xiao M, Tanaka K, Qian XM, Yamamoto K, Kumagai H (2000) High-yield production and characterization of α-galactosidase from *Bifidobacterium breve* grown on raffinose. Biotechnol Lett 22: 747-751.
46. Voet JG, Abeles RH (1970) The mechanism of action of sucrose phosphorylase. J Biol Chem 245: 1020-1031.
47. Kullin B, Abratt VR, Reid SJ (2006) A functional analysis of the *Bifidobacterium longum* cscA and scrP genes in sucrose utilization. Appl Microbiol Biotechnol 72: 975-981.
48. Trindade MI, Abratt VR, Reid SJ (2003) Induction of sucrose utilization genes from *Bifidobacterium lactis* by sucrose and raffinose. Appl Environ Microbiol 69: 24-32.
49. Barletta RG, Curtiss R (1989) Impairment if melibiose utilization in *Streptococcus mutans* serotype c gtfA mutants. Infect Immun 57: 992-995.
50. Russell RRB, Aduseopoku J, Sutcliffe IC, Tao L, Ferretti JJ (1992) A binding protein dependent transport system in *Streptococcus mutans* responsible for multiple sugar metabolism. J Biol Chem 267: 4631-4637.
51. Ajdic D, McShan WM, McLaughlin RE, Savic G, Chang J, et al. (2002) Genome sequence of *Streptococcus mutans* UA159, a cariogenic dental pathogen. Proc Natl Acad Sci USA 99: 14434-14439.

52. McLaughlin RE, Ferretti JJ (1996) The multiple-sugar metabolism (msm) gene cluster of *Streptococcus mutans* is transcribed as a single operon. FEMS Microbiol Lett 140: 261-264.

53. Ajdic D, Pham VTT (2007) Global transcriptional analysis of *Streptococcus mutans* sugar transporters using microarrays. J Bacteriol 189: 5049-5059.

54. Lauer E, Kandler O (1976) Mechanism of variation of acetate/lactate ratio during glucose fermentation by bifidobacteria. Arch Microbiol 110: 271-277.

55. van der Meulen R, Avonts L, De Vuyst L (2004) Short fractions of oligofructose are preferentially metabolized by *Bifidobacterium animalis* DN-173 010. Appl Environ Microbiol 70: 1923-1930.

56. van der Meulen R, Makras L, Verbrugghe K, Adriany T, De Vuyst L (2006) In vitro kinetic analysis of oligofructose consumption by bacteroides and bifidobacterium spp. indicates different degradation mechanisms. Appl Environ Microbiol 72: 1006-1012.

Legend to Figures

Fig. 1. A detailed 2-DE of the 400 µg whole cell extract soluble proteins (pH 3−10) of *Bifidobacterium animalis* subsp. *lactis* Bl-04 grown on MRS medium with 1% glucose. Numbered spots are chosen for analysis by in-gel digestion and mass spectrometry.

Fig. 2. A detailed 2-DE of the 300 µg whole cell extract soluble proteins (pH 3−7) of *Bifidobacterium animalis* subsp. *lactis* Bl-04 grown on MRS medium with 1% glucose. Numbered spots are chosen for analysis by in-gel digestion and mass spectrometry.

Fig. 3. Functional grouping of the 328 identified unique proteins on the 2-DE (pH 3–7 and 3–10) of *Bifidobacterium animalis* subsp. *lactis* Bl-04.

Fig. 4. Progenesis Samespots image of analyzed 2D-DIGE gel of *Bifidobacterium animalis* subsp. *lactis* Bl-04 grown with glucose and GOS as the carbon source. The numbers on the gel indicate differentially abundant spots (Fold change: $\geq$ 1.5; ANOVA $p \leq 0.05$; False discovery rate $q \leq 0.05$). The spots were analysed by in-gel digestion and mass spectrometry.

Fig. 5. Progenesis Samespots image of analyzed 2D-DIGE gel of *Bifidobacterium animalis* subsp. *lactis* Bl-04 grown with glucose and staychose (**A**), with glucose and raffinose (**B**) and with glucose and melibiose (**C**) as the carbon source. The numbers on the gel indicate differentially abundant spots (Fold change: $\geq$ 1.5; ANOVA $p \leq 0.05$; False discovery rate $q \leq 0.05$). The spots were analysed by in-gel digestion and mass spectrometry.

Fig. 6. Progenesis Samespots image of analyzed 2D-DIGE gel of *Bifidobacterium animalis* subsp. *lactis* Bl-04 grown with glucose and panose (**A**) and with glucose and isomaltose (**B**) as the carbon source. The numbers on the gel indicate differentially abundant spots (Fold change: $\geq$ 1.5; ANOVA $p \leq 0.05$; False discovery rate $q \leq 0.05$). The spots were analysed by in-gel digestion and mass spectrometry.

Fig. 7. Schematic representation of the differentially abundant proteins involved in the utilization of RFO and IMO. The genetic organization of the melibiose, raffinose fanily oligosaccharide and isomaltooligosaccharide induced, gene cluster, and sucrose uttilization gene loci are shown. The proteins identified by 2D-DIGE and MS analysis of cytosolic proteome (pH 3−7) are shown as arrows in black.

Fig. 1.

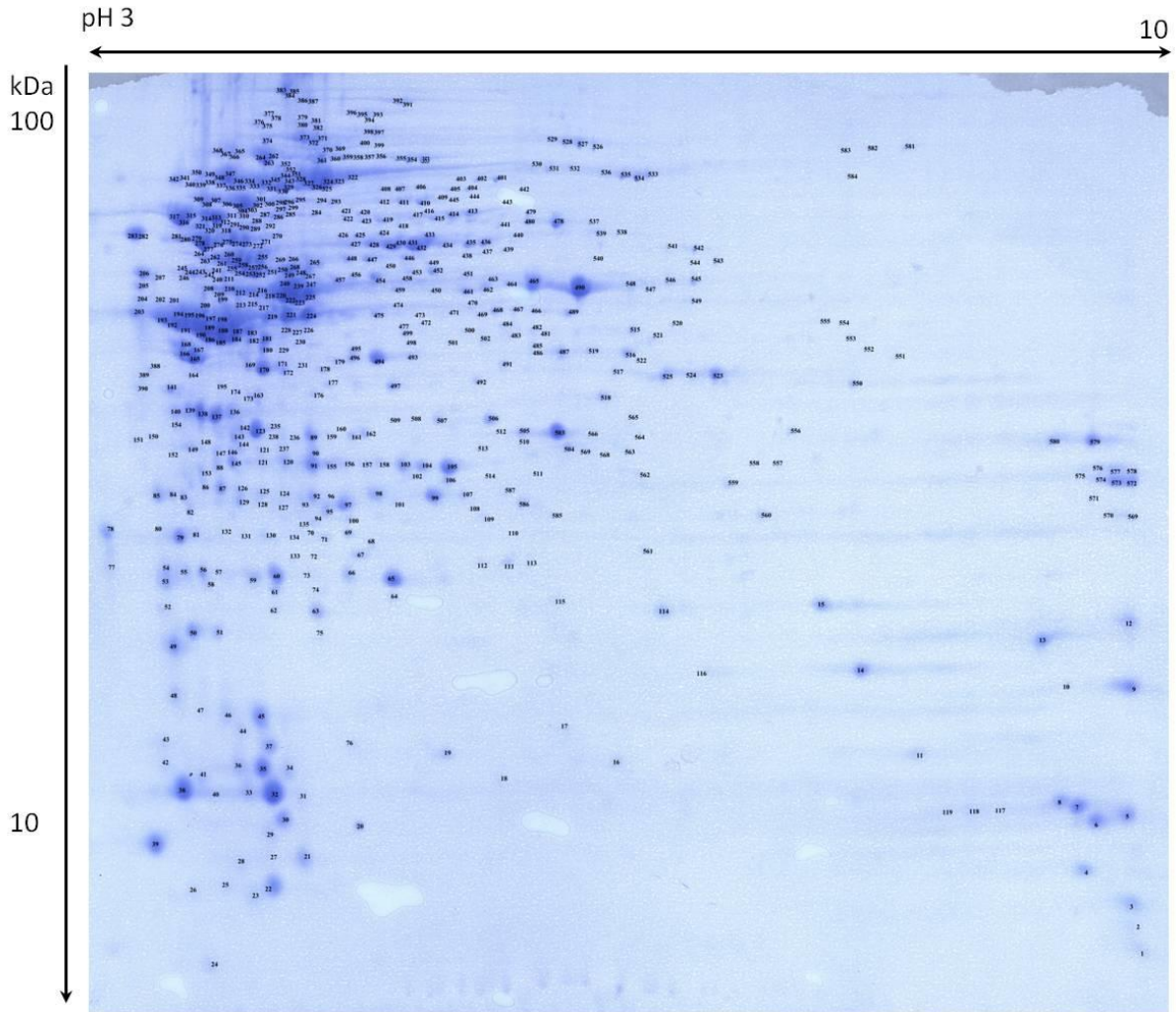

Fig. 2.

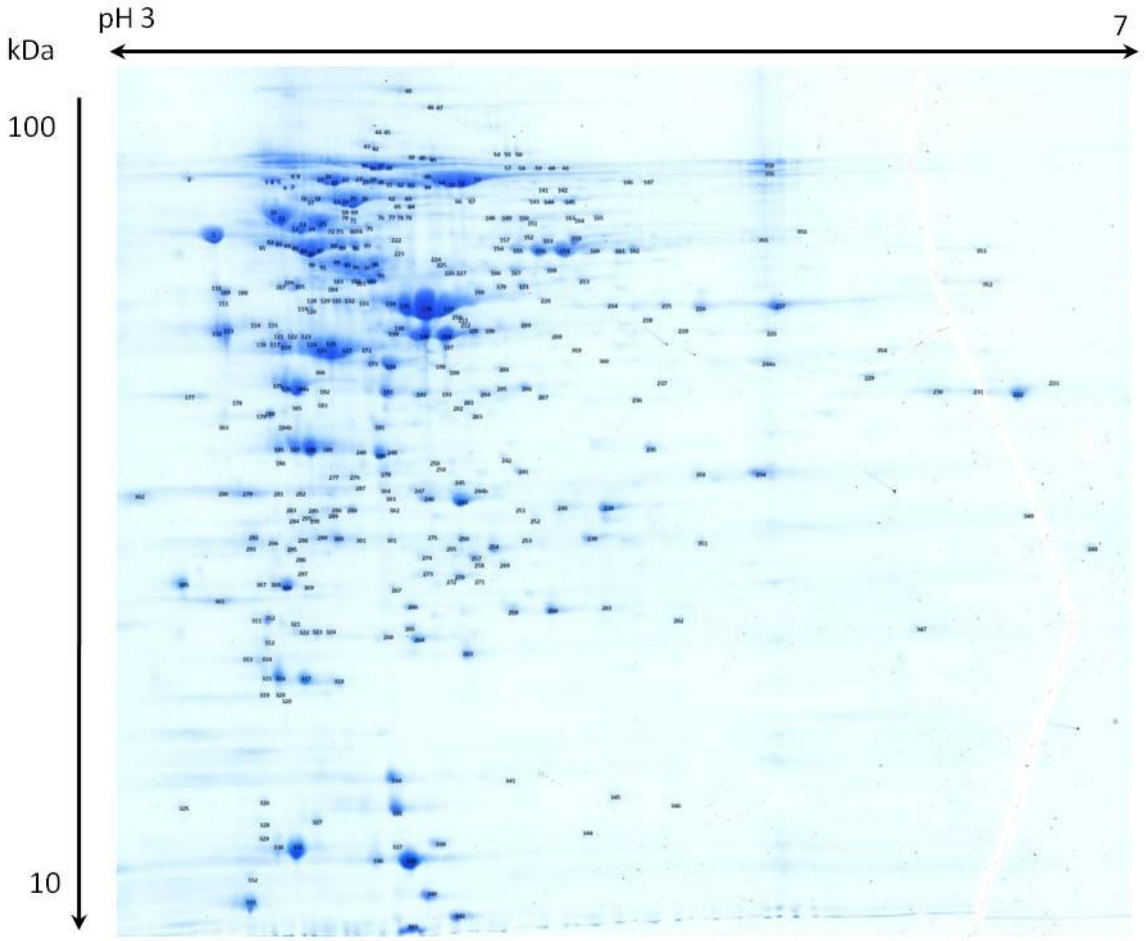

Fig. 3.

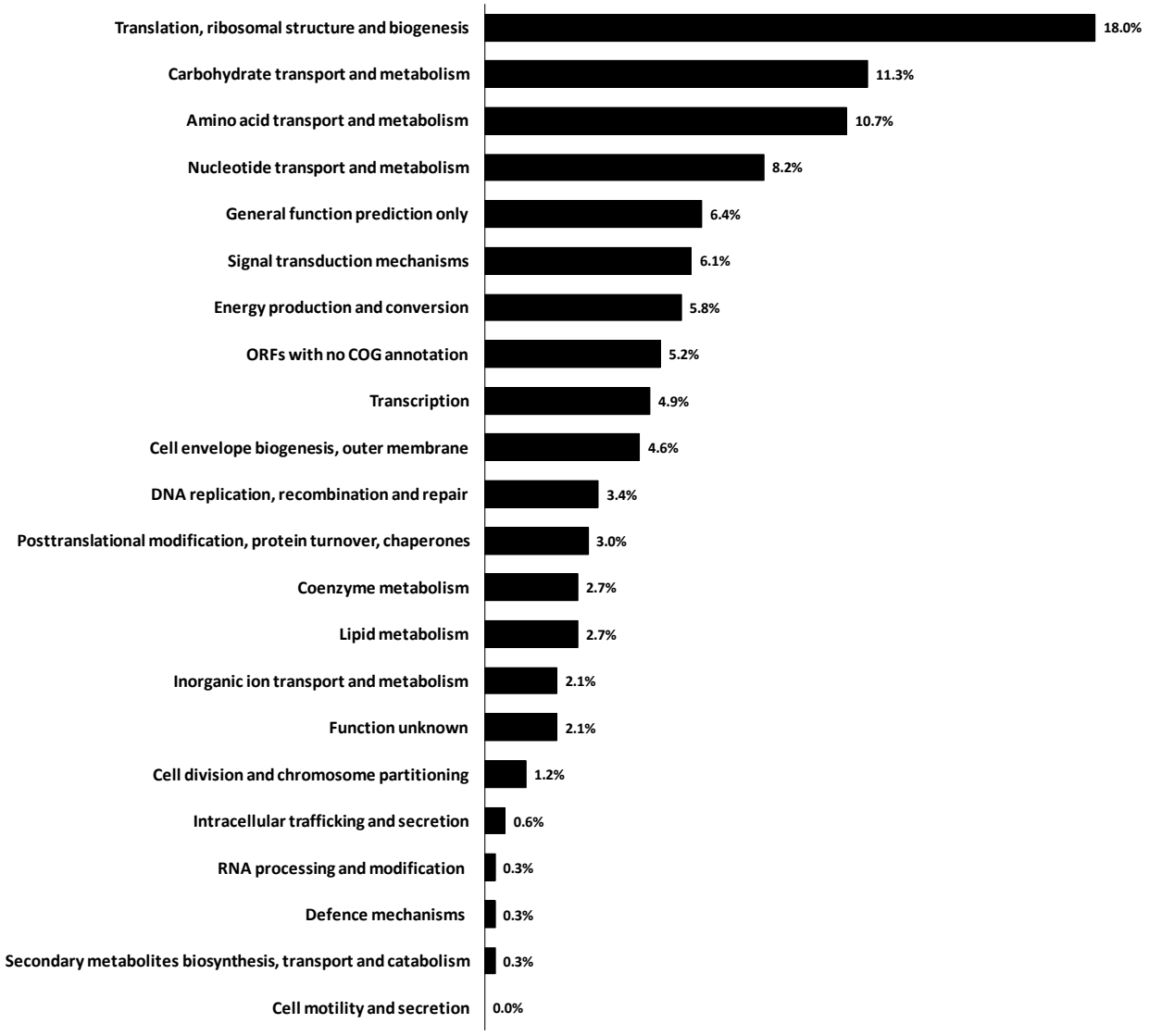
Translation, ribosomal structure and biogenesis
18.0%
Carbohydrate transport and metabolism
11.3%
Amino acid transport and metabolism
10.7%
Nucleotide transport and metabolism
8.2%
General function prediction only
6.4%
Signal transduction mechanisms
6.1%
Energy production and conversion
5.8%
ORFs with no COG annotation
5.2%
Transcription
4.9%
Cell envelope biogenesis, outer membrane
4.6%
DNA replication, recombination and repair
3.4%
Posttranslational modification, protein turnover, chaperones
3.0%
Coenzyme metabolism
2.7%
Lipid metabolism
2.7%
Inorganic ion transport and metabolism
2.1%
Function unknown
2.1%
Cell division and chromosome partitioning
1.2%
Intracellular trafficking and secretion
0.6%
RNA processing and modification
0.3%
Defence mechanisms
0.3%
Secondary metabolites biosynthesis, transport and catabolism
0.3%
Cell motility and secretion
0.0%

Fig. 4.

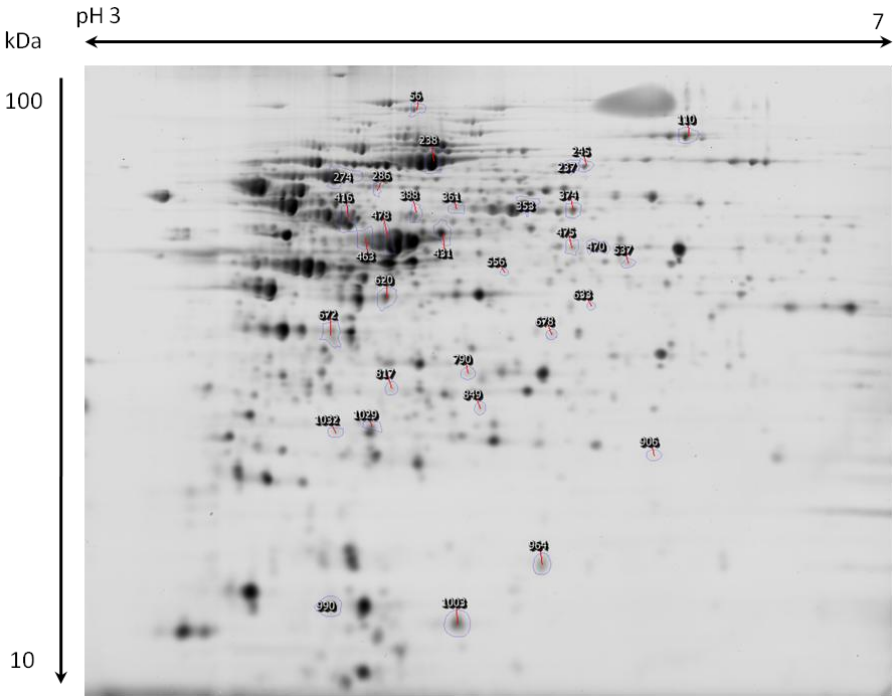
pH 3
7
kDa
100
10
55
110
238
245
237
274
285
316
383
361
353
374
478
475
470
337
463
431
559
620
633
572
678
750
817
849
1032
1029
908
964
930
1003

Fig. 5.

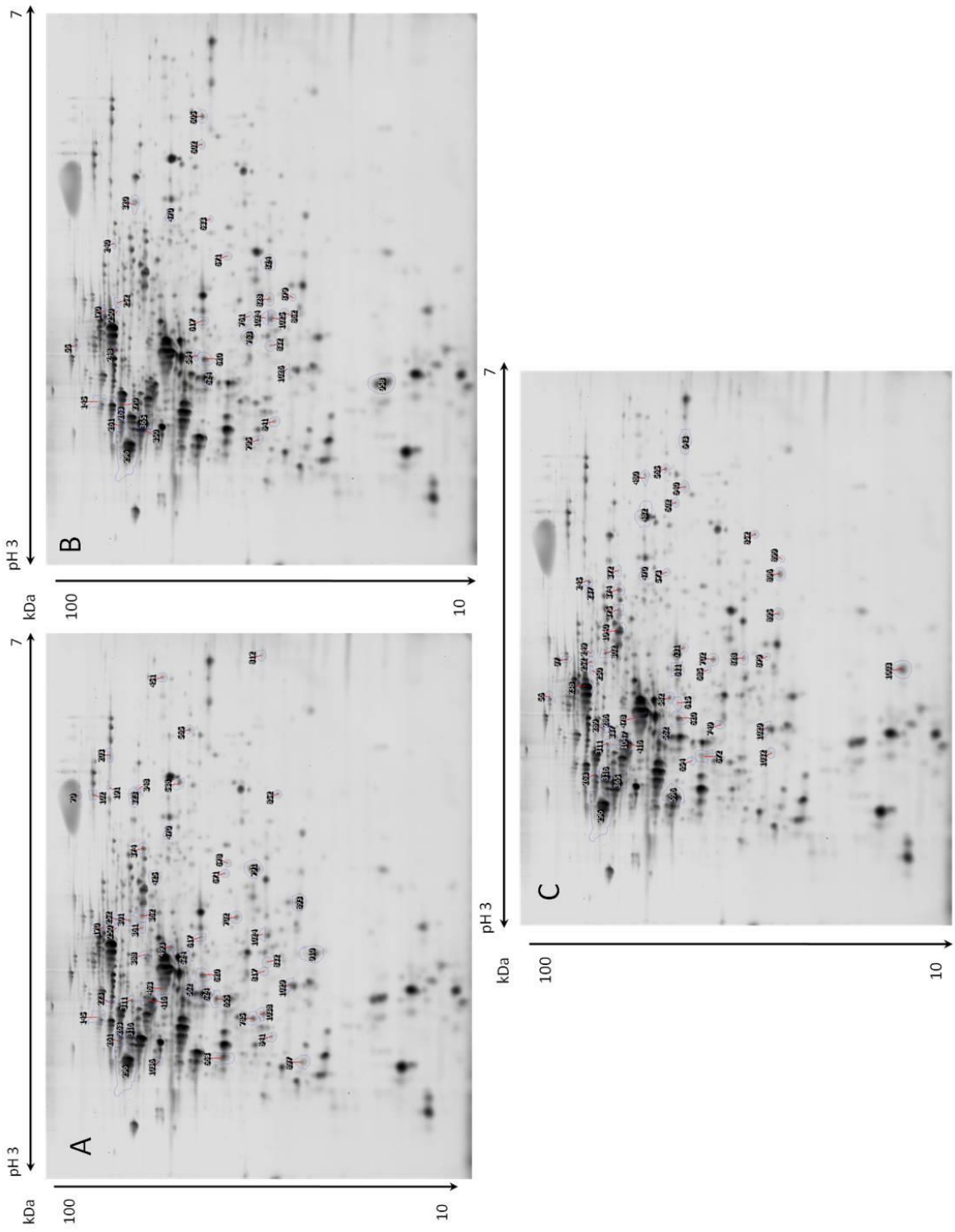

Fig. 6.

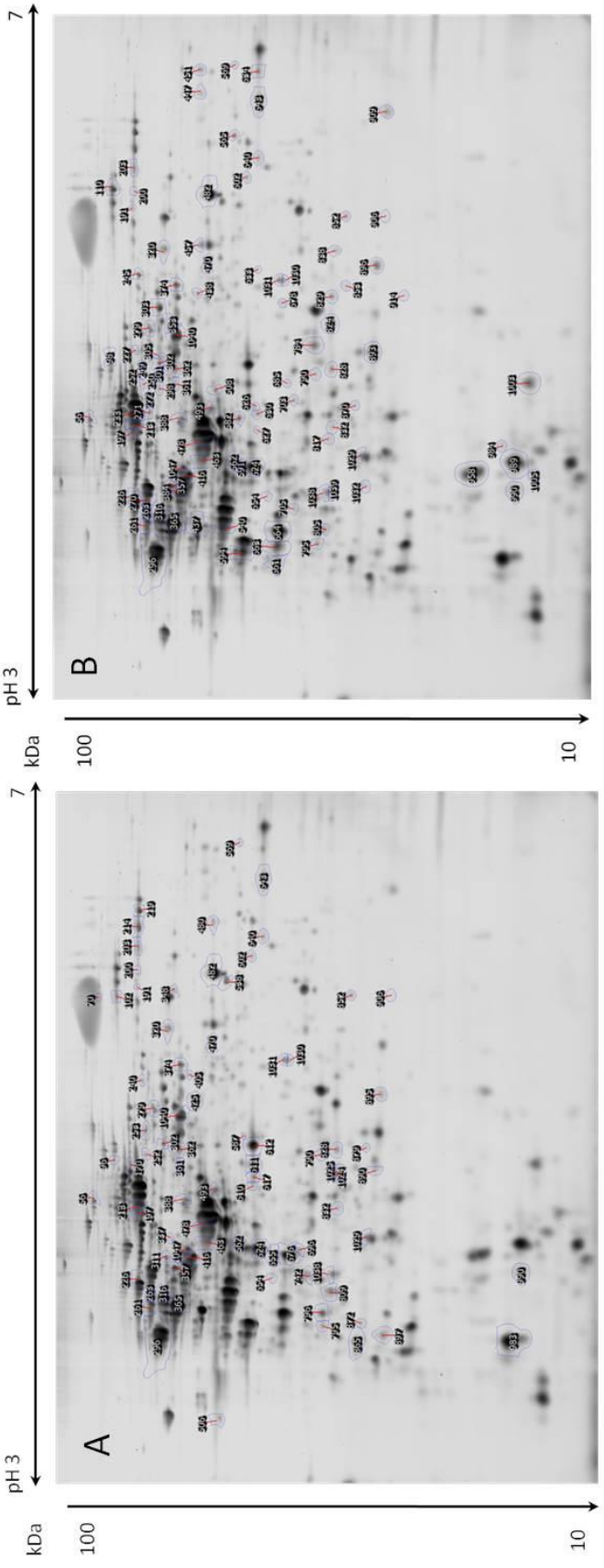

Fig. 7.

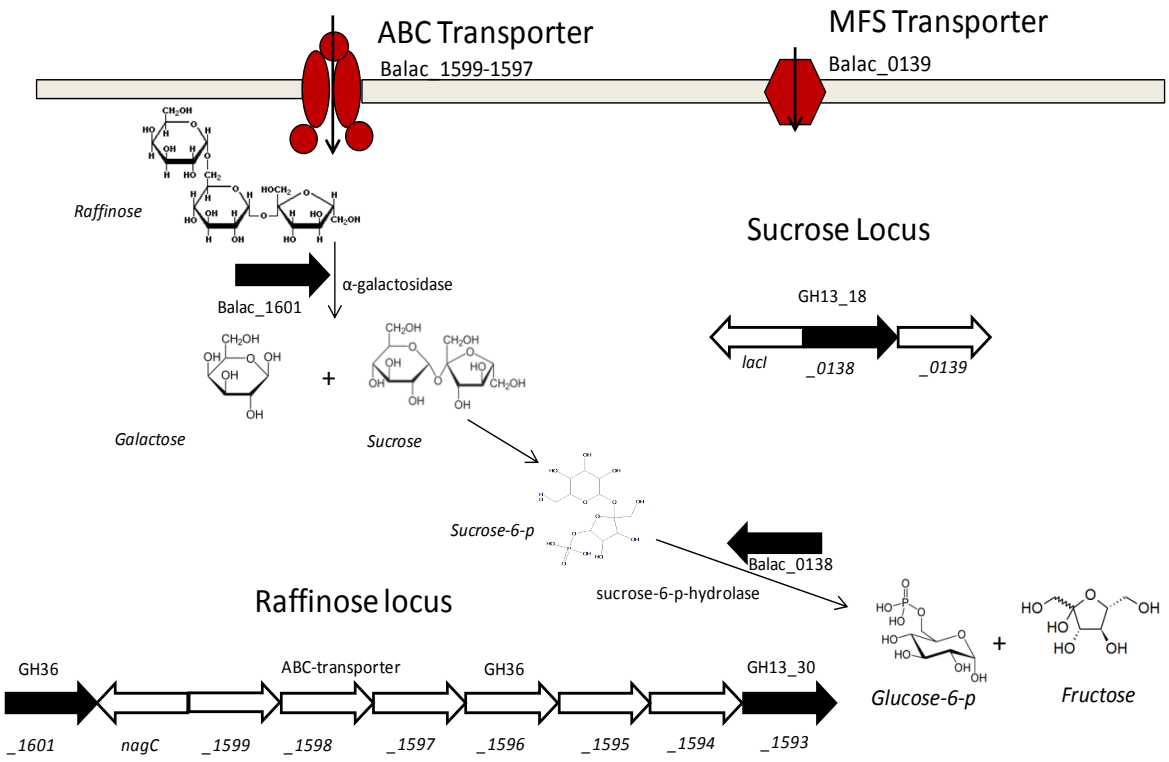
ABC Transporter
Balac_1599-1597
MFS Transporter
Balac_0139
Raffinose
Balac_1601
α-galactosidase
Galactose
Sucrose
Sucrose Locus
GH13_18
lacI
_0138
_0139
Sucrose-6-p
Balac_0138
sucrose-6-p-hydrolase
Raffinose locus
GH36
ABC-transporter
GH36
GH13_30
_1601
nagC
_1599
_1598
_1597
_1596
_1595
_1594
_1593
Glucose-6-p
Fructose

Table 1: Protein identifications of differentially abundant spots (≥ 1.5-fold spot volume ratio change and ANOVA $p \leq 0.05$) of *Bifidobacterium animalis* subsp. *lactis* grown on SEM medium with 1% glucose and 1% GOS.

Spot	Accession	Protein name	Mascot score	*Mr* /p*I*	Anova (*p*) (DIGE)	Fold	COG Functional role*
849	gi|241190131	L-ribulose-5-phosphate 4-epimerase	417	24576/5.06	2.53E-05	+3.7	G
110	gi|241190429	bifunctional acetaldehyde-CoA/alcohol dehydrogenase	397	105257/5.69	0.006	+2.6	C
620	gi|241190508	UDP-glucose 4-epimerase	427	34894/4.81	0.007	+2.4	M
56	gi|241190667	Carbamoylphosphate synthase large subunit	415	125134/4.9	0.0009531	+2.2	EF
388	gi|241190132	L-arabinose isomerase	343	55406/4.90	0.007	+2.1	G
286	gi|241190531	beta-galactosidase	393	69369/4.78	0.002	+2.0	G
374	gi|241190571	inosine-5'-monophosphate dehydrogenase	537	58116/5.3	0.0005322	+2.0	F
431	gi|241190489	aminopeptidase C	330	48233/4.97	0.000745	+1.9	E
238	gi|241191000	X5P/F6P phosphoketolase	441	84552/4.95	0.003	+1.9	G
678	gi|241191290	ATP binding protein of ABC transporter for glutamate_aspartate	377	29894/5.24	0.005	+1.8	E
245	gi|241191166	dipeptide transport ATP-binding protein	267	83448/5.33	0.002	+1.8	R
237	gi|241191166	dipeptide transport ATP-binding protein	374	84828/5.29	0.006	+1.6	R
353	gi|241190474	phosphoglucomutase	400	60826/5.16	0.008	+1.6	G
274	gi|241190872	transketolase	386	74062/4.67	0.003	+1.6	G
1032	gi|241191249	histidinol dehydrogenase	330	22768/4.66	0.004	-3.2	E
990	gi|241190823	hypothetical protein Balac_0787	129	11541/5.01	0.009	-3.1	−
1029	gi|241190089	oxidoreductase	191	23011/4.76	0.0007991	-2.3	R
906	gi|241190812	ribosome recycling factor	97	21331/5.52	0.007	-2.2	J
790	gi|241190653	phosphoribosylaminoimidazole-succinocarboxamidesynthase	359	27087/5.03	0.002	-2.1	F
1003	gi|241190258	hypothetical protein Balac_0197	150	12297/5.28	0.008	-2	S
470	gi|241190472	seryl-tRNA synthetase	266	42494/5.35	0.004	-1.9	J
463	gi|241190661	elongation factor Tu	170	44726/4.76	0.002	-1.8	J
537	gi|241190463	transcription elongation factor NusA	173	38588/5.64	0.003	-1.8	K

672	gi|241191625	thioredoxin reductase	219	30210/4.66	0.014	-1.8	O
475	gi|241191613	ATP binding protein of ABC transporter for sugars	171	42016/5.29	0.015	-1.7	G
633	gi|241191186	Glyceraldehyde-3-phosphate dehydrogenase	339	33607/5.35	0.003	-1.7	G
361	gi|241191011	pyruvate kinase	235	58913/5.00	0.01	-1.7	G
817	gi|241190768	elongation factor Tu	183	44281/4.91	0.015	-1.6	IQR
478	gi|241191613	2,3-bisphosphoglycerate-dependent phosphoglycerate mutase	171	27636/5.33	0.003	-1.5	G
964	gi|241190504	Hypothetical redox protein	301	15191/5.36	0.01	-1.5	O

*COG Functional role: J, Translation, ribosomal structure and biogenesis; G, Carbohydrate transport and metabolism; E, Amino acid transport and metabolism; F, Nucleotide transport and metabolism, R, General function prediction only; O, Signal transduction mechanisms; C, Energy production and conversion, −, ORFs with no COG annotation; K, Transcription; M, Cell envelope biogenesis, outer membrane; L, DNA replication, recombination and repair; T, Posttranslational modification, protein turnover, chaperones; H, Coenzyme metabolism; I, Lipid metabolism; P, Inorganic ion transport and metabolism; S, Function unknown; D, Cell division and chromosome partitioning; U, Intracellular trafficking and secretion; A, RNA processing and modification; V, Defence mechanisms; Q, Secondary metabolites biosynthesis, transport and catabolism; N, Cell motility and secretion

Table 2A: Protein identifications of differentially abundant spots (≥ 1.5-fold spot volume ratio change and ANOVA $p \leq 0.05$) of *Bifidobacterium animalis* subsp. *lactis* grown on SEM medium with 1% glucose and 1% stachyose.

Spot	Accession	Protein name	Mascot score	*Mr* /p*I*	Anova (*p*) (DIGE)	Fold	COG Functional role*
252	gi|241191604	alpha-galactosidase	232	81516/5.03	0.0003917	+5.0	G
250	gi|241191604	alpha-galactosidase	170	81792/5.00	0.003	+4.3	G
620	gi|241190508	UDP-glucose 4-epimerase	427	34894/4.81	0.0008372	+3.7	M
451	gi|241190304	UDP-N-acetylglucosamine1-carboxyvinyltransferase	352	45842/5.97	0.008	+2.9	M
893	gi|241190445	50S ribosomal protein L5	328	22228/5.09	0.009	+2.6	J
470	gi|241190472	seryl-tRNA synthetase	266	42494/5.35	0.001	+2.3	J
678	gi|241191290	ATP binding protein of ABC transporter for glutamate_aspartate	377	29894/5.24	0.00000929	+2.3	E
852	gi|241191594	NAD-dependent protein deacetylase	141	24522/5.53	0.001	+2.2	K
263	gi|241191596	oligo-1,6-glucosidase	123	7627/4.59	0.0002007	+2.2	G
841	gi|241190572	oligoribonuclease	172	25224/4.57	0.001	+2.1	A
316	gi|241191015	30S ribosomal protein S1	313	64174/4.59	0.002	+2.0	J
538	gi|241190463	transcription elongation factor NusA	234	39474/5.58	0.0003608	+2.0	K
388	gi|241190132	L-arabinose isomerase	343	55406/4.9	0.001	+1.9	G
374	gi|241190571	inosine-5'-monophosphate dehydrogenase	537	58116/5.30	0.008	+1.9	F
296	gi|241191566	molecular chaperone DnaK	433	66884/4.50	0.0004101	+1.9	O
812	gi|241191244	1-(5-phosphoribosyl-5-[(5-phosphoribosylaminomethylideneamino]imidazole-4-carboxamide isomerase)	176	26196/4.71	0.00005617	+1.9	E
562	gi|241190280	myo-inositol-1-phosphate synthase	335	37518/4.74	0.006	+1.8	I
785	gi|241190700	response regulator of two-component system	367	27141/4.63	0.013	+1.8	TK

565	gi|241190137	Tryptophanyl-tRNA synthetase	174	37415/5.85	0.015	+1.8	J
624	gi|241190210	ketol-acid reductoisomerase	372	34533/4.73	0.00005012	+1.8	EH
1036	gi|241190779	threonine synthase	144	47914/4.51	0.0002614	+1.8	E
897	gi|241191102	ATP-dependent Clp protease proteolytic subunit 2	104	2191/4.45	0.004	+1.7	OU
524	gi|241191186	Glyceraldehyde-3-phosphate dehydrogenase	342	39783/4.90	0.007	+1.7	G
702	gi|241190946	ABC transporter ATP-binding protein	301	28895/5.04	0.008	+1.7	O
1029	gi|241190089	oxidoreductase	191	23011/4.76	0.009	+1.7	R
910	gi|241190664	elongation factor P	290	20863/4.91	0.005	+1.6	J
416	gi|241190200	sucrose phosphorylase	262	51899/4.69	0.007	+1.6	G
1038	gi|241190569	Sua5/YciO/YrdC family protein	220	26061/4.65	0.013	+1.6	J
261	gi|241191596	oligo-1,6-glucosidase	82	76822/4.57	0.014	+1.6	G
323	gi|241190709	hypothetical protein Balac_0668	302	63377/5.52	0.0002135	+1.6	–
311	gi|241190948	ABC-type transport system for Fe-S cluster assembly permease component	439	64971/4.69	0.0005644	+1.6	O
655	gi|241190306	glycerol-3-phosphate dehydrogenase	264	31909/4.70	0.001	+1.5	C
791	gi|241190494	2,3-bisphosphoglycerate-dependent phosphoglycerate mutase	545	2706/5.21	0.002	+1.5	G
301	gi|241190670	dihydroxy-acid dehydratase	273	66406/5.03	0.005	+1.5	EG
425	gi|241191067	6-phosphogluconate dehydrogenase	274	50146/5.18	0.006	+1.5	G
493	gi|241190804	isocitrate dehydrogenase	185	41069/4.93	0.01	+1.5	C
170	gi|241191107	formate acetyltransferase	407	89654/5.08	0.002	-5.3	C
832	gi|241190768	L-2,3-butanediol dehydrogenase/acetoinreductase	198	28506/5.10	0.00004879	-5.2	IQR
70	gi|241190407	hypothetical protein Balac_0352	356	134591/5.66	0.004	-4.9	–
203	gi|241190264	polyphosphate kinase	114	83817/5.86	0.002	-3.5	P
1024	gi|241190768	L-2,3-butanediol dehydrogenase/acetoinreductase	466	28506/5.10	0.00006948	-3.2	IQR
102	gi|241190429	bifunctional acetaldehyde-CoA/alcohol dehydrogenase	180	100490/5.69	0.0008908	-2.6	C

361	gi|241191011	pyruvate kinase	235	49697/5.28	0.0000405	-2.2	G
617	gi|241190361	GTPase ObgE	144	61812/5.09	0.003	-2.1	R
663	gi|241190893	bile salt hydrolase, choloylglycine hydrolase	148	35286/4.70	0.003	-2.0	M
348	gi|241190372	propionyl-CoA carboxylase beta chain	297	58221/5.82	0.013	-2.0	I
463	gi|241190661	elongation factor Tu	170	44281/4.91	0.00005892	-1.8	J
191	gi|241191473	Trehalose-6-phosphate hydrolase	152	81871/5.57	0.007	-1.7	G
223	gi|241190140	glycogen phosphorylase	150	92737/4.94	0.003	-1.6	G
817	gi|241190768	L-2,3-butanediol dehydrogenase/acetoinreductase	183	28506/5.10	0.009	-1.6	IQR
671	gi|241190342	reductase	241	37488/5.44	0.012	-1.6	C
362	gi|241191011	pyruvate kinase	314	49697/5.28	0.008	-1.5	G

*COG Functional role: J, Translation, ribosomal structure and biogenesis; G, Carbohydrate transport and metabolism; E, Amino acid transport and metabolism; F, Nucleotide transport and metabolism, R, General function prediction only; O, Signal transduction mechanisms; C, Energy production and conversion, −, ORFs with no COG annotation; K, Transcription; M, Cell envelope biogenesis, outer membrane; L, DNA replication, recombination and repair; T, Posttranslational modification, protein turnover, chaperones; H, Coenzyme metabolism; I, Lipid metabolism; P, Inorganic ion transport and metabolism; S, Function unknown; D, Cell division and chromosome partitioning; U, Intracellular trafficking and secretion; A, RNA processing and modification; V, Defence mechanisms; Q, Secondary metabolites biosynthesis, transport and catabolism; N, Cell motility and secretion

Table 2B: Protein identifications of differentially abundant spots (≥1.5-fold spot volume ratio change and ANOVA $p \leq 0.05$) of *Bifidobacterium animalis* subsp. *lactis* grown on SEM medium with 1% glucose and 1% raffinose.

Spot	Accession	Protein name	Mascot score	*Mr* /p*I*	Anova (*p*)	Fold	COG Functional role*
250	gi|241191604	alpha-galactosidase	170	81792/5.00	0.02	+3.2	G
252	gi|241191604	alpha-galactosidase	232	81516/5.03	0.013	+2.7	G
620	gi|241190508	UDP-glucose 4-epimerase	427	34894/4.81	0.004	+2.2	M
296	gi|241191566	molecular chaperone DnaK	433	66884/4.50	0.001	+2.2	O
350	gi|241190697	chaperonin GroEL	294	60986/4.54	0.003	+2.1	O
365	gi|241190697	chaperonin GroEL	515	58754/4.57	0.007	+1.9	O
841	gi|241190572	oligoribonuclease	172	25224/4.57	0.014	+1.9	A
263	gi|241191596	oligo-1,6-glucosidase	123	7627/4.59	0.016	+1.8	G
624	gi|241190210	ketol-acid reductoisomerase	372	34533/4.73	0.007	+1.8	EH
879	gi|241190669	Guanylate kinase	155	23254/5.05	0.007	+1.7	F
470	gi|241190472	seryl-tRNA synthetase	266	42494/5.35	0.002	+1.6	J
55	gi|241190667	Carbamoylphosphate synthase large subunit	289	48144/4.88	0.007	+1.6	EF
584	gi|241191452	homoserine O-succinyltransferase	140	36592/4.82	0.0009344	+1.6	E
270	gi|241190872	transketolase	324	75442/4.64	0.004	+1.6	G
240	gi|241191166	dipeptide transport ATP-binding protein	203	84552/5.24	0.009	+1.5	R
795	gi|241190653	phosphoribosylaminoimidazole-succinocarboxamidesynthase	198	26898/4.51	0.006	+1.5	F
261	gi|241191596	oligo-1,6-glucosidase	182	76822/4.57	0.031	+1.5	G
633	gi|241191186	Glyceraldehyde-3-phosphate dehydrogenase	339	33607/5.35	0.012	+1.5	G
1025	gi|241190768	L-2,3-butanediol dehydrogenase/acetoinreductase	383	25548/4.97	0.0002132	-5.5	IQR

832	gi|241190768	L-2,3-butanediol dehydrogenase/acetoinreductase	198	25629/4.88	0.00002664	-5.3	IQR
1024	gi|241190768	L-2,3-butanediol dehydrogenase/acetoinreductase	466	25845/4.97	0.0007374	-4.8	IQR
602	gi|241190317	Ribokinase family sugar kinase	292	35357/5.84	0.000557	-4.0	G
170	gi|241191107	formate acetyltransferase	407	94491/4.98	0.008	-3.8	C
671	gi|241190342	reductase	241	30313/5.19	0.0008577	-3.0	C
605	gi|241190317	Ribokinase family sugar kinase	273	35254/5.84	0.3731	-2.9	G
958	gi|241190788	hypothetical protein Balac_0750	203	15247/4.70	0.003	-1.8	R
617	gi|241190361	GTPase ObgE	144	34997/4.97	0.012	-1.8	R
824	gi|241190731	polyphosphate glucokinase	76	25791/5.17	0.008	-1.7	KG
828	gi|241190731	polyphosphate glucokinase	207	2571/5.04	0.014	-1.6	KG
248	gi|241191022	glycogen branching enzyme	346	8262/4.85	0.015	-1.6	G
320	gi|241190709	hypothetical protein Balac_0668	217	63696/5.42	0.016	-1.6	−
761	gi|241190869	hypothetical protein Balac_0839	118	27789/4.98	0.005	-1.5	G
862	gi|241191021	transcriptional regulator	466	24171/4.99	0.004	-1.5	K

*COG Functional role: J, Translation, ribosomal structure and biogenesis; G, Carbohydrate transport and metabolism; E, Amino acid transport and metabolism; F, Nucleotide transport and metabolism, R, General function prediction only; O, Signal transduction mechanisms; C, Energy production and conversion, −, ORFs with no COG annotation; K, Transcription; M, Cell envelope biogenesis, outer membrane; L, DNA replication, recombination and repair; T, Posttranslational modification, protein turnover, chaperones; H, Coenzyme metabolism; I, Lipid metabolism; P, Inorganic ion transport and metabolism; S, Function unknown; D, Cell division and chromosome partitioning; U, Intracellular trafficking and secretion; A, RNA processing and modification; V, Defence mechanisms; Q, Secondary metabolites biosynthesis, transport and catabolism; N, Cell motility and secretion

Table 2C: Protein identifications of differentially abundant spots (≥ 1.5-fold spot volume ratio change and ANOVA $p \leq 0.05$) of *Bifidobacterium animalis* subsp. *lactis* grown on SEM medium with 1% glucose and 1% melibiose.

Spot	Accession	Protein name	Mascot score	*Mr*/p*I*	Anova (*p*) (DIGE)	Fold	COG Functional Role*
252	gi|241191604	alpha-galactosidase	232	81516/5.03	0.002	+3.4	G
620	gi|241190508	UDP-glucose 4-epimerase	427	34894/4.81	0.002	+3.1	M
250	gi|241191604	alpha-galactosidase	170	81792/5.00	0.0015	+2.8	G
302	gi|241190670	dihydroxy-acid dehydratase	470	66246/5.06	0.0005674	+2.2	EG
249	gi|241191005	glycogen operon protein GlgX	126	82068/5.06	0.0004014	+2.1	G
852	gi|241191594	NAD-dependent protein deacetylase	141	24522/5.53	0.012	+2.1	K
374	gi|241190571	inosine-5'-monophosphate dehydrogenase	537	58116/5.30	0.000146	+2.0	F
365	gi|241190697	chaperonin GroEL	515	58754/4.57	0.002	+1.9	O
482	gi|241191613	ATP binding protein of ABC transporter for sugars	322	41378/5.60	0.003	+1.9	G
263	gi|241191596	oligo-1.6-glucosidase	123	7627/4.59	0.003	+1.9	G
245	gi|241191166	dipeptide transport ATP-binding protein	267	83448/5.33	0.004	+1.9	R
565	gi|241190137	Tryptophanyl-tRNA synthetase	174	37415/5.85	0.0003011	+1.8	J
316	gi|241191015	30S ribosomal protein S1	313	64174/4.59	0.0008851	+1.8	J
615	gi|241190508	UDP-glucose 4-epimerase	182	35048/4.88	0.012	+1.8	M
337	gi|241191221	UDP-N-acetylmuramate--L-alanine ligase	85	61942/4.75	0.009	+1.7	M
237	gi|241191166	dipeptide transport ATP-binding protein	374	84828/5.29	0.0003814	+1.6	R
562	gi|241190280	myo-inositol-1-phosphate synthase	335	37518/4.74	0.00004229	+1.6	I
1047	gi|241191445	F0F1 ATP synthase subunit beta	535	53972/4.72	0.002	+1.6	C
375	gi|241190571	inosine-5'-monophosphate dehydrogenase	378	57797/5.21	0.003	+1.6	F
286	gi|241190896	thioredoxin reductase-like protein	393	69369/4.78	0.007	+1.6	O

372	gi|241190386	protease or peptidase	213	58435/5.38	0.012	+1.6	O
311	gi|241190948	ABC-type transport system for Fe-S cluster assembly permease component	439	64971/4.69	0.013	+1.6	O
879	gi|241190669	Guanylate kinase	155	23254/5.05	0.5515	+1.5	F
480	gi|241191613	ATP binding protein of ABC transporter for sugars	165	41697/5.69	0.001	+1.5	G
416	gi|241190200	sucrose phosphorylase	262	51899/4.69	0.002	+1.5	G
97	gi|241191008	DNA polymerase I	238	107742/5.04	0.002	+1.5	L
238	gi|241191000	putative phosphoketolase	441	84552/4.95	0.006	+1.5	G
749	gi|241190851	succinyl-CoA synthetase subunit alpha	203	28112/4.79	0.006	+1.5	C
296	gi|241191566	molecular chaperone DnaK	433	66884/4.50	0.01	+1.5	O
56	gi|241190667	Carbamoylphosphate synthase large subunit	415	125134/4.90	0.011	+1.5	EF
702	gi|241190946	ABC transporter ATP-binding protein	301	28895/5.04	0.011	+1.5	O
596	gi|241190873	transaldolase	534	35871/4.52	0.012	+1.5	G
1032	gi|241191249	histidinol dehydrogenase	330	22768/4.66	0.0004245	-3.9	E
1029	gi|241190089	oxidoreductase	191	23011/4.76	0.0001958	-2.4	R
895	gi|241190445	50S ribosomal protein L5	164	22066/5.20	0.0005478	-2.2	J
896	gi|241190821	Uracil-DNA glycosylase. putative	245	21932/5.36	0.013	-2	L
899	gi|241190311	AcrR-type transcriptional regulator	119	21799/5.42	0.013	-2	
640	gi|241191238	L-lactate dehydrogenase 2	167	33504/6.00	0.014	-2	C
654	gi|241190306	glycerol-3-phosphate dehydrogenase	113	32012/4.64	0.003	-1.9	C
643	gi|241191238	L-lactate dehydrogenase 2	326	33401/6.00	0.0006494	-1.8	C
470	gi|241190472	seryl-tRNA synthetase	266	42494/5.35	0.001	-1.8	J
1040	gi|241191011	pyruvate kinase	451	58435/5.14	0.00003524	-1.7	G
631	gi|241190260	phosphodiesterase	520	33761/5.08	0.001	-1.7	C
828	gi|241190731	polyphosphate glucokinase	207	2571/5.04	0.003	-1.7	KG
602	gi|241190317	Ribokinase family sugar kinase	292	35357/5.32	0.012	-1.7	G
685	gi|241190789	phosphoglycerate mutase	306	29489/5.00	0.015	-1.7	G

478	gi|241190661	elongation factor Tu	259	41697/4.82	0.0001849	-1.6	J
672	gi|241191625	thioredoxin reductase	219	3021/4.66	0.001	-1.6	O
1003	gi|241190258	hypothetical protein Balac_0197	150	12297/5.00	0.001	-1.6	S
573	gi|241190288	hypothetical protein Balac_0227	197	37107/5.37	0.004	-1.6	R
611	gi|241190809	30S ribosomal protein S2	187	35099/5.00	0.005	-1.6	J
582	gi|241190503	Universal stress protein	146	36643/4.90	0.0003764	-1.5	T

*COG Functional role: J, Translation, ribosomal structure and biogenesis; G, Carbohydrate transport and metabolism; E, Amino acid transport and metabolism; F, Nucleotide transport and metabolism, R, General function prediction only; O, Signal transduction mechanisms; C, Energy production and conversion, −, ORFs with no COG annotation; K, Transcription; M, Cell envelope biogenesis, outer membrane; L, DNA replication, recombination and repair; T, Posttranslational modification, protein turnover, chaperones; H, Coenzyme metabolism; I, Lipid metabolism; P, Inorganic ion transport and metabolism; S, Function unknown; D, Cell division and chromosome partitioning; U, Intracellular trafficking and secretion; A, RNA processing and modification; V, Defence mechanisms; Q, Secondary metabolites biosynthesis, transport and catabolism; N, Cell motility and secretion

Table 3A: Protein identifications of differentially abundant spots (≥ 1.5-fold spot volume ratio change and ANOVA $p \leq 0.05$) of *Bifidobacterium animalis* subsp. *lactis* grown on SEM medium with 1% glucose and 1% panose.

Spot	**Accession**	**Protein name**	**Mascot score**	***Mr*/p*I***	**Anova (*p*)**	**Fold**	**COG Functional role***
852	gi|241191594	NAD-dependent protein deacetylase	141	24522/5.53	0.008025	+3.4	K
506	gi|241190365	Transcription antiterminator	259	40555/4.27	0.001	+3.2	K
263	gi|241191596	oligo-1,6-glucosidase	235	7627/4.59	0.0002323	+3.1	G
252	gi|241191604	alpha-galactosidase	335	81516/5.03	0.013	+3.1	G
470	gi|241190472	seryl-tRNA synthetase	155	42494/5.35	0.0001037	+2.6	J
302	gi|241190670	dihydroxy-acid dehydratase	470	66246/5.06	0.0006334	+2.3	EG
796	gi|241190494	2,3-bisphosphoglycerate-dependent phosphoglycerate mutase	266	26898/4.55	0.003	+2.3	G
365	gi|241190697	chaperonin GroEL	217	58754/4.57	0.0006899	+2.2	O

1038	gi|241191585	NADPH-flavin oxidoreductase	451	26061/4.65	0.008	+2.2	C
562	gi|241190280	myo-inositol-1-phosphate synthase	123	37518/4.74	0.0002543	+2.1	I
624	gi|241190210	ketol-acid reductoisomerase	198	34533/4.73	0.006	+2.1	EH
482	gi|241191613	ATP binding protein of ABC transporter for sugars	509	41378/5.60	0.001	+2.0	G
296	gi|241191566	molecular chaperone DnaK	383	66884/4.50	0.002	+2.0	O
569	gi|241191273	4-hydroxy-3-methylbut-2-en-1-yl diphosphatesynthase	197	37312/6.12	0.014	+2.0	I
357	gi|241190474	phosphoglucomutase	537	60508/4.67	0.0002975	+1.9	G
1029	gi|241190089	oxidoreductase	187	23011/4.76	0.0006402	+1.9	R
316	gi|241191015	30S ribosomal protein S1	185	64174/4.59	0.006	+1.9	J
374	gi|241190571	inosine-5'-monophosphate dehydrogenase	114	58116/5.30	0.0004365	+1.8	F
493	gi|241190804	isocitrate dehydrogenase	191	41069/4.93	0.0005736	+1.8	C
655	gi|241190306	glycerol-3-phosphate dehydrogenase	515	31909/4.70	0.002	+1.8	C
897	gi|241191102	ATP-dependent Clp protease proteolytic subunit 2	415	2191/4.45	0.003	+1.8	OU
337	gi|241191221	UDP-N-acetylmuramate--L-alanine ligase	308	61942/4.75	0.011	+1.8	M
405	gi|241190741	dihydrolipoamide dehydrogenase	144	53812/5.26	0.013	+1.8	C
879	gi|241190669	Guanylate kinase	262	23254/5.05	0.00004702	+1.7	F
696	gi|241190385	aldo/keto reductase family oxidoreductase	128	29057/4.72	0.001	+1.7	C
226	gi|241190660	elongation factor G	322	85657/4.63	0.008	+1.7	J
1047	gi|241191445	F0F1 ATP synthase subunit beta	398	53972/4.72	0.011	+1.7	C
1040	gi|241191011	pyruvate kinase	66	58435/5.14	0.0001956	+1.6	G
311	gi|241190948	ABC-type transport system for Fe-S cluster assembly permease component	314	64971/4.69	0.002	+1.6	O
983	gi|241190405	50S ribosomal protein L7/L12	170	13219/4.40	0.004	+1.6	J
742	gi|241190728	morphine 6-dehydrogenase	278	28193/4.65	0.004	+1.6	R
676	gi|241190810	elongation factor Ts	264	30056/4.70	0.007	+1.6	J

872	gi|241191244	1-(5-phosphoribosyl-5-[(5-phosphoribosylaminomethylideneamino]imidazole-4-carboxamide isomerase)	113	2374/4.52	0.01	+1.6	E
809	gi|241190470	ribose-5-phosphate isomerase A	433	26223/4.61	0.01	+1.6	G
1031	gi|241190342	reductase	292	30056/5.31	0.014	+1.6	C
56	gi|241190667	Carbamoylphosphate synthase large subunit	382	125134/4.90	0.0007002	+1.5	EF
416	gi|241190200	sucrose phosphorylase	439	51899/4.69	0.0009437	+1.5	G
279	gi|241190843	hypothetical protein Balac_0807	267	73786/5.15	0.002	+1.5	K
425	gi|241191067	6-phosphogluconate dehydrogenase	104	50146/5.18	0.004	+1.5	G
480	gi|241191613	ATP binding protein of ABC transporter for sugars	225	41697/5.69	0.004	+1.5	G
1030	gi|241190342	reductase	203	29813/5.31	0.005	+1.5	C
865	gi|241190928	Ribosomal protein L25	399	2409/4.48	0.009	+1.5	J
388	gi|241190132	L-arabinose isomerase	167	55406/4.90	0.01	+1.5	G
261	gi|241191596	oligo-1,6-glucosidase	471	76822/4.57	0.011	+1.5	G
538	gi|241190463	transcription elongation factor NusA	274	39474/5.58	0.014	+1.5	K
795	gi|241190653	phosphoribosylaminoimidazole-succinocarboxamidesynthase	165	26898/4.51	0.014	+1.5	F
70	gi|241190407	hypothetical protein Balac_0352	180	120717/5.52	0.01	-4.3	−
203	gi|241190264	polyphosphate kinase	458	87865/5.86	0.0006028	-4.1	P
832	gi|241190768	L-2,3-butanediol dehydrogenase/acetoinreductase	249	25629/4.88	0.0002888	-3.6	IQR
200	gi|241191232	hypothetical protein Balac_1208	326	88141/5.68	0.0007811	-3.5	R
1025	gi|241190768	L-2,3-butanediol dehydrogenase/acetoinreductase	168	25548/4.97	0.0004042	-3.1	IQR
610	gi|241190809	30S ribosomal protein S2	250	35151/4.95	0.001	-3.1	J
906	gi|241190812	ribosome recycling factor	313	21331/5.52	0.0004173	-2.9	J
602	gi|241190317	Ribokinase family sugar kinase	372	35357/5.84	0.002	-2.9	G
214	gi|241190264	polyphosphate kinase	207	87037/5.86	0.003	-2.8	P

640	gi|241191238	L-lactate dehydrogenase 2	297	33504/6.00	0.004	-2.7	C
348	gi|241190372	propionyl-CoA carboxylase beta chain	531	61145/5.54	0.006	-2.6	I
361	gi|241191011	pyruvate kinase	466	58913/5.00	0.02201	-2.5	G
320	gi|241190709	hypothetical protein Balac_0668	387	63696/5.42	0.1656	-2.5	−
990	gi|241190823	hypothetical protein Balac_0787	451	11541/4.65	0.014	-2.4	−
611	gi|241190809	30S ribosomal protein S2	591	35099/5.00	0.0005575	-2.3	J
197	gi|241191000	putative phosphoketolase	407	88141/4.86	0.011	-2.3	G
102	gi|241190429	bifunctional acetaldehyde-CoA/alcohol dehydrogenase	249	106085/5.52	0.004	-2.2	C
1024	gi|241190768	L-2,3-butanediol dehydrogenase/acetoinreductase	494	25845/4.97	0.007	-2.2	IQR
213	gi|241191000	putative phosphoketolase	356	87037/4.89	0.001	-2.1	G
890	gi|241190445	50S ribosomal protein L5	176	22525/4.99	0.005	-2.1	J
219	gi|241190264	polyphosphate kinase	310	86485/5.86	0.008	-2.1	P
617	gi|241190361	GTPase ObgE	343	34997/4.97	0.0008641	-2	R
463	gi|241190661	elongation factor Tu	209	44726/4.76	0.001	-2	J
654	gi|241190306	glycerol-3-phosphate dehydrogenase	508	32012/4.64	0.002	-2	C
643	gi|241191238	L-lactate dehydrogenase 2	185	33401/6.00	0.005	-2	C
587	gi|241191399	glycosyltransferase	182	36386/5.08	0.01	-2	M
170	gi|241191107	formate acetyltransferase	535	94491/4.98	0.008	-1.9	C
362	gi|241191011	pyruvate kinase	359	58913/5.04	0.001	-1.8	G
191	gi|241191473	Trehalose-6-phosphate hydrolase	152	88969/5.56	0.012	-1.8	G
895	gi|241190445	50S ribosomal protein L5	232	22066/5.20	0.015	-1.8	J
240	gi|241191166	dipeptide transport ATP-binding protein	196	84552/5.24	0.003	-1.7	R
253	gi|241190140	glycogen phosphorylase	151	80963/5.10	0.004	-1.7	G
612	gi|241190809	30S ribosomal protein S2	129	35099/5.06	0.009	-1.7	J
790	gi|241190653	phosphoribosylaminoimidazole-succinocarboxamidesynthase	250	27087/5.03	0.012	-1.7	F
478	gi|241190661	elongation factor Tu	234	41697/4.82	0.01019	-1.6	J

96	gi|241191480	valyl-tRNA synthetase	198	108018/5.02	0.002	-1.6	J
828	gi|241190731	polyphosphate glucokinase	164	2571/5.04	0.006	-1.5	KG

*COG Functional role: J, Translation, ribosomal structure and biogenesis; G, Carbohydrate transport and metabolism; E, Amino acid transport and metabolism; F, Nucleotide transport and metabolism, R, General function prediction only; O, Signal transduction mechanisms; C, Energy production and conversion, −, ORFs with no COG annotation; K, Transcription; M, Cell envelope biogenesis, outer membrane; L, DNA replication, recombination and repair; T, Posttranslational modification, protein turnover, chaperones; H, Coenzyme metabolism; I, Lipid metabolism; P, Inorganic ion transport and metabolism; S, Function unknown; D, Cell division and chromosome partitioning; U, Intracellular trafficking and secretion; A, RNA processing and modification; V, Defence mechanisms; Q, Secondary metabolites biosynthesis, transport and catabolism; N, Cell motility and secretion

Table 3B: Protein identifications of differentially abundant spots (≥ 1.5-fold spot volume ratio change and ANOVA $p \leq 0.05$) of *Bifidobacterium animalis* subsp. *lactis* grown on SEM medium with 1% glucose and 1% isomaltose.

Spot	**Accession**	**Protein name**	**Mascot score**	***Mr*/p*I***	**Anova (*p*) (DIGE)**	**Fold**	**COG Functional role***
252	gi|241191604	alpha-galactosidase	232	81516/5.03	0.0000389	+11.2	G
250	gi|241191604	alpha-galactosidase	170	81792/5.00	0.0009143	+8	G
451	gi|241190304	UDP-N-acetylglucosamine1-carboxyvinyltransferase	352	45842/5.97	0.0008448	+4.7	M
633	gi|241191186	Glyceraldehyde-3-phosphate dehydrogenase	339	33607/5.35	0.00003908	+4.6	G
249	gi|241191005	glycogen operon protein GlgX	126	82068/5.06	0.00009128	+3.2	G
272	gi|241191552	methionyl-tRNA synthetase	203	74890/4.95	0.0008658	+3.2	J
569	gi|241191273	4-hydroxy-3-methylbut-2-en-1-yl diphosphatesynthase	151	37312/6.12	0.003	+2.9	I
263	gi|241191596	oligo-1,6-glucosidase	123	76270/4.59	0.0005277	+2.8	G
870	gi|241191609	deoxycytidine triphosphate deaminase	92	23767/4.94	0.0001457	+2.6	F
353	gi|241190474	phosphoglucomutase	400	60826/5.16	0.00001167	+2.5	G
1029	gi|241190089	oxidoreductase	191	23011/4.76	0.000323	+2.4	R
110	gi|241190429	bifunctional acetaldehyde-CoA/alcohol dehydrogenase	397	105257/5.69	0.001	+2.3	C

852	gi|241191594	NAD-dependent protein deacetylase	141	24522/5.53	0.0003636	+2.3	K
447	gi|241190304	UDP-N-acetylglucosamine1-carboxyvinyltransferase	387	46001/5.97	0.014	+2.3	M
482	gi|241191613	ATP binding protein of ABC transporter for sugars	322	41378/5.60	0.0003708	+2.2	G
1047	gi|241191445	F0F1 ATP synthase subunit beta	535	53972/4.72	0.0002322	+2.2	C
1032	gi|241191249	histidinol dehydrogenase	330	22768/4.66	0.005	+2.2	E
893	gi|241190445	50S ribosomal protein L5	328	22228/5.09	0.0006042	+2.1	J
374	gi|241190571	inosine-5'-monophosphate dehydrogenase	537	58116/5.30	0.0001217	+2.1	F
508	gi|241190770	tyrosyl-tRNA synthetase	171	40400/4.98	0.0008026	+2	J
365	gi|241190697	chaperonin GroEL	515	58754/4.57	0.0006345	+2	O
630	gi|241190190	fructose-bisphosphate aldolase	204	33761/4.92	0.0002316	+2	G
438	gi|241191595	threonine dehydratase	255	47117/5.27	0.0004706	+2	E
388	gi|241190132	L-arabinose isomerase	343	55406/4.90	0.00006148	+1.9	G
227	gi|241190371	JadJ	101	85657/5.09	0.01	+1.9	I
853	gi|241191204	hypothetical protein Balac_1180	137	24495/5.29	0.0007814	+1.8	−
302	gi|241190670	dihydroxy-acid dehydratase	470	66246/5.06	0.0003967	+1.8	EG
565	gi|241190137	Tryptophanyl-tRNA synthetase	174	37415/5.85	0.0007447	+1.8	J
245	gi|241191166	dipeptide transport ATP-binding protein	267	83448/5.33	0.001	+1.7	R
416	gi|241190200	sucrose phosphorylase	262	51899/4.69	0.0001131	+1.7	G
301	gi|241190670	dihydroxy-acid dehydratase	273	66406/5.03	0.0004106	+1.7	EG
271	gi|241191552	methionyl-tRNA synthetase	271	74890/4.92	0.003	+1.7	J
562	gi|241190280	myo-inositol-1-phosphate synthase	335	37518/4.74	0.00005233	+1.7	I
316	gi|241191015	30S ribosomal protein S1	313	64174/4.59	0.011	+1.6	J
56	gi|241190667	Carbamoylphosphate synthase large subunit	415	125134/4.90	0.005	+1.6	EF
303	gi|241191433	diaminopimelate decarboxylase	359	66087/5.22	0.005	+1.6	E
493	gi|241190804	isocitrate dehydrogenase	185	41069/4.93	0.003	+1.6	C
261	gi|241191596	oligo-1,6-glucosidase	82	76822/4.57	0.01	+1.6	G
298	gi|241190361	GTPase ObgE	290	66565/4.99	0.01	+1.6	R

470	gi|241190472	seryl-tRNA synthetase	266	42494/5.35	0.01	+1.6	J
457	gi|241190673	cyclopropane-fatty-acyl-phospholipid synthase	222	45523/5.43	0.003	+1.5	M
279	gi|241190843	hypothetical protein Balac_0807	267	73786/5.15	0.00007065	+1.5	K
626	gi|241191065	hypothetical protein Balac_1039	284	34070/4.93	0.003	+1.5	G
902	gi|241190542	hypoxanthine-guanine phosphoribosyltransferase	472	21665/4.54	0.0006402	+1.5	F
624	gi|241190210	ketol-acid reductoisomerase	372	34533/4.73	0.008	+1.5	EH
305	gi|241191423	long-chain-fatty acid CoA ligase	475	65449/5.08	0.003	+1.5	I
296	gi|241191566	molecular chaperone DnaK	433	66884/4.50	0.004	+1.5	O
357	gi|241190474	phosphoglucomutase	509	60508/4.67	0.003	+1.5	G
384	gi|241190350	glucose-6-phosphate isomerase	255	56522/4.65	0.012	+1.5	G
1040	gi|241191011	pyruvate kinase	451	58435/5.14	0.002	+1.5	G
896	gi|241190821	Uracil-DNA glycosylase, putative	245	21932/5.36	0.00001353	-6.9	L
990	gi|241190823	hypothetical protein Balac_0787	129	11541/4.65	0.0004729	-4.2	−
1003	gi|241190258	hypothetical protein Balac_0197	150	12297/5	0.00008026	-3.2	S
909	gi|241190812	ribosome recycling factor	351	21219/7.85	0.006	-3.0	J
956	gi|241190962	3-dehydroquinate dehydratase	82	15269/5.69	0.0003593	-2.9	E
989	gi|241190823	hypothetical protein Balac_0787	205	4.74/5.01	0.0005827	-2.9	−
640	gi|241191238	L-lactate dehydrogenase 2	167	33504/6.00	0.0002105	-2.9	C
197	gi|241191000	putative phosphoketolase	508	88141/4.86	0.004	-2.8	G
984	gi|241191037	peptidyl-prolyl cis-trans isomerase	163	13219/4.80	0.00003749	-2.6	−
643	gi|241191238	L-lactate dehydrogenase 2	326	33401/6.00	0.00004103	-2.5	C
832	gi|241190768	L-2,3-butanediol dehydrogenase/acetoinreductase	198	25629/4.88	0.00001199	-2.5	IQR
200	gi|241191232	hypothetical protein Balac_1208	308	88141/5.68	0.005	-2.4	R
663	gi|241190893	bile salt hydrolase, choloylglycine hydrolase	148	30468/4.51	0.0003166	-2.3	M
828	gi|241190731	polyphosphate glucokinase	207	25710/5.04	0.00001994	-2.3	KG
906	gi|241190812	ribosome recycling factor	97	21331/5.52	0.009	-2.3	J

654	gi|241190306	glycerol-3-phosphate dehydrogenase	113	32012/4.64	0.0003306	-2.2	C
213	gi|241191000	putative phosphoketolase	398	87037/4.89	0.0004891	-2.1	G
361	gi|241191011	pyruvate kinase	235	58913/5.00	0.002	-2.1	G
664	gi|241190893	bile salt hydrolase, choloylglycine hydrolase	309	30468/4.55	0.001	-2.0	M
790	gi|241190653	phosphoribosylaminoimidazole-succinocarboxamidesynthase	359	27087/5.03	0.002	-2.0	F
685	gi|241190789	phosphoglycerate mutase	306	29489/5.00	0.007	-2.0	G
817	gi|241190768	L-2,3-butanediol dehydrogenase/acetoinreductase	183	25980/4.83	0.0001795	-1.9	IQR
661	gi|241191009	Putative response regulator	196	30571/4.56	0.012	-1.9	T
594	gi|241190873	transaldolase	376	36026/4.47	0.0001764	-1.8	G
829	gi|241191023	Putative response regulator	318	25710/5.26	0.002	-1.8	TK
1005	gi|241191436	Putative translation initiation inhibitor	139	13926/4.70	0.004	-1.8	J
582	gi|241190503	Universal stress protein	146	36643/4.90	0.0008694	-1.8	T
784	gi|241190494	2,3-bisphosphoglycerate-dependent phosphoglycerate mutase	520	27168/5.11	0.002	-1.7	G
540	gi|241191043	enolase	503	39371/4.56	0.013	-1.7	G
602	gi|241190317	Ribokinase family sugar kinase	292	37762/35357	0.007	-1.7	G
634	gi|241190783	ribose-phosphate pyrophosphokinase	328	37067/33607	0.0006434	-1.7	FE
703	gi|241190946	ABC transporter ATP-binding protein	149	28868/4.95	0.015	-1.6	O
320	gi|241190709	hypothetical protein Balac_0668	217	63696/5.42	0.003	-1.6	−
838	gi|241190710	hypothetical protein Balac_0669	149	25332/5.41	0.002	-1.6	−
705	gi|241190728	morphine 6-dehydrogenase	147	28841/4.61	0.013	-1.6	R
795	gi|241190653	phosphoribosylaminoimidazole-succinocarboxamidesynthase	198	26898/4.51	0.002	-1.6	F
233	gi|241191000	putative phosphoketolase	354	85104/4.92	0.001	-1.6	G
270	gi|241190872	transketolase	324	75442/4.64	0.003	-1.6	G
478	gi|241190661	elongation factor Tu	259	41697/4.82	0.00001842	-1.5	J
463	gi|241190661	elongation factor Tu	170	44726/4.76	0.0001908	-1.5	J

824	gi|241190731	polyphosphate glucokinase	76	25791/5.17	0.002	-1.5	KG
362	gi|241191011	pyruvate kinase	314	58913/5.04	0.006	-1.5	G

*COG Functional role: J, Translation, ribosomal structure and biogenesis; G, Carbohydrate transport and metabolism; E, Amino acid transport and metabolism; F, Nucleotide transport and metabolism, R, General function prediction only; O, Signal transduction mechanisms; C, Energy production and conversion, −, ORFs with no COG annotation; K, Transcription; M, Cell envelope biogenesis, outer membrane; L, DNA replication, recombination and repair; T, Posttranslational modification, protein turnover, chaperones; H, Coenzyme metabolism; I, Lipid metabolism; P, Inorganic ion transport and metabolism; S, Function unknown; D, Cell division and chromosome partitioning; U, Intracellular trafficking and secretion; A, RNA processing and modification; V, Defence mechanisms; Q, Secondary metabolites biosynthesis, transport and catabolism; N, Cell motility and secretio

CHAPTER 6

Structural basis for xylooligosaccharide uptake by the probiotic *Bifidobacterium animalis* spp. *lactis* Bl-04

Structural basis for xylooligosaccharide uptake by the probiotic *Bifidobacterium animalis* spp. *lactis* Bl-04

Morten Ejby,[1] Andreja Vujicic-Zagar,[2] Folmer Fredslund,[3] Birte Svensson, [1] Dirk Jan Slotboom,[2] and Maher Abou Hachem[1*]

1. Enzyme and Protein Chemistry, Department of Systems Biology, Technical University of Denmark, Søltofts Plads, Building 224, DK-2800 Kgs. Lyngby, Denmark.

2. Membrane Enzymology, Institute for Biomolecular Sciences & Biotechnology, Rijksuniversiteit Groningen, Nijenborgh 4, 9747 AG Groningen, The Netherlands.

3. MaxLab, MAX IV Laboratory, Lund University, Ole Römers väg 1, 221 00 LUND, Sweden

*Corresponding authors: Maher Abou Hachem, Enzyme and Protein Chemistry, Department of Systems Biology, the Technical University of Denmark, Søltofts Plads, Building 224, DK-2800 Kgs. Lyngby, Denmark

Phone: +45 45252740; +45 45252741; Fax:+45 45886307

Email: maha@bio.dtu.dk

Capsule

Background:

Xylooligosaccharides (XOS) selectively stimulate the growth of probiotic bifidobacteria, thus acting as prebiotics. Several intracellular glycoside hydrolases (GHs) involved in the degradation of XOS have been characterized to date, but molecular insight on XOS uptake by bifidobacteria is lacking. An operon including a transcriptional regulator, three GH43 enzymes, and an ATP-binding cassette (ABC) transporter is implicated in XOS uptake and degradation in the probiotic *Bifidobacterium animalis* subsp. *lactis* Bl-04, and the ABC transport system of this operon is conserved across different *Bifidobacterium* species.

Results:

SBP of the ABC transport system of the XOS operon from *Bifidobacterium animalis* subsp.*lactis* Bl-04 (*Bl*XBP) was produced and its ligand preference and affinity determined. The crystal structures of *Bl*XBP in complex with xylotriose, xylotetraose and xylohexaose were determined, thus providing a structural rationale for the binding data and highlighting structural elements responsible for XOS recognition and binding.

Conclusion:

*Bl*XBP shows a narrow preference with optimal affinity for undecorated or arabinosyl decorated XOS ligands of degree of polymerization of $3-4$. Binding kinetics play a role in the selectivity with the association rate (k_{on}) as a major contributor to the affinity.

Significance:

This data, presenting the first structure of a xylooligosaccharide specific SBP from a probiotic bacterium, provide novel insight into the biochemical and structural basis of XOS utilization by bifidobacteria and contribute to a better understanding of *Bifidobacterium animalis* subsp. *lactis* Bl-04's role in the gut microbiome.

Abstract

The xylooligosaccharides (XOS) binding protein of the ABC import system (*Bl*XBP) has been produced in *Escherichia coli* and biophysically and structurally characterised. Surface plasmon resonance binding assays showed that *Bl*XBP was specific for XOS with a degree of polymerization (DP) 2− 6 with optimal affinity (K_d ~100 nM) for xylotetraose followed by xylotriose. Differences in binding affinity was governed largely by the association rate (k_{on}), while k_{off} had a more modest contribution to binding affinities, except for xylobiose, which displayed the highest k_{off}. The binding affinity and kinetics of arabinose decorated XOS were similar to undecorated counterparts, thus providing evidence that arabinoxylan fragments are efficiently captured by the ABC import system. The binding affinity towards xylotriose and xylotetraose was corroborated using fluorescence emission spectroscopy and isothermal titration calorimetry that revealed that the binding free energy was dominated by a favourable enthalpy, which was off-set by a large unfavourable entropy change.

The crystal structures of *Bl*XBP in complex with xylotriose, xylotetraose and xylohexaose were determined and showed a binding cleft large enough to accommodate the preferred ligand xylotetraose. The helical structure of xylan fragments was recognized by aromatic stacking of xyloxyl rings 1, 3 and 4, in addition to several direct and solvent mediated hydrogen-bonds that contribute to the binding enthalpy. Binding of larger ligands requires conformational changes in a lid loop that contributes to the structural plasticity of *Bl*XBP. This data bring novel insight into the molecular basis for XOS uptake by bifidobacteria, and xylan utilization by the gut microbiome.

Introduction

The human gut hosts a highly diverse microbial community (1) giving rise to the most densely populated ecological niche in nature (2). Despite the diversity and dynamic nature of the gut microbiome, the majority of species it constitutes belong to a few dominant phyla, with *Firmicutes* being the most abundant followed by *Bacteroidetes*, *Actinobacteria* and *Proteobacteria* (3). The abundance of actinobacteria owes to the *Bifidobacterium* members constituting the third most abundant genus in the gut. Bifidobacteria are considered beneficial for human health and include several probiotic strains able to prevent or alleviate infectious diarrhea through their modulation of the immune system and to confer host resistance against colonization of pathogens (4-6). An important attribute of probiotic bacteria is their ability to utilize a variety of non-digestible oligosaccharides by the human host, which provides an advantage in the highly competitive gut niche (7). Specifically, the occurrence of certain ATP-binding cassette (ABC) carbohydrate transporters in bifidobacteria and high acetate production associated with carbohydrate metabolism have been correlated to probiotic traits such as protection from pathogenic infection in mice (8). Thus the activity and abundance of probiotics can be modulated by prebiotics, mainly comprising non-digestible oligosaccharides and certain polysaccharides (9).

Xylan is the main constituent of hemicellulose in the plant cell wall of monocotyledons and the second most abundant non-starch polysaccharide after cellulose in many cereal grains, where it occurs as decorated arabinoxylan and amounts to 25 – 40% (w/w) of the dietary fiber content in grains (10,11). Hence, human diet is rich in arabinoxylan, that reaches the colon intact and is degraded mainly by species belonging to the *Bacteroides* and *Roseburia* genera that possess extracellular endo-xylanases necessary for the degradation of the xylan backbone (12). The endo-xylanases releases both undecorated xylooligosaccharides (XOS) and decorated arabinooligosaccharides (AXOS), some of which escape uptake by the arabinoxylan degraders and become accessible for other species (13). Growth on AXOS and XOS, however, is limited to a few taxa amongst oligosaccharide degraders (14). Several gut commensals and potential pathogens *e.g.* members of the *Clostridium* and *Escherichia* genera are unable to utilize this substrate (15). Bifidobacteria possess glycoside hydrolases (GHs) capable of degradating XOS and AXOS to arabinose and xylose (16,17). This is highlighted by the widespread ability of

different *Bifidobacterum* species to grow on XOS and AXOS in mono-cultures (18). Some species *e.g. B. adolecencis, B. catenulatum, B. lactis and B. pseudolomgum,* were shown to grow more efficiently on XOS as compared to xylose, suggesting the existence of an oligosaccharide specific transport system (14,19). Larger increase in *B. animalis* subsp. *lactis* count was measured on XOS compared to the well established prebiotic fructooligosaccharides (FOS) in a colon simulator study, thus highlighting the potential of the former substrate as a selective prebiotic for bifidobacteria (20). Recently, a genetic locus encoding a LacI transcriptional regulator, a GH43 β-xylosidase and 2 GH43 arabinofuranosidases, and an ATB-binding cassette (ABC) transport system was shown to confer XOS utilization in *B. animalis* subsp. *lactis* BB-12 using combined transcriptome and proteome analysis (21). The organization of this locus is identical to other *B. lactis* strains including the widely used probiotic *B. animalis* subsp. *lactis* Bl-04 (22), and the ABC system in the locus is conserved in different *Bifidobaterium* species. The ligand preference and the structural basis for XOS recognition by the transporter, however, are currently unknown. Canonical ABC import systems share a common structural organization comprising two transmembrane domains (TMDs) that form the translocation pore, two intracellular nucleotide binding domains that power the transport process by harnessing energy from ATP hydrolysis, and an extracellular solute binding protein (SBP). The affinity and the specificity of ABC import systems is governed by their SBPs responsible for high affinity capture of substrates for uptake across the membrane (23).

Here, the ligand preference, binding energetics and kinetics of the SBP responsible for the capture of both XOS and AXOS in *B. animalis* spp. *lactis* Bl-04 are reported. The complex structures between this SBP and three different XOS ligands are also determined, presenting the first structural data on XOS capture by an ABC import system in probiotic bacteria and providing novel insight on the structural basis of XOS uptake by a physiologically important group of the gut microbiome.

Experimental procedures

Chemicals.

All chemicals used in this study were of analytical grade. Carbohydrate ligands with purities in : XOS Longlive 95P (84% xylooligosaccharides composed of 43% xylobiose (X2), 30% xylotriose (X3), 10% xylotetraose (X4), 17% dp≥X5), 13.5 % other

monosaccharides) was from Shandong Biotechnology (Heze China) (20). Xylooligosachharides X2–X4 >95%, X5 and X6 ~95% were from Megazyme (Wicklow, Ireland). Arabinoxylooligosaccharides (AXOS), all ~95% pure with degrees of polymerization (DP) 3–5 were a kind gift from Dr. Barry McCleary (Megazyme), and their structure and composition was as follows: AX2: [α-L-Ara*f*-(1,3)]-β-D-Xyl*p*-(1,4)-D-Xyl*p*; AX3(1): mixture of [α-L-Ara*f*-(1,2)]-β-D-Xyl*p*-(1,4)-β-D-Xyl*p*-(1,4)-D-Xyl*p* (90%) + β-D-Xyl*p*-(1,4)-[α-L-Ara*f*-(1,3)]-β-D-Xyl*p*-(1,4)-D-Xyl*p* (10%); AX3(2): xylotriose substituted with a single arabinosyl residue, precise structure not determined; AX4: β-D-Xyl*p*-(1,4)-[α-L-Ara*f*-(1,3)]-β-D-Xyl*p*-(1,4)-β-D-Xyl*p*-(1,4)-D-Xyl*p* (80%) + β-D-Xyl*p*-(1,4)-[α-L-Ara*f*-(1,2)]-β-D-Xyl*p*-(1,4)-β-D-Xyl*p*-(1,4)-D-Xyl*p* (20%). Xylose, sucrose, cellobiose, melibiose, isomaltose, raffinose, fructo-oligosaccharides from chicory (DP 2–60 average of 10) were >98%. Pure (Sigma-Aldrich, St.Louis, MO, USA). Commercial β-galactooligosacchride mix with degree of polymerization (DP) 2–6, 95% pure was a gift from Sampo Lathinen at DuPont Nutrition and Health, Kantvik, Finland (24).

Cloning, expression and purification of the XOS solute binding protein

Chromosomal DNA of *Bifidobacterium animalis* subsp *lactis* Bl-04 (22) was isolated from bead beated MRS grown cells according to (25). The gene fragment encoding the xylooligosaccharide binding protein of the ATP-binding cassette (ABC) transporter in the XOS utilization operon (locus tag number, *balac_0514*, GenBank accession number NC_01281; 609361..610638; GI:241190066) without the signal peptide predicted by SignalP v.3.0 (26) (basepairs 1–54) was cloned using the sense primer: 5´-CTA**GCTAGC**ATGAGCGCATGTGGCGGG-3´ and antisense primer: 5´-CCG**GAGCTC**TCAGCCCTTCTGGGCGG-3´ and the TaKaRa PrimeStar high GC PCR kit (Takara Bio Inc., Otsu, Shiga, Japan) using the NheI and XhoI restriction sites (bold) and pET28a(+) (Novagen, Darmpstadt Germany) to yield the expression vector pET28aBalac_0514, which was transformed into *Escherichia coli* DH5□ and selected on LB plates supplemented with 50 µg/ml kanamycin. Following restriction analysis and full sequencing, pET28aBalac_0514 was transformed into *E. coli* BL21(DE3) and B834DE3 (Novagen) for expression of unlabelled and selenomethionine labelled protein respectively. The recombinant xylooligosaccharide binding protein, designated as *Bl*XBP, was produced as an N-terminal fusion of a thrombin cleavable hexa-histidine tag with the *Bl*XBP mature

peptide lacking the native transit peptide (amino acid residues 1–18), but having a six amino acid insertion (GSHMAS) flanking the N-terminus of the protein following the tag cleavage.

E. coli BL21(DE3) cells harboring pET28Balac_0514 were used to produce *Bl*XBP in a 5 L Biostat B (B. Braun Biotech International, Melsungen, Germany) bioreactor as previously described (27) except for induction OD_{600} and temperature which were 7.5 and 20 °C, respectively. The fermentation was harvested after 16 h of induction by centrifugation (10000 x *g*, 20 min, 4°C) yielding ~200 g cell wet weight. The cell pellet was resuspended in HisA buffer (10 mM Hepes, 500 mM NaCl, 10 mM imidazole, 10% glycerol (pH 7.5)) and disrupted by high pressure homogenization at 1000 bar (Stansted Fluid Power, Stansted, UK). Disintegrated cells were benzonase nuclease treated (Invitrogen, Carlsbad, CA, US; 30 min at room temperature) and centrifuged (20000 x g , 40 min, 4 °C). The supernatant was sterile filtered (0.45 µm) and loaded onto a 5 ml HisTrap HP column (GE Healthcare, Uppsala, Sweden). After washing by HisA (10 column volumes), bound protein was eluted with a linear gradient of 10 column volumes to 100% HisB (HisA but with 400 mM imidazole instead of 10 mM). Fractions enriched with *Bl*XBP, identified by SDS-PAGE, were concentrated and loaded on a gel filtration on a Hiload Superdex 200 16/60 column (GE Healthcare) and eluted with 10 mM MES, 150 mM NaCl, pH 6.5 at 1 ml/min. *Bl*XBP-containing fractions were pooled, concentrated and dialysed against (10 mM MES, pH 6.5), loaded onto a 6 ml anion exchange Resource Q column (GE Heathcare) and eluted by a 3 stepNaCl gradient resulting in ~2.5 mg homogenous *Bl*XBP per g cell pellet. Chromatographic steps were performed using an ÄKTA-AVANT chromatograph (GE Healthcare) at 4 °C. The His tag was removed using human thrombin (Calbiochem, Merck, Darmstadt, Germany) as recommended by the manufacturer.

Differential scanning calorimetry (DSC)

DSC analysis was performed to assess the conformational integrity of the apo (unliganded) recombinant protein and possible stabilization due to ligand binding. A VP-DSC calorimeter (MicroCal, Northampton, MA, USA) with a cell volume of 0.52061 ml was used and samples were scanned in the temperature interval 20–90 °C at 1 $°C \cdot min^{-1}$. *Bl*XBP (11.3 µM) was dialysed in 1000 volumes of either 20 mM MES, pH 6.5 with or without

2.5 mg/ml commercial XOS mixture (~5 mM assuming an average DP of 3 and 84% purity), and degassed for 10 min at 20 °C. Baseline scans collected with buffer in the reference and sample cells were subtracted from sample scans. Origin v7.038 software with a DSC add-on module was used for assigning T_m and the unfolding enthalpy accessed by fitting a non-two state model to the thermogram.

Surface plasmon resonance (SPR)

Affinity of *Bl*XBP for the different xylooligosaccharides was determined using a Biacore T100 (GE Healthcare). *Bl*XBP, diluted into 10 mM Na-acetate pH 4.1 to 2.3 µM, was immobilized on a CM5 sensor chip using a random amine coupling kit (GE Healthcare) to a density of 2900 response units (RU). Sensograms were recorded at 25 ºC in 20 mM Na_2HPO_4/citrate; 150 mM NaCl; pH 6.5, 0.005% (v/v) P20 surfactant (GE Healthcare) at a flow of 30 µl/min, with an association time of 90 s, and dissociation time of 240 s. Experiments were performed in triplicates in the range 3 nM–10 µM for X3–X5, and AXOS; X2 and X6 were from 0.5 µM–1 mM all dissolved in the same buffer as above. To investigate the specificity of *Bl*XBP binding was tested towards 5 mM of xylose, cellobiose, raffinose, sucrose, melibiose, isomaltose; FOS and GOS in the same buffer. The pH dependence of the binding affinity of *Bl*XBP to xylotetraose was investigated at 8 different pH values in the range pH3–9 (Supplementary Fig. 4), while dependence of binding on temperature was examined in the range 15–30 ºC. Data analysis was carried out using the Biacore T100 evaluation software, and equilibrium dissociation constants (K_d) were calculated by fitting either the steady state response data or the full sensograms to a one site binding model allowing the determination of binding kinetics. The van 't Hoff non-linear equation was used to extract the thermodynamic parameters of binding from the temperature dependence of *Bl*XBP.

Isothermal titration calorimetry (ITC)

Binding of X3 and X4 to recombinant *Bl*XBP was measured using an ITC_{200} microcalorimeter (MicroCal) at 25 ºC in 10 mM sodium phosphate, pH 6.5. *Bl*XBP (14 or 25 µM) in the sample cell (200 µl), was titrated by a first injection of 0.5 µl followed by 18

× 2 µl injections of carbohydrate ligand (140 or 250 µM) with 120 s between injections. Data was analyzed using the MicroCal software provided (29).

Fluorescence titration spectroscopy

Intrinsic tryptophan emission was measured on a Spex Fluorlog 322 fluorescence spectrometer (HORIBA Jobin Yvon, Irvine, California, US) in a 1 ml stirred quartz cuvette at 25 °C. Purified *Bl*XBP diluted in 10mM sodium phosphate, pH 6.5 to 4 µM and pre-equilibrated for 5 min was titrated with 0.5 mM of X3 or X4 in 0.5 µl steps. Instrument settings and data analysis were as previously reported (30). The ligand specific contribution to fluorescence quenching was corrected for in all measurements.

Crystallization and structure determination

*Bl*XBP and selenomethionine labeled *Bl*XBP (15 mg/ml in 10 mM MES, pH 6.5 and 150 mM NaCl) were used to screen for crystallisation conditions. Crystals grew only in the presence of xylooligosaccharide (1 mM) after 30 h incubation at 5°C by vapor diffusion in hanging drops from the following condition: 1:1 ratio of *Bl*XBP and reservoir 0.1 M Tris pH 7.5, 47% PEG 300 and 5% PEG 1000. Due to the high concentrations of PEG in the reservoir solution no further cryoprotectant was needed and the crystals were flash frozen directly in liquid nitrogen. Diffaction data was collected to 3.1 Å for the selenomethionine *Bl*XBP:X4, 2.2 Å for *Bl*XBP:X4, 2.4 Å for *Bl*XBP:X3 and 2.6 Å for *Bl*XBP:X6 complexes at the SLS beamlines PXI and PXIII, Villigen, Switzerland. The structure of selenomethionine *Bl*XBP was solved using the single anomalous diffraction (SAD) method with the experimental phase information obtained from data collected at the Selenium K-edge. All datasets were processed with XDS (31). The program Phenix.AutoSol [29] identified 15 out of 17 selenomethionine residues present in the *Bl*XBP. An initial partial model was obtained with AutoBuild and further corrections and model building using the program Coot resulted in a 75% complete model The latter model was used in molecular replacement to solve the structure of *Bl*XBP:X4 . The model was further completed using automatic and manual model building and the structure was refined using Phenix.Refine randomly setting aside 5% of the reflections (and monitoring R_{cryst}/R_{free} factors). The *Bl*XBP:X3 and *Bl*XBP:X6 structures were solved using the protein part of the *Bl*XBP:X4

structure. The *Bl*XBP:X4 R_{free}-set was used for *Bl*XBP:X3. Ligand molecules were included after the protein parts were build and water molecules were manually added. The overall quality of all models was checked using the MolProbity server [30].

Results

Production and Purification of recombinant Bl*XBP*

The *balac_0514 gene* in the *B. animalis* spp. *lactis* Bl-04 genome (22), annotated as a putative sugar transporter solute-binding protein (Pfam family: SBP_bac_1 (PF05147) (32), was predicted to have XOS specificity based on gene landscape analysis and comparison to the XOS utilization cluster identified in the homolog from *B. animalis* spp. *lactis* strain BB-12 (21). Recombinant unlabelled and selenomethionine labelled *Bl*XBP were produced and purified at yields of (~2.5 mg/ g of cell wet weight). *Bl*XBP occurred as a mixture of monomer and dimer in solution based on analytical size exclusion chromatography and static light scattering (Supplementary Fig. 1).

Thermal Stability

The conformational stability of *Bl*XBP was evaluated by differential scanning calorimetry (DSC) (33). The thermogram of the apo-protein displayed a well defined albeit broad asymmetric thermal transition with an assigned T_m of 65.0 °C for the main peak and a shoulder at ≈ 70 °C (Fig. 1A) attesting the conformational integrity and stability of the recombinant protein, but suggesting a complex unfolding behaviour. Indeed, the unfolding thermogram was best described by a non-two-state model with two thermal transitions deconvoluted (T_{m1} =65.0 °C and T_{m2} =70.8 °C) with an overall calorimetric enthalpy of 404 kJ/mol. The presence of ~ 450 fold excess of a XOS mixture resulted in an increase of T_m and calorimetric enthalpy to 69.5°C and 543 kJ/mol, respectively. The narrow cooperative thermal transition was also best described by a non-two-state model, in this case however a single peak was adequate to describe the transition suggesting the overlap of the two processes which were deconvoluted in the apo form of the protein (Fig. 1). Thus, significant stabilisation of *Bl*XBP mounting to 25% increase in calorimetric enthalpy occurred in presence of XOS, supportive of the functionality of the protein and the predicted specificity towards XOS.

Specificity and affinity of Bl*XBP*

Binding of *Bl*XBP to xylooligosaccharides with DP 2–6, arabinosyl decorated xylooligosaccharides (DP 3–5) in additions to 8 other mono-, di- and oligosaccharides was analyzed by surface plasmon resonance. Only XOS and AXOS resulted in significant binding at the tested concentrations, and good quality data (Fig. 2) enabled discerning the kinetics of binding of the different ligands. *Bl*XBP displayed highest affinity towards X4 with a K_d = 45 nM followed closely by AX3(1), AX3(2) AX2 and X3 (Table 1). The affinity towards xylobiose was ~200 fold lower than X4 owing to a lower association rate constant (k_{on}) and faster dissociation (k_{off}) (Table 1). Similarly, the relative affinity compared to X4 dropped about 12 and 400 fold for X5 and X6, respectively (Table 1) owing largely to decreased k_{on}, whereas k_{off} changed only modestly. The presence of an arabinosyl sidechain contributed to affinity and binding kinetics in a similar way as adding a backbone xylosyl (Table 1, Fig. 2).

The temperature dependence of binding in the range 15–30°C (Supplementary Table 1) was used to analyse the energetics of *Bl*XBP binding to X4. The non-linear van´t Hoff plot was used for this analysis (Supplementary Fig. 2) and showed a favorable van´t Hoff standard enthalphy change ΔH° = -100 kJ/mol, which was complemented by an unfavorable entropy change of TΔS° kJ/mol = -62. The thermodynamic parameters for binding of X3 andX4 were determined using ITC and the obtained binding isotherms were sigmoidal (Fig. 3), which allowed the determination of binding stoichiometry (*n*) to 0.95 and 0.83 for X3 and X4, respectively. The binding affinity was the highest for xylotetraose and the magnitude of the binding constants was in very good agreement with those obtained from SPR and fluorescent spectroscopy measurements (Table 2). For X3 and X4, the energetics of binding were similar but the magnitude of the enthalpy and entropy changes were larger than those determined by the indirect van´t Hoff extrapolation (Supplementary Table 1).

Crystallization, data collection and structure determination

Crystallization was performed using the hanging drop vapor-diffusion method at 278K. The initial condition was obtained with the Cryo crystallization screen (Emerals BioSystems, MA, USA). Crystals were only obtained in the presence of 1 mM

xylooligosaccharide ligands in drops containing solution E5 (Tris pH 7, 40% PEG-300 and 5% PEG-1000). This condition was optimized to (0.1 M Tris pH 7.5, 47% PEG-300 and 5% PEG-1000), which resulted in rod shaped crystals that grew in 30 h. The crystals of the SeMet-*Bl*XBP in complex with X4 were assigned into the orthorhombic space group $P2_12_12$ with one molecule in the asymmetric unit. The crystals of *Bl*XBP in complex with X3 and X4 belonged to the same space group, while *Bl*XBP in complex with X6 crystals were assigned into the monoclinic P121 space group with two molecules in the asymmetric unit. A model of *Bl*XBP was build based on single-anomalous dispersion (SAD) X-ray diffraction data from SeMet labeled *Bl*XBP in complex with X4 and used as search model for molecular replacement in native datasets of *Bl*XBP co-crystalized with X3, X4 and X6 at 2.4 Å, 2.2 Å and 2.6 Å respectively. The data collection and refinement statistics are shown in Table 3. The final models of *Bl*XBP in complex with X3, X4 and X6 were refined to R_{cryst} /R_{free} values 0.21/0.26, 0.27/0.29 and 0.21/0.26 for complexes with X4, X3 and X6 respectively. The three complexes are very similar in conformation and superposition of the individual monomers results in an overall RMSD of 0.27 Å between aligned C-alpha atoms. The final models and refined electrondesity maps are provided in the supplementary material of the thesis.

Overall three-dimensional structure

*Bl*XBP displays a bilobate architecture that consists of two domains of different size joined by a tripartite hinge region with the ligand binding site buried at the interface between the two domains (Fig. 4), consistent with a type I and cluster B assignment according to secondary structure topology based and structural alignment classification systems, respectively. The N-terminal domain (domain I) (1–143; 318–362) consists of 7 α-helices and 5 β-strands, two of which form a part of the hinge region and continue into the C-terminal domain (domain II) (147–314; 365–425). Domain II consists of 11 α-helices and 4 β-strands. The domain is stabilized by a disulphide bridge between Cys 209 and Cys 227. The tripartite hinge region comprises two β-strands arranged in an anti-parallel β-sheet spanning the 2 domains (144–146; 315–317) and the loop region 363–365.

Ligand binding site.

The crystal structures of *Bl*XBP in complex with X3 and X4 show well defined densities for 3 and 4 xylose units, respectively in the binding site in contrast to the X6 complex where only 5 xylose units are visible in the electron density map. The XOS ligands are oriented with the non-reducing end docked against domain II. The xylose units are numbered starting with 1 at the non-reducing end. Residues from both domains contribute to the binding of the XOS ligand: residues from the C-terminal domain II are both involved in polar contacts and van der Waals interactions through aromatic ring stacking with first two xylose units from the non-reducing end of the XOS ligand, while the N-terminal domain I exclusively makes polar contacts including a number of water mediated hydrogen bonds. The xylooligosaccharides are recognized by aromatic stacking interactions with Trp195, Trp277,Trp 384 and Phe350 but also polar interactions with residues His199 and Asp386 are coordinating the two xylose units 1 and 2 (Fig. 5 and 6). The hydroxyl groups of the ligands form direct hydrogen bonds to the side chains of Asn72, His199, Gln254 and to the peptide backbone (Fig. 6), but especially hydrogen bonds mediated through ordered water in the binding pocket seem to have an important contribution to the binding. In all three complex structures ordered water molecules mediate hydrogen bonds between the ligands and the protein, and the binding pocket contain ordered waters. Thus water-mediated hydrogen bonds between the ligands and the protein contribute greatly to the ligand protein interactions (Fig. 5). The main difference between the 3 complex structures is the conformational change in loop region Asn39–Glu44 that forms a lid that blocks the entrance to the binding site in the X3 structure but bends out towards the solvent side in the X4 and X6 structures, this region makes hydrogen bonds form the C_{α}-peptide backbone to the XOS ligand. (Shown in Fig. 6).

Discussion

Although the concept of stimulation of probiotic bacteria by prebiotic carbohydrates is currently well established (34), the molecular mechanisms governing prebiotic selectivity remain elusive. Several transcriptional studies implicated a diversity of carbohydrate transport systems in uptake of oligosaccharides, which are subsequently degraded by

intracellular enzymes in probiotic bacteria (21,35,36). By contrast, data on the molecular properties of carbohydrate transport systems is essentially lacking on the protein level with the exception of the lacto-*N*-biose solute binding protein from *Bifidobacterium longum* (37). In the present study, the binding properties and the structure of the xylooligosaccharide specific solute binding protein that mediates high affinity uptake of XOS via an ABC transport system within the *Bifidobacterium* genus is presented.

The ligand specificity of Bl*XBP*

*Bl*XBP displays no detectable binding activity towards xylose or arabinose, and the specificity of the protein was also evident from the lack of detectable binding to various di- and oligosaccharides tested. By contrast, *Bl*XBP displayed significant plasticity with regard to the size and side chain substitution of xylooligosaccharide being able to accommodate undecorated and arabinose decorated xylooligosaccharides with similar affinity (Table 1). Notably, AXOS at both the C2 and C3 of the non-reducing end xylosyl as in AX2 and AX3(1), respectively, or internally as in AX4 (Table 1). This data is consistent with the growth of bifidobacteria on arabinoxylooligosaccrharides and with the presence of AXOS specific arabinofuranosidases of mainly GH43 but also GH51 in bifidobacteria (38). On the other hand the relatively sharp size preference of *Bl*XBP for DP 3–5 (optimum affinity for DP4) is intriguing as characterized intracellular bifidobacterial β-xylosidases of GH8 (reducing end xylanase), GH43 and GH120 do not seem to display the same substrate preference. Common to these enzyme families is that they display high activity on XOS ligands with DP from 3–6 (17,39). While GH120 and GH8 enzymes from bifidobacteria displayer higher activity on longer substrates and are essentially inactive on xylobiose, GH43 enzymes displays high levels of activity on the disaccharide, in addition to their activity on longer ligands (17). Thus, additional factors such as the competitive niche in the gut appear to have exerted evolutionary pressure to select for the ligand preference of the XOS ABC transport system in bifidobacteria (will be discussed in more detail below).

Structural, kinetic and thermodynamic aspects of XOS recognition

The affinity of *Bl*XBP to its ligands was characterized by large changes in the association rate (k_{on}), while changes in the dissociation rate were modest with the exception for X2 (Table 1, Supplementary Fig. 3). The magnitude of k_{off} reflects the short range interactions between the protein and the ligand, while k_{on} is influenced by diffusion and by favorable electrostatics when the protein and the ligand are within the encounter complex distance (40). The observed changes in k_{off} are in excellent agreement with the determined complex structures revealing a binding site accommodating X4. Thus, fewer interactions are possible with X2 compared to X3 or X4, rationalizing the 16 fold faster k_{off} compared to X4 (Table 1). Ligands longer than X4 will protrude out of the binding site without being able to form additional contacts with the protein as compared to X4 (Fig. 5) consistent with the almost invariant k_{off} for X4–X6. The arabinoxylated XOS conform largely to the same k_{off} trend, with slightly lower values for AX2 and slightly higher values for the larger decorated ligands. The more than 20 fold lower k_{on} of X2 as compared to X3 is intriguing and may be possibly explained by formation of fewer contacts and possibility to bind in more than one binding mode resulting in slower transition from the open to the bound conformation of the binding protein (41-43). The estimated stoichiometry from the SPR data (Table 2) is similar for X2 and X3, consistent with the binding of a single X2 molecule in the active site of *Bl*XBP, confirming that the binding of this smaller ligand is thermodynamically sufficient to elicit the required conformational change, at the penalty of slower kinetics. Interestingly, a similar trend of slower k_{on} governed the affinity to the larger ligands X5 and X6. The binding of these ligands would require additional structural rearrangements (Fig. 5), which evidently results in slower k_{on} values. Thus the binding kinetics modulate the ligand preference of *Bl*XBP for optimal recognition of ligands of DP 3–4.

The thermodynamic signature of *Bl*XBP binding to X3 and X4 was similar and revealed an enthalpically dominated binding, which is compensated by large entropic penalties. This energetic finger print is in excellent agreement with the structural data showing extensive protein-ligand interactions involving a combination of aromatic stacking and a hydrogen bonding network including direct and solvent mediated contacts, which contribute to the binding enthalpy. The unfavorable entropy is likely to arise from the ordering of water molecules in the binding pocket and the loss of conformational freedom of both the ligand and the protein side chains and domains that typically possess rotational freedom along the

hinge region (44). It was not possible to obtain crystal of *Bl*XBP in the unliganded apo form, which is indicative of considerable loss of protein flexibility upon ligand binding. Nonetheless, the entropy of ordering the solvent molecules seems to be crucial in the entropic off-set of binding, as the blood antigen binding protein from *Streptococcus pneumonia* which does not contain ordered solvent molecules shows a significantly lower entropic compensation of the favourable binding enthalpy (ca 10% ΔH as compared to ca 76% for *Bl*XBP). The energetic fingerprint of *Bl*XBP is similar to the lacto-*N*-biose binding potein from *B. longum* (37), which also employs ordered solvent molecules to mediate a hydrogen bonding network to the bound ligand.

Biological implications of the ligand preference of BlXBP: xylan catabolism in the gut

Plant cell wall polysaccharides, including arabinoxylan fibres that are abundant in human diet, offer members of the gut microbiome an important source of carbon and energy. Although xylan metabolism in the colon is not fully understood, it has been suggested that species from the *Bacteroides* and *Roseburia* genera that possess modular GH10 endoxylanases are the prevalent xylanotyic taxa (45). This is consistent with the presence of at least one gene encoding an extracellular modular GH10 endoxylanase appended to one or more putative xylan specific carbohydrate biding modules of CBM4, CBM6 or CBM22 (46) or CBM9 (47) in *e.g. Roseburia intestinalis* and in species of *Bacteroides*. Xylan utlisation in *Bacteroides* has been shown to be mediated by a specific PULs (polysaccharide utilization loci) similar to the SUS (starch utilization system), where extracellular modular GH10 enzymes capture the substrate by means of their appended CBMs and hydrolyse it to large fragments that are subsequently transported via the SusC translocation protein to the periplasm for further degradation to monosaccharides, which are taken up by MFS (major facilitator superfamily) transporters (48). Notably, the affinity of CBM22 and CBM6 increases with ligand size with highest affinities measured for xylohexaose with K_d values typically typically in the low μM range (49). Accordingly, it is unlikely that smaller xylan fragments are captured efficiently by the *Bacteorides* uptake system or by *Roseburia* assuming a similar CBM mediated binding mechanism. It is predicted that xylan degradation occurs mainly in the proximal colon (50). Thus it is likely that a gradient of increasing concentration of smaller xylooligosaccharides would be

formed downstream in the colon, providing a nichè for bacteria like *Bifidobaterium animalis* subsp. *lactis* with efficient XOS uptake and utilization systems.

References

1. Eckburg, P. B., Bik, E. M., Bernstein, C. N., Purdom, E., Dethlefsen, L., Sargent, M., Gill, S. R., Nelson, K. E., and Relman, D. A. (2005) Diversity of the human intestinal microbial flora. *Science.* **308**, 1635-1638
2. Xu, J., Mahowald, M. A., Ley, R. E., Lozupone, C. A., Hamady, M., Martens, E. C., Henrissat, B., Coutinho, P. M., Minx, P., Latreille, P., Cordum, H., Van Brunt, A., Kim, K., Fulton, R. S., Fulton, L. A., Clifton, S. W., Wilson, R. K., Knight, R. D., and Gordon, J. I. (2007) Evolution of Symbiotic Bacteria in the Distal Human Intestine. *PLos Biol.* **5**, 1574-1586
3. Arumugam, M., Raes, J., Pelletier, E., Le Paslier, D., Yamada, T., Mende, D. R., Fernandes, G. R., Tap, J., Bruls, T., Batto, J.-M., Bertalan, M., Borruel, N., Casellas, F., Fernandez, L., Gautier, L., Hansen, T., Hattori, M., Hayashi, T., Kleerebezem, M., Kurokawa, K., Leclerc, M., Levenez, F., Manichanh, C., Nielsen, H. B., Nielsen, T., Pons, N., Poulain, J., Qin, J., Sicheritz-Ponten, T., Tims, S., Torrents, D., Ugarte, E., Zoetendal, E. G., Wang, J., Guarner, F., Pedersen, O., de Vos, W. M., Brunak, S., Dore, J., Weissenbach, J., Ehrlich, S. D., and Bork, P. (2011) Enterotypes of the human gut microbiome. *Nature*. **473**, 174-180
4. Picard, C., Fioramonti, J., Francois, A., Robinson, T., Neant, F., and Matuchansky, C. (2005) Bifidobacteria as probiotic agents – physiological effects and clinical benefits. *Aliment. Pharmacol. Ther*. **22**, 495-512
5. Roberfroid, M. (2007) Prebiotics: The concept revisited. *J. Nutr.* **137**, 830S-837S
6. Wallace, T. C., Guarner, F., Madsen, K., Cabana, M. D., Gibson, G., Hentges, E., and Sanders, M. E. (2011) Human gut microbiota and its relationship to health and disease. *Nutr. Rev.* **69**, 392-403
7. O'Flaherty, S., and Klaenhammer, T. R. (2010) The role and potential of probiotic bacteria in the gut, and the communication between gut microflora and gut/host. *Int. Dairy J.* **20**, 262-268

8. Fukuda, S., Toh, H., Hase, K., Oshima, K., Nakanishi, Y., Yoshimura, K., Tobe, T., Clarke, J. M., Topping, D. L., Suzuki, T., Taylor, T. D., Itoh, K., Kikuchi, J., Morita, H., Hattori, M., and Ohno, H. (2011) Bifidobacteria can protect from enteropathogenic infection through production of acetate. *Nature.* **469**, 543-U791
9. Gibson, G. R., and Roberfroid, M. B. (1995) Dietray modulation of the human colonic microbiota-introducing the concept of prebiotics. *J. Nutr.* **125**, 1401-1412
10. Van Craeyveld, V., Swennen, K., Dornez, E., Van de Wiele, T., Marzorati, M., Verstraete, W., Delaedt, Y., Onagbesan, O., Decuypere, E., Buyse, J., De Ketelaere, B., Broekaert, W. F., Delcour, J. A., and Courtin, C. M. (2008) Structurally different wheat-derived arabinoxylooligosaccharides have different prebiotic and fermentation properties in rats. *J. Nutr.* **138**, 2348-2355
11. Nyman, M., Siljestrom, M., Pedersen, B., Knudsen, K. E. B., Asp, N. G., Johansson, C. G., and Eggum, B. O. (1984) Dietary fiber content and composition in 6 cereals at different extraction rates. *Cereal Chem.* **61**, 14-19
12. Chassard, C., Goumy, V., Leclerc, M., Del'homme, C., and Bernalier-Donadille, A. (2007) Characterization of the xylan-degrading microbial community from human faeces. *FEMS Microbiol. Ecol.* **61**, 121-131
13. Flint, H. J., Duncan, S. H., Scott, K. P., and Louis, P. (2007) Interactions and competition within the microbial community of the human colon: links between diet and health. *Environ. Microbiol.* **9**, 1101-1111
14. Crittenden, R., Karppinen, S., Ojanen, S., Tenkanen, M., Fagerstrom, R., Matto, J., Saarela, M., Mattila-Sandholm, T., and Poutanen, K. (2002) In vitro fermentation of cereal dietary fibre carbohydrates by probiotic and intestinal bacteria. *J. Sci. Food Agric.* **82**, 781-789
15. Moura, P., Barata, R., Carvalheiro, F., Girio, F., Loureiro-Dias, M. C., and Esteves, M. P. (2007) In vitro fermentation of xylo-oligosaccharides from corn cobs autohydrolysis by Bifidobacterium and Lactobacillus strains. *LWT-Food Sci. Technol.* **40**, 963-972
16. Lagaert, S., Pollet, A., Delcour, J. A., Lavigne, R., Courtin, C. M., and Volckaert, G. (2010) Substrate specificity of three recombinant alpha-L-arabinofuranosidases from *Bifidobacterium adolescentis* and their divergent action on arabinoxylan and arabinoxylan oligosaccharides. *Biochem. Biophys. Res. Commun.* **402**, 644-650

17. Lagaert, S., Pollet, A., Delcour, J. A., Lavigne, R., Courtin, C. M., and Volckaert, G. (2011) Characterization of two beta-xylosidases from *Bifidobacterium adolescentis* and their contribution to the hydrolysis of prebiotic xylooligosaccharides *Appl. Microbiol. Biotechnol.* **92**, 1179-1185
18. Makelainen, H., Saarinen, M., Stowell, J., Rautonen, N., and Ouwehand, A. C. (2010) Xylo-oligosaccharides and lactitol promote the growth of *Bifidobacterium lactis* and *Lactobacillus* species in pure cultures *Benef. Microbes.* **1**, 139-148
19. Palframan, R., Gibson, G. R., and Rastall, R. A. (2003) Development of a quantitative tool for the comparison of the prebiotic effect of dietary oligosaccharides. *Lett. Appl. Microbiol.* **37**, 281-284
20. Mäkeläinen, H., Forssten, S., Saarinen, M., Stowell, J., Rautonen, N., and Ouwehand, (2009) Xylo-oligosaccharides enhance the growth of bifidobacteria and *Bifidobacterium lactis* in a simulated colon model. *Benef. Microbes.* **1**, 81-91
21. Gilad, O., Jacobsen, S., Stuer-Lauridsen, B., Pedersen, M. B., Garrigues, C., and Svensson, B. (2010) Combined transcriptome and proteome analysis of *Bifidobacterium animalis* subsp. *lactis* BB-12 grown on xylo-oligosaccharides and a model of their utilization. *Appl. Environ. Microbiol.* **76**, 7285-7291
22. Barrangou, R., Briczinski, E. P., Traeger, L. L., Loquasto, J. R., Richards, M., Horvath, P., Coute-Monvoisin, A. C., Leyer, G., Rendulic, S., Steele, J. L., Broadbent, J. R., Oberg, T., Dudley, E. G., Schuster, S., Romero, D. A., and Roberts, R. F. (2009) Comparison of the complete genome sequences of *Bifidobacterium animalis* subsp. *lactis* DSM 10140 and Bl-04. *J. Bacteriol.* **191**, 4144-4151
23. Eitinger, T., Rodionov, D. A., Grote, M., and Schneider, E. (2011) Canonical and ECF-type ATP-binding cassette importers in prokaryotes: diversity in modular organization and cellular functions. *FEMS Microbiol. Rev.* **35**, 3-67
24. Barrangou, R., Azcarate-Peril, M. A., Duong, T., Conners, S. B., Kelly, R. M., and Klaenhammer, T. R. (2006) Global analysis of carbohydrate utilization by *Lactobacillus acidophilus* using cDNA microarrays. *Proc. Natl. Acad. Sci. U.S.A.* **103**, 3816-3821
25. Sambrook, J., and Russell, D. W. (2006) Purification of nucleic acids by extraction with phenol:chloroform. *Cold Spring Harb Protoc.* pdb.prot4455

26. Bendtsen, J. D., Nielsen, H., von Heijne, G., and Brunak, S. (2004) Improved prediction of signal peptides: SignalP 3.0. *J. Mol. Biol.* **340**, 783-795
27. Fredslund, F., Abou Hachem, M., Larsen, R. J., Sorensen, P. G., Coutinho, P. M., Lo Leggio, L., and Svensson, B. Structure of alpha-galactosidase from *Lactobacillus acidophilus* NCFM: Insight into tetramer formation and substrate binding. *J. Mol. Biol.* **412**, 466-480
28. Slotboom, D. J., Duurkens, R. H., Olieman, K., and Erkens, G. B. (2008) Static light scattering to characterize membrane proteins in detergent solution. *Methods.* **46**, 73-82
29. Wiseman, T., Williston, S., Brandts, J. F., and Lin, L. N. (1989) Rapid measurement of binding constants and heats of binding using a new titration calorimeter. *Anal. Biochem.* **179**, 131-137
30. Erkens, G. B., and Slotboom, D. J. (2010) Biochemical characterization of ThiT from *Lactococcus lactis*: A thiamin transporter with picomolar substrate binding affinity. *Biochemistry.* **49**, 3203-3212
31. Kabsch, W. (2010) XDS. *Acta Crystallogr. D Biol. Crystallogr.* **66**, 125-132
32. Tam, R., and Saier, M. H., Jr. (1993) Structural, functional, and evolutionary relationships among extracellular solute-binding receptors of bacteria. *Microbiol. Rev.* **57**, 320-346
33. Bruylants, G., Wouters, J., and Michaux, C. (2005) Differential scanning calorimetry in life science: Thermodynamics, stability, molecular recognition and application in drug design. *Curr. Med. Chem.* **12**, 2011-2020
34. Kolida, S., and Gibson, G. R. (2011) Synbiotics in Health and Disease. *Annu. Rev. Food Sci. Technol.* **2**, 373–93
35. Turroni, F., Bottacini, F., Foroni, E., Mulder, I., Kim, J. H., Zomer, A., Sanchez, B., Bidossi, A., Ferrarini, A., Giubellini, V., Delledonne, M., Henrissat, B., Coutinho, P., Oggioni, M., Fitzgerald, G. F., Mills, D., Margolles, A., Kelly, D., van Sinderen, D., and Ventura, M. Genome analysis of *Bifidobacterium bifidum* PRL2010 reveals metabolic pathways for host-derived glycan foraging. *Proc. Natl. Acad. Sci. U.S.A.***107**, 19514-19519
36. Andersen, J. M., Rodolphe Barrangou, Maher Abou Hachem, Sampo J. Lahtinen, Yong Jun Goh, Birte Svensson, and Klaenhammer, T. R. (2012) Transcriptional

analysis of prebiotic uptake and catabolism by *Lactobacillus acidophilus* NCFM. *PLoS ONE.* **7**:e44409.

37. Suzuki, R., Wada, J., Katayama, T., Fushinobu, S., Wakagi, T., Shoun, H., Sugimoto, H., Tanaka, A., Kumagai, H., Ashida, H., Kitaoka, M., and Yamamoto, K. (2008) Structural and thermodynamic analyses of solute-binding protein from *Bifidobacterium longum* specific for core 1 disaccharide and lacto-N-biose I. *J. Biol. Chem.* **283**, 13165-13173
38. van den Broek, L. A. M., Lloyd, R. M., Beldman, G., Verdoes, J. C., McCleary, B. V., and Voragen, A. G. J. (2005) Cloning and characterization of arabinoxylan arabinofuranohydrolase-D3 (AXHd3) from *Bifidobacterium adolescentis* DSM20083. *Appl. Microbiol. Biotechnol.* **67**, 641-647
39. Lagaert, S., Van Campenhout, S., Pollet, A., Bourgois, T. M., Delcour, J. A., Courtin, C. M., and Volckaert, G. (2007) Recombinant expression and characterization of a reducing-end xylose-releasing exo-oligoxylanase from *Bifidobacterium adolescentis*. *Appl. Environ. Microbiol.* **73**, 5374-5377
40. Sheinerman, F. B., Norel, R., and Honig, B. (2000) Electrostatic aspects of protein-protein interactions. *Curr. Opin. Struct. Biol.* **10**, 153-159
41. Park, K., Lee, L. H., Shin, Y.-B., Yi, S. Y., Kang, Y.-W., Sok, D.-E., Chung, J. W., Chung, B. H., and Kim, M. (2009) Detection of conformationally changed MBP using intramolecular FRET. *Biochem. Biophys. Res. Commun.* **388**, 560-564
42. Sooriyaarachchi, S., Ubhayasekera, W., Park, C., and Mowbray, S. L. (2010) Conformational changes and ligand recognition of *Escherichia coli* D-xylose binding protein revealed. *J. Mol. Biol.* **402**, 657-668
43. Bjorkman, A. J., and Mowbray, S. L. (1998) Multiple open forms of ribose-binding protein trace the path of its conformational change. *J. Mol. Biol.* **279**, 651-664
44. Jelesarov, I., and Bosshard, H. R. (1999) Isothermal titration calorimetry and differential scanning calorimetry as complementary tools to investigate the energetics of biomolecular recognition. *J. Mol. Recognit.* **12**, 3-18
45. Mirande, C., Kadlecikova, E., Matulova, M., Capek, P., Bernalier-Donadille, A., Forano, E., and Bera-Maillet, C. (2010) Dietary fibre degradation and fermentation by two xylanolytic bacteria *Bacteroides xylanisolvens* XB1A and *Roseburia intestinalis* XB6B4 from the human intestine. *J. Appl. Microbiol.* **109**, 451-460

46. Czjzek, M., Bolam, D. N., Mosbah, A., Allouch, J., Fontes, C. M. G. A., Ferreira, L. M. A., Bornet, O., Zamboni, V., Darbon, H., Smith, N. L., Black, G. W., Henrissat, B., and Gilbert, H. J. (2001) The location of the ligand-binding site of carbohydrate-binding modules that have evolved from a common sequence is not conserved. *J. Biol. Chem.* **276**, 48580-48587
47. Boraston, A. B., Creagh, A. L., Alam, M. M., Kormos, J. M., Tomme, P., Haynes, C. A., Warren, R. A. J., and Kilburn, D. G. (2001) Binding specificity and thermodynamics of a family 9 carbohydrate-binding module from *Thermotoga maritima* xylanase 10A. *Biochemistry.* **40**, 6240-6247
48. Dodd, D., Mackie, R. I., and Cann, I. K. (2011) Xylan degradation, a metabolic property shared by rumen and human colonic bacteroidetes. *Mol Microbiol.* **79**, 292-304
49. McCartney, L., Blake, A. W., Flint, J., Bolam, D. N., Boraston, A. B., Gilbert, H. J., and Knox, J. P. (2006) Differential recognition of plant cell walls by microbial xylan-specific carbohydrate-binding modules. *Proc. Natl. Acad. Sci. U.S.A.* **103**, 4765-4770
50. Pochart, P., Lemann, F., Flourie, B., Pellier, P., Goderel, I., and Rambaud, J. C. (1993) Pyxigraphic sampling to enumerate methanogens and anaerobes in the right colon of healthy humans. *Gastroenterology.* **105**, 1281-1285
51. Wallace, A. C., Laskowski, R. A., and Thornton, J. M. (1995) LIGPLOT: a program to generate schematic diagrams of protein-ligand interactions. *Protein Eng.* **8**, 127-134

Legend to Figures

Fig. 1. Thermrostability of *Bl*XBP analysed by differential scanning calorimetry: Top: Reference and base line subtracted thermogram of the unfolding of the apo *Bl*XBP (solid line). The complex unfolding transition is best described by a non-two-state model with two peaks. The fit to the thermogram (dashed line) is shown as well as the deconvuluted transitions. Bottom: Reference and base line subtracted thermogram of the unfolding of the *Bl*XBP bound to XOS (solid line). A non-two-state single peak model is fitted (dotted line) to the *Bl*XBP-XOS thermogram (solid line).

Fig. 2. Binding kinetics of XOS to *Bl*XBP as analysed by surface plasmon resonance at 25 °C in in 20 mM Na_2HPO_4/citrate; 150 mM NaCl; pH 6.5, 0.005% (v/v) P20 surfactant. Blank and reference cell corrected sensograms (grey) and one binding site global fits (solid black lines) to five ligand concentrations from 19.5 to 312.5 nM A) xylotetraose (X4), B) xylopentaose (X5), C) arabino-xylotriose-1 (AX3(1)), D) arabino-xylotriose-2 (AX3(2)).

Fig. 3. Isothermal titration calorimetry analysis of *Bl*XBP with X3 and X4. A) The thermograms (X3 above X4) and binding isotherms (bottom panel: X3 squares, X4 circles) are shown. The analysis is performed at 25 °C and pH 6.5 using 250 µM of each ligand in the syringe and 25 µM *Bl*XBP in the cell.

Fig. 4. Ribbon representation of the overall structure of *Bl*XBP complexed with X4. Two globular domains, the smaller N-terminal lobe (Domain 1, brown) on the right, and the larger C-terminal lobe (domain 2, green) on the left, are linked by three hinge regions (grey). The ligand X4 molecule is shown as a ball-and-stick model numbered from the non-reducing end.

Fig. 5. Comparison of the structures of *Bl*XBP in complex with X3 and X4. Close-up view of the sugarbinding site. **A**: *Bl*XBP complexed with X3. **B**: *Bl*XBP complexed with X4.

Fig. 6. Comparison of the binding site of *Bl*XBP in complex with X3 and X4. LigPlot (51) representation of binding interactions.

Table 1. Kinetics of xylooligosaccharide binding to *Bl*XBP as measured by surface plasmon resonance

Oligo	k_{on}	k_{off}	K_d	R_{max}	χ^2
	$M^{-1}s^{-1}$ x10^4	s^{-1} x 10^{-2}	M		
X2	56.5 ± 1.7	50.25 ± 0.80	9.00 x10^{-6}	9.6 ± 0.15	0.11
X3	1254.0 ± 15.0	12.79 ± 0.10	1.02 x10^{-7}	16.23 ± 0.1	0.1
X4	1019.0 ± 9.1	4.61 ± 0.04	4.53 x10^{-8}	18.17 ± 0.06	0.09
X5	86.1 ± 0.9	5.66 ± 0.05	6.57 x10^{-7}	19.17 ± 0.08	0.17
X6	1.8 ± 0.01	4.42 ± 0.01	2.50 x10^{-5}	14.83 ± 0.04	0.19
AX2	650.5 ± 13.4	5.19 ± 0.10	8.10 x10^{-8}	11.77 ± 0.1	0.17
AX3(1)	1098.7 ± 10.3	7.78 ± 0.04	7.08 x10^{-8}	13.93 ± 0.06	0.14
AX3(2)	1083.0 ± 12.5	8.89 ± 0.07	8.20 x10^{-8}	14.2 ± 0.07	0.12
AX4	90.2 ± 2.0	14.01 ± 0.27	1.55 x10^{-6}	10.43 ± 0.07	0.13

Table 2. Thermodynamic parameters and binding constants obtained by ITC. Binding data determined from SPR and fluorescence spectroscopy measurements are shown for comparison

	$\Delta G°$	$\Delta H°$	$T\Delta S°$	K_d	*n*
	kJ mol^{-1}	kJ mol^{-1}	kJ mol^{-1}	M x10^{-9}	
X3[a]	-39.13	-165.5	-126.4	141	0.95
X4[a]	-39.51	-163.2	-123.7	126	0.83
X4[b]	-42	-100	-62	45	0.70
X3[c]	-41.4	ND	ND	75	1.13
X4[c]	-40.7	ND	ND	57	1.09

[a]Determined by ITC.
[b]Determined by SPR and the thermodynamics were calculated from the non-linear van´t Hoff analysis using the temperature dependence SPR data (Supplementary material Table 2).
[c]Determined by fluorescence emission spectroscopy.

Table 3 Data collection and refinement statistics

*Bl*XBP	X4	X3	X6
Wavelength (Å)	0.97935	0.97935	0.97935
Resolution range (Å)	45.80 - 2.2 (2.3 - 2.2)	45.8 - 2.4 (2.5 - 2.4)	44.5 - 2.6 (2.7 - 2.6)
Space group	P 2_1 2_1 2	P 2_1 2_1 2	P 1 2_1 1
Unit cell	68.045 124.049 61.334 90 90 90	68.045 124.049 61.334 90 90 90	67.013 119.882 67.749 90 95.64 90
Unique reflections [α]	27024 (2590)	20785 (1861)	32071 (2570)
Completeness (%)[α]	99.52 (97.48)	98.76 (90.12)	97.16 (78.50)
R-meas (%)[α]	5.6 (152.0)	5.9 (150.9)	14.2 (96.0)
Mean I/σ(I) [α]	17.65 (2.12)	20.88 (2.24)	8.97 (1.82)
Wilson B-factor	55.59	62.33	42.65
R-factor [β]	0.2072 (0.4323)	0.2668 (0.4372)	0.2080 (0.3016)
R-free [β]	0.2576 (0.4453)	0.2902 (0.4558)	0.2607 (0.3479)
Number of atoms	3110	3002	6004
macromolecules	3002	3002	6004
Ligands	59	NA	NA
Water	49	NA	792
Protein residues	396	396	
RMS (bonds)	0.007	0.007	0.009
RMS (angles)	1.3	1.05	1.16
Ramachandran favored (%)	98	98	97
Ramachandran outliers (%)	0	0	0.25
Clashscore	8.96	6.78	11.77
Average B-factor	23.3	23.6	25
macromolecules	23.6	23.6	25
Solvent	13.8	--	--

[α] Values in the parenthesis are for the highest resolution shell.
[β] Values in the parenthesis are for before refinement.

Fig. 1.

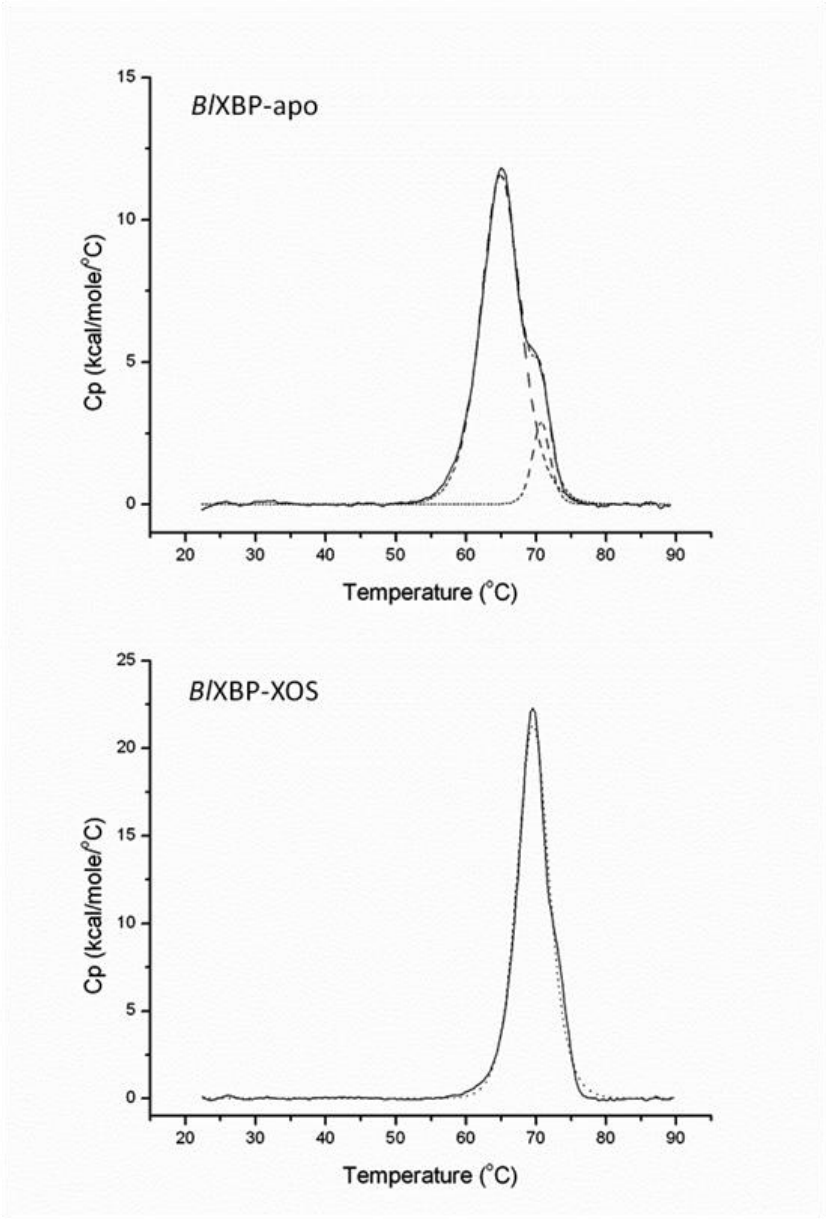
BlXBP-apo
Cp (kcal/mole/°C)
Temperature (°C)
BlXBP-XOS
Cp (kcal/mole/°C)
Temperature (°C)

Fig. 2.

.

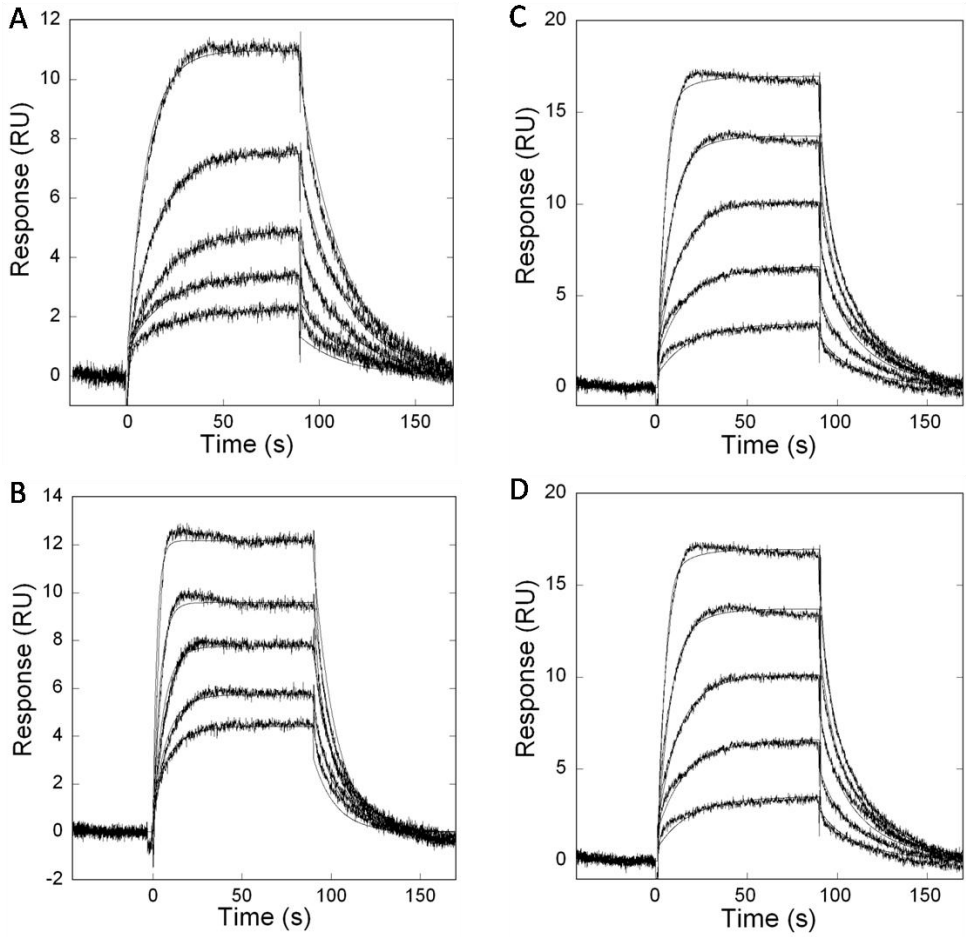

Fig. 3.

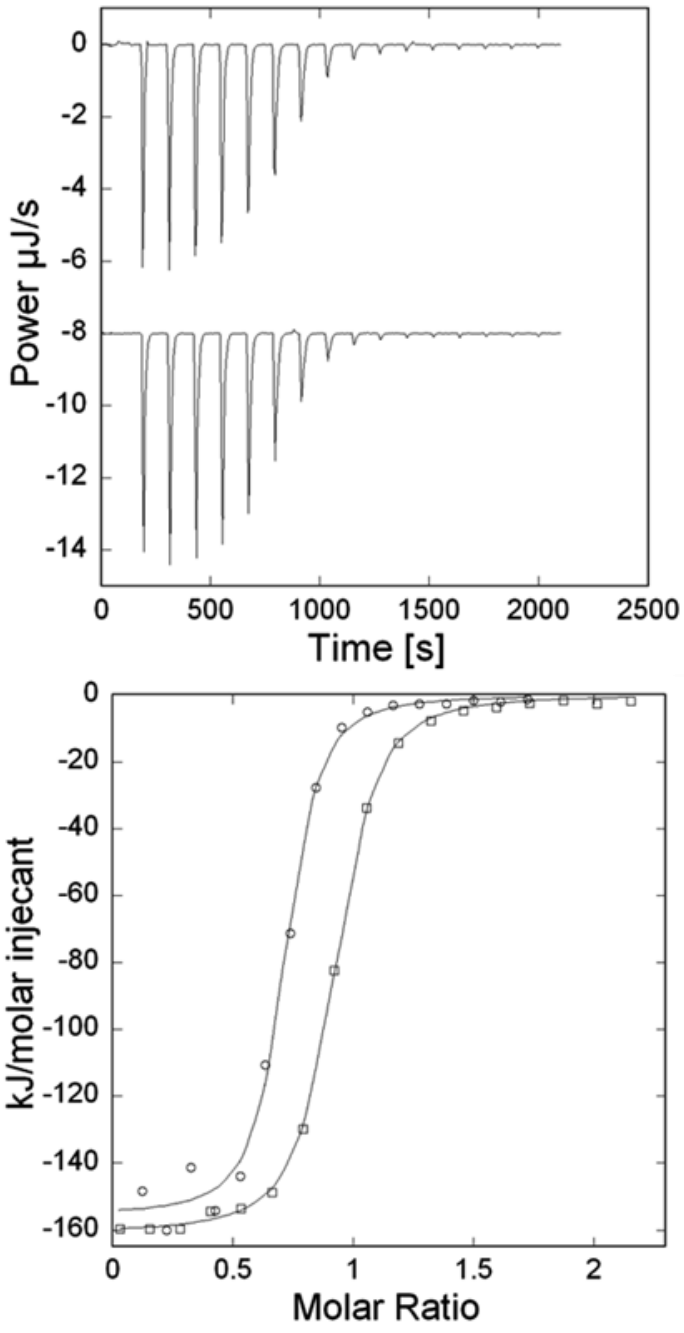
Power µJ/s
0
-2
-4
-6
-8
-10
-12
-14
0
500
1000
1500
2000
2500
Time [s]
kJ/molar injecant
0
-20
-40
-60
-80
-100
-120
-140
-160
0
0.5
1
1.5
2
Molar Ratio

Fig. 4.

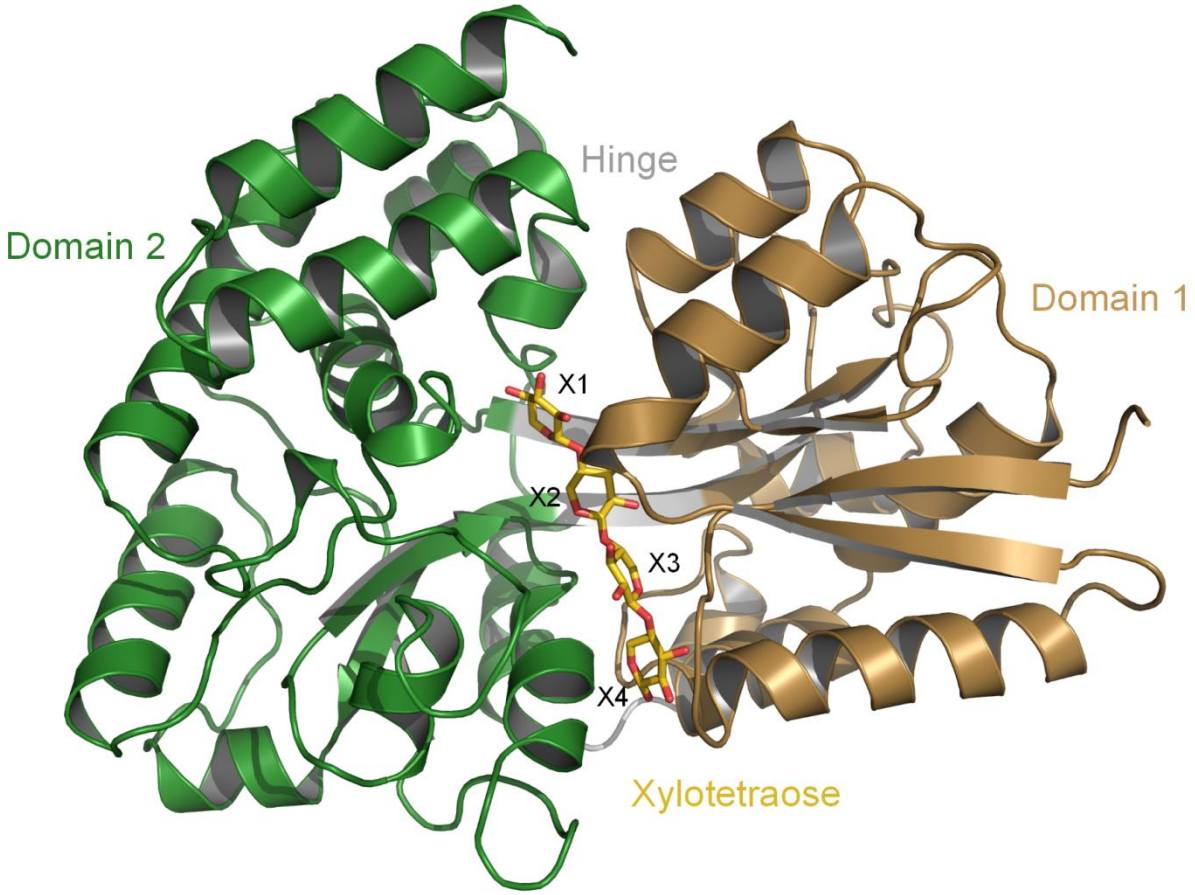

Fig. 5.

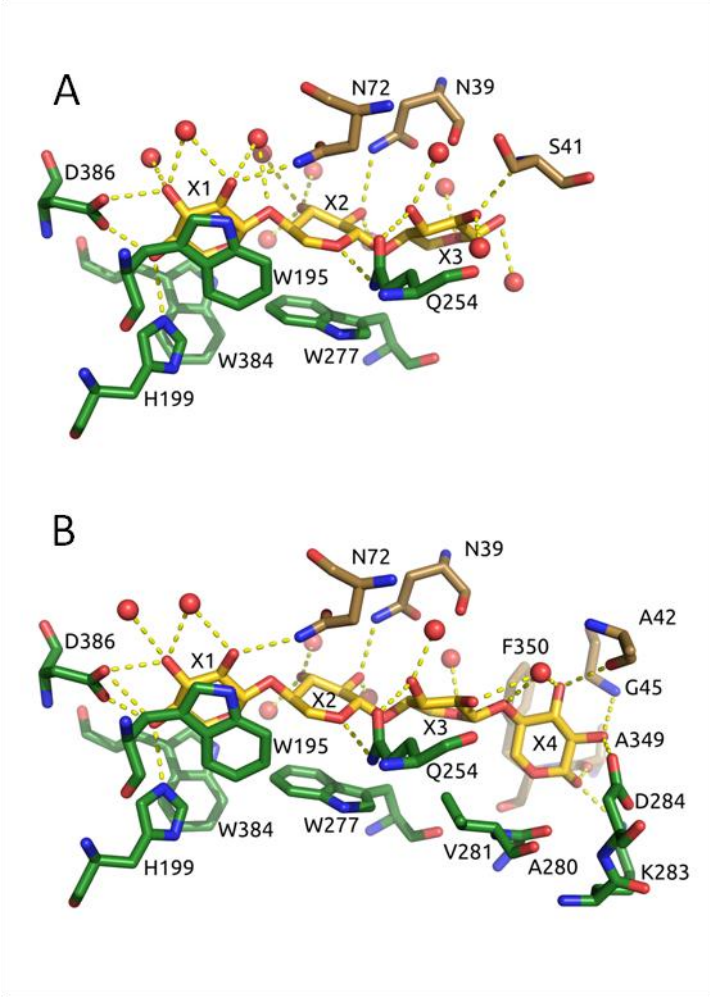
A
N72
N39
S41
D386
X1
X2
X3
W195
Q254
W384
W277
H199
B
N72
N39
A42
D386
F350
X1
G45
X2
X3
X4
A349
W195
Q254
D284
W384
W277
V281
A280
K283
H199

Fig. 6.

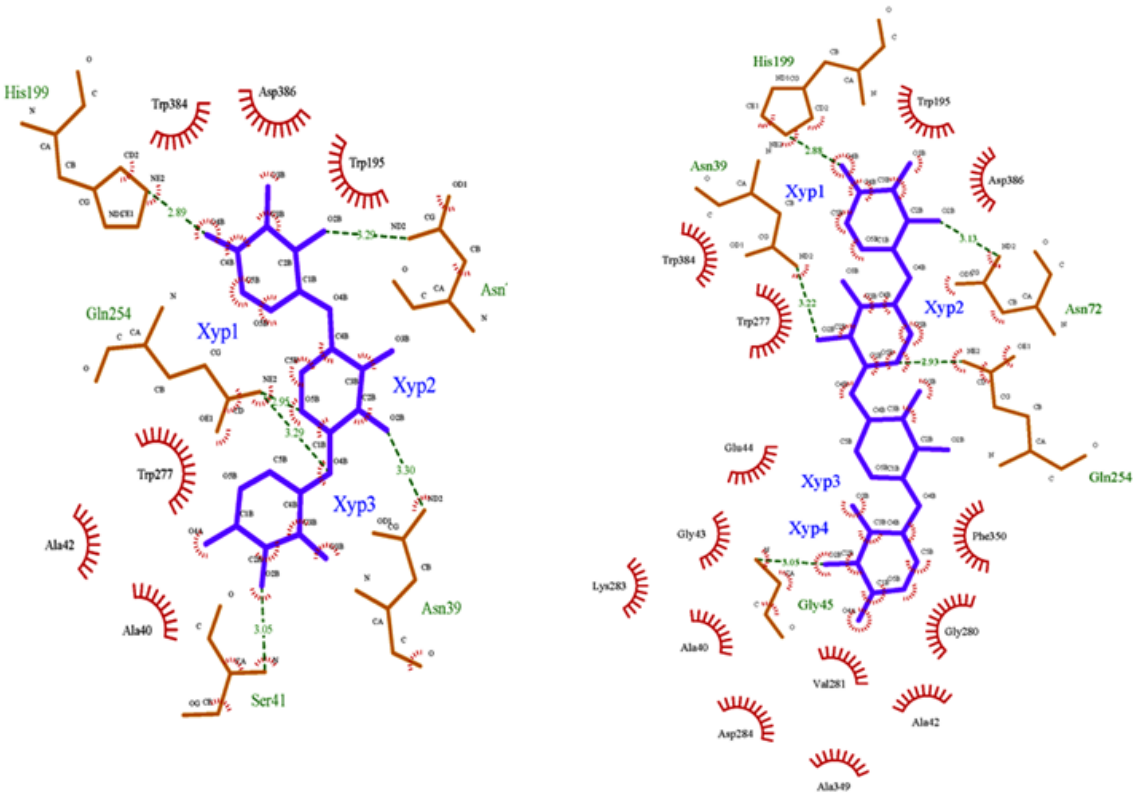
His199
Trp384
Asp386
Trp195
Asn
Gln254
Xyp1
Xyp2
Trp277
Xyp3
Ala42
Asn39
Ala40
Ser41
His199
Trp195
Asn39
Xyp1
Asp386
Trp384
Xyp2
Asn72
Trp277
Glu44
Gln254
Xyp3
Gly43
Xyp4
Phe350
Lys283
Gly45
Gly280
Ala40
Val281
Ala42
Asp284
Ala349

CHAPTER 7

Discussion

7 DISCUSSION

The present study is part of a larger effort with the goal of providing new insight to the beneficial effects of carbohydrates on probiotic bacteria at the molecular level and identifying carbohydrate active enzymes and proteins central to probiotic metabolism ("*Gene discovery and molecular interactions in prebiotics/probiotics systems. Focus on carbohydrate prebiotics*" (project no. 2101-07-0105)). The project is multi disciplinary and involves genome mining for functional units for utilization of non-digestible carbohydrates, colon simulator studies [1] and human intervention studies (van Zanten et. al. submitted manuscript) combined with protein characterization of carbohydrate active enzymes and transcriptome [2, 3] and proteome analysis of the probiotic bacteria utilizing selected carbohydrates in batch single cultures [4]. The crucial points of the concept of probiotics and prebiotics are the beneficial effect on the human host and the selective metabolism of the probiotic bacteria towards the probiotic compounds [5]. In this study I have focused on the latter part involving proteomics and protein characterization. The specific goal for my part of this project has been to establish the proteomes of the probiotic bacteria NCFM and Bl-04 using 2-DE based proteomics and differential proteome analysis with prebiotic carbohydrates to identify the changes in proteome when utilizing potential prebiotic carbohydrates. I have further focused on carbohydrates transport systems involved in uptake of potential prebiotic carbohydrates, specifically the ABC-transporter associated solute binding protein involved in the transport of XOS from Bl-04.

7.1 REFERENCE PROTEOMES OF NCFM AND BL-04

The advantage of proteomics compared to genomics is the ability to identify the proteins expressed in the cell at a given time, thereby monitoring the physiological state of the organism while fermenting potential probiotic carbohydrates. In the present study, the detailed reference proteome maps of *Lactobacillus acidophilus* NCFM and *Bifidobacterium animalis* subsp. *lactis* Bl-04 was established using two-dimensional gel electrophoresis, and have been and will be made public available. For NCFM 507 and 150 protein identifications were made from the CBB stained 2D-gel representing 275 and 102 unique proteins (pH 3−7 and pH 6−11). While from the whole cell extract proteome of Bl-04, 328 unique protein identifications were made from 870 protein identifications (pH 3−7 and pH 3−10). The purpose of the reference proteomes is to describe the probiotic

bacteria's physiology at the proteome level where proteins represent the actual functional molecules required by all life processes in the cell. Reference map serves as a blue print for comparative proteomics study to further increase our knowledge on the physiology. From the comparison of frequency of unique identifications to total number of identifications in the 2 organisms, it is evident that many proteins exist in multiple forms due to protein post-translational modifications, indicating multiple functions of a protein. The observed frequency of unique identifications is similar to other reported bacterial 2-DE reference proteomes [6-9]. Why are the proteins in the bacterial cell and specifically in our case the enzymes of the carbohrydate metabolism targets for multiple PTM? Regulation of function seems to be the most likely explanation. Within this project I have not been able to address this question, and gel-free proteomic methods are better suited for this task [10]. Multiple functions of one protein species have been reported and dubbed moonlighting proteins [11]. Interestingly several proteins involved in carbohydrate metabolism and translation from lactobacilli and bifidobacteria have been shown to moonlight in bacteria-host interactions, *e.g*. as adhesins or plasminogen receptors [12-16], and perhaps the PTM are involved in regulating these moonlighting functions.

The distribution of unique identifications into functional categories reveals a similar pattern for the two organisms, with the highest number of proteins belonging to carbohydrate metabolism, energy conversion and protein synthesis (chapter 2, Fig. 3 and chapter 5, Fig. 3). This distribution is also found in other reported bacterial 2-DE reference proteomes [6-9]. Noticeably 4.7 and 12.5% of the proteins species identified in the reference map for NCFM and Bl-04 respectively were annotated as hypothetical proteins, but can no longer be perceived as such. All proteins predicted to be involved in carbohydrate metabolism have been identified on the 2DE gels. NCFM is homofermentative and uses glycolysis for the utilization of carbohydrates, with lactate as the primary end product metabolite. Bl-04 is heterofermentative and uses the bifid shunt for utilization of carbohydrates and mixture of acetate, lactate, formate and ethanol are the end product metabolites. NCFM produces both enantiomers L-lactate and D-lactate, L-lactate is readily taken up by the colonic epithelia and used as energy source while D-lactate is degraded more slowly and is the cause of D-lactic acidosis in some cases [17]. The short chain fatty acids from Bl-04 metabolism have anti-inflammatory effects and promote defence functions of gut epithelial cells [18-20]. Carbohydrate sources have been

shown to play a major role in determining the final end product metabolite in NCFM and Bl-04 [21].

7.2 DIFFERENTIAL PROTEOME ANALYSIS

7.2.1 NCFM

Two different carbohydrates, lactitol and raffinose were used for the differential proteome analysis. Lactitol is a well established prebiotic with proven beneficial effects [22, 23], while raffinose is a potential prebiotic and is a major constituent of diet involving soya beans [24]. The 2-DE DIGE experiments with NCFM grown on lactitol and raffinose identified the glycoside hydrolases responsible for initiating the break down of these two potential prebiotics, namely GH2 β-galactosidase LacLM and GH36 α-galactosidase MelA. The hydrolysis product galactose from lactitol and raffinose induced the expression of enzymes of the Leloir pathway for galactose metabolism. The glucitol/sorbitol part of lactitol was metabolized via a PTS-II component. The sucrose part of raffinose also induced the expression of a sucrose-6-phosphate hydrolase, and is the primary enzyme involved in the metabolism of sucrose generated from raffinose. Furthermore the various changes in the abundance of proteins involved in carbohydrate metabolism were identified.

Various enzymes involved in CCR mediated regulation in the presence of lactitol were identified by DIGE analysis. In low G+C Gram-positive bacteria, PTS protein and HPr are the master regulators of carbon flow and metabolism. The phosphorylation and dephosphorylation of these proteins control the carbon metabolism via CCR [25, 26]. PTS phosphotransferase activity and the phosphoenolpyruvate-to-pyruvate ratio regulates the concentrations of metabolites such as fructose-1,6-bis-P, ATP, PP_i and P_i, which in turn control the HPr kinase activity [26-28]. The key gene products involved in the regulation, i.e. catabolite control protein A (CcpA), HPr, HPrK/P and PTS, were consistently highly abundant in the NCFM transcriptome, which suggested the regulation to occur at the protein rather than the transcriptional level [29]. In *Streptococcus* sp. transport of lactose via lactose permease containing the IIA domain was found to be regulated at the protein level by different HPr forms [30]. A similar mechanism is possible in NCFM owing to the absence of other transporters for lactose and the presence of a highly homologous lactose permease with IIA domain. The cellular concentration of pyruvate kinase, which has control over the phosphoenolpyruvate-to-pyruvate ratio, was more abundant, consistent with CCR.

Lactate dehydrogenase converts the generated pyruvate into lactate, NCFM has two lactate dehydrogenase enzymes D-lactate dehydrogenase and L-lactate dehydrogenase. L-lactate is the form preferred by the colon epithelia while D-lactate can induce acidosis in the host [17]. In the case of lactitol two forms of D-lactate dehydrogenase were found to be differentially abundant, with one being up-regulated and the other being down-regulated durring growth on lactitol. With growth on raffinose, D-lactate dehydrogenase and L-lactate dehydrogenase were found to be differentially abundant with upregulation of L-lactate dehydrogenase and downregulation of D-lactate dehydrogenase, indicating a shift from the end product enatiomer ratio of lactic acid.

7.2.2 BL-04

The established prebiotics galactooligosaccharides, isomaltooligosaccharides (panose and isomaltose) and potential prebiotics melibiose, raffinose family oligosaccharides (raffinose and stachyose) were used for the differential proteome analysis with Bl-04. The 2D-DIGE analysis with GOS, RFO and IMO revealed various proteins involved in the metabolism of these carbohydrates. A GH42 β-galactosidase was found to be differentially abundant with GOS, and is the primary enzyme in the utilization of β-galactosyl linked oligosaccharides. Glycoside hydrolases GH36 α-galactosidase (Balac_1601), GH13_31 oligo-1,6-glucosidase (Balac_1593) and GH13_18 sucrose phosphorylase (Balac_0138) were found to be upregulated during growth on melibiose, raffinose family oligosaccharides and isomaltooligosaccharides. In Bl-04 the gene cluster involved in the metabolism of α-galactose linked sugars includes two α-galactosidases (Balac_1596 and Balac_1601), components of the ABC transporter for sugars, oligo-1-6-glucosidase. The gene cluster is similar to the multiple sugar metabolism gene cluster in Gram-positive bacteria capable of utilizing melibiose, raffinose and isomalooligosaccharides. The presence and induction of oligo-1-6-glucosidase indicates transcriptional regulation and induction by α-galactose linked sugars and the capability of the gene cluster in Bl-04 to utilize multiple sugars.

Various proteins of the bifid shunt including L-ribulose-5-phosphate 4-epimerase, phosphoketolase, phosphoglucomutase, transketolase, 2,3-bisphosphoglycerate-dependent phosphoglycerate mutase, glyceraldehyde-3-phosphate dehydrogenase, pyruvate kinase, formate acetyl transferase, L-2,3-butanedioldehydrogenase/acetoinreductase and L-lactate

dehydrogenase were found to be differentially abundant with these prebiotic oligosaccharides candidates as carbon source.

The prebiotic carbohydrate sources have been shown to influence abundance of the proteins of the bifid shunt and play a role in the production of end product metabolites. In the present study, the differential abundance of isoforms of L-lactate dehydrogenase 2 involved in the inter conversion of pyruvate to L-Lactate and the bifunctional acetaldehyde-CoA/alcohol dehydrogenase involved in the inter conversion of acetaldehyde to ethanol also suggests changes in the end product metabolites with prebiotic carbohydrates.

7.3 XOS TRANSPORT IN BL-04

In order to try to understand the selectiveness of XOS towards bifidobacteria the structure and biochemical properties of the XOS uptake ABC-transporter associated SBP *Bl*XBP was charaterized. *Bl*XBP displayed no detectable binding activity towards xylose or arabinose but a relatively sharp size preference for XOS and AXOS with DP 3–5 with an optimum affinity for DP4. This observation can perhaps inspire to the production of probiotic products containing oligosaccharides with optimal DP for the probiotic strains that is targeted.

The affinity of *Bl*XBP to its ligands was characterized by large changes in the association rate (k_{on}), while changes in the dissociation rate were modest with the exception for X2. The magnitude of k_{off} reflects the short range interactions between the protein and the ligand, while k_{on} is influenced by diffusion and by favorable electrostatics when the protein and the ligand are within the encounter complex distance [31]. The trend of a slower k_{on} was also observed governing the affinity to the larger ligands X5 and X6. The binding of these ligands would require additional structural rearrangements, which results in slower k_{on} values. Thus the binding kinetics modulates the ligand preference of *Bl*XBP for optimal affinity to ligands of DP 3–4. The thermodynamic signature of *Bl*XBP binding to X3 and X4 was similar and revealed an enthalpic dominated binding, which is compensated by large entropic penalties. This energetic fingerprint is in excellent agreement with the structural data showing extensive protein-ligand interactions involving a combination of aromatic stacking and a hydrogen bonding network including direct and solvent mediated contacts, which contribute to the binding enthalpy. A similar mode of binding was also

observed for Lactose-N-biose SBP from probiotic *Bifidobacerium longum* [32]. The unfavorable entropy is likely to arise from the ordering of water molecules in the binding pocket and the loss of conformational freedom of both the ligand and the protein side chains and domains that typically possess rotational freedom along the hinge region [33]. Previously the binding constants of two other XOS binding SBP have been reported *Streptomyces thermoviolaceus* and *Caldanaerobius polysaccharolyticus* [34, 35] with high affinity towards xylobiose and xylotriose respectively. In the present moment it is unclear, what the underlying molecular basis is that determines the difference in ligand preference, but further structural analysis may elucidate this. This work contributes to the understanding of the molecular mechanism for probiotic selectiveness of probiotic carbohydrates.

References

1. van Zanten GC, Knudsen A, Röytiö H, Forssten S, Lawther M, Blennow A, Lahtinen SJ, Jakobsen M, Svensson B, Jespersen L: **The effect of selected synbiotics on microbial composition and short-chain fatty acid production in a model system of the human colon**. *PLoS One* 2012, **7**:e47212.
2. Andersen JM, Barrangou R, Abou Hachem M, Lahtinen S, Goh YJ, Svensson B, Klaenhammer TR: **Transcriptional and functional analysis of galactooligosaccharide uptake by lacS in *Lactobacillus acidophilus***. *Proc Natl Acad Sci USA*, **108**:17785-17790.
3. Andersen JM, Barrangou R, Hachem MA, Lahtinen SJ, Goh Y-J, Svensson B, Klaenhammer TR: **Transcriptional analysis of prebiotic uptake and catabolism by *Lactobacillus acidophilus* NCFM**. *PLoS One* 2012, **7**:e44409.
4. Majumder A, Sultan A, Jersie-Christensen RR, Ejby M, Schmidt BG, Lahtinen SJ, Jacobsen S, Svensson B: **Proteome reference map of *Lactobacillus acidophilus* NCFM and quantitative proteomics towards understanding the prebiotic action of lactitol**. *Proteomics* 2011, **11**: 3470-3481.
5. Roberfroid M, Gibson GR, Hoyles L, McCartney AL, Rastall R, Rowland I, Wolvers D, Watzl B, Szajewska H, Stahl B *et al*: **Prebiotic effects: metabolic and health benefits**. *Br J Nutr* 2010, **104**:S1-63.
6. Yuan J, Zhu L, Liu XK, Zhang Y, Ying TY, Wang B, Wang JJ, Dong H, Feng EL, Li Q

et al: **A proteome reference map and proteomic analysis of *Bifidobacterium longum* NCC2705**. *Mol Cell Proteomics* 2006, **5**:1105-1118.

7. Cohen DPA, Renes J, Bouwman FG, Zoetendal EG, Mariman E, de Vos WM, Vaughan EE: **Proteomic analysis of log to stationary growth phase *Lactobacillus plantarum* cells and a 2-DE database**. *Proteomics* 2006, **6**:6485-6493.
8. Buttner K, Bernhardt J, Scharf C, Schmid R, Mader U, Eymann C, Antelmann H, Volker A, Volker U, Hecker M: **A comprehensive two-dimensional map of cytosolic proteins of *Bacillus subtilis***. *Electrophoresis* 2001, **22**:2908-2935.
9. Guillot A, Gitton C, Anglade P, Mistou MY: **Proteomic analysis of *Lactococcus lactis*, a lactic acid bacterium**. *Proteomics* 2003, **3**:337-354.
10. Soufi B, Soares NC, Ravikumar V, Macek B: **Proteomics reveals evidence of cross-talk between protein modifications in bacteria: focus on acetylation and phosphorylation**. *Curr Opin Microbiol* 2012, **15**:357-363.
11. Jeffery CJ: **Moonlighting proteins: old proteins learning new tricks**. *TIG* 2003, **19**:415-417.
12. Candela M, Bergmann S, Vici M, Vitali B, Turroni S, Eikmanns BJ, Hammerschmidt S, Brigidi P: **Binding of Human Plasminogen to Bifidobacterium**. *J Bacteriol* 2007, **189**:5929-5936.
13. Castaldo C, Vastano V, Siciliano RA, Candela M, Vici M, Muscariello L, Marasco R, Sacco M: **Surface displaced alfa-enolase of *Lactobacillus plantarum* is a fibronectin binding protein**. *Microb Cell Fact* 2009, **8**: 14.
14. Katakura Y, Sano R, Hashimoto T, Ninomiya K, Shioya S: **Lactic acid bacteria display on the cell surface cytosolic proteins that recognize yeast mannan**. *Appl Environ Microbiol* 2010, **86**:319-326.
15. Sanchez B, Urdaci MC, Margolles A: **Extracellular proteins secreted by probiotic bacteria as mediators of effects that promote mucosa-bacteria interactions**. *Microbiology* 2010, **156**:3232-3242.
16. Candela M, Biagi E, Centanni M, Turroni S, Vici M, Musiani F, Vitali B, Bergmann S, Hammerschmidt S, Brigidi P: **Bifidobacterial enolase, a cell surface receptor for human plasminogen involved in the interaction with the host**. *Microbiology* 2009, **155**:3294-3303.
17. Uchida H, Yamamoto H, Kisaki Y, Fujino J, Ishimaru Y, Ikeda H: **D-lactic acidosis in**

short-bowel syndrome managed with antibiotics and probiotics. *J Pediatr Surg* 2004, **39**:634-636.

18. Saulnier DMA, Spinler JK, Gibson GR, Versalovic J: **Mechanisms of probiosis and prebiosis: considerations for enhanced functional foods**. *Curr Opin Biotechnol* 2009, **20**:135-141.
19. Fukuda S, Toh H, Hase K, Oshima K, Nakanishi Y, Yoshimura K, Tobe T, Clarke JM, Topping DL, Suzuki T *et al*: **Bifidobacteria can protect from enteropathogenic infection through production of acetate**. *Nature* 2011, **469**:543-549.
20. Tedelind S, Westberg F, Kjerrulf M, Vidal A: **Anti-inflammatory properties of the short-chain fatty acids acetate and propionate: A study with relevance to inflammatory bowel disease**. *World J Gastroentero* 2007, **13**:2826-2832.
21. Goderska K. NJ, Czarnecki Z.: **Comparision of growth of *Lactobacillus acidophilus* and *Bifidobacterium bifidum* species in media suplemented with selected saccharides including prebiotics**. *Acta Sci Pol, Technol Aliment* 2008, **7**:5-20.
22. Ouwehand AC, Tiihonen K, Saarinen M, Putaala H, Rautonen N: **Influence of a combination of *Lactobacillus acidophilus* NCFM and lactitol on healthy elderly: intestinal and immune parameters**. *Br J Nutr* 2009, **101**:367-375.
23. Makivuokko H, Forssten S, Saarinen M, Ouwehand A, Rautonen N: **Synbiotic effects of lactitol and *Lactobacillus acidophilus* NCFM™ in a semi-continuous colon fermentation model**. *Benef Microbes* 2010, **1**:131-137.
24. Kumar V, Rani A, Goyal L, Dixit AK, Manjaya JG, Dev J, Swamy M: **Sucrose and raffinose family oligosaccharides (RFOs) in soybean seeds as influenced by genotype and growing location**. *J Agric Food Chem* 2010, **58**:5081-5085.
25. Monedero V, Maze A, Boel G, Zuniga M, Beaufils S, Hartke A, Deutscher J: **The phosphotransferase system of *Lactobacillus casei* : Regulation of carbon metabolism and connection to cold shock response**. *J Mol Microbiol Biotechnol* 2007, **12**:20-32.
26. Deutscher J, Francke C, Postma PW: **How phosphotransferase system-related protein phosphorylation regulates carbohydrate metabolism in bacteria**. *Microbiol Mol Biol Rev* 2006, **70**:939-1031.
27. Dossonnet V, Monedero V, Zagorec M, Galinier A, Perez-Martinez G, Deutscher J: **Phosphorylation of HPr by the bifunctional HPr kinase/P-Ser-HPr phosphatase**

from *Lactobacillus casei* controls catabolite repression and inducer exclusion but not inducer expulsion. *J Bacteriol* 2000, **182**:2582-2590.

28. Kotrba P, Inui M, Yukawa H: **Bacterial phosphotransferase system (PTS) in carbohydrate uptake and control of carbon metabolism**. *J Biosci Bioeng* 2001, **92**:502-517.
29. Barrangou R, Azcarate-Peril MA, Duong T, Conners SB, Kelly RM, Klaenhammer TR: **Global analysis of carbohydrate utilization by *Lactobacillus acidophilus* using cDNA microarrays**. *Proc Natl Acad Sci USA* 2006, **103**:3816-3821.
30. Hols P, Hancy F, Fontaine L, Grossiord B, Prozzi D, Leblond-Bourget N, Decaris B, Bolotin A, Delorme C, Ehrlich SD *et al*: **New insights in the molecular biology and physiology of *Streptococcus thermophilus* revealed by comparative genomics**. *FEMS Microbiol Rev* 2005, **29**:435-463.
31. Sheinerman FB, Norel R, Honig B: **Electrostatic aspects of protein-protein interactions**. *Curr Opin Struct Biol* 2000, **10**:153-159.
32. Suzuki R, Wada J, Katayama T, Fushinobu S, Wakagi T, Shoun H, Sugimoto H, Tanaka A, Kumagai H, Ashida H *et al*: **Structural and thermodynamic analyses of solute-binding protein from *Bifidobacterium longum* specific for core 1 disaccharide and lacto-N-biose I**. *J Biol Chem* 2008, **283**:13165-13173.
33. Jelesarov I, Bosshard HR: **Isothermal titration calorimetry and differential scanning calorimetry as complementary tools to investigate the energetics of biomolecular recognition**. *J Mol Recognit* 1999, **12**:3-18.
34. Han Y, Agarwal V, Dodd D, Kim J, Bae B, Mackie RI, Nair SK, Cann IKO: **Biochemical and structural insights into xylan utilization by the thermophilic bacterium *Caldanaerobius polysaccharolyticus***. *J Biol Chem* 2012, **42**: 34946-34960.
35. Tsujibo H, Kosaka M, Ikenishi S, Sato T, Miyamoto K, Inamori Y: **Molecular characterization of a high-affinity xylobiose transporter of *Streptomyces thermoviolaceus* OPC-520 and its transcriptional regulation**. *J Bacteriol* 2004, **186**:1029-1037.